

Generating functions and attractor flow for $\mathcal{N} = 2$ BPS structures

Dissertation zur Erlangung des Doktorgrades

an der

Fakultät für Mathematik, Informatik und

Naturwissenschaften

Fachbereich Physik

der

Universität Hamburg

vorgelegt von

Daniel Siphon Fritz Bryan

Hamburg

2023

Gutachter/innen der Dissertation:

Dr. Murad Alim

Prof. Dr. Timo Weigand

Zusammensetzung der Prüfungskommission:

Dr. Murad Alim

Prof. Dr. Timo Weigand

Prof. Dr. Jan Louis

Prof. Dr. Daniela Pfannkuche

Prof. Dr. Gregor Kasieczka

Vorsitzende/r der Prüfungskommission:

Prof. Dr. Daniela Pfannkuche

Datum der Disputation:

07.12.2023

Vorsitzender Fach-Promotionsausschuss PHYSIK:

Prof. Dr. Markus Drescher

Leiter des Fachbereichs PHYSIK:

Prof. Dr. Wolfgang J. Parak

Dekan der Fakultät MIN:

Prof. Dr.-Ing. Norbert Ritter

Eidesstattliche Versicherung

Hiermit versichere ich an Eides statt, die vorliegende Dissertationsschrift selbst verfasst und keine anderen als die angegebenen Hilfsmittel und Quellen benutzt zu haben.

Hamburg, den 2. Oktober 2023

A handwritten signature in black ink that reads "Daniel Bryan". The script is cursive and fluid.

Unterschrift Daniel Siphon Fritz Bryan

Abstract

This thesis studies wall crossing phenomena in BPS structures associated to 4d $\mathcal{N} = 2$ QFTs including both Argyres-Douglas and Seiberg-Witten theories. The BPS spectrum is determined in each region of the moduli space, bounded by walls of marginal stability, both by using attractor flow methods and by deriving a generating function with Fourier coefficients that jump as a wall is crossed. The attractor flow methods are applied using existence conditions for the BPS states on the endpoints of the flow lines which split when a composite line flows into a wall. For $\mathcal{N} = 4$ dyonic black holes the wall crossing of $\frac{1}{4}$ BPS states is known to be determined by the Weyl denominator of a Borcherds-Kac-Moody algebra. This has a different Fourier expansion in the different chambers, which represents a jump in the degeneracies of black holes with specific charges.

In this work, analogs of these counting functions are found for $\mathcal{N} = 2$ BPS structures. These correspond to the Weyl denominator formulae in the case of ADE type Lie algebras, where the root system describes the charges of the BPS particles. The resulting formulae contain information about the spectra of BPS and framed BPS states in Weyl chambers within the moduli spaces of these theories. The regions in the moduli space with fixed spectra are found to be bounded by walls, including the Weyl chamber boundaries and an additional wall of marginal stability. In some examples of uncoupled BPS structures this can then be reproduced by the Stokes phenomena of the Borel summation of the topological string free energy.

Zusammenfassung

Die vorliegende Arbeit beschäftigt sich mit Wall-Crossing Phänomenen von BPS Zuständen in 4d $\mathcal{N} = 2$ supersymmetrischen Quantenfeldtheorien, einschließlich Argyres-Douglas und Seiberg-Witten Theorien. Das BPS Spektrum wird in den verschiedenen Regionen des Modulraums bestimmt, die durch die “Walls of marginal stability” begrenzt werden. Dies geschieht zunächst durch die Anwendung von Attractor-Flow Methoden und danach durch die Herleitung einer erzeugenden Funktion mit Koeffizienten, die beim Überqueren einer Wall sich verändern. Die Attractor-Flow-Methoden werden angewandt, indem die Existenzbedingungen für BPS-Zustände an den Endpunkten der Flusslinien betrachtet werden. Diese Linien verzweigen sich, wenn eine Linie, die zu einem zusammengesetzten BPS-Zustand gehört, in eine Wall fließt.

Für $\mathcal{N} = 4$ supersymmetrische Schwarze Löcher mit elektrischer und magnetischer Ladung werden die Wall-Crossing-Phänomene von $\frac{1}{4}$ -BPS-Zuständen durch den Weyl-Nenner für die Borcherds-Kac-Moody-Algebra beschrieben. Diese Funktion hat unterschiedliche Fourier-Entwicklungen in den verschiedenen Weyl-Kammern. Dies repräsentiert einen Sprung im Entartungsgrad der Schwarzen Löcher mit spezifischer Ladung. In dieser Arbeit werden Analoga dieser erzeugenden Funktion für BPS-Strukturen in $\mathcal{N} = 2$ supersymmetrischen Theorien gefunden. Diese Analoga sind die Weyl-Nenner-Formeln für ADE Lie-Algebren, in denen die Wurzeln die Ladung der BPS-Teilchen beschreiben. Mithilfe dieser Formeln kann man Informationen über das Spektrum der BPS- und gerahmten BPS-Zustände ablesen. Die Regionen des Modulraums, in denen die Spektren konstant sind, werden durch die Walls begrenzt. Diese Walls umfassen die Grenzen der Weyl-Kammern, aber auch eine zusätzliche Wall of marginal stability. In einigen Beispielen entkoppelter BPS-Strukturen lassen sich diese Phänomene auch mit den Stokes-Sprüngen der Borel-Summierung der freien Energien des topologischen Strings beschreiben.

Acknowledgements

The research in this thesis was supported by the DFG Emmy Noether Grant on “Building blocks of physical theories from the geometry of quantization and BPS states”, number AL1407/2-1. I am also very grateful for the financial support from the Friedrich-Naumann Foundation (FNF) for Freedom, further supported by the Ministry for Education and Research of Germany, from which I received a scholarship from 01.05.2020-31.07.2022.

Firstly, I am deeply grateful to my advisor Dr. Murad Alim for supporting and guiding me throughout this time and suggesting research questions and ideas. He helped guide the research patiently throughout and suggested connections between BPS structures that led to promising results. His encouragement to develop independence and professionalism in my research helped me enormously over the course of this work and will undoubtedly serve me well in the future. I am very happy to have been offered the opportunity of working with him. Furthermore, I am also grateful for the support from my co-advisor Prof. Dr. Jan Louis.

During the course of the PhD, I greatly benefited from discussions and conversations with other PhD students and postdoctoral researchers. I would therefore also like to thank Dr. Martin Vogrin, Dr. Ivan Tulli, Dr. Florian Beck and Dr. Arpan Saha for helpful discussions on various topics in mathematics and physics. Finally, I would also like to thank my family for their unwavering support during this time.

Contents

1	Introduction	1
2	BPS states and Argyres-Douglas theories	7
2.1	Introduction to $4d \mathcal{N} = 2$ QFTs	8
2.1.1	Moduli space	9
2.1.2	Argyres-Douglas theories and their string theory construction	10
2.1.3	Seiberg-Witten theory	12
3	BPS structures and invariants	13
3.1	BPS structures and Donaldson-Thomas invariants	13
3.1.1	Refinement of BPS indices	14
3.1.2	BPS invariants and wall crossing from quantum dilogarithms	16
4	BPS quivers in $\mathcal{N} = 2$ QFTs	20
4.1	Construction of quivers	20
4.1.1	Construction of quiver moduli space	21
4.2	Quiver descriptions	24
4.2.1	Representations and subrepresentations	24
4.2.2	Quiver mutations and dualities	26
4.3	Examples	28
4.3.1	Argyres-Douglas A_1	28
4.3.2	Argyres-Douglas A_2	28
4.3.3	Seiberg-Witten theory	29
4.3.4	Resolved conifold	30
5	Wall crossing formulae and framed BPS states	31

5.1	Primitive wall crossing formula	31
5.2	Semi-primitive wall crossing formula	32
5.3	Framed BPS states and galaxies	34
5.3.1	Core charges and orbiting charges	35
5.3.2	Hilbert space and generating function of framed BPS states	37
5.4	D6-D2-D0 system on the conifold	40
6	Exact WKB method	45
6.1	Schrödinger equation and quantum periods	45
6.1.1	WKB for the cubic curve	48
6.2	Borel transformation of periods	49
6.2.1	Definition of Borel transform	49
6.2.2	Application to quantum periods	50
6.2.3	TBA equations	51
7	Attractor flow in $\mathcal{N} = 2$ supergravity	55
7.1	Introduction to attractor flow of BPS states	55
7.1.1	Wall crossing and attractor flow in $\mathcal{N} = 2$ supergravity	56
7.2	Application to 1 parameter case	60
7.2.1	Path of steepest descent	62
7.2.2	Curves and periods	62
7.2.3	Picard-Fuchs equations and solutions	63
8	Attractor flow examples	68
8.1	Attractor flow for A_1 -theory	68
8.2	Attractor flow for Argyres–Douglas A_2 theory	70
8.2.1	Walls, branch cuts and flow lines	70
8.2.2	Attractor flow first realisation	71
8.2.3	Attractor flow second realisation	78
8.3	Attractor flow in Seiberg–Witten $SU(2)$	90
8.3.1	Concluding remarks	96
9	$\mathcal{N} = 4$ black hole partition functions	98

9.1	History of black hole partition functions	98
9.1.1	Black hole entropy in Strominger-Vafa black holes	98
9.2	BPS charges and degeneracies in $\mathcal{N} = 4$ black holes	99
9.3	Derivation of generating function for black hole	101
9.3.1	Heterotic description for purely electric and magnetic states	102
9.3.2	Type II description of electric and magnetic states	104
9.3.3	Partition function of dyons from type II description	106
9.3.4	Expansion of $K3$ elliptic genus	109
9.3.5	The 1-loop integral	110
9.4	Generating function as partition function	112
9.5	Modularity, contour prescription, and wall crossing	114
9.5.1	Modularity and limits of Igusa cusp form	114
9.5.2	Contour prescription	115
9.5.3	Walls and central charges in $\mathcal{N} = 4$	117
10	$\mathcal{N} = 4$ BPS generating function and Lie algebras	119
10.1	Wall crossing and BPS generating function for subalgebras	120
10.2	Subalgebras of Borcherds-Kac-Moody	122
10.2.1	Weyl denominator for the subalgebras	122
10.2.2	Degeneracies	123
10.3	\hat{A}_1 as a subalgebra	124
10.3.1	Extracting generating function for \hat{A}_1	126
10.3.2	Contour prescription for \hat{A}_1	127
10.4	Wall crossing for \hat{A}_1 in $\mathcal{N} = 4$	128
10.4.1	Wall crossing	129
10.4.2	Jumping between chambers	130
10.4.3	Wall crossing in terms of highest weights	132
11	$\mathcal{N} = 2$ analogs of the generating functions	135
11.1	BPS root systems and Lie algebras	135
11.1.1	Weyl denominator and generating function	137
11.2	\hat{A}_1 root system in $\mathcal{N} = 2$	139
11.2.1	Change in highest weight	140

11.2.2	Counting roots and weights in Verma modules	141
11.3	Example 1: Jafferis-Moore D6-D2-D0 bound state	145
11.4	Example 2: Seiberg-Witten theory	146
11.4.1	Seiberg-Witten walls	148
11.5	Argyres-Douglas A_2	156
11.5.1	Introduction to counting function for Argyres-Douglas A_2 theory	156
11.5.2	A_2 Weyl character	156
11.5.3	Wall crossing and change of basis for denominator	157
12	Uncoupled BPS structures and topological strings	165
12.1	Deformed and resolved conifold	165
12.1.1	Deformed conifold generating function	166
12.1.2	Resolved conifold	167
12.1.3	Gamma and G -functions	168
12.2	Multiple gamma functions	169
12.2.1	Relation between integral representations	171
12.2.2	Relation between G and zeta function	171
12.2.3	Removal of logarithm in gamma function	172
12.2.4	Concluding remarks	174
13	Summary	176
A	BPS states and central charges	179
A.1	Expansion of central charges around singular points	179
A.1.1	Argyres-Douglas A_2 realised on $\Sigma_{A_2}^I$	179
A.1.2	Argyres-Douglas A_2 realised on $\Sigma_{A_2}^{II}$	181
A.1.3	Seiberg-Witten SU(2) theory	182
B	\hat{A}_1 changes in representation	184
B.1	Original generating function	184
B.1.1	Changes in highest weight	185
B.2	A_2 Weyl character changes in representation	187
B.2.1	Weyl denominator expansions	187

C	Integral representations of double gamma function	189
C.1	Derivation of relation	189
C.2	Writing relation as an integral representation	190

1 | Introduction

This thesis is concerned with the wall crossing of BPS structures that arise from BPS states present in special 4d $\mathcal{N} = 2$ QFTs. These theories also have a type II string theory construction on a Calabi-Yau 3-fold. In this thesis a new generating function is constructed that encodes these wall crossing phenomena. Wall crossing in general involves jumps in the number of BPS states, and the associated BPS invariants, across a boundary within the deformation space of parameters describing the theory. This occurs as composite BPS states become unstable and decay into constituents. The boundary is called the wall of marginal stability and the space of parameters describing the deformations of the theory is known as the moduli space. Physically, for a QFT or string theory, this can be interpreted as a deformation space of the low energy effective action or the space of couplings.

A BPS state is a special type of supersymmetric state that is annihilated by the supercharges. There is a condition, known as the BPS bound, which is saturated from below by the BPS states: their mass and the modulus of their central charges are equal, otherwise the mass is greater. BPS states also have a geometrical description as D-branes arising from string theory. In this case, one looks at the target space of the string theory in which the BPS states are described by special submanifolds wrapped within this space. BPS states can be considered topological data of a theory - they are topologically protected against quantum corrections. This means that the number of states should not change under continuous deformation of the moduli of a theory unless a wall of marginal stability is crossed. Therefore, this has led to descriptions of strong/weak coupling dualities and has inspired a large body of research looking for non-perturbative formulations of QFTs and string theories as well as a description of black hole microstates.

An important result in the study of 4d $\mathcal{N} = 2$ QFTs was that of Seiberg-Witten theory [1] due to the exact description of the low energy effective action. This has later been found to have a BPS spectrum represented by the full \hat{A}_1 root system at weak coupling and just 2 basis states in the strong coupling region on the other side of the wall [2, 3, 4]. Subsequently, similar results have been found for Argyres-Douglas theories [5, 6, 7, 8, 9], with ADE type root systems describing the charges of the BPS states. The most basic example of wall crossing involves the simple (also known as primitive) case representing a jump between 2 and 3 BPS states. One can interpret this as a composite BPS dyon splitting into electric and magnetic constituents during wall crossing. This occurs when the central charges of the BPS states, which are complex numbers, align on the wall of marginal stability.

There is also an equivalent 2d description of this wall crossing that predated this [10] and was further developed in [11, 3]. This involved counting solitons in Landau-Ginsburg theories which are the analog of the 4d BPS states. The models themselves were constructed from [12, 13] massive deformations of superconformal points [14, 15]. Further important contributions to the study of wall crossing were made by Gaiotto, Moore and Neitzke (GMN), first by reducing wall crossing phenomena found in the 4d models to $\mathbb{R}^3 \times S^1$ [16], then by introducing a new type of wall crossing [17]. This involved bound states of the original BPS states that exist in the theory with a large core object. These combinations are called framed BPS states [17, 18] and their walls are referred to as BPS walls. The new walls are of particular interest as they can be organised into Weyl chambers and constrain the wall crossing behavior of the original BPS states in the theory.

The BPS invariants in the $\mathcal{N} = 2$ theories that are discussed in this thesis are found by counting the states using BPS indices for the hyper and vector multiplets in the theory. When embedded in string theory, they have also been found to have a description [19, 20, 21] as topological invariants of the target spaces, such as Donaldson-Thomas (DT) [19, 22, 23] and Gopakumar-Vafa (GV) [24, 25, 26, 27] invariants, which have been further related to Gromov-Witten invariants for some examples in the DT-GW correspondence from MNOP [28, 29]. They can therefore be encoded by particular functions known as the generating functions of these invariants and can be read off from topological string partition functions in specific examples. Wall crossing for these BPS structures has also been encoded in generating functions by considering products of operators representing BPS states that match on either side of the wall, as found by Kontsevich and Soibelman [30], and interpreted physically in [16, 31, 32, 33, 34]. Furthermore, the jumps in the BPS indices can often be generated simultaneously when crossing a wall using results known as the wall crossing formulae. These are well known [35, 36] in the primitive and semi-primitive cases, the latter involving bound states of a single BPS state with multiple copies of another [37, 34, 18, 38].

Conversely, one can also work backwards if the BPS invariants and their wall crossing phenomena are known. One writes down a generating function for these invariants which determines the BPS spectrum in every region of the moduli space. This then becomes a candidate for a non-perturbative partition function for a generalised lattice of BPS states. This direction of research is developed in this thesis for particular testing cases, given by Seiberg-Witten and simple A_1, A_2 type Argyres-Douglas theories, with known patterns of wall crossing. This should then be generalisable to other BPS structures such as those described by ADE type root systems.

In parallel, BPS states have been counted for $\mathcal{N} = 4$ black holes where the first microstate description in terms of BPS states was given by Strominger and Vafa [39] for 5d black holes on $K3 \times S^1$. Later the partition function for dyonic 4d black holes on $K3 \times T^2$ was also derived by Dijkgraaf, Verlinde, Verlinde [40] and built on by [41]. This partly followed the older known computation [42] for the $\mathcal{N} = 2$ BPS algebras of perturbative BPS states, described by Harvey and Moore [43, 44], starting from 1996. The result of this was that the partition function for dyonic black holes could be written as the weight 10 Siegel modular

form known as the Igusa cusp form. This is also the Weyl denominator of a Borcherds-Kac-Moody algebra and is extensively discussed by Gritsenko and Nikulin [45, 46, 47].

Since then, there has been extensive research on using this dyon counting formula to extract degeneracies for particular charges [48, 49, 50, 51]. This is done by extracting Fourier coefficients as well as by using a specific contour prescription for the different charges that can be deformed into each other. The prescription must satisfy parity and S-duality constraints. The dyons (which are black holes with multiple centers) can undergo wall crossing in that they split into electric and magnetic constituents. This has been studied by Cheng and Verlinde [52, 53] and further discussed in [54], first using the contour prescription in which wall crossing happens as poles are crossed, and then by considering the jumps in a highest weight of Verma modules. In this work this result is used to construct an analog for BPS states in the 4d $\mathcal{N} = 2$ theories.

The attractor flow on the moduli space of BPS solutions in supergravity is another important concept in the study of wall crossing and has been worked on extensively in [55, 36, 56, 57, 58]. One can use existence conditions on the endpoints of the central charges to determine the spectrum within each chamber and the wall crossing between the chambers. A BPS state is excluded if its flow line terminates at a regular point in the moduli space. Wall crossing can be seen here by the attractor flow line of a composite BPS state splitting into the flow lines of the constituents at the wall. A BPS state can exist if the flow terminates at a singular point where the central charge vanishes. This method is applied to Seiberg-Witten and Argyres-Douglas theories in this thesis.

The central charges can also be used as arguments in the $\mathcal{N} = 2$ analogs of the generating function. In this case, the existence conditions for the BPS states then map onto counts of BPS states in the generating function in the different regions of the moduli space. This is what allows a generating function for a particular root system to count the BPS states of distinct theories, with different central charges, but retaining the same BPS root system. Finally, this thesis directly discusses connections between the wall crossing of BPS counting functions derived here and non-perturbative topological string partition functions. In the example of the resolved conifold with an \hat{A}_1 root system [59, 20, 60] the free energies can be expressed as a Borel transform and have been found [61] to take different values depending on which ray the integral is taken along, hereby encoding the Jafferis-Moore wall crossing.

Contribution of this thesis

In the first research work in this thesis “Special geometry, quasi-modularity and attractor flow for BPS structures” [62], included in chapters 7 and 8, we extend the attractor flow literature [55, 36, 56, 57, 58] to the BPS structures of Argyres-Douglas A_1, A_2 models and Seiberg-Witten theory. We use the solutions of the Picard-Fuchs equations to find the moduli dependent central charges of the BPS states. This then allows the attractor flow to be plotted using the gradient flow lines which are then continued through branch cuts when necessary. The existence conditions at the ends of these lines then determine the BPS

spectrum in the different chambers.

In the second work “Generating functions for $\mathcal{N} = 2$ BPS structures”, presented in chapters 10 and 11 of this thesis, we generalise the results of Cheng and Verlinde [52, 53] to construct an $\mathcal{N} = 2$ analog counting function. When the central charges are included in the argument of this function, this then reproduces the BPS spectra in all regions of the moduli space for the 4d $\mathcal{N} = 2$ QFT examples, including Argyres-Douglas theories with A_1, A_2 root systems, and BPS structures with the affine root system \hat{A}_1 . This includes both Seiberg-Witten theory and the D6-D2-D0 brane system on the resolved conifold described by Jafferis-Moore [37] and further studied by [59, 63, 20, 61]. This counting function, as in the $\mathcal{N} = 4$ examples, is the Weyl denominator or character of a Verma module with the highest weight counting the BPS states. This highest weight jumps when a BPS wall, in the form of a Weyl chamber boundary, is crossed. The construction of the generating function should be generalisable to ADE type Argyres-Douglas theories.

Outline of thesis

- The introductory chapter 2 introduces the concept of a BPS bound [64, 65] and the history of the development of BPS states in super Yang-Mills (SYM) theory and string theory. Seiberg-Witten theory [1] and Argyres-Douglas theories [5] are introduced. The interpretation of the BPS states as D-branes [66], wrapped on cycles in the target space of the string theory, is introduced on both the type IIA and type IIB side.
- Chapter 3 describes the relations between BPS state counts using indices and geometric invariants [19] of the underlying target spaces including Donaldson-Thomas [22, 23] invariants and their refinement [34, 67] for hyper and vector multiplets. This is then used to explain the Konsevich-Soibelman [30] wall crossing formulae with the key examples of wall crossing including the primitive case and that for Seiberg-Witten theory.
- Chapter 4 reviews the background and development of the theory of quivers in the context of counting BPS states [68, 69, 70, 4, 71]. The theory of quiver representations and mutations are discussed and it is shown how the spectrum of BPS states is determined in the different regions of the moduli space. Interpreting the mutations as Weyl reflections is of particular importance as these are later used in section 11 to change the basis of positive roots in the generating function that is constructed. The root systems of the quivers can be derived from BPS algebras [43, 44].
- Chapter 5 describes the formulae for the change of the BPS indices across a wall known as the wall crossing formulae [36]. The primitive and semiprimitive examples are reviewed. The concept of framed BPS state [17] is introduced, but following the supergravity description [18]. Here, the walls for framed BPS states are known as BPS walls and can be related to Weyl chambers of the associated root system describing the states. In 5.4 the D6-D2-D0 system developed by Jafferis Moore [37] is reviewed and written in terms of the roots of the affine Lie algebra \hat{A}_1 .
- Chapter 6 describes the Exact WKB method applied to the cubic curve.
- Chapters 7 and 8 include my contributions to the preprint “Special geometry, quasi-modularity and attractor flow for BPS structures” [62]. We use solutions to the Picard-Fuchs equations and the monodromies to determine the central charges for the BPS

states in Argyres-Douglas A_1, A_2 and Seiberg-Witten theory. We plot the gradient flow lines and use existence conditions to reproduce the spectra in the different chambers.

- In chapter 9 the BPS configurations and wall crossing phenomena in $\mathcal{N} = 4$ black holes are introduced in sections 9.1 and 9.2. In section 9.3 the derivation of the generating function of dyonic black holes by Dijkgraaf, Verlinde, Verlinde [40] is reviewed and described as a partition function of dyons. The wall crossing for the decomposition of dyons is discussed in section 9.5 via the contour prescription.
- Chapters 10 and 11 describe a research project “Generating functions for $\mathcal{N} = 2$ BPS structures”. In chapter 10 we extract generating functions for subalgebras from the $\mathcal{N} = 4$ dyon counting formula and continue to apply the prescription for wall crossing described by Cheng and Verlinde [52, 53] for the full generating function in terms of a change in a highest weight of the Verma module. In chapter 11 we use this to construct analog generating functions for $\mathcal{N} = 2$ theories using their root systems. Specifically, the D6-D2-D0 wall crossing 11.3 and Seiberg-Witten theory 11.4 for \hat{A}_1 . We also look at the Argyres-Douglas A_2 theory 11.5.
- Chapter 12 discusses the relation between the generating functions constructed and topological string partition functions for uncoupled BPS structures, for example, on the resolved conifold [61] and the A_1 model. In this case, the Borel transform of the free energy generates the wall crossing.

Publications

The work in this thesis resulted in the following manuscripts:

- M. Alim, F. Beck, A. Biggs, D. Bryan, *Special geometry, quasi-modularity and attractor flow for BPS structures*, arXiv:2308.16854 [hep-th], 2023;
- M. Alim, D. Bryan, *Generating functions for $\mathcal{N} = 2$ BPS structures*, to appear.

2 | BPS states and Argyres-Douglas theories

A class of theories, defined on special loci in the moduli space of particular 4d $\mathcal{N} = 2$ QFTs, and associated to a Lie algebra, are known as ADE type Argyres-Douglas [5, 6, 7, 8, 9] theories. In these models, the wall crossing phenomena for the BPS states are particularly well understood, making them an ideal testing case for more general ideas about BPS structures and wall crossing. There are several ways to construct Argyres-Douglas and related gauge theory models from higher dimensional theories. One can use the constructions to obtain information about these full theories simply by studying the Argyres-Douglas model. Examples of this include a 10 dimensional type II string theory construction of ADE type gauge theories [72, 73, 74, 75, 68, 76, 77], and Argyres-Douglas theories [8, 9], that has developed since these models were originally derived. String theory constructions such as these contain Dp -branes as submanifolds embedded within the target space, which describe open strings with both Dirichlet and von Neumann boundary conditions [78], and give rise to $p + 1$ dimensional worldvolume theories. Type IIA and type IIB string theories contain branes with even and odd p respectively. They carry electric and magnetic Ramond-Ramond (RR) charges and can be taken to represent the charged BPS states.

One can use the BPS spectrum, the set of existing states, to study the wall crossing. This means that some BPS states are only stable in certain regions in the moduli space. The boundary separating these regions is known as the *wall of marginal stability*. This condition for stable BPS states is also known as Π -stability [70]¹. These BPS states then decay into constituents when this wall is crossed. However, within these regions the number of BPS states remain constant under variation of the moduli and can thus be considered a topological quantity. In this thesis 2 types of supersymmetric BPS multiplets are described. These include the hypermultiplet which describes scalars and fermionic matter, and the vector multiplet which includes a vector boson.

¹This is a generalisation of the μ -stability condition of vector bundles first described mathematically in [79].

2.1 Introduction to 4d $\mathcal{N} = 2$ QFTs

There exist classes of Yang-Mills theories that contain such BPS multiplets and have also led to significant physical contributions, for example, they have been used extensively for building unification models. Yang-Mills (YM) theories [80, 81] can be represented by an $SU(N)$ gauge group or other compact, non-abelian Lie group. Importantly, there are also supersymmetric SYM of this form which are interesting due to many exact results being known. For example, 4d $\mathcal{N} = 2$ gauge theories are a particularly interesting case to study because these systems can be solved exactly at low energies. The theories with rank r gauge group G have a holomorphic prepotential $\mathcal{F}(A)$, in r multiplets A^i ,² which are chiral and abelian. Perturbative quantum corrections to this prepotential exist only at one loop order. At low energies an effective action for the quantum theory was put forward in the literature [1, 66, 82, 83, 84] and can be written in $\mathcal{N} = 1$ language as:

$$\mathcal{L} = \frac{1}{4\pi} \text{Im} \left[\int d^4\theta \sum_i \frac{\partial \mathcal{F}(A)}{\partial A^i} \bar{A}^i + \int d^2\theta \left(\frac{1}{2} \sum_{ij} \tau_{ij}(A) W_\alpha^i W^{\alpha j} \right) \right], \quad (2.1.1)$$

W_α represents a vectormultiplet, $\mathcal{K}(A, \bar{A})$ is the Kähler potential on the moduli space, and $\tau_{ij}(A)$ are the complexified effective gauge couplings.

This theory is determined by the prepotential $\mathcal{F}(A)$ such that

$$\mathcal{K}(A, \bar{A}) = \text{Im} \left[\frac{\partial \mathcal{F}(A)}{\partial A^i} \bar{A}^i \right], \quad \tau_{ij}(A) = \frac{\partial^2 \mathcal{F}(A)}{\partial A^i \partial A^j}, \quad A_{iD} = \frac{\partial \mathcal{F}(A)}{\partial A^i}, \quad (2.1.2)$$

where A_{iD} is the dual component under electric-magnetic duality. We have a charge lattice $\Gamma = \Gamma^e \oplus \Gamma^m$ for the $U(1)$ charges, arranged into the vector (q, p) , that is split into the electric and magnetic sublattices. From this one can define a symplectic pairing on the lattice for 2 dyons $\gamma_k \in \Gamma$ ($k = 1, 2$), also known physically as the Dirac pairing

$$\langle \gamma_k, \gamma_l \rangle = \sum_i (p_k)^i (q_l)_i - (p_l)^i (q_k)_i, \quad k, l \in \{1, 2\}. \quad (2.1.3)$$

It is also important to understand that this Lagrangian description only works at low energies [1]. This is because electric and magnetic monopoles under the $U(1)$ lattice charges are mutually non local. This means that their symplectic product from (2.1.3) is non-vanishing. Such a Lagrangian, as given in (2.1.1), can only ever contain local degrees of freedom - no known duality can transform a purely electric lagrangian into one coupled to both electric and magnetic monopoles whilst retaining Lorentz invariance.

²The index i labels generators of the Cartan subalgebra. α are spinor indices which are suppressed on the chiral multiplets.

2.1.1 Moduli space

One can now introduce a set of complex numbers defining a coordinate on the moduli space \mathcal{B} , such that $u = (u_1, \dots, u_r) \in \mathcal{B}$.³ This space parameterises the vacua of the theory, which, in the case of an $\mathcal{N} = 2$ gauge theory, is also known as the Coulomb branch or vectormultiplet moduli space [85]. One can also use these moduli to specify a hyperelliptic curve that realises the theory. In the classical theories [83, 84, 86] one obtains gauge symmetry at the singularities of this curve which act as symmetry enhancement points. This is then broken to $U(1)^r$ at a generic point in the moduli space $u \in \mathcal{B}$. Recalling the charge lattice, one can consider this mathematically as a local system Γ over the base \mathcal{B} containing the lattice fiber $\Gamma_u \simeq \mathbb{Z}^{2r}$. Physically, this can be interpreted as the separate set of electric and dual magnetic charges for each multiplet.

Theories with 1-dimensional moduli spaces

The focus of the research in this thesis is on one-dimensional moduli spaces, parameterised by a single complex variable u , with a single set of electric and magnetic charges (q, p) . The multiplets discussed above (2.1.1-2.1.2) have scalar components given by $a(u)$ and the dual $a_D(u)$. The central charges of the BPS states can now be defined in terms of the electric and magnetic charges as

$$Z_\gamma(u) = qa(u) + pa_D(u). \quad (2.1.4)$$

One remembers that for BPS states the mass equals the modulus of the central charge. The prepotential and central charges of the theory are determined by a Riemann surface, denoted by Σ_u , called the Seiberg-Witten curve and can be considered part of a deformation family. In this way one can define a specific theory from a specially chosen Riemann surface, which can include various deformations of singularities. The electric and magnetic functions $a(u)$ and $a_D(u)$ in (2.1.4) are determined by period integrals on this curve over the cycles γ_1 and $\gamma_2 \in H_1(\Sigma_u, \mathbb{Z})$ such that

$$a(u) = \int_{\gamma_1} \lambda_u, \quad a_D(u) = \int_{\gamma_2} \lambda_u, \quad \Pi = \begin{pmatrix} a_D \\ a \end{pmatrix} \in \Gamma^\vee \otimes_{\mathbb{Z}} \mathbb{C}, \quad (2.1.5)$$

where Π is the period vector and λ_u is a meromorphic differential on the surface chosen for the particular theory one is considering.⁴

³In general this can also be written as a polynomial in terms of the scalar fields in the multiplet ϕ as $u_k = \text{Tr}[\phi^k]$.

⁴See sec. 7.2.2 for the specific curves studied in this thesis.

Monodromies

The functions $a(u)$ and $a_D(u)$ in (2.1.5) are in general multivalued such that if one takes a path in the moduli space around a singular point s , each function can now be written as a linear combination of the electric and magnetic functions before the path was taken. This can be seen by crossing branch cuts in the moduli space. This is called monodromy and there is a monodromy matrix M_s associated to each singular point. The matrix acts on Π^t . In a non-local theory, the monodromies do not commute. One can take loops around multiple singular points to derive relations between the monodromies, such that if one knows the monodromies around a particular set of singular points one can compute those for the remaining points. This is used extensively in the research on attractor flow presented in chapters 7 and 8. One can now look at specific examples of theories.

2.1.2 Argyres-Douglas theories and their string theory construction

In general an Argyres-Douglas theory [5, 6] is a supersymmetric QFT that arises from the deformation of ADE type singularities on the curve. Argyres-Douglas points exist in the moduli space at the points where the curves have cusps. An ADE type singularity can be defined as an orbifold fixed point which is locally written as \mathbb{C}^2/Γ . Here $\Gamma \hookrightarrow SU(2)$ is a finite subgroup with an ADE classification. These quotient spaces are isomorphic to curves with cuspidal singularities at the origin. For example, one can look at a general A_{n-1} theory as shown by [86] and further reviewed in [66, 71]. For these models the most general type of deformation can be written in terms of the hyperelliptic curves

$$\Sigma_u : \quad y^2 - x^n + \sum_{0 \leq k < n} u_k x^k = 0 \quad \longrightarrow \quad y^2 - W_{A_{n-1}}(x, u_1, \dots, u_{n-1}) = 0, \quad (2.1.6)$$

where $y^2 - x^n = 0$ was the original A_{n-1} singular curve now embedded in (2.1.6).⁵

These singularities can also be resolved as ALE spaces, which provides a good way of visualising them. This stands for ‘‘Asymptotically Locally Euclidean’’ [87] space and is a hyperkähler manifold. In this space the singularities are resolved as a set of Riemann spheres touching in the form of a Dynkin diagram (see Fig. 2.1). Essentially, one now has spheres in place of the initial singular points.

This can be done by including extra quadratic variables to the polynomial in the curve

⁵For full $SU(n)$ SYM deformed by a dynamic scale Λ one must square the polynomial $W_{A_{n-1}}(x, u_1, \dots, u_k)$ in (2.1.6) and obtains genus $g = n - 1$ hyperelliptic curves from the deformation of the singularity [66, 71, 84, 86].

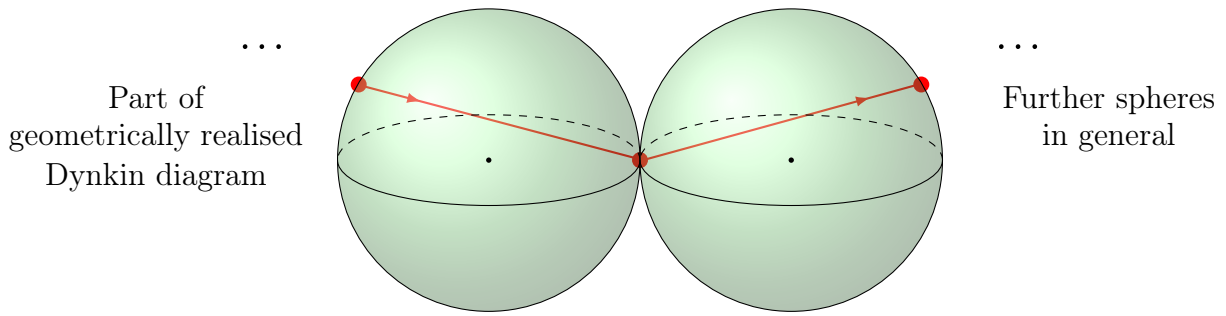


Figure 2.1: Showing part of a general resolution of an ADE singularity with touching spheres. The Dynkin diagrams can be drawn by connecting the red dots.

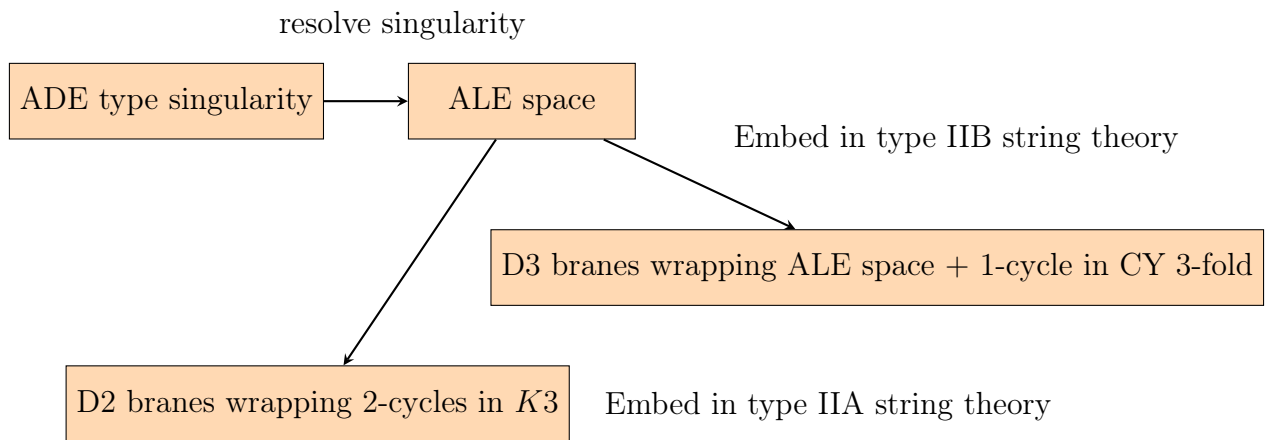


Figure 2.2: Embedding ADE type singularities in string theory.

containing the singular points e.g. $W_{A_{n-1}}(x_1, u_1, \dots, u_k)$ such that this is replaced with

$$W_{A_{n-1}}(x_1, u_1, \dots, u_k) + x_2^2 + x_3^2. \quad (2.1.7)$$

String theory construction

This form of resolution of the singularities has been very useful for further embedding these spaces in higher dimensional theories, for example, by using ALE fibrations (see Fig. 2.2). For example, type IIA strings have been studied on a $K3$ manifold in the literature [68, 72, 73, 74, 75], and reviewed in [66], where one considers BPS states as D2-branes wrapping 2 cycles around the spheres. On the type IIB side the BPS states are represented by D3 branes wrapping 3-cycles in CY 3-folds [76, 77, 9] given by the deformation families X_u . For these 3-folds one can now define:

$$\text{the central charge and mass} \quad Z_\gamma(u) = \int_{X_u} \gamma \wedge \Omega_u \equiv \int_\gamma \Omega_u, \quad M_\gamma(u) = \int_\gamma |\Omega_u|, \quad (2.1.8)$$

$$\text{the BPS bound} \quad \int_{\gamma} |\Omega_u| \geq \left| \int_{\gamma} \Omega_u \right|, \quad \gamma \in H^3(X_u, \mathbb{Z}), \quad u \in \mathcal{B}, \quad (2.1.9)$$

where Ω_u is a holomorphic (3,0)-form on the CY 3-fold. The meromorphic 1-forms λ_u in (2.1.5), which are used to compute the period integrals over 1-cycles in the Riemann surface realising the theory, are now reductions of this holomorphic (3,0)-form. This will be further used in chapter 7 of this thesis to evaluate the attractor flow of the central charges.

Wall crossing

The BPS spectra and their wall crossing phenomena are particularly well understood in the case of ADE type Argyres-Douglas theories because the charges of the BPS states are represented by the roots of the semi-simple ADE Lie algebra. In these cases, there are composite roots representing BPS states that combine the charges of the basis states. The walls of marginal stability MS are now loci in this space of deformations of the singularity where the composite roots split up. For 2 charges γ_1, γ_2 to combine, this condition is given by the alignment of the central charges $Z_{\gamma_1}(u), Z_{\gamma_2}(u)$:

$$MS_{\gamma_1, \gamma_2} := \left\{ u \in \mathcal{B} \mid Z_{\gamma_1}(u)/Z_{\gamma_2}(u) \in \mathbb{R} \right\}. \quad (2.1.10)$$

Therefore, these examples become particularly good for testing general ideas about wall crossing phenomena.

2.1.3 Seiberg-Witten theory

In [1] a 4d SYM theory was constructed by Seiberg and Witten with $SU(2)$ gauge symmetry. One can treat this theory according to the previous section 2.1.1 with complex 1 dimensional moduli space. The full quantum theory, however, has particularly interesting behavior of its BPS spectrum. When one writes down the electric and magnetic functions $a(u)$ and $a_D(u)$ one finds these have a monodromy group given by $\Gamma(2)$, a congruence subgroup of $SL(2, \mathbb{Z})$. This allows the moduli space to be parameterised by the quotient of the upper-half plane by this group: $\mathbb{H}^+/\Gamma(2)$.

In the weak coupling region these monodromies can be used to generate an infinite spectrum of BPS states described by the root system of the affine Lie algebra \hat{A}_1 . This includes infinitely many dyons, a monopole, and a W-boson. On the other hand, in the strong coupling region only 2 basis states of this root system exist due to the wall of marginal stability separating the regions. Here only one monopole and one dyon are left over.

3 | BPS structures and invariants

The BPS states in the theories discussed in the previous section 2.1 can in many cases be counted in the different regions (or chambers) in the moduli space. This count of BPS states can be used to derive geometric invariants such as Donaldson-Thomas (DT) [22, 23] and Gopakumar-Vafa (GV) invariants [25, 24]. Physically, the DT invariants enumerate BPS particles with spin in 4d $\mathcal{N} = 2$ QFTs, the latter GV invariants can be found from the genus expansion of the topological string free energy. If one lifts to M-theory in 11 dimensions the GV invariants count electrically charged M2 branes. The research in this thesis develops a new formulation for counting the BPS states in $\mathcal{N} = 2$ QFTs and the string models they are embedded in. However, to do this one must first reproduce the correct count and spectrum of the BPS states in the different chambers and the associated geometric invariants, that have been previously derived, using various formulations in the literature. These include the quantum dilogarithm identities of [30], quiver descriptions [68, 69, 4, 88] and wall crossing formulae [35, 36]. The various descriptions are reviewed in the following chapters 3, 4 and 5. In this chapter 3 the definitions of BPS invariants and their wall crossing are reviewed through quantum dilogarithm identities, which are simple formulae that encapsulate the wall crossing phenomena.

3.1 BPS structures and Donaldson-Thomas invariants

For theories with a string theory construction, BPS states can be counted by associating various invariants to a target space X , which can be taken as the internal CY 3-fold. These include BPS and Donaldson-Thomas invariants [19]. This formulation has been taken from these physical theories and defined mathematically as a BPS structure by [21]¹. In general, one can define a BPS structure as (Γ, Z, Ω) , where Γ is the charge lattice, the central charge $Z : \Gamma \rightarrow \mathbb{C}$ is defined as a homomorphism from the lattice to the complex numbers, and $\Omega(\gamma) \in \mathbb{Q}$ is the BPS invariant associated to the electric and magnetic charge $\gamma \in \Gamma$. This can be determined by taking a trace on the Hilbert space of BPS states. The BPS invariant is the same when one takes the opposite charge $\Omega(\gamma) = \Omega(-\gamma)$. Donaldson-Thomas invariants were first described by [22, 23] in the mathematics literature but it was found by Joyce and

¹This was based on the previous works [89, 90] and the stability structures of graded Lie algebras arising from the charges in [30].

Song [19] that they can be nicely mapped to the BPS invariants [19, 20, 21]

$$\text{DT}(\gamma) = \sum_{\gamma=m\alpha} \frac{1}{m^2} \Omega(\alpha) \in \mathbb{Q}, \quad (3.1.1)$$

where one has $m \in \mathbb{Z}$, so that when one takes $\gamma \in \Gamma$ to be a point in the charge lattice one still has a charge in the lattice after dividing by m . Donaldson-Thomas invariants were originally understood mathematically as a count of (semi-)stable² sheaves on X in particular rational combinations of cohomology classes defined by the Chern character of the sheaves. One can invert the above expression (3.1.1) to write the BPS invariants in terms of the Donaldson-Thomas invariants [21], where the function $\mu(m)$ is the Mobius function

$$\Omega(\gamma) = \sum_{\gamma=m\alpha} \frac{\mu(m)}{m^2} \text{DT}(\alpha) \in \mathbb{Q}. \quad (3.1.2)$$

3.1.1 Refinement of BPS indices

The BPS invariants $\Omega(\gamma)$ can also be refined. This means that each invariant can be split into parts, each part giving further information about the BPS configuration. To see this one must look at the BPS invariant as a trace over the BPS Hilbert space \mathcal{H}_{BPS} . However, one must first carry out a decomposition of the full BPS Hilbert space \mathcal{H}_{BPS} into that of individual charges [34]. The Hilbert space now becomes $\mathcal{H}_{BPS} = \oplus_{\gamma \in \Gamma} H_{BPS}(\gamma)$ [33]. In $\mathcal{N} = 2$ supersymmetric QFTs (including gauge and effective supergravity theories) constructed on a CY target space, BPS states in the additional 3+1 dimensions are defined by both the 3-component of the angular momentum in space $2J_3 \in \mathbb{Z}$ [36, 33, 34] and the charge $\gamma \in \Gamma$ in the lattice. Hence, a BPS invariant described above for a state with a single set of electric and magnetic charges $\gamma = (q, p)$, as described in section 2.1.1, can be refined by decomposing it into invariants describing the possible spin components.

Trace on Hilbert space

All BPS configurations in $\mathcal{N} = 2$ theories are supersymmetric multiplets, consisting of a set of constituent states with a particular spin; the smallest possible example of such a configuration is a hypermultiplet. The states in this hypermultiplet can be looked at as particles in the 4d Minkowski spacetime which have spin around their center of mass within the \mathbb{R}^3 space. These spin degrees of freedom of the hypermultiplet are present in all possible longer multiplets, therefore, to give a simple form for the refined index, they can be factored

²The stability condition used here is called Gieseker Stability and for algebraic curves is equivalent to the previously mentioned stability condition on vector bundles.

out of the BPS Hilbert space [36, 34, 67, 33]. The Hilbert space looks like

$$\mathcal{H}_{BPS} = \left(\left[\frac{1}{2}\right] + 2[0]\right) \otimes \mathcal{H}'_{BPS}, \quad (3.1.3)$$

after the factorisation. Here the Hilbert space, denoted by \mathcal{H}'_{BPS} in (3.1.3), is defined as the “reduced Hilbert space”, and is the space from which one can use the second helicity supertrace [91] to extract the refined BPS invariants. The refined BPS index [33] can now be computed in the form

$$\Omega^{ref}(\gamma, u, y) = \text{Tr}_{\mathcal{H}'_{BPS}(\gamma, u)}(-y)^{2J'_3} = \sum_{p \in \mathbb{Z}} \Omega_p^{ref}(\gamma, u, y)(-y)^p. \quad (3.1.4)$$

Here Ω_p^{ref} are refined BPS indices, meaning that they include the counts of the spin using the variable y (which can in string theory on a compact CY 3-fold be interpreted as a spacetime graviphoton background [34]). In this case, using the index formula (3.1.4) above, Ω_p^{ref} takes into account the spin degeneracy and can be read off from the y expansion of $\Omega^{ref}(\gamma, u, y)$. Here u is again the point in the moduli space, on which the chambers and any possible walls of marginal stability can exist.

Examples of refined indices

In the case of a hypermultiplet we have

$$\Omega_0^{ref} = 1, \quad \Omega_{p \neq 0}^{ref} = 0, \quad (3.1.5)$$

and for a vector multiplet

$$\Omega_{-1}^{ref} = 1, \quad \Omega_1^{ref} = 1. \quad (3.1.6)$$

This can alternatively be written as $\Omega^{ref}(\gamma, u, y) = -y - y^{-1}$ [33]. The BPS invariants can be recovered from the refined BPS invariants in the semi-classical limit. This can be taken as $y \rightarrow 1$. In this case, we reproduce the BPS invariants for hypermultiplets and vector multiplets, with charges γ_h and γ_v , respectively:

$$\Omega(\gamma_h, u) = 1, \quad \Omega(\gamma_v, u) = -2. \quad (3.1.7)$$

These are the well-known (un-refined) BPS invariants that appear in the BPS structures associated to the 4d $\mathcal{N} = 2$ QFTs discussed in section 2.1.2 including Argyres-Douglas and Seiberg-Witten theories. For example, the BPS configurations of Argyres-Douglas theories of ADE type consist of BPS hypermultiplets, whereas Seiberg-Witten $SU(2)$ theory contains an additional vector multiplet boson. These BPS invariants can also be derived from a suitable generating function in the cases for which this is known. For example, in the case of the BPS structure of the resolved conifold, it has been shown by [19] that these BPS invariants

can be derived from a generating function [59, 92] for non-commutative Donaldson-Thomas invariants (NCDT). This is elaborated on in sections 4.3.4 and 5.4.

Relation to Gopakumar-Vafa invariants

There is a way to derive BPS invariants from a topological string free energy. This is done by splitting it into contributions from constant and non-constant pseudoholomorphic maps into the target space, the non-constant maps representing extended objects in the CY 3-fold X . Physically, these are M2 branes (or D2-D0 boundstates in type IIA string theory) wrapped on genus g curves within this space [24, 25]. This part of the free energy can be expanded as

$$F(\lambda, t) = \sum_{\beta, g \geq 0, k > 0} \text{GV}(g, \beta) \frac{1}{k} \left(2 \sin \left(\frac{k\lambda}{2} \right) \right)^{2g-2} e^{kt_\beta}, \quad (3.1.8)$$

where λ is the topological string coupling, $\beta \in H_2(X, \mathbb{Z})$, and t_β is the associated Kähler parameter. $\text{GV}(g, \beta)$ are the Gopakumar-Vafa invariants, where those of genus-0 have been found to correspond to the BPS invariants of the form $\Omega(\pm\beta, n) = \text{GV}(0, \beta)$, $n \in \mathbb{Z}$, in some examples, such as the resolved conifold, and have been conjectured [26, 27, 19] to correspond to such BPS invariants for general CY 3-folds.

3.1.2 BPS invariants and wall crossing from quantum dilogarithms

It is also interesting to look at wall crossing in terms of the BPS invariants. For BPS states that are only stable in certain regions of the moduli space we expect the BPS invariants to vanish when the state decays into its constituents. In this case, it is useful to have a simple equation which describes the decay process of a BPS state across a wall of marginal stability in terms of its charges, and also encodes the BPS invariants of the states involved. Fortunately, such a formula has been introduced by Konsevich and Soibelman [30] in terms of products of special functions called quantum dilogarithms. Here the product on one side of the wall of marginal stability should match that on the other with the exponents corresponding to BPS invariants. The wall crossing is also described by [30] in terms of “motivic” DT invariants, which were later shown by Dimofte, Gukov and Soibelman [34, 33] to correspond to the refined DT invariants discussed here in the previous section 3.1.1. These wall crossing formulae can be arranged to show a wall crossing relation in the Argyres-Douglas A_2 [5] and Seiberg-Witten [1] theory. The quantum dilogarithm function [33, 93, 94] can be defined as:

$$E(x) = \sum_{n=0}^{\infty} \frac{(-qx)^n}{(1-q)\dots(1-q)^n} = \prod_{i=0}^{\infty} (1 + q^{i+\frac{1}{2}}x)^{-1}, \quad (3.1.9)$$

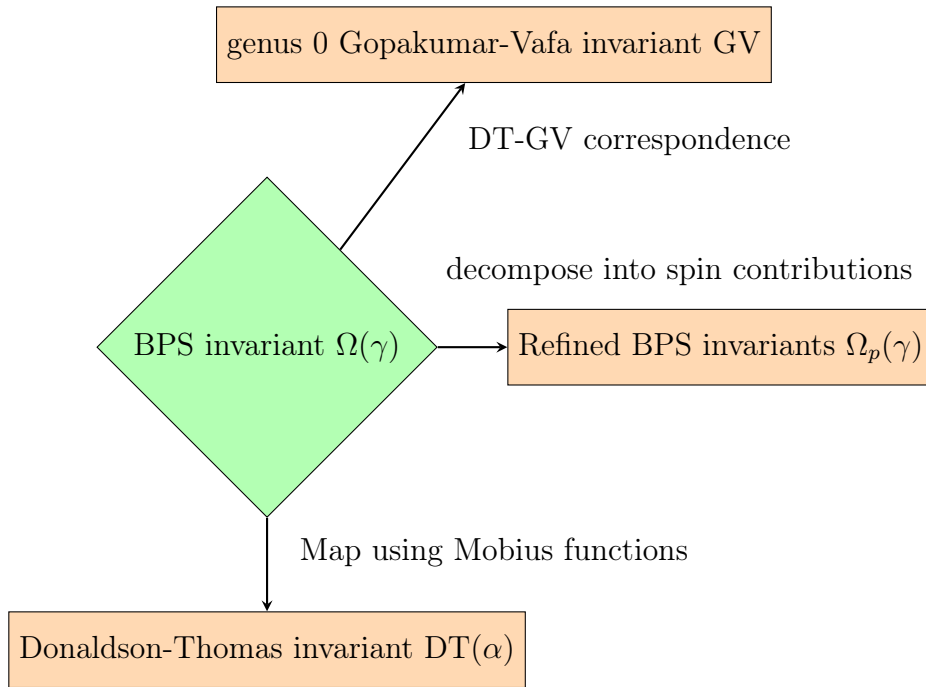


Figure 3.1: Diagram showing all the geometric invariants that arise from the BPS state count.

where x is a quantum operator such that for any two x_1, x_2 the relation $x_1 x_2 = q x_2 x_1$ is satisfied, and x_{12} is defined by $x_{12} = q^{-\frac{1}{2}} x_1 x_2 = q^{\frac{1}{2}} x_2 x_1$. The parameter $q^{\frac{1}{2}} = -e^{\hbar}$ describes the quantum deformation.

To write down a wall crossing formula one must first think about what must be substituted into the quantum dilogarithm (3.1.9). For this we must use the quantum operators described above to construct a general charge lattice Γ spanned by γ_1, γ_2 . For this one can define a quantum torus algebra. This is constructed by quantising the complex torus $\mathbf{T} = \Gamma^\vee \otimes \mathbb{C}^*$. In this case, one obtains the generators of the algebra $\hat{e}_{\gamma_1}, \hat{e}_{\gamma_2}$ (and $\hat{e}_0 = 1$) with $\gamma_1, \gamma_2 \in \Gamma$. This algebra is associative but non-commutative [30, 34]

$$\begin{aligned} \hat{e}_{\gamma_1 + \gamma_2} &= q^{\frac{1}{2}\langle \gamma_1, \gamma_2 \rangle} \hat{e}_{\gamma_1} \hat{e}_{\gamma_2}, \\ [\hat{e}_{\gamma_1}, \hat{e}_{\gamma_2}] &= (q^{\frac{1}{2}\langle \gamma_1, \gamma_2 \rangle} - q^{-\frac{1}{2}\langle \gamma_1, \gamma_2 \rangle}) \hat{e}_{\gamma_1 + \gamma_2}. \end{aligned} \quad (3.1.10)$$

Now this can be substituted into the quantum dilogarithm from [30, 33] using functions of the form

$$A_\gamma^{mot} := U_\gamma = \prod_{p \in \mathbb{Z}} E((-q^{\frac{1}{2}})^p \hat{e}_\gamma)^{(-1)^p \Omega_p^{ref}}, \quad (3.1.11)$$

where Ω_p^{ref} are refined BPS indices from section 3.1.1. A_γ^{mot} can be understood as elements of the quantum motivic torus. Now these are the functions that obey the wall crossing

formula - the product over the charges on one side of the wall should match that on the other. This is clear in the following 2 examples 3.1.2 and 3.1.2 below. For a 2 dimensional electric and magnetic charge lattice, the generators of the form \hat{e}_γ can be written in terms of the quantum operators x_1 and x_2 .³

Seiberg-Witten theory

Now we look back to the theories from sections 2.1.2-2.1.3 and compare the BPS invariants for the states in these theories to the exponents of the quantum dilogarithms in the wall crossing formula. It should be possible, using the operators in (3.1.11), to arrange the quantum dilogarithms into a product relation so that the exponents of the quantum dilogarithms on the left-hand side of the equation represent the BPS invariants on one side of the wall of marginal stability and those on the right-hand side represent those on the other. One can start by looking at the case for Seiberg-Witten SU(2) theory. For this example [33], we can write the functions U_γ , for $\gamma = n\gamma_1 + m\gamma_2$, as:

$$U_{n,m} = E(q^{-\frac{nm}{2}} x_1^n x_2^m) = \prod_{i=0}^{\infty} (1 + q^{i+\frac{1}{2}-\frac{nm}{2}} x_1^n x_2^m)^{-1}, \quad (3.1.12)$$

$$U_{2,0} = E(-q^{\frac{1}{2}} x_1^2)^{-1} E(-q^{-\frac{1}{2}} x_1^2)^{-1} = \prod_{i=0}^{\infty} (1 - q^{i+1} x_1^2)^{-1} \prod_{i=0}^{\infty} (1 - q^i x_1^2)^{-1}. \quad (3.1.13)$$

The first expression in (3.1.12), involving $U_{n,m}$, is a general expression for any BPS hypermultiplet, and can be taken to be the dyons found in Seiberg-Witten theory such that $(n, m) = (2k, 1), (2k - 2, -1)$, $k \in \mathbb{Z}$. The second expression for $U_{2,0}$ can be interpreted as the vector boson in Seiberg-Witten theory.

The next step is to look at the wall crossing encoded as a product relation. The functions $U_{n,m}$ can be written in a way that represents this wall crossing and might also be formulated as a generating function. This takes the form

$$U_{2,-1} U_{0,1} = U_{0,1} U_{2,1}, U_{4,1} \dots U_{2,0} \dots U_{6,-1} U_{4,-1} U_{2,-1}, \quad (3.1.14)$$

where one can clearly see the wall crossing in Seiberg-Witten theory, with the spectra on both sides of the wall in equation (3.1.14) being represented by the product of operators. On the left hand side of (3.1.14) we see the charges of a hypermultiplet monopole and dyon $(0, 1), (2, -1)$ represented because these are the only BPS states existing on this side of the wall, whereas on the other side we have the full infinite spectrum including the vector multiplet boson $(2, 0)$ in addition to the infinite spectrum of dyons with charges $(2k, 1), (2k + 2, -1)$, $k \in \mathbb{Z}$.

³It is also important to note that for a general generator in the lattice we have $\hat{e}_{n\gamma_1+m\gamma_2} = q^{-\frac{nm}{2}} \hat{e}_{\gamma_1}^n \hat{e}_{\gamma_2}^m$.

Argyres-Douglas A_2 theory

Such a relation also exists for the Argyres-Douglas A_2 theory. This can also be used as another opportunity to show a relation between the quantum dilogarithm operators and a Konsevich-Soibelman wall crossing formula [30]. In this case, the relation corresponds to the pentagon identity, first described in [93], which can be written as

$$\begin{aligned} E(x_1)E(x_2) &= E(x_2)E(x_{12})E(x_1), \\ U_{1,0}U_{0,1} &= U_{0,1}U_{1,1}U_{1,0}, \end{aligned} \tag{3.1.15}$$

where this is also the formula for primitive wall crossing. Equation (3.1.15) above then represents the most basic wall crossing process whereby a hypermultiplet dyon of charge $(1, 1)$ decays into an electric and magnetic monopole of charges $(1, 0)$ and $(0, 1)$ respectively. Hence, one can see the left-hand side the product representing the 2 basis particles whereas the right-hand side is a triple product representing 2 basis states and the composite.

4 | BPS quivers in $\mathcal{N} = 2$ QFTs

There is a class of supersymmetric QFTs with a BPS spectrum that can be described by a diagram called a quiver. This consists of a set of nodes connected by arrows. Quiver descriptions arose in the context of string theory to study D-brane systems that were used to geometrically engineer specific supersymmetric QFTs as worldvolume theories [68, 95, 96]. The spaces that were initially used for the construction of the quiver include the ALE spaces, which, as one can remember from section 2.1.2, are resolutions of ADE type orbifold singularities (remember Fig. 2.1) of the form \mathbb{C}^2/Γ , that are non-compact and hyperkähler. Γ being the finite subgroup of $SU(2)$. Quiver descriptions were subsequently found in the literature for the BPS states in ALE fibrations. Examples include the non-compact Calabi-Yau given by $\mathcal{O}_{\mathbb{P}^2}(-3)$ in [69] and type IIA string theory models close to the orbifold points of $\mathbb{C}^2/\mathbb{Z}_N$ [88]. In these cases, quiver representations can describe particular BPS states.

Because of these results, many supersymmetric QFTs that are embedded in these string theory constructions have subsequently been found to have a quiver description for their BPS states. This includes the Argyres-Douglas theories with ADE type root systems. It also applies to gauge theories containing massive hypermultiplet states [97] and other families of theories¹. There are methods that can be used to study wall crossing using a quiver i.e. to generate the spectrum of existing BPS states in different chambers in the moduli space. For example, such methods include using quiver mutations as well as the representation theory of quivers. These were reviewed in [71] and further worked on in [4, 99]. This is covered here in sections 4.2 and 4.2.5 respectively.

4.1 Construction of quivers

When one looks at 4d $\mathcal{N} = 2$ theories such as those in section 2.1 a quiver description can be constructed by considering the coulomb branch moduli $u \in \mathcal{B}$ again, which parameterize the masses and coupling constants. One remembers that in general, for a particular value of u , the gauge group splits into $U(1)^r$, $r = \text{rk}(G)$ and one has the BPS lattice Γ describing the electric and magnetic charges. (In general the lattice can also contain flavor charges with symmetry of rank f . The total rank of the lattice then becomes $2r + f$). The central charge

¹For example, those that can be constructed by wrapping M5 branes on Riemann surfaces with punctures [98].

in this context is defined as a homomorphism from the lattice into the complex numbers $Z(u) : \Gamma \rightarrow \mathbb{C}$.

To build a quiver Q for a particular theory, one must first take into account that the theory contains both particles and antiparticles. If one defines the spectrum of particles to have central charges in a chosen half plane \mathbb{H}^+ then the antiparticles have their central charges in \mathbb{H}^- (see Fig. 4.1 for an example). The theories we are looking at have CPT invariance which means that every particle has a corresponding antiparticle with opposite charge. To draw the quiver [4] one must first identify a basis of BPS hypermultiplet states that have central charges in a chosen half-plane. This is the minimum number of linearly independent states $(2r + f)$ from which one can generate the BPS spectrum. If one labels the basis γ_i then all charges in the lattice can be written in the form:

$$\gamma = \sum_{i=1}^{2r+f} n_i \gamma_i, \quad n_i \in \mathbb{N}^+. \quad (4.1.1)$$

Now a quiver Q can be drawn using the following rules:

- (i) For every basis state γ_i one must include a node.
- (ii) Take the inner product of the basis states [96, 3, 4, 71] $\langle \gamma_i, \gamma_j \rangle$ for all distinct γ_i, γ_j . This should correspond to the number of lines between the nodes labelled by γ_i and γ_j in the direction $j \rightarrow i$. These lines should only be drawn if $\langle \gamma_i, \gamma_j \rangle > 0$.

One can use the quiver to describe general composite BPS states of the form: $\gamma = \sum_i n_i \gamma_i$. For this one labels the nodes with i and arrows with b . For this description there is a gauge group $U(n_i)$ at the node i and a bifundamental matter field A_{ij} for every arrow between i and j . Hence, we now have a full gauge group from the product and matter fields of the form [4, 100]:

$$\text{Gauge group : } \prod_{\text{nodes } i} U(n_i), \quad \text{Matter fields : } \bigoplus_{\text{arrows } b} A_{ij}^b. \quad (4.1.2)$$

4.1.1 Construction of quiver moduli space

Now that we have defined the gauge group and matter fields one can look for the ground states of the supersymmetric quantum theory by determining whether the associated quiver moduli space exists. To do this for such a quiver construction one must now switch to the Higgs branch, which is the moduli space of $\mathcal{N} = 2$ hypermultiplets [85]. To construct a suitable moduli space, one must define, firstly Fayet-Iliopolus (FI) terms denoted by θ_i [70, 4, 100]. These parameters are determined by the central charges of the basis particles as the $U(1)$ charges at the nodes of the quiver couple to them. In the cases that the central

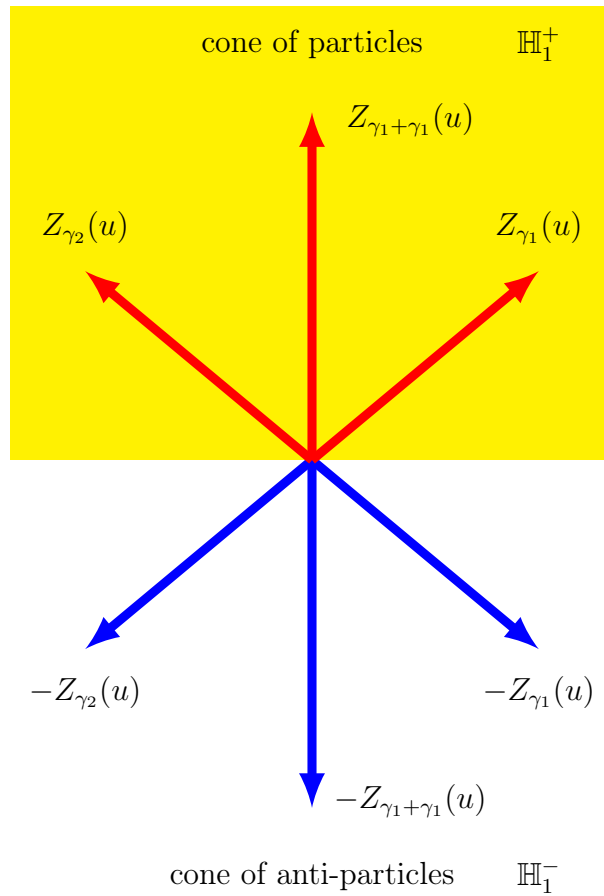


Figure 4.1: Example showing a cone of particles in the upper half-plane.

charges are closely aligned one can approximate the FI terms as

$$\theta_i = |Z_{\gamma_i}(u)|(\arg Z_{\gamma_i}(u) - \arg Z_\gamma(u)). \quad (4.1.3)$$

In the general case, one can write down a D-term equation of motion [4, 88] for every node existing within the quiver

$$\sum_{\text{arrows leaving } i} |A_{ij}^b|^2 - \sum_{\text{arrows entering } i} |A_{ki}^b|^2 = \theta_i. \quad (4.1.4)$$

Finally, in the cases where a quiver contains loops, the theory contains a function known as the superpotential \mathcal{W} . This superpotential is holomorphic and has various properties including gauge invariance. Its inputs are the fields A_{ij}^b . It is not determined by the quiver but has equations of motion [88, 4] that come from the F-term. These are

$$\frac{\partial \mathcal{W}}{\partial A_{ij}^b} = 0. \quad (4.1.5)$$

Form of moduli space

Now, using this information, one can write the moduli space of the BPS states \mathcal{M}_γ on the Higgs branch. If in general we have the gauge groups $U(n_i)$ (from (4.1.2)) for each node, the moduli space one looks for when considering a particular BPS state γ is the solution space of the above equations quotiented by the full gauge group [4]. This then becomes

$$\mathcal{M}_\gamma = \left\{ A_{ij}^b \left| \frac{\partial \mathcal{W}}{\partial A_{ij}^b} = 0, \sum_{\text{arrows leaving } i} |A_{ij}^b|^2 - \sum_{\text{arrows entering } i} |A_{ki}^b|^2 = \theta_i \right. \right\} / \prod_{i=1} U(n_i). \quad (4.1.6)$$

If this moduli space exists for a particular charge so does a corresponding BPS state. If one wants to determine the degeneracy of such states one needs to look at the possible spins. This information can be extracted from the cohomology of \mathcal{M}_γ . The moduli space \mathcal{M}_γ is a Kähler manifold. For Kähler manifolds there exists a special way to decompose the de Rham cohomology into forms constructed as an exterior product - a power of the Kähler form further multiplied by a kernel under the product with another power of this form. This is called the Lefschetz decomposition (see e.g. [101]). There are Lefschetz decompositions of the cohomology of the moduli space \mathcal{M}_γ that can be written as representations of $SU(2)$.

Constructing the BPS multiplets

The irreducible representations then become the BPS multiplets. However, if one is to consider all the spins, one must remember from section 3.1.1 that there is an additional hypermultiplet from the spin in spacetime that one must tensor this $SU(2)$ with ²

$$\text{Spin} = \text{Lefschetz} \otimes \left(\begin{bmatrix} 1 \\ 2 \end{bmatrix} + 2[0] \right). \quad (4.1.7)$$

The factor of $\frac{1}{2}$ being the intrinsic spin of the particle. If one just considers the spin from the perspective of the moduli space, the hypermultiplets have a Lefschetz multiplet with 0 length (in this case the moduli space \mathcal{M}_γ is just a point) whereas vector multiplets have length 2 (for example for $\mathcal{M}_\gamma \equiv \mathbb{P}^1$). In general, one can read off from (4.1.7) above that for a moduli space \mathcal{M}_γ of complex dimension d a BPS multiplet always exists with spin $\frac{d+1}{2}$. The most general equation for the dimension of the moduli space developed in [68, 4, 97] is

$$d = \sum_{A_{ij}^b} (n_i n_j) - \sum_{\text{nodes } i} n_i^2 - (\text{no. F-term constraints}) + 1, \quad (4.1.8)$$

²This has been used both to determine the dimensions of moduli spaces as well as to define refined BPS indices [4, 36, 34, 33, 67].

where the n_i come from the gauge groups at the nodes. This is derived by counting the degrees of freedom of the fields A_{ij}^b and subtracting those for the gauge group and the constraints imposed by the F-term. The extra +1 in (4.1.8) is added at the end to take into account an overall diagonal $U(1)_d \in$ factor because bifundamental fields do not obtain an extra charge if one can rotate all gauge factors simultaneously.

4.2 Quiver descriptions

There is an alternative way of looking at this problem. This works by solving the equations for the F-term constraints (4.1.5) and taking a quotient by the gauge group $\prod_i GL(n_i, \mathbb{C})$, where this is now complexified relative to that shown in (4.1.2). This is also another way of constructing the moduli space \mathcal{M}_γ in (4.1.6), for which one can also define stability conditions. This description of the problem can now be formulated in the language of quiver representations. These have been well understood mathematically [102, 103, 104] in terms of maps between vector spaces. A good overview of the connection between the mathematical and physical interpretation, including writing the maps as morphisms between categories, is given in the book on mirror symmetry [105].

4.2.1 Representations and subrepresentations

Definition 4.2.1. [4, 88, 97] To define a quiver representation R , associated to $\gamma = \sum_i n_i \gamma_i$ one must choose a complex vector space \mathbb{C}^{n_i} at every node of the quiver and also a set of linear maps $A_{ij}^b : \mathbb{C}^{n_i} \rightarrow \mathbb{C}^{n_j}$ defining the arrows between the nodes. Physically, this has been interpreted as the field configuration in a vacuum, where one has constant bi-fundamental fields A_{ij}^b (that still satisfy the F-term constraints). One can use their vacuum expectation values, VEVs, to form the maps between the nodes of the quiver.

Definition 4.2.2. [4, 88, 97] Next one can define a subrepresentation $S \subset R$ by considering a complex vector space contained in the one used to define the quiver representation $\mathbb{C}^{m_i} \subset \mathbb{C}^{n_i}$, and suitable linear maps at every arrow, that map these subspaces at the nodes to each other $a_{ij}^b : \mathbb{C}^{m_i} \rightarrow \mathbb{C}^{m_j}$. This constitutes a subrepresentation if all possible diagrams, of the form shown below, commute:

$$\begin{array}{ccc} \mathbb{C}^{n_i} & \xrightarrow{A_{ij}^b} & \mathbb{C}^{n_j} \\ \uparrow & & \uparrow \\ \mathbb{C}^{m_i} & \xrightarrow{a_{ij}^b} & \mathbb{C}^{m_j} \end{array}$$

For every quiver representation R , one must determine if it is stable with respect to the subrepresentations S and satisfies the conditions given by the D-term equations of motion. This is typically done by considering the central charges.

Stability of representations

One must remember that a quiver representation R , with the complex vector spaces given by \mathbb{C}^{n_j} , represents a charged BPS state of the form $\gamma = \sum_i n_i \gamma_i$ with central charge $Z_\gamma(u) = \sum_i n_i Z_{\gamma_i}(u)$. To construct a quiver description, one must have a cone of these central charges in a chosen half plane. A subrepresentation $S \subset R$ is thus a state, or linear combination of states, that form a constituent of this composite and becomes a decay product at the wall of marginal stability.³ One can denote a representation and subrepresentation R and S with charges γ_R, γ_S and assign the central charges $Z_{\gamma_R}(u), Z_{\gamma_S}(u)$ respectively. It can easily be seen that the nodes have no subrepresentations and hence are always stable. These give a single hypermultiplet.

A general representation R is stable under decay into a subrepresentation when for every S (excluding the trivial cases of 0 and R)

$$\arg(Z_{\gamma_S}(u)) < \arg(Z_{\gamma_R}(u)), \quad (4.2.1)$$

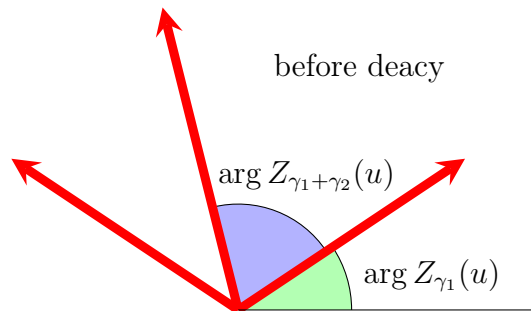


Figure 4.2: Example of representation before decay showing the larger argument.

so that we again have the condition of alignment of the central charges for wall crossing from section 2.1.2. It is interesting to note that close to alignment this condition can be written in terms of the equations of motion (4.1.3) for the D-term [4]. One can now also reformulate the moduli space (4.1.6) as

$$\mathcal{M}_\gamma = \left\{ R = \{A_{ij}^b : \mathbb{C}^{n_i} \rightarrow \mathbb{C}^{n_j}\} \left| \frac{\partial \mathcal{W}}{\partial A_{ij}^b} = 0, R \text{ has } \Pi \text{ stability} \right. \right\} / \prod_{i=1} Gl(n_i, \mathbb{C}). \quad (4.2.2)$$

³The stability under this decay is again called Π stability.

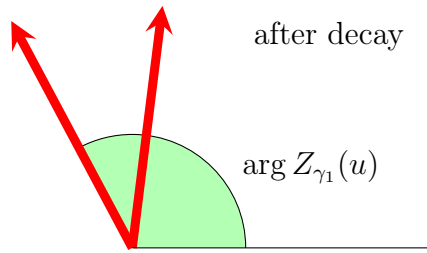


Figure 4.3: Representation after decay with the central ray now absent.

4.2.2 Quiver mutations and dualities

A quiver description requires a cone of central charges in a chosen half plane. Other than the wall of marginal stability, there is another kind of wall in the moduli space where this condition breaks down (these are often referred to as “walls of the second kind” [30, 4]). In this case, one can no longer construct the quiver on the other side of this type of wall. This occurs when at a point in the moduli space the imaginary part of the central charge for a particular BPS state becomes negative

$$\text{Im}(Z_\gamma(u)) > 0 \longrightarrow \text{Im}(Z_\gamma(u)) < 0. \quad (4.2.3)$$

When this occurs, the quiver description breaks down, and one must choose a different quiver with a new basis of charges that have central charges with a positive imaginary part. The transformation that acts between the quivers is known as a quiver mutation. Physically these mutations represent Seiberg dualities [106, 107, 108] which are S-dualities of the low energy theory that can exchange electric and magnetic charges. This is formulated in [109] for the ADE examples.

Change of basis

Alternatively, one can use a different quiver to describe a new basis for the same charges at the same point in the moduli space. In order to construct such a quiver one has to have a cone of particles in the chosen half plane \mathbb{H}^+ , however, one can simply rotate the half plane such that some particles become antiparticles in the new half plane (see Fig. 4.4 for an example). Then one can choose a new basis of charges such that all particles again exist within the new half plane: this change of basis is the quiver mutation.

Transformation of charges

A quiver mutation is possible due to the CPT invariance of the theory such that the particles and antiparticles can be exchanged. For example, take a particle with charge γ_1 where the

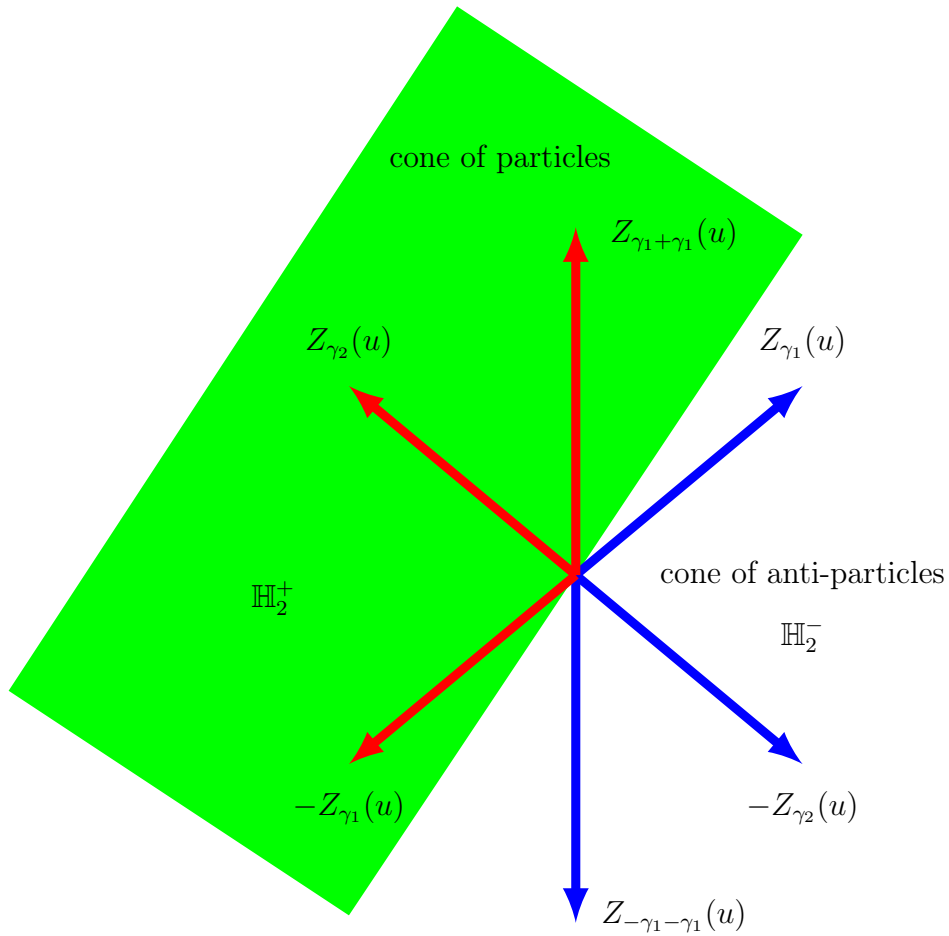


Figure 4.4: A change in the definition of the upper half-plane \mathbb{H}_2^+ also generates a change of basis of particles or quiver mutation.

imaginary part of the central charge changes sign. One now looks for a dual quiver that this quiver can be mapped to: $Q \rightarrow Q'$. In this case, one must use the following basis change so that this charge is mapped to its negative

$$\gamma'_1 = -\gamma_1. \quad (4.2.4)$$

The other BPS states become [4, 71, 109]:

$$\gamma'_i = \begin{cases} \gamma_i + \langle \gamma_i, \gamma_1 \rangle \gamma_1, & \text{for } \langle \gamma_i, \gamma_1 \rangle > 0, \\ \gamma_i, & \text{for } \langle \gamma_i, \gamma_1 \rangle \leq 0. \end{cases} \quad (4.2.5)$$

From this information in (4.2.4) and (4.2.5) a new quiver can be constructed. This new quiver Q' has the same nodes as the original. It has arrows, now encoding fields of the form

A'_{ij} , that take the place of the original arrow.

These rules should be sufficient to mutate the quivers with 2 nodes and no superpotential that are investigated in this thesis. The quiver mutations (4.2.5) can also be described as Weyl reflections when one constructs Weyl chambers from the basis of charges. This will become important later in chapter 11 as when one looks at potential new generating functions such as the Weyl denominator or Weyl character one must be able to distinguish these mutations from an actual change in the number of BPS states.

4.3 Examples

Now one can look to specific simple examples where the quiver representations for the BPS states, mutation sequences for the spectrum, and the possible inclusions of subrepresentations are known. Here we can return to the Argyres-Douglas and Seiberg-Witten theories from sections 2.1.2-2.1.3. The wall crossing for these theories was already shown in terms of quantum dilogarithm identities in section 3.1.2 but this can be further demonstrated here. This can be done by looking at inclusions of quiver subrepresentations into the representations for these models or by using quiver mutations to generate the spectrum on either side of the wall of marginal stability. Here we show the quiver for each example and explain how the spectrum is determined in all chambers from a mutation sequence or by using the representations and the subrepresentations. Here the latter have the interpretation as decay products of a composite BPS states.

4.3.1 Argyres-Douglas A_1

This is the simplest possible BPS structure that one can represent with a quiver. It is a single BPS hypermultiplet with charge γ . In this case, one can define the quiver representation simply by a single complex vector space: \mathbb{C} . There cannot be any subrepresentations for this, meaning that this remains stable everywhere in the moduli space. The quiver itself is just a single node with no arrows:



4.3.2 Argyres-Douglas A_2

This is the first BPS structure that undergoes wall crossing. For this example, the theory is described by a quiver with 2 nodes. This is drawn using the rule for drawing arrows with the product $\langle \gamma_2, \gamma_1 \rangle = 1$, where $\gamma_1 = (1, 0)$ and $\gamma_2 = (0, 1)$. There is one arrow labelled as b_1 between them:

$$\gamma_1 \quad \bullet \xrightarrow{b_1} \bullet \quad \gamma_2$$

In this case, it is possible to decay into subrepresentations which can be written as inclusions of the quiver representations shown below. The possible subrepresentations include:

$$\begin{array}{ccc} \mathbb{C} & \longrightarrow & \mathbb{C} \\ \uparrow & & \uparrow \\ 0 & \longrightarrow & \mathbb{C} \end{array}$$

as well as,

$$\begin{array}{ccc} \mathbb{C} & \longrightarrow & \mathbb{C} \\ \uparrow & & \uparrow \\ \mathbb{C} & \longrightarrow & 0 \end{array}$$

The condition for the decay of this representation into these subrepresentations is that of the real ratio of the central charges. It is also possible to generate the spectrum of this theory using quiver mutations. On one side of the wall of marginal stability one can generate just the basis states - the electric and magnetic monopoles and their antiparticles $\pm\gamma_1, \pm\gamma_2$. On the other side one can also generate the sum and its antiparticle $\pm(\gamma_1 + \gamma_2)$ - the dyon in the theory.

4.3.3 Seiberg-Witten theory

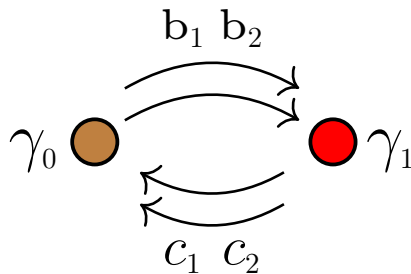
In this well known example, the quiver (4.3.3) is found extensively in the literature [3, 4, 33, 97, 100, 2] and has 2 nodes but also 2 arrows labelled as b_1 and b_2 . These are obtained following the rule that there must be $\langle \gamma_2, \gamma_1 \rangle = 2$ edges between the nodes, where the charges are given by $\gamma_1 = (2, -1)$ and $\gamma_2 = (0, 1)$:

$$\gamma_1 \quad \bullet \xrightarrow{b_1 \ b_2} \bullet \quad \gamma_2$$

This again undergoes wall crossing as the central charges align. On one side of the wall of marginal stability there are infinitely many ways to mutate this quiver (4.3.3) generating the full spectrum of Seiberg-Witten theory at weak coupling with charges $k\gamma_1 + (k + 1)\gamma_2$, $(k + 1)\gamma_1 + k\gamma_2$ and their antiparticles. This includes the infinite spectrum of dyons, a monopole, and a W-boson. The W-boson is found as the accumulation ray of the mutated charges given by the sum $\gamma_1 + \gamma_2$ and its antiparticle. On the other side the mutations can only generate the basis states γ_1, γ_2 and their antiparticles. These being the dyon and the monopole.

4.3.4 Resolved conifold

We now know that quivers describing the BPS spectra of Argyres-Douglas theories are constructed from the resolution of ADE type singularities [71]. However, there are also other models that have a quiver description arising from the resolution of a singularity. An example of this is the resolved conifold, which, as with the case of the quiver discussed for Seiberg-Witten theory, has multiple arrows. This is formed by a non-commutative resolution of the conifold singularity, a singular point in the 3-fold which can locally be written as $Z = \{x_1x_2 - x_3x_4 = 0\} \subset \mathbb{C}^4$. Here it is the Calabi-Yau algebra ⁴, resulting from this resolution [59, 111], that is non-commutative. This can be represented by a quiver, [19, 59] with 2 vertices $Q_0 = \{\gamma_0, \gamma_1\}$, and 2 pairs of edges in opposite directions between the vertices $b_1, b_2 : \gamma_0 \rightarrow \gamma_1$ and $c_1, c_2 : \gamma_1 \rightarrow \gamma_0$. In this final example, the quiver can be depicted as



Physically, this quiver describes D2-D0 branes within the resolved conifold. This results in a quiver quantum mechanics with no wall of marginal stability, although the same combinations of charge vectors represent the BPS states as in the full spectrum of Seiberg-Witten theory. If one wants to include a magnetic charge in the model one can wrap a D6 brane around the entire conifold. From the D2-D0 states bound to this D6 brane, one can now write down framed representations for this quiver (4.3.4) (which pair the representations with a map to a vector space which is fixed and graded [112]) ⁵ that can become unstable. This is also an example of a quiver with a superpotential as it has closed loops. This superpotential is in general given by the functions on the edges (if we write them, using the arrow labels, as b_1, b_2, c_1, c_2), which can be written as $\mathcal{W} = b_1c_1b_2c_2 - b_1c_2b_2c_1$. Later in sec. 5.4 it will be shown, if the magnetic D6 brane is included, how one can derive the BPS invariants from this resolution by defining a partition function with non-commutative NCDT invariants as its expansion coefficients.

⁴A Calabi-Yau manifold can be re-formulated as a polynomial algebra following Ginsburg [110] and can have properties such as associativity and non-/commutativity.

⁵These were first constructed by Nakajima [113] to define quiver varieties. They will also become important for understanding the framed BPS states in sec. 5.3.

5 | Wall crossing formulae and framed BPS states

There are ways of computing the change in the BPS index and the refined BPS index across a wall of marginal stability. These are known as wall crossing formulae and can be derived by looking at the Hilbert space of the composite BPS state and considering all the possible decompositions into constituents. Then one must find suitable tensor products of the Hilbert spaces of the constituents and then sum over the possible decompositions correctly [35, 36]. One can then calculate the change in the indices. This has been used extensively in the split attractor flow literature, which will be discussed later in detail in chapter 7 of this thesis. Whenever such a flow line hits a wall of marginal stability, for example in [36], BPS indices of composite states can be computed by taking products of constituents comprising the split flows. This has been used and extended for many examples of wall crossing in [114, 115, 116, 18].

These results are well understood for the simple case of a composite state splitting into 2 basis states, known as primitive, and also semi-primitive case of n copies of one state bound to another, where prescriptions exist for the change $\Delta\Omega(u, \gamma, y)$ and $\Delta\Omega(u, \gamma)$ across a wall. In this chapter 5 the examples of the primitive and the semi-primitive wall crossing formulae are reviewed as well as the relation to BPS galaxies of bound states consisting of a heavy core charge and an orbiting charge. This is demonstrated for an example from Jafferis-Moore [37] of a heavy D6 brane bound to configurations of D2/D0 branes.

5.1 Primitive wall crossing formula

There is a well known relation for the change in the BPS index $\Omega(\gamma, u)$ in $\mathcal{N} = 2$ theories at a point u within a chamber in the moduli space just after crossing the wall of marginal stability at u_{ms} . This holds when 2 constituent states, with charges γ_1, γ_2 , which cannot be decomposed further, combine into a composite state with charge $\gamma = \gamma_1 + \gamma_2$. This is known as the primitive wall crossing formula and is constructed from the fact that the Hilbert space for the composite state is a tensor product of that for the constituents [35]. The formula

takes the form [36, 37], for the BPS invariants, of the equation

$$\Delta\Omega(\gamma, u) = (-1)^{\langle\gamma_1, \gamma_2\rangle-1} |\langle\gamma_1, \gamma_2\rangle| \Omega(\gamma_1, u_{ms}) \Omega(\gamma_2, u_{ms}). \quad (5.1.1)$$

This can be generalised to the refined BPS invariants from section 3.1.1 if one includes the additional parameter y

$$\Delta\Omega(\gamma, u, y) = (-1)^{\langle\gamma_1, \gamma_2\rangle-1} ch_{|\langle\gamma_1, \gamma_2\rangle|}(y) \Omega(\gamma_1, u_{ms}, y) \Omega(\gamma_2, u_{ms}, y), \quad (5.1.2)$$

where the character $ch_{|\langle\gamma_1, \gamma_2\rangle|}(y)$ is of a representation of $SU(2)$ with a dimension $|\langle\gamma_1, \gamma_2\rangle|$ of the form $ch_{|\langle\gamma_1, \gamma_2\rangle|} = ch_{\rho_{|\langle\gamma_1, \gamma_2\rangle|}}$ ¹. This takes into account the $so(3)$ spin in spacetime of the electromagnetic field of the particles, given by $J_{\gamma_1, \gamma_2} = \frac{1}{2}(|\langle\gamma_1, \gamma_2\rangle| - 1)$. If there is only one decay pathway of a composite BPS particle into its constituents, of the form $\gamma = \gamma_1 + \gamma_2$, then this is the formula that should be applied.

5.2 Semi-primitive wall crossing formula

Now we look for a wall crossing formula for states with charges of the form $\gamma_c + n\gamma_h$. This is a special type of configuration where parallel charges, known as halo charges, bind to a core on a sphere of fixed radius (see Fig. 5.1). There is one wall at which infinitely many electric halo charges, of the form $n\gamma_h$, bind to a single core monopole charge γ_c . A good example of this is the case of infinitely many D0 branes binding to a D6 brane, with large mass, in the resolved conifold. One can look for an equation describing the possible BPS indices for the states, and how they jump, as the halo configurations become stable at the wall. This allows one to compute the change in the BPS indices for all n . This is known as the semi-primitive wall crossing formula first derived by Denef and Moore [36] and applied in [37, 34, 18, 38]. In general, the semi-primitive formula can be described by a sum over the changes in the BPS indices under wall crossing. This is given by

$$\Omega(\gamma_c; u) + \sum_{n \geq 1} \Delta\Omega(\gamma_c + n\gamma_h; u) \mathbf{X}_{\gamma_h}^n = \Omega(\gamma_c; u_{ms}) \prod_{k \geq 1} (1 - (-1)^{k\langle\gamma_c, \gamma_h\rangle} \mathbf{X}_{\gamma_h}^k)^{k|\langle\gamma_c, \gamma_h\rangle| \Omega(k\gamma_h; u_{ms})}, \quad (5.2.1)$$

where one introduces the variable \mathbf{X}_γ to encode the charges such that it obeys the condition $\mathbf{X}_{\gamma_1 + \gamma_2} = \mathbf{X}_{\gamma_1} \mathbf{X}_{\gamma_2}$. These are coordinates on a fiber T_u of the complex torus $\mathbf{T} = \Gamma^\vee \otimes \mathbb{C}^*$ from (3.1.10) but this time just in the semi-classical limit [16]. If the basis in the charge lattice is given by γ_i such that $\mathbf{X}_i := \mathbf{X}_{\gamma_i}$, a general charge in the spectrum of BPS states can be written in the form $\mathbf{X}_\gamma = \prod_i \mathbf{X}_{\gamma_i}^{n_i}$.

This semi-primitive wall crossing formula (5.2.1) can be constructed just as in the primitive case by considering the products of Hilbert spaces. Indeed, one can start by considering a

¹ $\rho_{|\langle\gamma_1, \gamma_2\rangle|}$ is the highest weight.

Hilbert space consisting of the core charge γ_c and the single halo γ_h . However, we remember that in the semi-primitive case we must generalise to charges of the form $\gamma_c + n\gamma_h$, with core γ_c , to which multiples of the halo charge $n\gamma_h$ become bound to as the wall is crossed. The changes in the BPS indices can be seen most clearly by considering the product step by step and then using it to construct a generating function in the variable X_γ .



Figure 5.1: Core and halos.

Now one can proceed to construct the generating function by starting to use the Hilbert space products [117]. As there are now multi-particle halo states, one must include the internal Fock space of bosonic and fermionic creation and annihilation operators, to count the halo states present for a particular charge. Then one takes suitable products of the contributions of the individual charges that are active. Using the new variables X_γ , defined here, one can expand the contribution of these factors to the BPS invariants in terms of the generating function

$$G_{\gamma_c}^{Halo}(u) = \sum_{n=0}^{\infty} \Omega(\gamma_c + n\gamma_h; u) X_{\gamma_c + n\gamma_h}, \quad (5.2.2)$$

where the $\Omega(\gamma_c + n\gamma_h; u)$ are the BPS indices counting the states in this way. If one has a region in which only the core charge exists, one can simply write the function as

$$G_{\gamma_c}(u) = X_{\gamma_c}. \quad (5.2.3)$$

Now we are crossing one wall but we can treat this as infinitely many overlapping walls for every possible state. As one gradually moves in the moduli space, one can cross a wall for a particular halo configuration, say from a region u_- to u_+ . As this occurs a state with charge $\gamma_c + n\gamma_h$ comes into existence. For every such state that enters the spectrum one must consider a new factor representing the contribution of the Fock space for the new halo particle now bound to the core. For example, as the wall for γ_h is crossed, this is taken into

account by including an extra factor such that the new generating function becomes

$$G_{\gamma_c}^{Halo}(u) = (1 - (-1)^{\langle \gamma_h, \gamma_c \rangle} \mathbf{X}_{\gamma_h})^{|\langle \gamma_h, \gamma_c \rangle| \Omega(\gamma_h; u_{ms})} \mathbf{X}_{\gamma_c}, \quad (5.2.4)$$

where one has now acted with a symplectomorphism on T_u , and $\sigma(\gamma_h) = (-1)^{\langle \gamma_h, \gamma_c \rangle}$ is a quadratic refinement used to generate the torus algebra². One must continue by considering all the BPS halo states $n\gamma_h$ as they enter the spectrum, so one has to continue to add factors until an infinity of BPS states contribute to the generating function

$$G_{\gamma_c}^{Halo}(u) = \prod_{n=1}^{\infty} (1 - (-1)^{\langle n\gamma_h, \gamma_c \rangle} \mathbf{X}_{\gamma_h}^n)^{| \langle n\gamma_h, \gamma_c \rangle | \Omega(\gamma_h; u_{ms})} \mathbf{X}_{\gamma_c}, \quad (5.2.5)$$

which now reproduces the right hand side of the initial equation (5.2.1). It can therefore be seen that, when crossing this single wall, one obtains the same result as if an infinite product is taken on overlapping walls that are crossed simultaneously. This can then be expanded and matched to the left hand side to obtain the changes in the BPS indices $\Delta\Omega(\gamma_c + n\gamma_h; u)$ as the wall is crossed.

5.3 Framed BPS states and galaxies

Framed BPS states were introduced in [17] as BPS states in 4d $\mathcal{N} = 2$ theories that can bind with a particular class of operators. These are called line operators as they are inserted on a straight line. Examples of line operators include the t'Hooft-Wilson operators defined in [118, 119]. When they only carry electric charge, they have a physical interpretation as Wilson Lines. The name ‘‘framed’’ comes from the framed quiver representations [113, 112] that describe them. In the context of framed BPS states the original BPS states that are bound to the line operator are referred to as ‘‘vanilla’’ BPS states. Framed BPS states are interesting because of their effect on the vanilla BPS degeneracies. This situation can be looked at as a large central object probing the system of BPS states, in an Argyres-Douglas theory for example, and can be used to recover the Konsevich-Soibelman wall crossing formula [30] for these vanilla BPS states.

Framed BPS states are also interesting in the context of the research presented in this thesis because the wall crossing of framed BPS states can be matched with Weyl chambers in a way that is analogous to that in Cheng and Verlinde [52, 53], which is suggestive of a new form of generating function (see chapters 10 and 11). There is also a supergravity perspective from which to view framed BPS states in the context of halo states bound to a large core charge (the analog of the line operator) which was developed in [57, 100, 120]. Importantly, this was then further developed into a direct analog in terms of a generating function, from the QFT perspective [17] for framed BPS states, in [18] by constructing a more general configuration of orbiting charges known as a BPS galaxy. This is then further reviewed in

² $\sigma(\gamma_h)X_{\gamma_h}$ is a Hamiltonian that gives the generator e_{γ_h} [16].

[117]. The configuration has appropriate inner products between the charges that match the construction of the framed BPS states in [17].

5.3.1 Core charges and orbiting charges

One can consider a more general configuration, of a core charge and orbiting charges, than those looked at for the semi-primitive wall crossing formula (5.2.1) in chapter 5.2. Here “orbiting” refers to 4d solutions in $\mathcal{N} = 2$ effective supergravity³. These can be bound in many more possible configurations. As before, the core is denoted by γ_c , and the sum of the orbiting charges is denoted by γ_{orb} . This is then defined as a BPS galaxy with total charge $\gamma_t = \gamma_c + \gamma_{orb}$. To define the core one must first define $U(1)$ electric and magnetic charges γ_0 and γ'_0 respectively. After this, one can use an example of a core charge of the form [18, 117]:

$$\begin{aligned} \gamma_c &= \Lambda^2 \gamma_0 + \Lambda \gamma'_0 + \delta, & \text{such that,} \\ \gamma_t &= \gamma_c + \gamma_{orb}, & \text{and the products are,} \end{aligned} \tag{5.3.1}$$

$$\langle \gamma_0, \gamma'_0 \rangle = 1, \quad \delta, \gamma_{orb} \in \Gamma_0^\perp := \{ \gamma : \langle \gamma_0, \gamma \rangle = \langle \gamma'_0, \gamma \rangle = 0 \},$$

where Λ is an anisotropic scaling, and one lets the charge δ be perpendicular to the core electric and magnetic charges. There is an additional lattice of orthogonal charges relative to the initial $U(1)$ charges described before (5.3.1). These are the orbiting charges that are bound to the core as a whole. The sum of these charges is denoted by $\gamma_{orb} \in \Gamma_0^\perp$. This whole configuration is then described as a BPS galaxy as we now have the single core charge and in general we can have composite bound states in orbit in many possible configurations. The orbiting charges don't have to be pure halo states as they can be configurations within Γ_0^\perp that are non-local relative to each other. There can also be mixed states meaning that charges can be exchanged between the core and the orbiting charges. This arises due to quantum tunnelling in the full non-perturbative theory.

Looking back at the semi-primitive wall crossing formula (5.2.1) in chapter 5.2, one can continue looking at charges of the form $\gamma_c + n\gamma_h$ to use as an example of mixed states. The BPS indices for these charges cannot simply be decomposed into the product of constituents. This means that $\Omega(\gamma_c + n\gamma_h; u) \neq \Omega(\gamma_c; u)\Omega(n\gamma_h; u)$. This is because the states in the Hilbert space can mix in such a way that one can redefine which charges in $\gamma_c + n\gamma_h$ belong to the core and the halo. The alternative decompositions of the charge $\gamma_c + n\gamma_h$ take the form of a core with charge $\gamma_c + m\gamma_h$ and halo charge with $(n - m)\gamma_h$. Furthermore, in general one can also include additional orbital charges of the form $n\gamma_h + \delta$ combined with a core of $\gamma_c - \delta$. However, all these effects can be suppressed by taking a limit of large charges in the core.

³See section 7 for a detailed description of multi-centered bound states in supergravity.

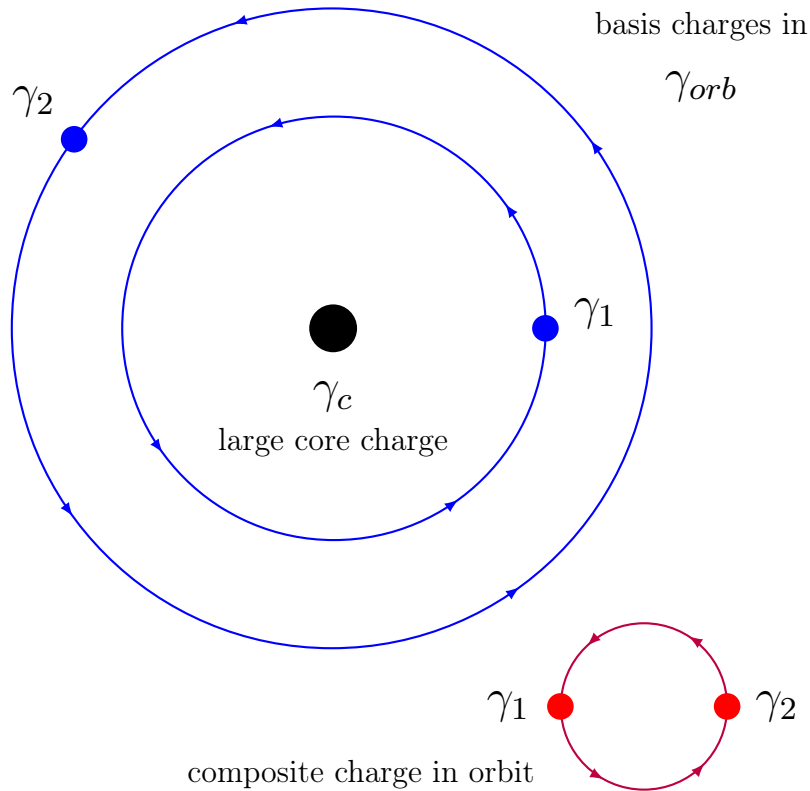


Figure 5.2: Example BPS galaxy with possible basis and composite configurations in orbit of the large core γ_c .

Limit of large charges

The effects of mixed states can be taken into account following the example of [18] by using the fact that these effects do not occur if one takes the core charge to be large. One can take the limit $\Lambda \rightarrow \infty$ so that the core becomes such a BPS state with large charge and mass. There are several physical arguments explaining that, in the $\Lambda \rightarrow \infty$ limit, the extra decompositions from non-perturbative quantum effects disappear. Two main reasons are:

- (i) Entropic suppression of the fragmentation of black holes; this is exponential as the charge becomes large [121, 122, 117]. A good example for this is the Reissner-Nordström black hole where one can consider a charge Q splitting into components $Q = Q_1 + Q_2$. The change of entropy from this decomposition is

$$\delta S = \pi Q^2 - \pi Q_1^2 - \pi Q_2^2 = 2\pi Q_1 Q_2. \quad (5.3.2)$$

In this case, the amplitude for this decomposition falls off in the change in the entropy (the difference between the entropy of the composite and 2 separate constituents) as $e^{-\frac{1}{2}\delta S}$. Therefore, as $Q \rightarrow \infty$ the amplitude associated to this splitting tends to 0.

- (ii) Alternatively, one can look at the core γ_c and consider a potential halo charge of the form $\gamma_i \in \Gamma_0^\perp$. For this example, one can determine if a transfer of the charge γ_i from the core to the halo [18] is possible. The argument for the absence of mixed states [57, 18, 117] can be seen by looking at the distance between the core and this halo charge

$$r = \langle \gamma_c, \gamma_i \rangle \frac{1}{2\text{Im}(Z_{\gamma_i} e^{i\alpha})}, \quad (5.3.3)$$

$e^{i\alpha}$ is obtained by taking the phase of the total central charge $Z(\gamma_c + \gamma_i; u_\infty)$ after an infinite time evolution. In this case, because of the scaling Λ in the γ_c we have $r \rightarrow \infty$ as $\Lambda \rightarrow \infty$ and the quantum tunnelling amplitude tends to 0 because of the large separation of the core and the orbiting charge. Therefore, a transfer between the core and the halo cannot happen with a large core charge.

5.3.2 Hilbert space and generating function of framed BPS states

From the limit described in the previous subsection 5.3.1, a closed system of BPS states is obtained with a core charge γ_c and various configurations of states bound to the core. The core charge is now fixed. Therefore, with all the composite BPS configurations containing the same core charge - one can factor the core out of the Hilbert space and construct a quotient Hilbert space [117]. This is defined as

$$\mathfrak{h}_{\gamma_c}(\gamma_{orb}; u) = \frac{\mathfrak{h}_{\gamma_c + \gamma_{orb}}}{\mathfrak{h}_{\gamma_c}}, \quad (5.3.4)$$

where we remember that γ_{orb} is the sum of the charges orbiting the core. These BPS states are defined as framed, which can be interpreted as in [17]. The index of these framed BPS states is given by

$$\underline{\Omega}_{\gamma_c}(\gamma_{orb}; u) = \lim_{\Lambda \rightarrow \infty} \text{Tr}_{\mathfrak{h}_{\gamma_c}(\gamma_{orb}; u)} (-1)^{2J_3}, \quad (5.3.5)$$

with spin $2J_3$, which is analogous to the BPS indices from [34], defined in section 3.1.1. These BPS numbers are locally constant but undergo wall crossing when a new particle γ enters the BPS galaxy. To see this, consider this new particle in the galaxy with central charge: $Z(\gamma, u)$. This charge γ can be chosen to be in the perpendicular space $\gamma \in \Gamma_0^\perp$, so the resulting generating function (5.3.8) for these framed indices only depends on a charge of the form $\gamma_{orb} + \delta$.

BPS walls and Weyl chambers

The wall for the new particle γ to enter the BPS galaxy occurs when this central charge is parallel with the sum of all the central charges within the BPS galaxy [18, 117], after

the new particle has entered. This total central charge after the new particle has entered is denoted by: $Z(\gamma_c + \gamma_{orb} + \gamma; u)$. The dependence on γ_{orb} is removed by taking the $\Lambda \rightarrow \infty$ limit discussed above in section 5.3.1. Now the wall is defined by

$$W_\gamma := \left\{ Z(\gamma_0, u) \parallel Z(\gamma, u) : \text{Im}[Z(\gamma, u)\bar{Z}(\gamma_0, u)] = 0 \longrightarrow \text{Im}\left[\frac{Z(\gamma, u)}{\zeta}\right] = 0 \right\}, \quad (5.3.6)$$

where ζ can be considered a phase.

This wall therefore depends just on the large part of the core and the halo. It is called a BPS wall and is distinct from the wall of marginal stability for the decomposition of the vanilla BPS states γ , without the presence of a BPS galaxy. The configurations with charges proportional to the charge γ are removed or added from the orbit of the core when W_γ is crossed. Later, in chapter 11, we also match the BPS walls to the boundaries of the Weyl chambers, of the particular root system, associated to the Lie algebra describing the vanilla BPS states of the 4d $\mathcal{N} = 2$ theory. This is interesting as this is a setting in which new candidate generating functions, such as the Weyl denominator formula, can be conjectured to exist that count the introduction of new halo states as changes in the highest weight of a module or representation. However, we can now look at the effects of crossing BPS walls on the currently known generating function of the indices in (5.3.5).

This effect of crossing a BPS wall on this generating function can be determined by using the same principle as for the semi-primitive wall crossing formula. The configuration has total charge $\gamma_t = \gamma_c + \gamma_{orb}$ and the contribution of the charge γ to the new wall crossing formula is

$$(1 - (-1)^{\langle \gamma, \gamma_t \rangle} \mathbf{X}_\gamma^n)^{|\langle \gamma, \gamma_t \rangle| \Omega(\gamma; u_{ms})}, \quad (5.3.7)$$

where one can then multiply by these factors successively for each γ to obtain the generating function. The expansion of the generating function for framed BPS states becomes

$$G_{\gamma_c}^{\gamma_{orb}}(u) := \sum_{\gamma_{orb} \in \Gamma_0^\perp} \underline{\Omega}_{\gamma_c}(\gamma_{orb}; u) \mathbf{X}_{\delta + \gamma_{orb}}. \quad (5.3.8)$$

One can then read off the framed BPS indices in (5.3.5) from this expansion (5.3.8). These generating functions can be applied to $\mathcal{N} = 2$ theories with an effective supergravity description which arise when taking local limits of compact CY 3-folds that give rise to the effectively non-compact Argyres-Douglas and Seiberg-Witten theories. In these cases, the charges γ can be chosen as the charges present in the respective models. They can then be interpreted as the charges of BPS solutions in a chosen $\mathcal{N} = 2$ supergravity theory probed by a large core charge.

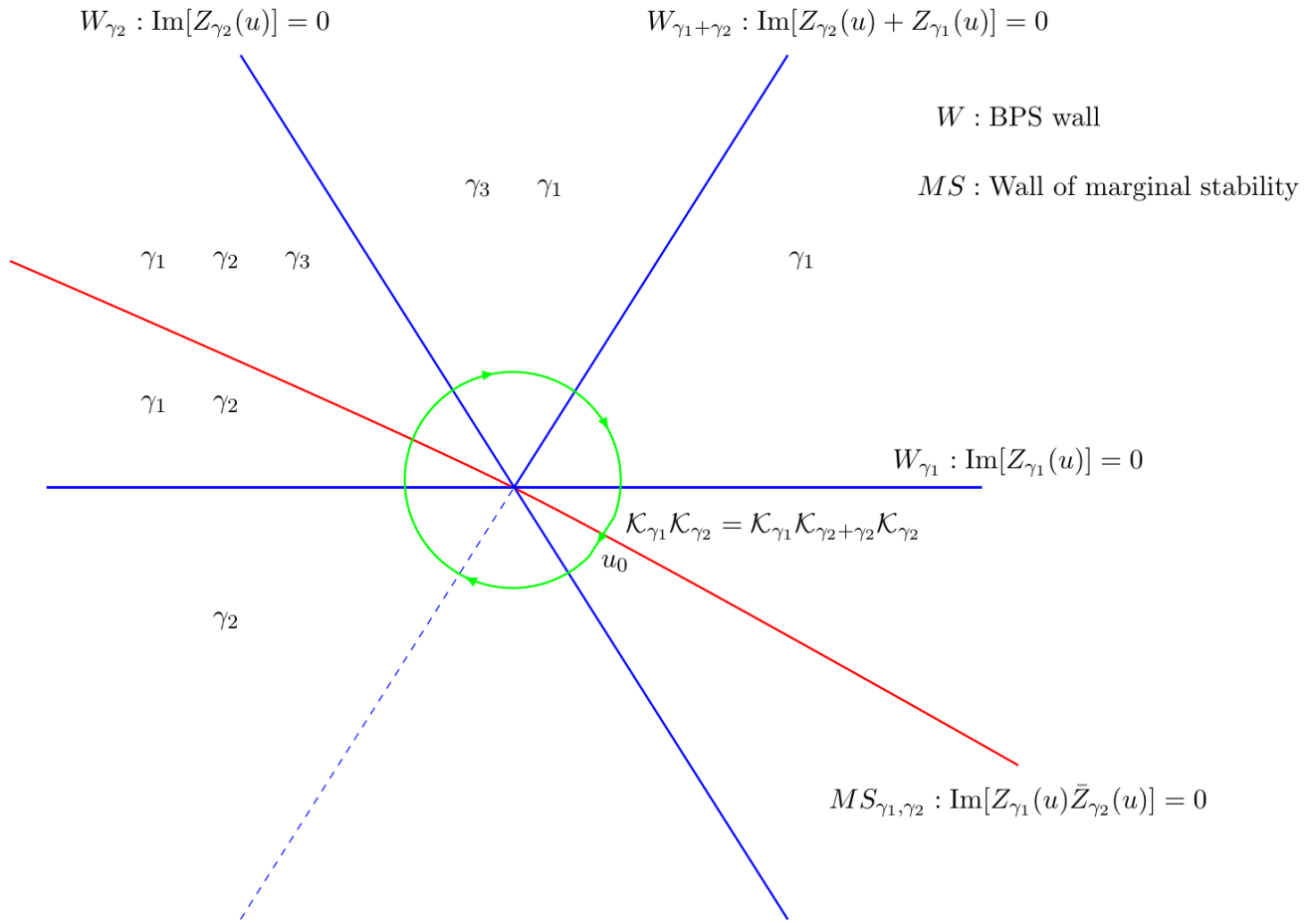


Figure 5.3: This diagram shows the BPS walls for the framed BPS states in blue intersecting on the wall of marginal stability in red where one has zoomed in. The green line is the path in the moduli space which can be taken to show the wall crossing formula.

Konsevich-Soibelman operator

It is possible to write the generating function in terms of the Konsevich-Soibelman (KS) operators from [30] (unlike those looked at in section 3.1.2, we are now considering the semi-classical limit) representing the $\mathcal{N} = 2$ charges and their wall crossing behavior from either the line operator or large charge formulation [17, 18]. These have, as an exponent, the BPS index $\Omega(\gamma; u)$ of the pure $\mathcal{N} = 2$ theory without any additional charges associated with a BPS galaxy. As mentioned above, these are also known as “vanilla” BPS indices. Equation (5.3.7), describing the contribution of the semi-primitive wall crossing formula to the framed generating function, can be simplified by introducing the operator $D_\gamma \mathbf{X}_{\gamma_t} := \langle \gamma, \gamma_t \rangle \mathbf{X}_{\gamma_t}$ to remove the explicit dependence on γ_{orb} . This operator can act separately on individual terms in the generating function representing a different total charge. One can now write down the factor (5.3.7) as a Konsevich-Soibelman operator

$$\mathcal{K}_\gamma := (1 - (-1)^{D_\gamma \mathbf{X}_\gamma})^{D_\gamma}. \quad (5.3.9)$$

Hence, these transformations can be used to construct the generating function by acting with the operator $\mathcal{K}_\gamma^{\Omega(\gamma,u)}$ if a wall W_γ is crossed. This is interesting as one can now see how wall crossing works in the pure $\mathcal{N} = 2$ theory by thinking about the generating function of framed BPS indices. This generating function is equivalent when one takes equivalent paths in the moduli space, crossing all BPS walls for framed states, on both sides of the wall of marginal stability of the pure theory. This can be seen as shown in Figure 5.3 by starting at a point u_0 and taking a loop in the moduli space crossing all walls and including the KS operator associated with a particular BPS wall as the loop crosses that particular wall. For example, in the A_2 root system we have $\mathcal{K}_{\gamma_1}\mathcal{K}_{\gamma_2} = \mathcal{K}_{\gamma_2}\mathcal{K}_{\gamma_1+\gamma_2}\mathcal{K}_{\gamma_1}$ representing the construction of the generating function from factors on either side of the wall of marginal stability.

A collection of intersecting rays in which some rays only exist on one side of the intersection is also known as a scattering diagram. Figure 5.3 shows this for the A_2 case. These were originally introduced by Gross and Siebert [123] in the context of mirror symmetry. The scattering diagrams for the Seiberg-Witten and A_2 examples were worked out by Bridgeland in [124].

5.4 D6-D2-D0 system on the conifold

There is another well known case of a system of BPS states describing configurations that are bound to a large core. This is the example of type IIA string theory on the conifold [37, 59, 38]. Here, an initially compact CY 3-fold X is considered which contains a projective line $\mathbb{P}^1 \subset X$. The local limit of the CY is taken, meaning one zooms in around the conifold singularity so that one can effectively treat this as a non-compact manifold given by the rank 2 bundle $\mathcal{O}(-1) \oplus \mathcal{O}(-1) \rightarrow \mathbb{P}^1$. The \mathbb{P}^1 zero section can be contracted by letting its Kähler modulus tend to 0 such that the conifold singularity exists at this point. This example has been extremely useful because the wall crossing has been later shown to be related to non-perturbative topological string partition functions on this target space [61], and has reproduced the Donaldson-Thomas partition functions in [28, 29] that have been useful for demonstrating the correspondence between Donaldson-Thomas and Gromov-Witten invariants. One can also use this partition function to read off the values of non-commutative (NCDT) invariants, described by Joyce and Song in [19], and then further use these to calculate the vanilla BPS indices discussed in section 3.1.1 for the hyper and vector multiplets respectively.

The D0-D2-D6 partition function is another framed BPS index and this model can be considered as a pure D6 brane on the conifold with possible combinations of D0-D2 branes bound to it [37]. In this model, the BPS walls for a new state to become bound to the core have been shown to depend on the Kähler moduli of the target space as well as another real number describing a phase of the core charge [37]. The target space in this case is a CY 3-fold X . A scaling factor Λ is chosen for which the local limit is taken as $\Lambda \rightarrow \infty$.

This is analogous to the limit of large charges taken in section 5.3.1 and indeed this is the limit of large D6 brane charge. The partition function has been derived by starting in the region where only the core D6 brane exists [37, 36]. In this first region, the BPS partition function is just $Z_{\text{D6-D2-D0}} = 1$. The other walls have been determined by considering where the central charges align. To define the central charges, one must define the charges. These charges take the form: ⁴

$$\gamma_1 + \gamma_2 = \gamma = 1 - \tilde{m}\beta + \tilde{n}dV, \quad \text{where} \quad \gamma_1 = a + \mathcal{D} - \beta_h + n_h dV, \quad \tilde{m}, \tilde{n}, n_h \in \mathbb{Z}, \quad (5.4.1)$$

$$a \in H^0(X; \mathbb{R}), \quad \beta \in H^4(X; \mathbb{R}), \quad \mathcal{D} \in H^2(X; \mathbb{R}), \quad dV \text{ generates } H^6(X; \mathbb{Z}),$$

$$\mathcal{P}, \mathcal{P}' \in H^2(X, \mathbb{R}), \text{ such that } \mathcal{P} \cdot \beta = 1, \quad \mathcal{P}' \cdot \beta = 0,$$

$$\text{and one can also define } \beta_h \cdot \mathcal{P} = m_h, \quad \beta_h \cdot \mathcal{P}' = M_h.$$

The central charges associated to this system [37] can be written as ⁵

$$\begin{aligned} Z_{\gamma_1} &= \frac{a}{6} \Lambda^3 e^{3i\phi} + \frac{\mathcal{D}}{2} \cdot (\Lambda e^{i\phi} \mathcal{P}' + z\mathcal{P})^2 - M_h \Lambda e^{i\phi} - m_h z - n_h, \\ Z_{\gamma_2} &= \frac{1}{6} \Lambda^3 e^{3i\phi} - \tilde{m}z - \tilde{n} - Z_{\gamma_1}, \end{aligned} \quad (5.4.2)$$

where we consider a Kähler parameter of the form $t = z\mathcal{P} + \Lambda e^{i\phi} \mathcal{P}'$, and $z \in \mathbb{C}$, $\phi \in \mathbb{R}$. The wall crossing has been well understood for the range $\phi \in (0, \pi)$ and $\text{Im}(z) > 0$. Now one takes the limit $\Lambda \rightarrow \infty$ for a large core D6 charge and looks for values of a, \mathcal{D}, M_h ⁶ that allow for the existence of walls, in this limit, that represent the formation of bound states to this core. After this one is left with charges of the form

$$\gamma_1 = 1 - m'\beta + n'dV \quad \text{and} \quad \gamma_2 = -m\beta + ndV, \quad (5.4.3)$$

where the numbers have been relabelled. ⁷ Remembering to take the limit [37], this results in the central charges of the form

$$\begin{aligned} \lim_{\Lambda \rightarrow \infty} Z(\gamma_1; t) : \quad Z(\gamma_1; t) : \Lambda^3 e^{3i\phi} - m'z - n' &\rightarrow \Lambda^3 e^{3i\phi}, \\ \lim_{\Lambda \rightarrow \infty} Z(\gamma_2; t) : \quad Z(\gamma_2; t) = -mz - n. & \end{aligned} \quad (5.4.4)$$

The walls of marginal stability occur at the points at which the central charges align. This is also equivalent to the attractor flow stability condition (e.g. Denef [56]) which for this

⁴Here the dot product is the intersection product in cohomology $\alpha_1 \cdot \alpha_2 := \int_X \alpha_1 \wedge \alpha_2$.

⁵One can interpret this physically as z and ϕ parameterizing the magnetic field of the resulting theory.

⁶E.g. $a = 0, 1$, $\mathcal{D} = 0$, $M_h = 0$.

⁷The relabelling depends on the parameters chosen and the labelling of γ_1 and γ_2 .

system corresponds to

$$\langle \gamma_1, \gamma_2 \rangle \text{Im}[Z(\gamma_1; t) \bar{Z}(\gamma_2; t)] = -n \text{Im}(e^{3i\phi}(-mz^* - n)) > 0. \quad (5.4.5)$$

Now one can see that the positions of the walls depend just on $z \in \mathbb{C}$ and the angle $\phi \in (0, \pi)$

$$\phi = \frac{1}{3} \arg(-mz - n) + \frac{2\pi k}{3}. \quad (5.4.6)$$

Here we have $k \in \mathbb{Z}$. The total space spanned by z and ϕ has real dimension 3, with the walls here being a codimension 1 real space. For a fixed choice of k one can write all the possible walls [37, 38] in the form (for $m > 0$)

$$\begin{aligned} \mathcal{W}_n^m &= \{(z, \phi) : \phi = \frac{1}{3} \arg(z + \frac{n}{m}) + \frac{\pi}{3}\}, \\ \mathcal{W}_n^{-m} &= \{(z, \phi) : \phi = \frac{1}{3} \arg(z - \frac{n}{m})\}, \\ \tilde{\mathcal{W}}_n^{-m} &= \{(z, \phi) : \phi = \frac{1}{3} \arg(z - \frac{n}{m}) + \frac{2\pi}{3}\}. \end{aligned} \quad (5.4.7)$$

The regions between the walls are written as $[\mathcal{W}_{n_1}^{m_1}, \mathcal{W}_{n_2}^{m_2}]$ as one moves in the direction of increasing ϕ . Now we can construct the generating function in this case by starting in the right chamber in Fig. 5.4 and reducing ϕ . We review this here with fixed z but this can in general be varied. Walls are encountered as the composite states $\gamma_1 + \gamma_2$ form. These walls are initially of the form \mathcal{W}_n^m and are located at $\phi = \frac{1}{3} \arg(z - |\frac{n}{m}|) + \frac{\pi}{3}$. Now one must look more specifically at the system of D0-D2-D6 branes. One can start by noting that the BPS states discussed above that become bound to the core correspond to either primitive D0-D2 fragments or pure D0 branes. The D2-D0 fragments represent BPS hypermultiplets as discussed in section 3.1.1.

This means the particles associated to this charge are fermionic, implying that multiple particles cannot occupy the same quantum state. Therefore, one cannot have multiple D2-D0 fragments bound to the core and the only walls one is left with are those with $\mathcal{W}_n^{\pm 1}$ shown on Fig. 5.4. The D0 branes represent BPS vector multiplets and behave as bosons. In contrast to the fermions multiple particles can occupy the same state implying walls of the form \mathcal{W}_n^0 can exist. This is also interesting because these are roots of the \hat{A}_1 Lie algebra. It means that the walls can also be written as boundaries of the Weyl chambers of this Lie algebra. This will become important later in section 11.3, in the context of finding new generating functions, by looking for analogs of the $\mathcal{N} = 4$ generating functions in [52, 53].

However, we start by constructing the known partition function by crossing the walls successively. One starts with the D2-D0 walls. These exist as the D2-D0 fragments align with the core D6. This is started by applying the semi-primitive wall crossing formula to successive walls [37, 63] such that the partition function (5.4.8) in each region of the moduli space

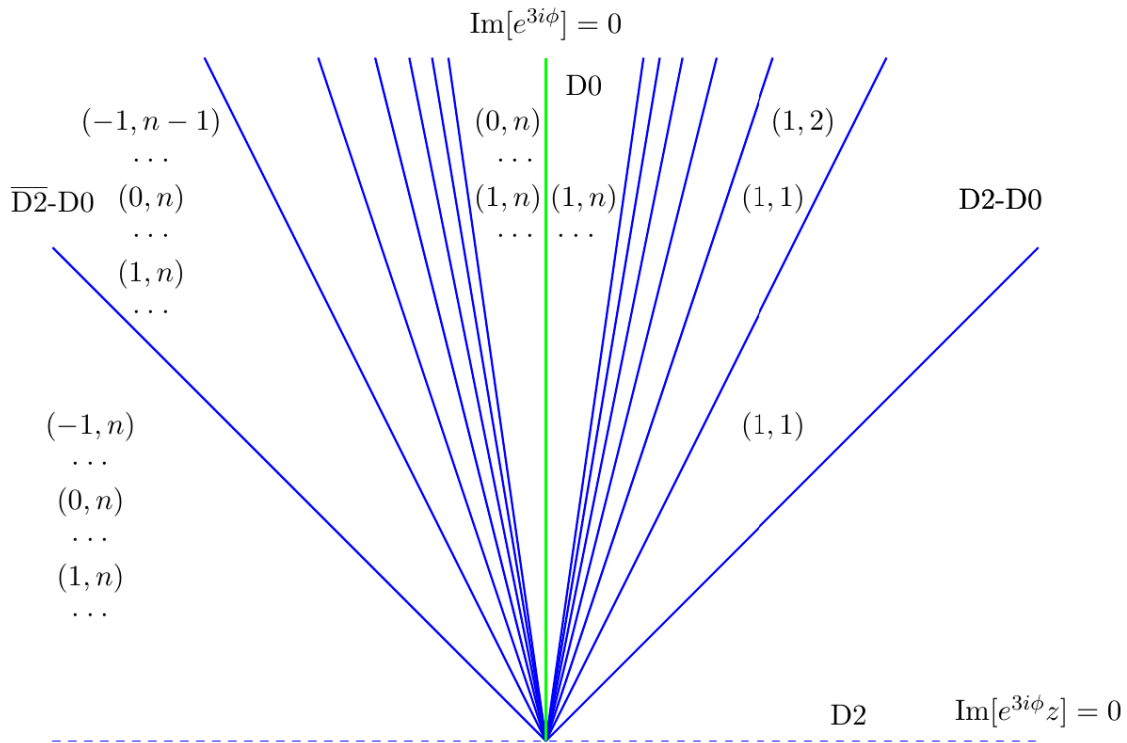


Figure 5.4: This shows the walls in blue for the binding of D2-D0 fragments to the D6 core. The D6-D0 wall is labelled in green. In this example, there can be infinitely many BPS states as n can tend to infinity.

$[\mathcal{W}_{n+1}^1, \mathcal{W}_n^1]$ then becomes

$$Z_n^+(u, v) = \prod_{j=1}^n (1 - (-u)^j v)^j, \quad (5.4.8)$$

where $u, v \in \mathbb{C}$.⁸ So, one continues to cross the walls of which there are infinitely many, which have the form \mathcal{W}_n^1 . Here one lets $n \rightarrow \infty$ which represents an increasing D0 charge of the fragment. There is an accumulation ray at $\phi = \frac{\pi}{3}$, which represents the wall for the bound state D6-D0. As one continues to successively cross the walls one continues to pick up factors [37, 63] as one takes the limit (5.4.9) approaching the accumulation ray

$$\lim_{n \rightarrow \infty} Z_n^+(u, v) = \prod_{k>0} (1 - (-u)^k v)^k = Z'_{DT}(u, v). \quad (5.4.9)$$

This is also known as the “reduced Donaldson-Thomas Partition function” for the previously known topological string partition function in [28]. Next one crosses the wall, or

⁸These chemical potentials can be matched with the Kähler parameter $t = z$, and coupling $\arg(\lambda) = 3\phi$, in a topological string partition function, where $u = -e^{i\lambda}$, $v = e^{2\pi it}$ [28, 29, 61].

accumulation ray, for the D6-D0 combination. For this one picks up the factor

$$M(u)^2 = \prod_{k>0} (1 - (-u)^k)^{-2k}. \quad (5.4.10)$$

where $M(u)$ is also known as the MacMahon function [28, 125]. This is now included in the partition function as

$$\lim_{n \rightarrow \infty} Z_n^-(u, v) = \prod_{k>0} (1 - (-u)^k)^{-2k} (1 - (-u)^k v)^k. \quad (5.4.11)$$

Now as one continues crossing walls one encounters next the walls that exist as the D6 composite brane central charge aligns with those of the fragments consisting of $\overline{D2} - D0$ brane combinations. These walls are now of the general form \mathcal{W}_n^{-m} , where $m = 1$, and lie at an angle given by $\phi = \frac{1}{3} \arg(z - |\frac{n}{m}|)$ for $m < 0, n > 0$. Now one can keep decreasing the angle ϕ and consider (5.4.12) the D6-D2-D0 partition function [37, 63, 126] in the chambers defined by $[\mathcal{W}_n^{-1} \mathcal{W}_{n+1}^{-1}]$

$$Z_n^-(u, v) = \prod_{k>0} (1 - (-u)^k)^{-2k} (1 - (-u)^k v)^k \prod_{r>n} (1 - (-u)^r v^{-1})^r. \quad (5.4.12)$$

Finally, we keep reducing the angle ϕ until all walls of the form \mathcal{W}_n^{-1} are crossed. One is now in the chamber defined by: $\frac{1}{3} \arg(z) < \phi < \frac{1}{3} \arg(z-1)$. One can call this the Szendrői region as the partition function within this region is exactly what Szendrői derived, by counting particular framed objects in the category of quiver representations [59, 19], constructed from a non-commutative resolution of the conifold. This was done by relating the counting function to the pyramid partition function of [126]. When taking the limit $\text{Im}(z) \rightarrow 0$, in this Szendrői region, one approaches conifold singularity at the chamber boundary as the $\mathbb{P}^1 \subset X$ contracts. The final form of this generating function [37, 59, 63, 126, 20] is

$$Z_{S_z}(u, v) = \prod_{k>0} (1 - (-u)^k)^{-2k} (1 - (-u)^k v)^k (1 - (-u)^k v^{-1})^k \quad (5.4.13)$$

$$= 1 + \sum_{p,q} \text{NCDT}_{p,q} u^p v^q. \quad (5.4.14)$$

One can use this final partition function (5.4.13) to define the non-commutative Donaldson-Thomas invariants NCDT, as in Joyce and Song [19], for framed quiver representations labelled by (p, q) . For this example, the quiver with 2 sets of arrows between the nodes has also been shown previously in section 4.3.4. This will later also be shown to match to Weyl chambers for \hat{A}_1 root system, which allows for another description of the wall crossing. For the resolved conifold one finds the well-known BPS invariants that are known from the $\text{GV}(0, \beta)$ invariants in [25, 24]. In this case, the BPS invariants are

$$\Omega(\pm\beta + ndV) = +1, \quad \forall n \in \mathbb{Z} \quad \Omega(ndV) = -2, \quad n \in \mathbb{Z} \quad n \neq 0. \quad (5.4.15)$$

6 | Exact WKB method

The WKB method (named after Wentzel, Kramers and Brillouin) was originally developed as a method for solving differential equations approximately - this was done in 1926. These differential equations are linear and have a coordinate dependence in their coefficients. This method is particularly useful for solving the Schrödinger equation in semiclassical approximations. More recently, this has been extended to the exact WKB analysis for one-dimensional cases. Remarkably, one can use such examples to consider quantum periods, as series expansions in \hbar around classical paths, that are Borel resummable along different rays. This exact WKB method was developed in [127, 128, 129, 130] and subsequently reviewed in [131, 132, 133]. This was done by interpreting the wavefunction in terms of these quantum or WKB periods. The classical periods that these are expanded about can be related back to the periods of the curves we are interested in for Seiberg-Witten and Argyres-Douglas theories. Importantly, this can help us interpret the periods used in the research on attractor flow described in chapters 7 and 8.

There has also been recent exploration in the literature for the periods of the quantised Seiberg-Witten curve in [134]. The quantisation of these curves is important from the perspective of counting BPS states as the quantum periods satisfy the system of TBA equations already used to derive the hyperkähler metric for the $\mathcal{N} = 2$ QFTs in the work of Gaiotto, Moore, Neitzke [16]. This implies that these TBA equations have poles in the period ratio representing the walls of marginal stability for the decay of composite BPS states, hereby dividing the moduli space into regions where different numbers of BPS states exist. Indeed, the concepts introduced in this chapter can therefore be added to the prescriptions used to count BPS states and describe the wall crossing phenomena discussed in chapters 3, 4 and 5.

6.1 Schrödinger equation and quantum periods

This discussion can be started by considering the Schrödinger equation describing the wavefunction of a particle with energy E moving in a potential $V(x)$ at a coordinate x . This particle is non-relativistic. However, unlike the situation for a particle, x is now complex to

allow for the exact resummation of the solutions. The equation can be written as

$$-\hbar^2\psi''(x) + (V(x) - E)\psi(x) = 0. \quad (6.1.1)$$

The exact WKB method [131, 132, 133] solves this equation by producing asymptotic expansions in \hbar . One starts with the substitution of the exponential of an integral over a path

$$\psi(x) = \exp\left[\frac{i}{\hbar} \int_{x_0}^x Q(x')dx'\right], \quad (6.1.2)$$

which when put in the equation gives

$$Q^2(x) - i\hbar \frac{dQ(x)}{dx} = p^2(x), \quad p(x) = (E - V(x))^{\frac{1}{2}}. \quad (6.1.3)$$

This is also known as a Riccati equation. The solution for the function $Q(x)$ can be found as a series in \hbar

$$Q(x) = \sum_{k=0}^{\infty} Q_k(x)\hbar^k, \quad (6.1.4)$$

where $Q_k(x)$ can be found using a recursion relation. One can split this series into 2 parts [133] corresponding to odd and even exponents of \hbar respectively

$$Q(x) = P(x) + Q_{odd}(x). \quad (6.1.5)$$

the odd part being the total derivative

$$Q_{odd}(x) = \frac{i\hbar}{2} \frac{d}{dx} \log P(x). \quad (6.1.6)$$

This can be put back into the expression for the wavefunction so that it becomes

$$\psi(x) = \frac{1}{\sqrt{P(x)}} \exp\left[\frac{i}{\hbar} \int_{x_0}^x P(x')dx'\right], \quad (6.1.7)$$

where $P(x)$ can be written in the form of the series

$$P(x) = \sum_{n \geq 0} p_n(x)\hbar^{2n}.$$

Here we have the classical momentum being defined as $p_0(x) = p(x)$ and the meromorphic differential $P(x)dx$. This is defined for the curve [133] containing both the energy and the

potential

$$y^2 = 2(E - V(x)), \quad (6.1.8)$$

however, we remember that x and y are now complex. Now if the potential $V(x)$ is polynomial in q then the equation above is a hyperelliptic curve known as the WKB curve. This is a Riemann surface Σ_{WKB} parameterized by moduli set in E and $V(x)$. We can define the periods of this curve using the differential $P(x)dx$ around the path given by the one-cycles $\gamma \in H_1(\Sigma_{WKB})$. These are known as quantum [132, 133] or WKB periods and are denoted as

$$\Pi_\gamma(\hbar) = \oint_\gamma P(x)dx, \quad \gamma \in H_1(\Sigma_{WKB}). \quad (6.1.9)$$

The Voros symbol is defined as the exponent of this period $\mathcal{V} = \exp(\frac{i}{\hbar}\Pi_\gamma)$. The quantum periods in (6.1.9) can also be written in terms of a power series in \hbar with even powers - just like we have described for $P(x)$. This is written as:

$$\Pi_\gamma(\hbar) = \sum_{n \geq 0} \Pi_\gamma^n(x) \hbar^{2n}, \quad \Pi_\gamma^n(x) = \oint_\gamma p_n(x)dx. \quad (6.1.10)$$

Therefore, the classical period that we have been looking at so far, introduced in section 2.1.1, in our discussion of $\mathcal{N} = 2$ QFTs, corresponds to

$$\Pi_\gamma^0(x) = \oint_\gamma p_0(x)dx. \quad (6.1.11)$$

It is interesting to look at a way to explicitly calculate the quantum corrections to this classical period. First, the energy and the potential are chosen such that they take the form of an $(r + 1)$ order polynomial

$$V(q) - E = x^{r+1} - u_1 x^{r-1} - \dots - u_r. \quad (6.1.12)$$

This is now a suitable curve representing deformations about singularities which can be chosen as the realisation of ADE type Argyres-Douglas theories. Here the period integral of the curve $\tilde{y}^2 = V(x) - E$ is given by

$$\Pi_\gamma^0(x) = i \oint_\gamma \tilde{y}dx. \quad (6.1.13)$$

One can then construct a meromorphic basis of differentials [133], used to construct higher order quantum corrections for the WKB period, from the derivative of the one used in the

classical period such that

$$\partial_{u_i} \tilde{y} dx = -\frac{x^{r-i}}{2\tilde{y}} dx, \quad i : 1, \dots, r. \quad (6.1.14)$$

This can then be used to expand the differentials $p_n(x)dx$ in terms of this basis. This means that each term in the expansion of the differential can be written as

$$p_n(x)dx = i \sum_{j=1}^r b_j^{(n)} \partial_{u_j} \tilde{y} dx + \partial_x(\dots), \quad (6.1.15)$$

with a total derivative as the second term that is integrated out when taking the period. The full series expansion, for the quantum corrections (6.1.10) to the classical period, is given as follows

$$\Pi_\gamma^{(n)} = \sum_{i=1}^r b_i^{(n)} \partial_{u_i} \Pi_\gamma^{(0)}. \quad (6.1.16)$$

This means that every term in the expansion of the quantum period can be written as a linear combination of derivatives of the classical period. The coefficients $b_i^{(n)}$ must be determined by doing the computation of the classical period and its derivatives for a specific curve.

6.1.1 WKB for the cubic curve

We can now look at the special case of the cubic curve the discussion for which was started in [132] and continued for [133]. In general, it can be written in terms of a 2d complex moduli space with (u_1, u_2)

$$\Sigma : y^2 = x^3 - u_1 x - u_2. \quad (6.1.17)$$

This curve has discriminant $\Delta = 4u_1^3 - 27u_2^2$. Now, using the argument above for the cubic, the quantum corrections can be derived as

$$\Pi_\gamma^{(n)} = b_1^{(n)} \partial_{u_1} \Pi_\gamma^{(0)} + b_2^{(n)} \partial_{u_2} \Pi_\gamma^{(0)}. \quad (6.1.18)$$

One can now choose, as an example, the elliptic curve corresponding to the realisation of the Argyres-Douglas A_2 theory. This takes the form of

$$\Sigma_{A_2} : y^2 = 4x^3 - 3\Lambda^2 x + u, \quad (6.1.19)$$

where one can hold the (dynamically generated) scale Λ constant such that we can consider u_1 fixed. In this case, one has the classical periods corresponding to the central charges of

the BPS states

$$\Pi_{\gamma_1}^{(0)} = iZ_{\gamma_1}(u), \quad \Pi_{\gamma_2}^{(0)} = iZ_{\gamma_2}(u), \quad (6.1.20)$$

which will be used later in chapters 7 and 8 to determine the existence of BPS states by using the gradient flow to determine the existence conditions for particular BPS states in different regions of the moduli space. One can also use these central charges and their derivatives (if known explicitly) to calculate the quantum corrections to the classical periods.

6.2 Borel transformation of periods

A Borel transformation is a special type of transform that acts on a power series and is extensively reviewed, for example in Sauzin [135], and in Sternin, Shatalov [136]. If the Borel transformation is analytic along a particular ray on the Borel plane, and a Laplace integral can be taken along this ray that is finite, then the original series is called Borel summable. This integral is now known as the Borel sum. Also, the integral must be taken along a chosen ray that avoids singularities. This enables the study of wall crossing, as when the ray is taken on either side of a line containing singularities the result is different - these jumps can then encode the wall crossing phenomena we are studying. This has become important in perturbative QFTs where an expansion that in general does not converge can be rewritten as an analytic function.

6.2.1 Definition of Borel transform

The Borel transformation acts on the series as

$$\mathcal{O}(z) = \sum_{l=0}^{\infty} c_l z^{-(a+l)} \rightarrow \mathcal{BO}(\zeta) = \sum_{l=0}^{\infty} \frac{c_l}{\Gamma(a+l)} \zeta^{a+l-1}. \quad (6.2.1)$$

The Borel sum manifests its self as an integral along a ray

$$\mathcal{S}_\theta \mathcal{O}(z) = \int_0^{e^{i\theta}\infty} d\zeta e^{-\zeta z} \mathcal{BO}(\zeta), \quad (6.2.2)$$

where the ray is usually taken to lie along the real axis, so that one can write the integral as

$$\mathcal{SO}(z) = \int_0^\infty d\zeta e^{-\zeta z} \mathcal{BO}(\zeta). \quad (6.2.3)$$

The relationship between the series expansions can be shown by substituting the expression for the Borel transform back into the integral

$$\mathcal{SO}(z) = \int_0^\infty \frac{d\zeta}{\zeta} e^{-\zeta z} \sum_{l=0}^{\infty} \frac{c_l}{\Gamma(a+l)} \zeta^{a+l} = \sum_{l=0}^{\infty} c_l z^{-(a+l)}. \quad (6.2.4)$$

These transformations can be applied here (subsec. 6.2.2 below) to the quantum periods. They will also become useful for determining wall crossing phenomena in non-perturbative topological string partition functions for uncoupled BPS structures in chapter 12, e.g. for the deformed conifold in subsection 12.1.1.

6.2.2 Application to quantum periods

The Borel transformation and resummation of the quantum periods (6.1.9) can be written in terms of $z = \frac{1}{\hbar}$ as in [133, 134]:

$$\hat{\Pi}_\gamma(\zeta) = \sum_{n \geq 0} \frac{1}{(2n)!} \Pi_\gamma^n \zeta^{2n}, \quad s(\Pi_\gamma) = \frac{1}{\hbar} \int_0^\infty e^{-\frac{\zeta}{\hbar}} \hat{\Pi}_\gamma(\zeta) d\zeta. \quad (6.2.5)$$

The quantum period is Borel summable in the form of (6.2.5) if the integral converges in the limit $\hbar \rightarrow 0$. This Borel resummation has been taken along the ray $\mathbb{R}_{>0}$. This can be generalised to any ray along an angle ϕ such that one can use the integral

$$s_\phi(\Pi_\gamma) = \frac{1}{\hbar} \int_0^{e^{i\phi}\infty} e^{-\frac{\zeta}{\hbar}} \hat{\Pi}_\gamma(\zeta) d\zeta, \quad (6.2.6)$$

where these periods in (6.2.6) are Borel summable along the ray, of angle ϕ , if we have Borel resumability for the series $\Pi_\gamma(e^{i\phi}\hbar)$. As Borel resummations are discontinuous along singularities we now have jumps in the Borel resummations for the periods (known as Stokes jumps) such that there is a discontinuity of the period $\hat{\Pi}_\gamma(\zeta)$ for a particular ray in ζ and angle ϕ . For this we can define $s_{\phi_+}(\Pi_\gamma)$ and $s_{\phi_-}(\Pi_\gamma)$ on either side of the ray. These then become

$$s_{\phi_\pm}(\Pi_\gamma)(e^{i\phi}\hbar) = \lim_{\delta \rightarrow 0} s(\Pi_\gamma)(e^{i\phi \pm i\delta}\hbar). \quad (6.2.7)$$

The discontinuity along the ray at ϕ can then be calculated by taking the difference

$$\text{disc}_\phi(\Pi_\gamma) = s_+(\Pi_\gamma) - s_-(\Pi_\gamma). \quad (6.2.8)$$

The ray at the angle ϕ is known as a Stokes ray. Hence, it is possible to define a Stokes automorphism across the ray that can act on a series. This can be written as follows

$$\mathcal{O}_\phi = s_+ \circ s_-^{-1}, \quad (6.2.9)$$

where we are treating s_+, s_- and \mathcal{O}_ϕ as operators. The direction can be reversed by taking \mathcal{O}_ϕ^{-1} . Here a structure has been constructed for the Stokes jumps that depends just on the quantum periods. Stokes jumps will be discussed again in chapter 12 in the context of non-perturbative topological string free energies.

6.2.3 TBA equations

The Thermodynamic Bethe Ansatz (TBA) is a way to calculate the energy of ground states in an integrable quantum field theory. It can be used to find thermodynamic quantities such as the distributions for the energy and momentum of states in the model as well as the free energy. It has been determined that the WKB periods can be encoded within such a TBA system of equations.

It is possible to construct a system of TBA equations using a Riemann-Hilbert problem for the periods. The problem was described by Voros in [137], for the example of the quartic potential. There are known solutions to this Riemann-Hilbert problem given by Giaotto, Moore, Neitzke [31], in the context of a QFT on $\mathbb{R}^3 \times S^1$, with a low energy 3d sigma model description. The target space of this sigma model has a hyperkähler metric which can be constructed from the solutions of this Riemann-Hilbert problem. These solutions form a system of TBA equations which have been shown recently by [138] to describe quantum periods of Argyres-Douglas theories. From these equations one can then derive the conditions for wall crossing from the period ratio.

For this one can look back at the curve and the potential (6.1.8-6.1.12) and look at the turning points on this potential as was done in [133]. In general, we can consider a potential $V_{r+1}(x)$ where we consider this a degree $r + 1$ polynomial in a Riemann surface. The curve itself is hyperelliptic and has genus $g = \frac{r}{2}$. From this curve it is possible to calculate the classical periods using the turning points of the curve. When considering the turning points one can look at a region in the moduli space where they all occur at real coordinates which can be arranged in order such that if one labels the points x_i they satisfy: $x_1 < x_2 < \dots < x_{r+1}$. The classical periods correspond to the cycles around particular turning points. The cycles γ_i , $i : 1, \dots, r$, are taken to be around $[x_i, x_{i+1}]$, which is an interval between the turning points. In this case, a configuration is chosen such that the odd and even classical periods or masses are

$$m_{2i-1} = \Pi_{\gamma_{2i-1}}^0 = 2 \int_{x_{2i-1}}^{x_{2i}} p(x) dx, \quad m_{2i} = i \Pi_{\gamma_{2i}}^0 = 2i \int_{x_{2i}}^{x_{2i+1}} p(x) dx. \quad (6.2.10)$$

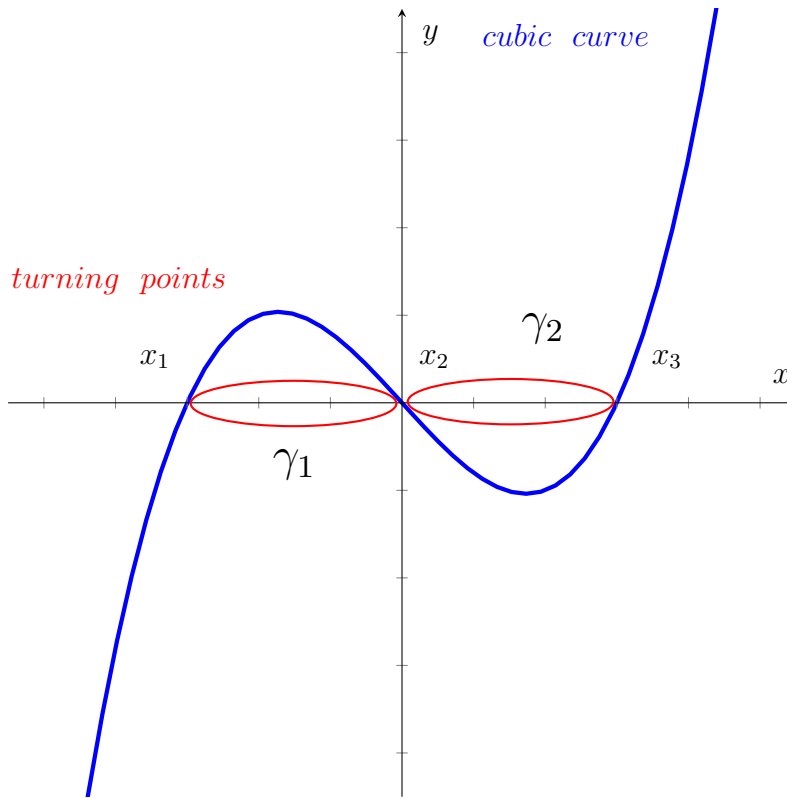


Figure 6.1: Plot of a cubic curve with turning points. The cycles can then be taken around these turning points.

Now one can look back at the quantum periods. For these periods discontinuity formulae have been derived for both odd and even cycles [133]. For example, the odd cycles satisfy

$$\text{disc } \Pi_{\gamma_{2i-1}} = -i\hbar \log(1 + e^{-\frac{i}{\hbar} \Pi_{\gamma_{2i-2}}(\hbar)}) - i\hbar \log(1 + e^{-\frac{i}{\hbar} \Pi_{\gamma_{2i}}(\hbar)}). \quad (6.2.11)$$

and a discontinuity relation for the even case can also be derived by exchanging cycles. One can then write these relations together, but one must first define:

$$\begin{aligned} -i\epsilon_{2i-1}(\theta + i\frac{\pi}{2} \pm i\delta) &= \frac{1}{\hbar} s_{\pm}(\Pi_{\gamma_{2i-1}})(\hbar), \\ -i\epsilon_{2i}(\theta) &= \frac{1}{\hbar} s(\Pi_{\gamma_{2i}})(\hbar), \end{aligned} \quad (6.2.12)$$

where $0 < \delta \ll 1$ is a small parameter. One also has $e^{i\theta} = \frac{1}{\hbar}$. Now we can define a new function with which one can completely encode all the discontinuities. This can be written as

$$L_a(\theta) = \log(1 + e^{\epsilon_a(\theta)}), \quad L_0(\theta), \quad L_{r+1}(\theta) = 0, \quad a : 1, \dots, r. \quad (6.2.13)$$

Now we can finally write the discontinuity formulae together as

$$\text{disc}_{\frac{\pi}{2}} \epsilon_a(\theta) = L_{a-1}(\theta) + L_{a+1}(\theta) \quad a : 1, \dots, r, \quad (6.2.14)$$

where the formulae constitute a Riemann-Hilbert problem for ϵ_a . These functions take the form $\epsilon_a = m_a e^\theta + \mathcal{O}(e^{-\theta})$, in the limit $\theta \rightarrow \infty$. This Riemann-Hilbert problem has a known solution [31, 133]. This is a set of TBA equations and reads as

$$\epsilon_a(\theta) = m_a e^\theta - \int_{\mathbb{R}} \frac{L_{a-1}(\theta')}{\cosh(\theta - \theta')} \frac{d\theta'}{2\pi} - \int_{\mathbb{R}} \frac{L_{a+1}(\theta')}{\cosh(\theta - \theta')} \frac{d\theta'}{2\pi} \quad a : 1, \dots, r. \quad (6.2.15)$$

This system was derived for a region in the moduli space where m_{2i-1} and m_{2i} are real. This region is also known as the minimal chamber. However, in general these are complex functions and take the form: $m_a = |m_a| e^{i\phi_a}$. This can be incorporated into the TBA equations by shifting the functions as follows

$$\tilde{L}_a(\theta) \rightarrow \tilde{L}_a(\theta - i\phi_a), \quad \tilde{\epsilon}_a(\theta) \rightarrow \epsilon_a(\theta - i\phi_a), \quad (6.2.16)$$

which can then be substituted into the TBA system to give

$$\tilde{\epsilon}_a(\theta) = m_a e^\theta - \int_{\mathbb{R}} \frac{\tilde{L}_{a-1}(\theta')}{\cosh(\theta - \theta' - i\phi_a + i\phi_{a-1})} \frac{d\theta'}{2\pi} - \int_{\mathbb{R}} \frac{\tilde{L}_{a+1}(\theta')}{\cosh(\theta - \theta' - i\phi_a + i\phi_{a+1})} \frac{d\theta'}{2\pi}. \quad (6.2.17)$$

Now one can consider the poles of (6.2.17). It can be seen [133] that there are poles at $|\phi_a - \phi_{a\pm 1}| = \frac{\pi}{2}$ such that the equations only hold in the region of the moduli space where $|\phi_a - \phi_{a\pm 1}| < \frac{\pi}{2}$. There are further poles at $\frac{(n+1)\pi}{2}$. These poles represent walls of marginal stability associated to BPS states existing in the spectrum. Now we look at the simplest example of the cubic with $r = 2$ that realises the A_2 model. Here one can move between 2 regions of the moduli space

$$\phi_2 - \phi_1 < \frac{\pi}{2} \quad \rightarrow \quad \phi_2 - \phi_1 > \frac{\pi}{2}, \quad (6.2.18)$$

where in this case the wall is crossed when $\phi_2 - \phi_1 = \frac{\pi}{2}$. For this example, considering that the functions in this case are at $m_1 = |m_1| e^{i\phi_1}$ and $m_2 = |m_2| e^{i\phi_2}$ this corresponds to a wall at

$$\text{Im} \left[\frac{\Pi_{\gamma_1}}{\Pi_{\gamma_2}} \right] = 0, \quad (6.2.19)$$

where one sees that (6.2.19) reproduces the equation of the wall in terms of a real ratio of the periods. From equations (6.1.20) and (6.2.10) one can see that this also holds in the classical limits that we are working in for the specific Argyres-Douglas or Seiberg-Witten theories when the appropriate curves are chosen on which to take the periods. In this case,

the period ratio is the wall of marginal stability. It is also interesting to note that the wall of marginal stability is represented by poles in a contour integral in a denominator of the form $\cosh(\theta - \theta' - i\phi_a + i\phi_{a-1})$. This form of integral for these $\mathcal{N} = 2$ theories is reminiscent of the situation in $\mathcal{N} = 4$ dyon counting formulae [40, 52, 53, 54]. However, in that case the integral was extracting Fourier coefficients. Later, in section 9.3 and chapter 11, it will be discussed if an exact analog can be found for the $\mathcal{N} = 2$ theories that counts BPS states with a similar contour prescription.

7 | Attractor flow in $\mathcal{N} = 2$ supergravity

In the previous chapters 3, 4, and 5, we have reviewed known prescriptions for computing the BPS spectrum in all the possible chambers in the moduli space for Argyres-Douglas theories. We now look for new methods that can reproduce these results and could be generalised to other BPS structures. We start by considering a very visual idea, known as attractor flow, that has been developed for $\mathcal{N} = 2$ supergravities, e.g. in [36, 56, 57]. We then apply it to effectively non-compact models described by local limits of compact Calabi-Yaus in which gravity decouples, as given by the decoupling limit in the work of Denef [139]. This can also be understood as zooming in close to the singularities where the CY becomes effectively non-compact. We look at the central charges of the BPS states, including those for the Argyres-Douglas theories described in the previous examples. This and the following chapter, 7 and 8, are based on the preprint “Special geometry, quasi-modularity and attractor flow for BPS structures” [62] done in collaboration with Alim, Beck and Biggs. Chapters 7 and 8 in this thesis include my contribution to this preprint, specifically the work on the attractor flow, with the addition of a brief review of the supergravity background in the first part of chapter 7.

7.1 Introduction to attractor flow of BPS states

BPS spectra in type II string theory on CY-3-folds, for example the quintic, have been studied in detail by Denef in the context of supergravity [57, 56], mapping the problem of determining the existence of BPS states within regions in the moduli space to the problem of determining solutions to the attractor flow equations. The attractor mechanism itself was first described in the context of extremal black hole solutions in $\mathcal{N} = 2$ supergravity [140]. The equations themselves subsequently emerged in [141, 142], and were formulated in terms of a time derivative in [143], such that the BPS mass is minimized in the limit of infinite time. BPS existence conditions were then formulated in terms of the value of the central charge at the end point of the attractor flow lines [55]. The reviews [144, 145] describe in detail the literature on attractor flow in the context of black hole solutions in supergravity, for example the radial flow of scalars with initial values at infinity to a fixed

point in the near horizon geometry, as well as the connection to the Bekenstein-Hawking entropy and the OSV conjecture ¹. The wall-crossing formulae we can recall from chapter 5.1, were developed in this context by Denef and Moore [36], giving a quantitative handle on the problem of determining the decay and recombination of BPS solutions. This was then further developed by [147], where the BPS index is explicitly determined from the split attractor flows. Importantly, it was found that the attractor flow splits as the composite states decay at a wall.

A significant contribution of the split attractor flow method, determining the BPS spectrum within different chambers of the moduli space, bounded by walls of marginal stability, was given in [57]. This was done for various examples, including type IIB string theory on the mirror quintic, and Seiberg-Witten theory in the low energy $\mathcal{N} = 2$ supergravity limit of type II string theory after gravity has been decoupled. The interpretation of the existence conditions for BPS states was further developed by finding the explicit black hole and empty hole (which have a central region with no energy)² solutions to the supergravity equations at the end point of the flow. Importantly, the existence conditions for Seiberg-Witten theory were determined in the context of monodromies around the singular points, which were then used to determine the known spectrum of BPS states. The method involved splitting the attractor flow of composite states at the wall of marginal stability and then allowing the resulting flow to pass through the relevant branch cuts.

In [56] the attractor flow method is extended to a detailed analysis of BPS type IIA D-branes on the quintic: here the attractor equations were written in the form of gradient flow of the central charges. The equations were solved approximately by minimizing the central charge using iterative methods and then the attractor flow lines were plotted. Existence conditions on the end point of the flow were considered as before.

Here, and in chapters 7-8, we re-derive and extend the results of [57] for Seiberg-Witten theory. We explicitly produce plots of iterative solutions to the attractor flow equations and find all possible flows between covers of the moduli space, using the existence conditions on these flows to determine the spectrum. We then extend this method to two parameterisations of the Argyres-Douglas A_2 theory and hereby determine the spectrum in this novel example. The A_1 model is also briefly discussed.

7.1.1 Wall crossing and attractor flow in $\mathcal{N} = 2$ supergravity

The attractor mechanism was first discovered for dyonic black holes in supergravity, where the black hole spacetime metric can be substituted into the supergravity action, and used to find the equations of motion. This also holds in the low energy effective supergravity limits of type IIB string theory: in our work we are considering the pure theory in the decoupling limit of the gravitational terms of the type IIB string, as described in [139].

¹This states that the black hole partition function is the modulus squared of the topological string partition function: $Z_{BH} = |Z_{top}|^2$ [146].

²See Fig. 7.2.

Our work involves $\frac{1}{2}$ BPS states on non-compact CY 3-folds, hence black holes cannot form from the resulting 4d solutions. However, there is still an interpretation as a supergravity solution. At special points in the moduli space these solutions can be interpreted in terms of Stromingers empty hole solutions [57] (shown in Fig. 7.2 with an empty central region with no energy).

The concept of attractor flow was originally interpreted as the minimisation of the BPS mass of the solution over time. This idea also holds in simple examples, such as the case of the A_2 or Seiberg-Witten theory. We start by following the paper by Denef, Green and Raugas [56], which investigates split attractor flows for the quintic, and then use their methods on the central charges of Argyres-Douglas theories, including the A_1 , A_2 models and Seiberg-Witten theory. Split attractor flows, which correspond to the multi-centered solutions splitting into multiple single-centered solutions, were used by [56] to find existence conditions on BPS states in the supergravity limit for the quintic.

4d metric

We derive the attractor flow on the moduli space by solving the BPS supergravity equations which can be found from the bosonic part of the 4d low energy limit of 10d type IIB string theory. One starts by studying a spherically symmetric metric (which is ideal for studying spherically symmetric solutions such as black holes), such that all quantities are just a function of a radial coordinate denoted by r [57]. In this case, the electric and magnetic charges of the supergravity solutions can be obtained by integrating the field strengths over a sphere at infinity. The solution then includes a radial function $U(r)$, which defines the metric. If this 4d spacetime metric is obtained in a low energy limit of type IIB string theory, $U(r)$ is also dependent on the period vector of the internal CY 3-fold [148, 149]. Furthermore, one has the scalar fields in the vectormultiplet of the theory $u^a(r)$, which define the moduli space [143]. This moduli space is a Kähler manifold [150].

There is also an alternative parameterisation in terms of the inverse radius $\tau = \frac{1}{r}$, where the radial function can be written as $U(\tau)$. To derive the attractor flow equations, one must first consider the equations of motion that can be derived from the 4d low energy bosonic supergravity action. One must then substitute a specific spacetime metric g_{ij} into the lagrangian, which can be found by first considering a general spherical 4d metric [56] of the form

$$ds^2 = -e^{2U(r)}(dt + w_i dx^i)^2 + e^{-2U(r)} dx^i dx^i. \quad (7.1.1)$$

Here \mathbf{x} is the coordinate vector centered at the origin, such that the radius is $r = |\mathbf{x}|$, and the vector $\mathbf{w} = w_i e_i$ describes the deformations of the metric. ³

One can let the metric become spherically symmetric by letting the components $w_i \rightarrow 0$, which then allows us to proceed in applying the method, from [56] for the quintic, to our

³This metric is asymptotically flat if $U(r), |\mathbf{w}| \rightarrow 0$ when $r \rightarrow \infty$.

Argyres-Douglas models. We consider that, in a supergravity theory, the BPS basis states have a 4d description in terms of such spherically symmetric solutions around a single point. They are thus called “single-centered”. Bound states of multiple BPS basis states have a description in terms of multiple solutions of the form just mentioned around different coordinate centers and are therefore called “multi-centered”.

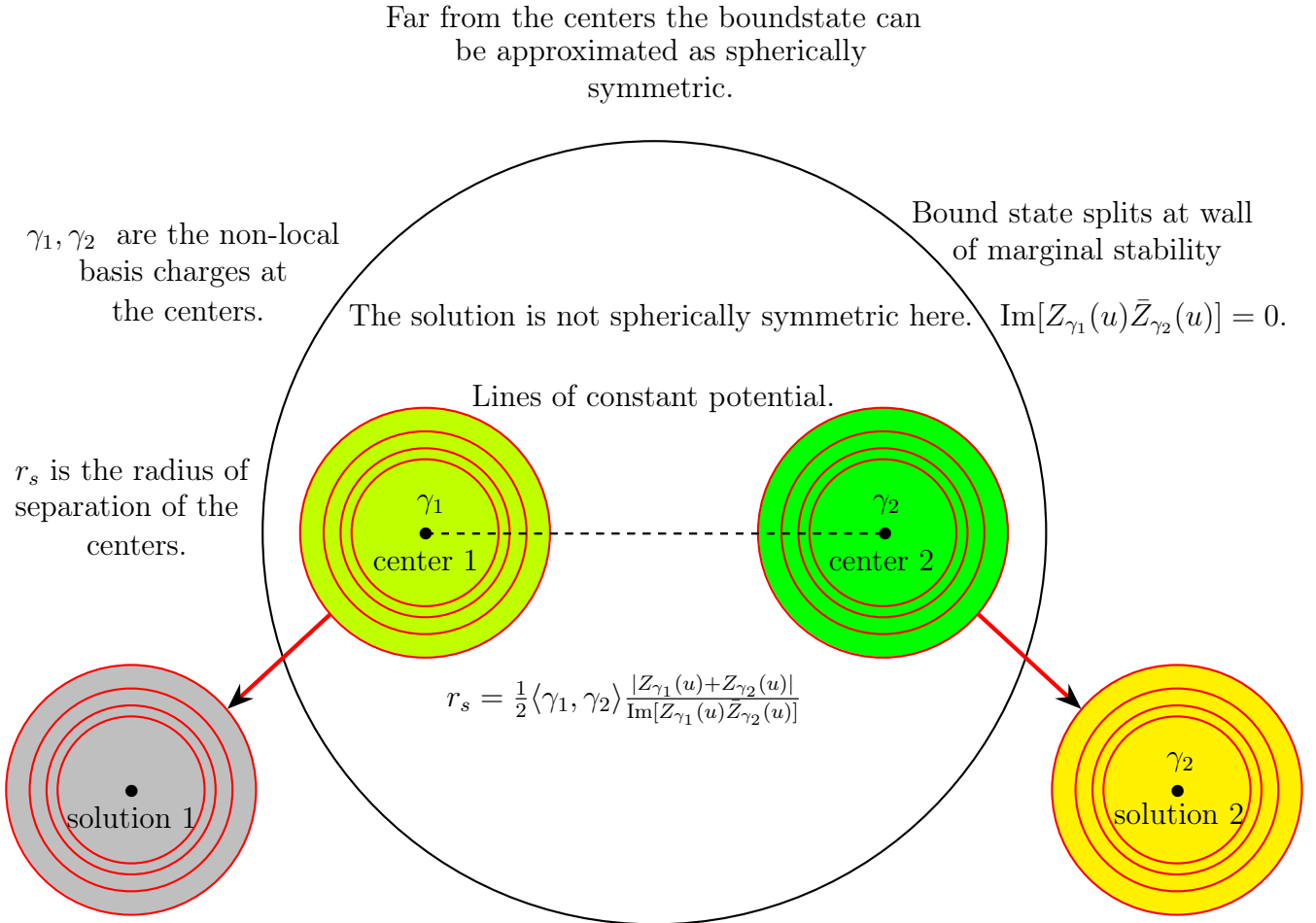


Figure 7.1: 2 centered solution: before and after it splits into 2 separate single-centered solutions.

This can be further understood by looking back to the metric and coordinate systems in (7.1.1-7.1.2): single-centered solutions in these models exist as BPS solutions, with metrics of the form (7.1.2), with spherical symmetry and charge located in spacetime at the origin. On the other hand, multi-centered solutions are not spherically symmetric, so in this case one must keep the deformed metric in (7.1.1). This changes the equations of motion that result when substituting the metric into the lagrangian. If the charges at the 2 centers are equal or parallel τ can be re-parameterised so that the attractor flow lines remain unaffected, otherwise one can take an approximation of spherical solutions at large distance from the two centers of the bound state. The spherically symmetric 4d space-time metric [56, 140, 143]

is given by the well known solution

$$ds^2 = -e^{2U(\tau)} dt^2 + e^{-2U(\tau)} dx^i dx^i. \quad (7.1.2)$$

We assume the solutions are asymptotically flat such that $U(\tau = 0) = 0$.

Supergravity equations of motion

This metric is what is substituted into the $\mathcal{N} = 2$, $d = 4$ supergravity action to derive the equations of motion. This is written in a 1 dimensional form in terms of the radial coordinate τ . The 1d effective action, in the time interval Δt , is denoted by S_{eff} [57]. This then becomes:

$$S_{eff} = \frac{S}{\Delta t} = -\frac{1}{2} \int_0^\infty d\tau \left(\dot{U}(\tau)^2 + \frac{1}{2} g_{a\bar{b}} \dot{u}^a \dot{\bar{u}}^{\bar{b}} + e^{2U(\tau)} V(u) \right) - \left(e^{2U(\tau)} |Z_\gamma(u)| \right)_{\tau=\infty}, \quad (7.1.3)$$

$$\text{where } V(u) = |Z_\gamma(u)|^2 + 4g^{a\bar{b}} \partial_a |Z_\gamma(u)| \bar{\partial}_{\bar{b}} |Z_\gamma(u)|.$$

Here the dot represents a derivative with respect to τ . The τ dependent coordinates at a point $u \in \mathcal{B}$ in the moduli space are written as $u^a(\tau)$, and $g^{a\bar{b}}$ is the inverse metric on the moduli space defined by

$$g_{a\bar{b}} = \partial_a \bar{\partial}_{\bar{b}} \mathcal{K}, \quad \text{where } \mathcal{K} = - \int_X i \ln \left(\Omega_0 \wedge \bar{\Omega}_0 \right). \quad (7.1.4)$$

Here, \mathcal{K} is the Kähler potential and Ω_0 is the holomorphic (3,0) form on the internal CY 3-fold X . This can be normalised as $\Omega = e^{\frac{\mathcal{K}}{2}} \Omega_0$ for later use in explicitly deriving the central charges. The central charge, denoted here again by $Z_\gamma(u)$, is dependent on the charges and the moduli. The supergravity equations of motion can be derived from this Lagrangian. This has been done in the spherically symmetric case for the single-centered BPS states with charge γ [143, 55, 56, 57]. They are given by

$$\partial_\tau U(\tau) = -e^{U(\tau)} |Z_\gamma(u)|, \quad (7.1.5)$$

$$\partial_\tau u^a = -2e^{U(\tau)} g^{a\bar{b}} \bar{\partial}_{\bar{b}} |Z_\gamma(u)|. \quad (7.1.6)$$

To solve these equations one would require the metric on the moduli space and the moduli dependence of the central charge. It has been found by [56], that unless one is at a singular or critical point of $|Z_\gamma(u)|$, the attractor flow equations (7.1.5-7.1.6) always drive the central charge to at least a local minimum in the moduli space. This can be understood [56] through the following equation:

$$\partial_\tau |Z_\gamma(u)| = -4e^{U(\tau)} g^{a\bar{b}} \partial_a |Z_\gamma(u)| \bar{\partial}_{\bar{b}} |Z_\gamma(u)| < 0. \quad (7.1.7)$$

Existence conditions for the BPS states

Given the positive definite metric and the positive product of the differentials of the central charges, there are several conditions on the existence of a BPS state with a particular central charge. These depend on the value of the central charge at the attractor point. The existence conditions were first described by Moore in [55] and applied in [56, 57, 62].

- (i) If $|Z_\gamma(u)| \neq 0$ at the modulus u_* (where $*$ denotes the attractor point) then the flow always exists as $\tau \rightarrow \infty$ and the equation describes a BPS black hole. In this case, the moduli tend towards their final value at the black hole horizon. Due to the non-compactness and decoupling from gravity, this is not the case in the A_2 model.
- (ii) If $|Z_\gamma(u)| = 0$ at u_* and u_* is a regular point in the moduli space then the above inequality is violated and no BPS states exist.
- (iii) If $|Z_\gamma(u)| = 0$ and u_* is a singular or boundary point in the moduli space then massless BPS states can exist. In this case one can interpret the resulting solution as an empty hole solution. Unlike a black hole this has no horizon but still has a core region. This core region being “empty” because it contains no energy (see Fig. 7.2). Such solutions are indeed possible in a non-compact CY 3-fold and occur in our research. These are the same solutions that exist for example at a conifold singularity [57].

7.2 Application to 1 parameter case

The main objective of our research is to find the solutions for Argyres-Douglas A_2 and Seiberg-Witten theory. These theories have a complex 1-dimensional moduli spaces with just 1 complex parameter u . Therefore, the attractor flow equations can be simplified in this 1-parameter case. In this case, all the components of the inverse metric vanish except for one, which can be written as $g^{u\bar{u}}$. Now looking back at equation (2.8) in Denef, Greene and Raugas [56], we have

$$\partial_\tau u = -2e^{U(\tau)} g^{u\bar{u}} \bar{\partial}_{\bar{u}} |Z_\gamma(u)|, \quad (7.2.1)$$

where τ is considered as a time parameter and is also the inverse of the radius of the solution $\tau = \frac{1}{r}$. One can now write the metric pre-factor to the derivative of the central charge as $\rho(\tau) = 2e^{U(\tau)} g^{u\bar{u}} > 0$ such that equation (7.2.1) [56, 57] becomes

$$\partial_\tau u = -\rho(\tau) \bar{\partial}_{\bar{u}} |Z_\gamma(u)|. \quad (7.2.2)$$

τ_* : value of τ at which moduli approach singular point

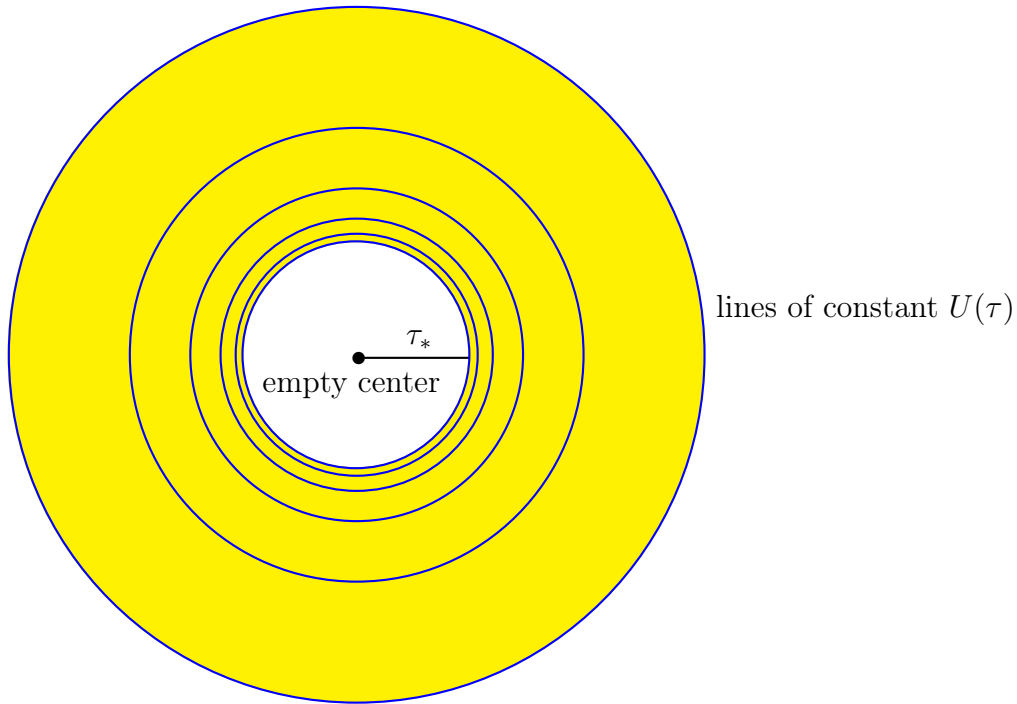


Figure 7.2: Solution with empty central region: the so called “empty” hole.

The time parameter τ can be re-parametrised to undo the dependence on $\rho(\tau)$:

$$\frac{1}{\rho(\tau)} \partial_\tau u = \partial_{\tau'} u = \frac{\partial \tau}{\partial \tau'} \partial_\tau u \longrightarrow \rho(\tau) = \frac{\partial \tau'}{\partial \tau}. \quad (7.2.3)$$

This is equivalent to writing the equations without the $\rho(\tau)$ and using a different definition of τ . It means that the attractor flow lines remain the same when the metric prefactor is reparameterized. So finally, in order to find a simple way to compute the flow lines, one can simply choose a parameterisation such that $\rho(\tau) = 1$. The attractor equation (7.2.2) can now simply be written as

$$\partial_\tau u = -\bar{\partial}_{\bar{u}} |Z_\gamma(u)|. \quad (7.2.4)$$

Furthermore, the inequality in (7.1.7) now becomes

$$\partial_\tau |Z_\gamma(u)| = -2\partial_u |Z_\gamma(u)| \bar{\partial}_{\bar{u}} |Z_\gamma(u)| < 0, \quad (7.2.5)$$

where this again shows that the flow lines always move towards a minimum value of the central charge. As stated in the literature [55, 57, 56], the attractor equations are the lines (or geodesics) of steepest descent of the central charge in the moduli space. Therefore, the only

required ingredient to input into the equations, to integrate and solve for these geodesics, is the moduli dependent central charge $|Z_\gamma(u)|$. The inverse metric factor $g^{u\bar{u}}$ can also be used if one wants to solve the exact equations of motion. However, this isn't necessary to determine the attractor flow lines as one can always use the τ re-parametrisation.

7.2.1 Path of steepest descent

The important thing to notice for this 1-parameter case is that the attractor flow lines are the lines of steepest descent for the modulus of $Z_\gamma(u)$. This greatly simplifies finding the attractor flow equations and allows us to write down the differential equation that must be solved for the attractor flow lines. $Z_\gamma(u)$ is a function of a complex 1-dimensional parameter u and its modulus can be written as $|Z_\gamma(u)|$. However, it can also be written as a function on \mathbb{R}^2 as $|Z_\gamma(x, y)|$. For a function in \mathbb{R}^2 the gradient is in the direction of the maximum rate of increase of the function

$$\nabla|Z_\gamma(x, y)| = \frac{\partial|Z_\gamma(x, y)|}{\partial x}\hat{e}_x + \frac{\partial|Z_\gamma(x, y)|}{\partial y}\hat{e}_y. \quad (7.2.6)$$

This path of steepest descent must therefore be tangent to $\nabla|Z_\gamma(x, y)|$ but in the opposite direction hence tangent to $-\nabla|Z_\gamma(x, y)|$. Therefore, the required differential equation describing the flow lines is

$$\frac{dy}{dx} = \frac{\left(\frac{\partial|Z_\gamma(x, y)|}{\partial y}\right)}{\left(\frac{\partial|Z_\gamma(x, y)|}{\partial x}\right)}. \quad (7.2.7)$$

When the expression for $|Z_\gamma(x, y)|$ is written in terms of x and y this equation should be integrated to find these flow lines. Unfortunately, this is not possible in the general case because the central charges involve hypergeometric functions with unknown integrals. However, the gradient flow can be computed iteratively and the attractor flow lines plotted from this. Also, in the limits around the singular points the integral can often be computed analytically.

7.2.2 Curves and periods

As explained previously in section 2.1.2, the BPS states in type IIB string theory arise from D3 branes wrapping 3-cycles in the threefold⁴. In the decoupling limit there is a one to one correspondence between the BPS supergravity solutions and the BPS states in the supersymmetric QFT with this brane construction. The D3 branes wrapped in the threefold have 1 dimensional slices on the Seiberg-Witten curve Σ_u embedded in the deformed CY-3-fold X_u which correspond to 1d cycles on this elliptic curve. The BPS central charge is

⁴These are also known as special Lagrangian submanifolds.

given by an integral over the normalised holomorphic (3,0) form Ω_u on the full CY-3-fold $Z_\gamma(u) = \int_\gamma \Omega_u$ and we take the reduction on the elliptic curve Σ . From this we obtain the meromorphic differential $\lambda_u = ydx$. The periods of the elliptic curve corresponding to the central charges then correspond to the integral of ydx over the cycles $\gamma_1, \gamma_2 \in H_1(\Sigma_u, \mathbb{Z})$ in the curve. In this work we will consider the following examples of BPS structures with complex one-dimensional moduli spaces \mathcal{B} and a dynamically generated scale Λ in the QFT defining the boundary of the strong and weak coupling regions [66]. These are associated to the physical theories. Their geometric realization, as outlined above, are given by the following curves. We denote these compactified elliptic curves by Σ :

1. Argyres–Douglas A_1 theory, realized geometrically by the curve:

$$\Sigma_{A_1} := \{y^2 = x^2 - 4u \in \mathbb{C}^2\}, \quad u \in \mathcal{B} = \mathbb{C}^* \quad (7.2.8)$$

2. Argyres–Douglas A_2 realized by:

$$\Sigma_{A_2}^I := \{y^2 = 4x^3 - 3\Lambda^2 x + u \in \mathbb{C}^2\}, \quad u \in \mathcal{B} = \mathbb{P}^1 \setminus \{\pm\Lambda^3, \infty\} \quad (7.2.9)$$

3. Argyres–Douglas A_2 realized by:

$$\Sigma_{A_2}^{II} := \{y^2 = (x - \Lambda^2)(x + \Lambda^2)(x - u) \in \mathbb{C}^2\}, \quad u \in \mathcal{B} = \mathbb{P}^1 \setminus \{\pm\Lambda^2, \infty\} \quad (7.2.10)$$

4. Seiberg–Witten $SU(2)$ realized by:

$$\Sigma_{SW} := \{y^2 = \frac{\Lambda^2}{x^3} + \frac{2u}{x^2} + \frac{\Lambda^2}{x} \in \mathbb{C} \times \mathbb{C}^*\}, \quad u \in \mathcal{B} = \mathbb{P}^1 \setminus \{\pm\Lambda^2, \infty\} \quad (7.2.11)$$

7.2.3 Picard-Fuchs equations and solutions

The next step is to choose the scaling $\Lambda = 1$. Now it is possible to derive Picard-Fuchs equations for the periods of the meromorphic differential. The derivation itself was done in [62] using the Griffiths pole order reduction methods. These were developed by Griffiths in [151, 152]. This then results in differential equations for the periods that can be solved. A particular linear combination of solutions can then be matched with the moduli dependent central charges of the BPS states using their monodromies. Here 4 examples and their associated Picard-Fuchs equations are briefly reviewed. The monodromies are shown for the singular points.

- (i) As in (7.2.8) the realisation of the A_1 curve is given by

$$\Sigma_{A_1} := y^2 = x^2 - 4u \in \mathbb{C}^2, \quad u \in \mathcal{B} = \mathbb{C}^*. \quad (7.2.12)$$

In this case, the Picard-Fuchs equation is simply

$$\partial_u(u\partial_u^2 f(u)) = 0. \quad (7.2.13)$$

such that one can immediately write the solution for the period as $f_1(u) = 2\pi i u$. There is another dual period taken over a cycle which is non-compact and can be determined by introducing a scale μ . This period is then given by

$$f_2(u) = u(\log u - 1) + \frac{\mu^2}{2} - 2u \log \mu + \mathcal{O}(1/\mu^2). \quad (7.2.14)$$

These are also the periods defining the special geometry in the Gaussian matrix model described in the Lecture notes [153]. There is another method that can be used to find the periods. This is to directly perform the period integrals on the curve over the cycles. The curve is a double cover of $\mathcal{C} = \mathbb{C}$, and has branch points at $\pm 2\sqrt{u}$. The compact cycle of the curve Σ is given by the lift of the cycle around the two branch points in the space \mathcal{C} . This cycle is denoted by A . The non-compact dual cycle is denoted by B , and is defined using the scale μ and considering the lift of the cycle around $2\sqrt{u}$ and μ .

The period integrals on the curve then reproduce the solutions to the Picard-Fuchs equation $y dx$ including

$$f_1(u) = \int_A y dx = 2\pi i u, \quad (7.2.15)$$

and the other period which is (μ -)regularized and dual to the first one

$$f_2(u) = \int_B y dx = u(\log u - 1) + \frac{\mu^2}{2} - 2u \log \mu + \mathcal{O}(1/\mu^2). \quad (7.2.16)$$

Once both periods are known one can determine the monodromy matrix about the singular point $u = 0$. This reads

$$M_0 = \begin{pmatrix} 1 & 1 \\ 0 & 1 \end{pmatrix}. \quad (7.2.17)$$

(ii) A realisation of the A_2 theory we worked with is given by the curve (based off (7.2.9)):

$$\Sigma_{A_2}^I := y^2 = 4x^3 - 3x - u \in \mathbb{C}^2, \quad u \in \mathcal{B} = \mathbb{P}^1 \setminus \{\pm 1, \infty\}. \quad (7.2.18)$$

The Picard-Fuchs equation associated to this curve is:

$$(1 - u^2)\partial_u^2 g(u) - \frac{5}{36}g(u) = 0. \quad (7.2.19)$$

The linearly independent solutions were found to be:

$$g_1(u) = \frac{3}{5\pi^{\frac{3}{2}}}(6\Gamma(\frac{7}{12})\Gamma(\frac{11}{12})F_2^1(-\frac{5}{12}, -\frac{1}{12}, \frac{1}{2}, u^2) - u\Gamma(\frac{1}{12})\Gamma(\frac{17}{12})F_2^1(\frac{1}{12}, \frac{5}{12}, \frac{3}{2}, u^2)), \quad (7.2.20)$$

$$g_2(u) = \frac{-3i}{5\pi^{\frac{3}{2}}}(6\Gamma(\frac{7}{12})\Gamma(\frac{11}{12})F_2^1(-\frac{5}{12}, -\frac{1}{12}, \frac{1}{2}, u^2) + u\Gamma(\frac{1}{12})\Gamma(\frac{17}{12})F_2^1(\frac{1}{12}, \frac{5}{12}, \frac{3}{2}, u^2)). \quad (7.2.21)$$

Here, the functions of the form $F_2^1(a, b, c, u)$ are hypergeometric. For $|u| < 1$ these functions are analytic and are represented by the hypergeometric series. For $|u| > 1$ one can find an analytic continuation such that the function again has such a series expansion. They are well known and described extensively for example in [154, 155], and in [156], along with many identities relating different hypergeometric and other special functions.

These solutions have the following monodromies about the singular points $-1, +1$ and ∞ , which can be taken around loops from a base point $u_b \in \mathcal{B}$ in the moduli space in a counterclockwise direction:

$$M_{+1} = \begin{pmatrix} 1 & -1 \\ 0 & 1 \end{pmatrix}, \quad M_{-1} = \begin{pmatrix} 1 & 0 \\ 1 & 1 \end{pmatrix}, \quad M_{\infty} = \begin{pmatrix} 0 & -1 \\ 1 & 1 \end{pmatrix}. \quad (7.2.22)$$

This can be seen by expanding the solutions around the singular points $u_s + \epsilon e^{i\theta}$, $\epsilon \in \mathbb{R}$ and taking the anti-clockwise loop $\theta : 0 \rightarrow 2\pi$. The expansions are shown in appendix part A, specifically part A.1.1 for this example. The third monodromy is determined by the other 2 such that $M_{\infty} = M_{+1}M_{-1}$. This can be seen by combining the loops around which the monodromies are taken.

(iii) The alternative realisation of the A_2 theory is given by the curve from (7.2.10):

$$\Sigma_{A_2}^I := y^2 = (x+1)(x-1)(x-u) \in \mathbb{C}^2, \quad u \in \mathcal{B} = \mathbb{P}^1 \setminus \{\pm 1, \infty\}. \quad (7.2.23)$$

The new Picard-Fuchs equation associated to this curve can be written as

$$u(u-1)\partial_u^2\pi(u) + (-2u+1)\partial_u\pi(u) + \frac{5}{4}\pi(u) = 0. \quad (7.2.24)$$

We solved these equations to obtain 2 linearly independent solutions:

$$\pi_1(u) = -\frac{8}{15}\sqrt{2}(-1+u^2)Q_{\frac{1}{2}}^2(u), \quad (7.2.25)$$

$$\pi_2(u) = -\frac{4}{15}\sqrt{2}i(-1+u^2)\pi P_{\frac{1}{2}}^2(u). \quad (7.2.26)$$

Here $P_{\frac{1}{2}}^2(u)$ is an associated Legendre polynomial (described for example in [157] and [156]) of fractional order corresponding to a solution of a hypergeometric differential Legendre equation. $Q_{\frac{1}{2}}^2(u)$ is the second solution of this hypergeometric differential equation. The numbers 2 and $\frac{1}{2}$ represent the degree and order respectively of the solution.

Again, in this case the monodromies around the singular points can be found (appendix A.1.2) by carrying out a series expansion at these points and then taking loops around them. For -1 and $+1$ we have:

$$M_{+1} = \begin{pmatrix} 1 & 0 \\ -2 & 1 \end{pmatrix}, \quad M_{-1} = \begin{pmatrix} 1 & 2 \\ 0 & 1 \end{pmatrix}, \quad M_{\infty} = \begin{pmatrix} 1 & 2 \\ -2 & -3 \end{pmatrix}. \quad (7.2.27)$$

(iv) Now we return to the curve for Seiberg-Witten theory in (7.2.11) while setting $\Lambda = 1$.

$$\Sigma_{SW} := \{y^2 = \frac{1}{x^3} + \frac{2u}{x^2} + \frac{1}{x} \in \mathbb{C} \times \mathbb{C}^*\}, \quad u \in \mathcal{B} = \mathbb{P}^1 \setminus \{\pm 1, \infty\} \quad (7.2.28)$$

For Seiberg-Witten theory the Picard-Fuchs equation becomes

$$(1-u^2)\partial_u^2 h(u) - \frac{1}{4}h(u) = 0. \quad (7.2.29)$$

This has solutions of the form

$$h_1(u) = -\frac{2^{\frac{1}{2}}}{\pi^{\frac{1}{2}}}\Gamma\left(\frac{3}{4}\right)^2 F_2^1\left(-\frac{1}{4}, -\frac{1}{4}, \frac{1}{2}, u^2\right) - u \frac{\Gamma\left(\frac{1}{4}\right)^2}{4\sqrt{2}\pi} F_2^1\left(\frac{1}{4}, \frac{1}{4}, \frac{3}{2}, u^2\right), \quad (7.2.30)$$

$$h_2(u) = -\frac{-i\sqrt{\pi}\Gamma\left(-\frac{1}{4}\right)}{8\Gamma\left(\frac{5}{4}\right)} F_2^1\left(-\frac{1}{4}, -\frac{1}{4}, \frac{1}{2}, u^2\right) - \frac{i\sqrt{\pi}\Gamma\left(\frac{5}{4}\right)}{\Gamma\left(\frac{3}{4}\right)} u F_2^1\left(\frac{1}{4}, \frac{1}{4}, \frac{3}{2}, u^2\right). \quad (7.2.31)$$

The monodromies in the case of Seiberg-Witten theory about the singular points $+1, -1$ and ∞ are well known [1]. However, as a different realisation of the curve has been used the monodromies that are obtained (from the expansions in appendix A.1.3) are also modified and are given by:

$$M_{+1} = \begin{pmatrix} 1 & 0 \\ -2 & 1 \end{pmatrix}, \quad M_{-1} = \begin{pmatrix} 1 & 2 \\ 0 & 1 \end{pmatrix}, \quad M_{\infty} = \begin{pmatrix} 1 & 2 \\ -2 & -3 \end{pmatrix}. \quad (7.2.32)$$

In this case, there are infinitely many covers for the central charges of the BPS states as one takes loops successively. This can also be used to generate the dyon spectrum in [1] and will be shown here in the next chapter 8 from the attractor flow.

The monodromies are determined by branch cuts (e.g. logarithmic) connecting the singular points. There is a further step necessary to conclude that these solutions to the Picard-Fuchs equations are indeed central charges of the BPS states of the physical theories we are working with. In general, any linear combination of solutions is also a solution so it is possible to choose a basis. A choice of basis in general produces different monodromies of the solutions around the singular points. To proceed, one must match these solutions with the central charges of the BPS states. This is done by matching the monodromies of the cycles around the singular points corresponding to the BPS states with the monodromies of solutions to the Picard-Fuchs equation. The monodromies for both the cycles and the solutions of the Picard-Fuchs equations for the first and second realisations of the A_2 case have indeed been found and matched in this way before this work was carried out.

8 | Attractor flow examples

Now the Picard-Fuchs equations are known and the solutions, with their monodromies, have been found and matched with the moduli dependent central charges, within the theories with complex 1-dimensional moduli spaces. This then allows us to apply the method of steepest decent from [56], described in section 7.2.1 and developed in [139], to such models originating from the literature [158, 159, 160, 161, 162] on type II effective field theories. We use this to find and plot the attractor flow lines iteratively (on MATHEMATICA) for all the cases mentioned above including the Argyres-Douglas A_1, A_2 theories [5, 9] as well as Seiberg-Witten theory [1]. In the cases with a wall of marginal stability between the weak and strong coupling regions, this is also plotted. The existence conditions on the endpoint of the flow [55, 56, 57] from subsection 7.1.1 are used to determine which BPS states exist in which chambers in the moduli space. Any split attractor flow lines are plotted. The branch cuts are also plotted, and when the flow lines enter or leave a cut they are continued through the branch cut by taking a loop around a singular point and acting on them with the appropriate monodromies from subsection 7.2.3.

8.1 Attractor flow for A_1 -theory

We proceed to derive the attractor flow for the A_1 -model. This arises from the deformed conifold, described for example in [60]. We are using the path of steepest descent method, described in subsection 7.2.1, to derive the flow lines. In this case, the central charge is simply $Z_{\gamma_1}(u) = u$.

- a.) We let $u := x + iy$ such that $|Z_{\gamma_i}(u)| := |Z_{\gamma_i}(x + iy)| \in \mathbb{R}^+$.
- b.) For $Z_{\gamma_1}(u) = u$ we have $|Z_{\gamma_1}(u)| = |u| = |x + iy| = \sqrt{x^2 + y^2}$.
- c.) We substitute this expression into the gradient flow equations to derive the attractor flow lines

$$\frac{dy}{dx} = \frac{\left(\frac{\partial|Z_{\gamma_i}(x,y)|}{\partial y}\right)}{\left(\frac{\partial|Z_{\gamma_i}(x,y)|}{\partial x}\right)} = \frac{\frac{y}{\sqrt{x^2+y^2}}}{\frac{x}{\sqrt{x^2+y^2}}} = \frac{y}{x}. \quad (8.1.1)$$

d.) The equation can be solved as

$$\frac{1}{y}dy = \frac{1}{x}dx \rightarrow y = Ax. \quad (8.1.2)$$

Hence, the equations $y = Ax$ from (8.1.1-8.1.2) describe the set of all straight lines L passing through the origin. The attractor flow lines then correspond to straight lines flowing to the origin. Now we can also look at this in terms of the time parameter τ . In this form, the attractor flow equation can be written as

$$\frac{dx}{d\tau} = -\frac{\partial|Z_{\gamma_i}(x,y)|}{\partial x} = -\frac{x}{\sqrt{x^2+y^2}} = -\frac{x}{\sqrt{(1+A^2)x^2}} = -\frac{1}{\sqrt{1+A^2}} = \alpha. \quad (8.1.3)$$

Therefore, the coordinate x is linear in the time coordinate such that:

$$x = \alpha\tau + \beta. \quad (8.1.4)$$

One can plot these attractor flow lines (see Fig. 8.1) on the moduli space as a radial flow flowing into the origin.

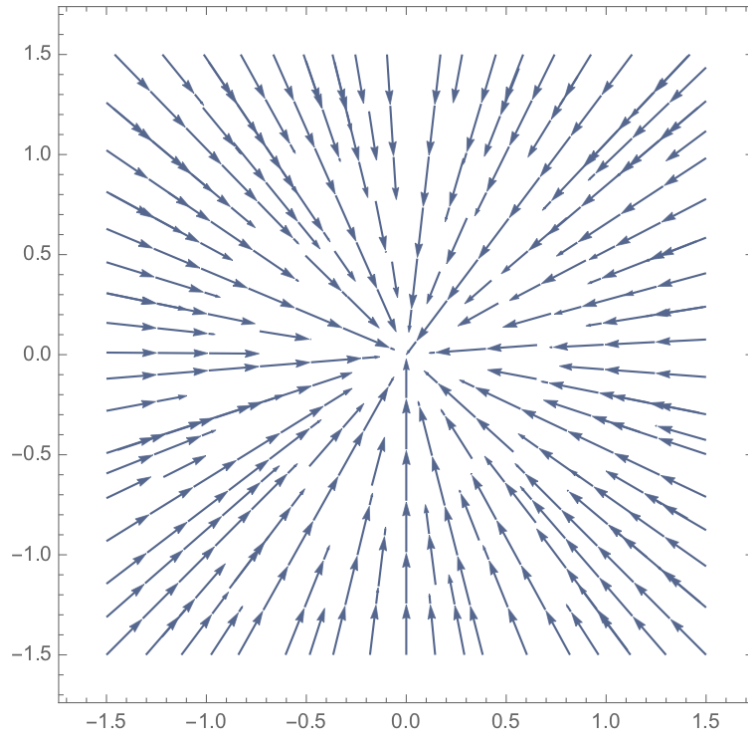


Figure 8.1: This diagram shows the attractor flow lines of A_1 flowing to its attractor point at the origin.

Final state in chamber

Hence, we can see that in this theory there is only 1 BPS state flowing to the attractor point at the origin. There are no walls of marginal stability or jumps in the number of BPS states.

Chamber	Existing charges	Count
1: All space	γ_1	1

Table 8.1: Single BPS state that exists everywhere in the moduli space.

8.2 Attractor flow for Argyres–Douglas A_2 theory

We now repeat this process for A_2 theory [5, 9]. We take the exact expressions for all possible linear combinations of the central charges $Z_{\gamma_i}(u)$, for each realisation of the theory, and derive the attractor flow lines from the gradient flow (see section 7.2.1) using MATHEMATICA. We let $u \rightarrow \frac{1}{u}$ to have the origin of the complex plane at infinity. We then proceed in the following way; we first let $u := x + iy \in \mathbb{P}^1$ such that the modulus of the central charge $|Z_{\gamma_i}(u)| := |Z_{\gamma_i}(x + iy)| \in \mathbb{R}^+$. As before, we substitute this expression into the gradient flow equations to derive the attractor flow lines

$$\text{gradient flow: } \frac{dy}{dx} = \frac{\left(\frac{\partial |Z_{\gamma_i}(x,y)|}{\partial y}\right)}{\left(\frac{\partial |Z_{\gamma_i}(x,y)|}{\partial x}\right)}. \quad (8.2.1)$$

8.2.1 Walls, branch cuts and flow lines

Wall of marginal stability and existence

We take into consideration the wall crossing phenomena in which a BPS exists (is stable) in one region of the u -plane, but is excluded by the existence conditions from [55, 56, 57] in another region (see section 7.1.1). Physically this corresponds to a region of the moduli space in which the composite BPS particle is unstable and decays into a combination of its constituents. For this we also plot the wall of marginal stability MS_{γ_1, γ_2} that bounds the stable and unstable regions on the u -plane: for the meromorphic differential $\tilde{y}dz$ from section 7.2.2 this is given by the locus of real ratio of the periods

$$MS_{\gamma_1, \gamma_2} : \frac{Z_{\gamma_1}(u)}{Z_{\gamma_2}(u)} \in \mathbb{R}. \quad (8.2.2)$$

The decay of a BPS state in a chamber is represented diagrammatically by split attractor flow lines: a flow line enters a chamber and would end at a regular point in the moduli space. Therefore, it is excluded in the chamber but still existed before it crossed the wall of marginal stability MS_{γ_1, γ_2} . In this case, the flow line hits the wall of marginal stability and splits into constituent BPS flow lines corresponding to BPS states that are stable within the region.

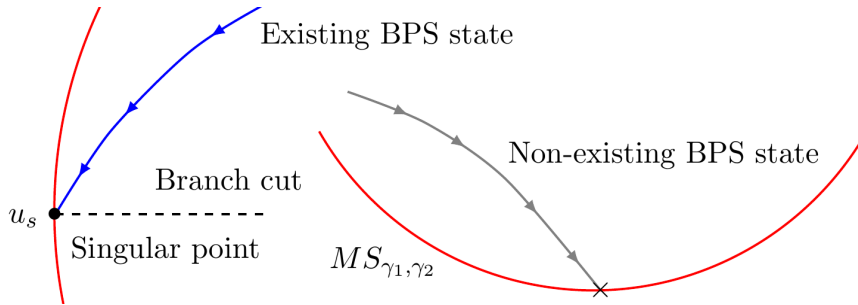


Figure 8.2: BPS state only exists if flow terminates at singular point u_s .

Comment on branch cuts

We also consider the branch cuts of the $Z_{\gamma_i}(u)$ in the u -plane. We find the branch cuts and plot the segments which affect the attractor flow lines. When an attractor flow line enters a branch cut, we follow [56, 57] by finding a path in the u -plane which connects the point at which the attractor flow line enters the branch cut (shown from above in Fig. 8.3) and leaves it (shown from below). We determine which singular points this path encloses and act on $Z_{\gamma_i}(u)$ with the monodromies M_{u_s} associated to the corresponding singular points $u_s \in \mathcal{B}$. We write $u = u_s + \epsilon e^{-i\theta}$, $\epsilon \in \mathbb{R}^+$, $\theta \in \{0, 2\pi\}$ and let $\theta : 0 \mapsto 2\pi$. The monodromies from section 7.2.3 can be read off from the expansions around the singular points given in appendix A.

We then continue this modified central charge through the branch cut. The same existence conditions then apply on the other side of the branch cut. If the state is excluded on the other side of the branch cut, by a regular termination point, then it also didn't exist before it entered the branch cut - up until the last point after it crossed the wall of marginal stability MS_{γ_1, γ_2} where it decayed into its constituent BPS states.

8.2.2 Attractor flow first realisation

We will start by using the curve $\Sigma_{A_2}^I$, for the first realisation, and consider flow lines of all possible $Z_{\gamma_i}(u)$. We plot a diagram Fig. 8.4 with the existing flow lines and the split attractor flow. When we compute the central charges and take the ratio we just obtain a

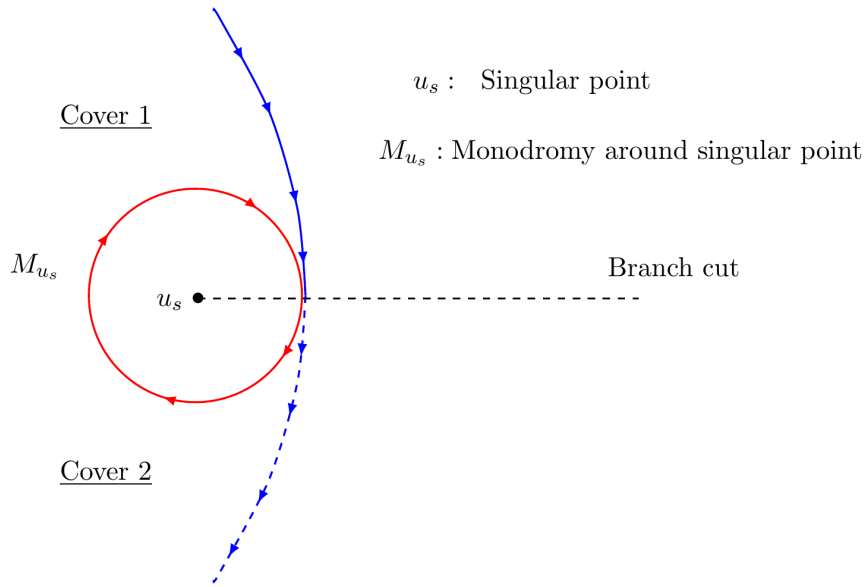


Figure 8.3: Single flow line passing through branch cut after acting with monodromy around singular point.

wall separating 2 chambers: an outer and inner region (see Fig. 8.4) labelled as A and B respectively. This is the standard realisation of the wall used the literature e.g. [31] and can be obtained by taking a slice in the complex 2d moduli space of $SU(3)$ [5] containing the Argyres-Douglas points [163]. In this parameterisation there are also 2 regions but with the wall shifted along the y -axis.

	Existing BPS states					Non-existing BPS states
Flow line						
Charges	γ_1	γ_2	$\gamma_1 + \gamma_2$	γ_1 continuation	γ_2 continuation	$\gamma_1 + \gamma_2$ outside wall

Table 8.2: Flow lines in Fig. 8.4.

Description of flow lines

$Z_{\gamma_1}(u)$ and $Z_{\gamma_2}(u)$ (7.2.20-7.2.21) are, for a particular cover, defined for $u \in \mathbb{P}^1 \setminus [-1, \infty)$ and $u \in \mathbb{P}^1 \setminus [1, \infty)$ respectively. They have $u^b \log u$ branch cuts $[-1, \infty)$ and $(\infty, 1]$ represented by and on Fig. 8.4 respectively, separating the regions B1 and B2. This allows for the analytic continuation of the central charges onto new covers. Their flow lines are represented on this diagram by blue and red lines, and flow to +1 and -1 respectively. Both are singular points, hence $Z_{\gamma_1}(u)$ and $Z_{\gamma_2}(u)$ exist everywhere. This holds in both the inner region B and outer region A.

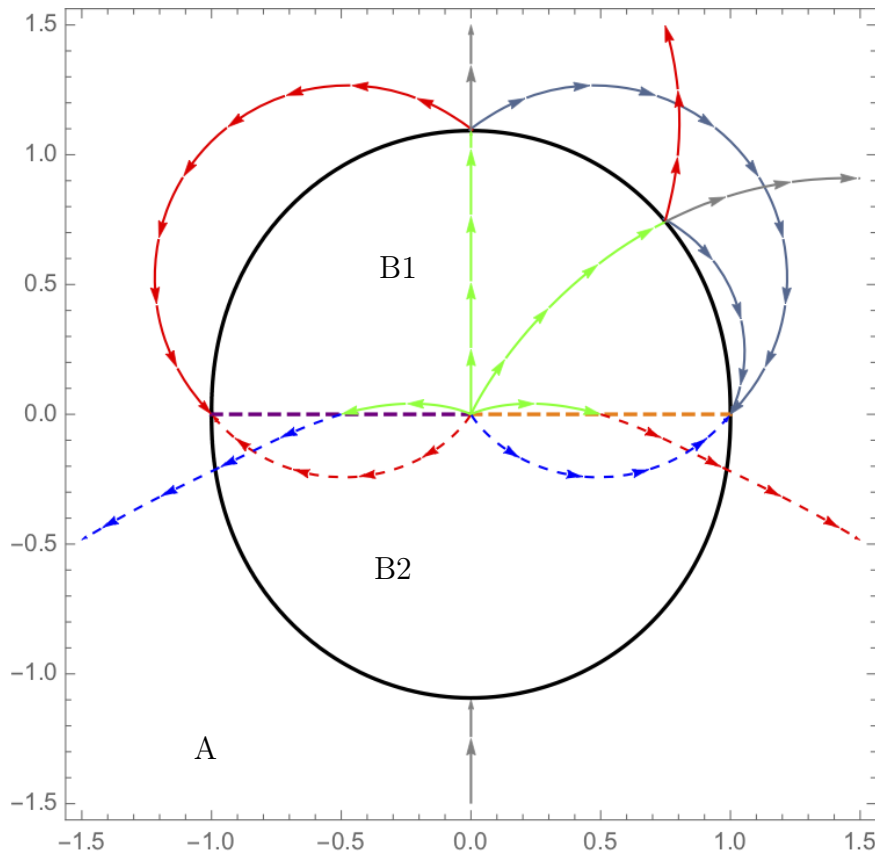


Figure 8.4: As before the black line is the wall of marginal stability.

- a.) The purple line represents the $Z_{\gamma_1}(u)$ branch cut and the orange line is that of $Z_{\gamma_2}(u)$. The blue and red flow lines represent $Z_{\gamma_1}(u)$ and $Z_{\gamma_2}(u)$ respectively.
- b.) The solid green line represents the sum of the basis states $Z_{\gamma_1}(u) + Z_{\gamma_2}(u)$. The dashed blue and red lines represent the analytic continuation of $Z_{\gamma_1}(u) + Z_{\gamma_2}(u)$ through the branch cuts of $Z_{\gamma_1}(u)$ and $Z_{\gamma_2}(u)$ respectively.

In this case, when the sum is analytically continued through the branch cuts, it becomes $Z_{\gamma_1}(u)$ around the left cut and $Z_{\gamma_2}(u)$ around the right cut. Again, the gray lines represent the unstable continuation of $Z_{\gamma_1}(u) + Z_{\gamma_2}(u)$ flow in the outer region A where it crashes at a regular point.

Wall crossing of dyon

The sum, represented by $\text{---}\rightarrow$, and written as $Z_{\gamma_1}(u) + Z_{\gamma_2}(u)$, has a more complicated

behavior. Its source is at infinity. It exists within the inner region B. However, outside this region, where it is represented by the gray line \longrightarrow , it flows to a regular point on the wall, is hereby excluded, and must therefore split into its constituent BPS states $Z_{\gamma_1}(u), Z_{\gamma_2}(u)$, as shown on the diagram above. The situation with the sum $Z_{\gamma_1}(u) + Z_{\gamma_2}(u)$ in the inner chamber B is more involved: it first appears that the attractor flow lines terminate at the same regular point in the moduli space as they do from the outside. However, in this case we must take the branch cuts of the basis charges into account.

We must now use the method introduced in 8.2.1. This means we analytically continue the flow of $Z_{\gamma_1}(u) + Z_{\gamma_2}(u)$ through the branch cuts between B1 and B2 by taking paths around the singular points at ± 1 and acting with the associated monodromy matrix, from (7.2.22), in the right direction. We look at 2 cases:

- (i) In the first case, represented by $---\blacktriangleright$, the analytic continuation of the central charges acts in a clockwise direction around -1 as

$$(M_{-1})^{-1} : Z_{\gamma_1}(u) \longmapsto Z_{\gamma_1}(u) - Z_{\gamma_2}(u), \quad (8.2.3)$$

$$\text{such that } Z_{\gamma_1}(u) + Z_{\gamma_2}(u) \longmapsto Z_{\gamma_1}(u).$$

This then leaves the branch cut in B2 as the dashed blue line.

- (ii) In the second case, represented by $----\blacktriangleright$, the continuation acts in a counter-clockwise direction around $+1$:

$$M_{+1} : Z_{\gamma_2}(u) \longmapsto Z_{\gamma_2}(u) - Z_{\gamma_1}(u), \quad (8.2.4)$$

$$\text{such that } Z_{\gamma_1}(u) + Z_{\gamma_2}(u) \longmapsto Z_{\gamma_2}(u),$$

and leaves the branch cut in B2 as the dashed red line.

Hence, one can see from (8.2.3-8.2.4), when the sum in the upper half plane is continued through the branch cuts, where it flows in, it subsequently flows out in the lower half plane as one of the basis states. This then flows to the singular points ± 1 and therefore exists.

One can use the analytic continuation of the central charges to find a region in which the sum of a particle and an antiparticle, e.g. $\gamma_1 - \gamma_2$, can exist. In the region B2 on the diagram Fig. 8.4, taken below the 2 branch cuts and above the outer lower arc ¹, the central charge of the basis states $Z_{\gamma_1}(u), Z_{\gamma_2}(u)$ becomes either $Z_{\gamma_1}(u) - Z_{\gamma_2}(u)$ or $-Z_{\gamma_1}(u) + Z_{\gamma_2}(u)$. This depends on which branch cut the analytic continuation is done through, the sign of the basis state before the continuation. There are now 2 possible covers one must consider for the central charges with either $\gamma_1 - \gamma_2$ or $-\gamma_1 + \gamma_2$ existing on it. .

¹This is the lower part of the central chamber.

Exclusion of higher linear combinations $nZ_{\gamma_1}(u) + mZ_{\gamma_2}(u)$

After this we consider the general state $n\gamma_1 + m\gamma_2$. For this, one needs to consider termination points corresponding to

$$nZ_{\gamma_1}(u) + mZ_{\gamma_2}(u) = 0, \quad (8.2.5)$$

for all (n, m) . If the point is a regular point on the wall, the state doesn't exist. In the discussion below we will show that all states other than $(0, 1)$, $(1, 0)$ and $(1, 1)$ are excluded by regular termination points on segments of the wall. This is done by considering the alignment or anti-alignment of the central charges (described in Fig. 8.5) on the wall and the range of the ratio on paths between singular points. If there is a change in sign along the path then equation (8.2.5) has a solution and a combination is excluded.

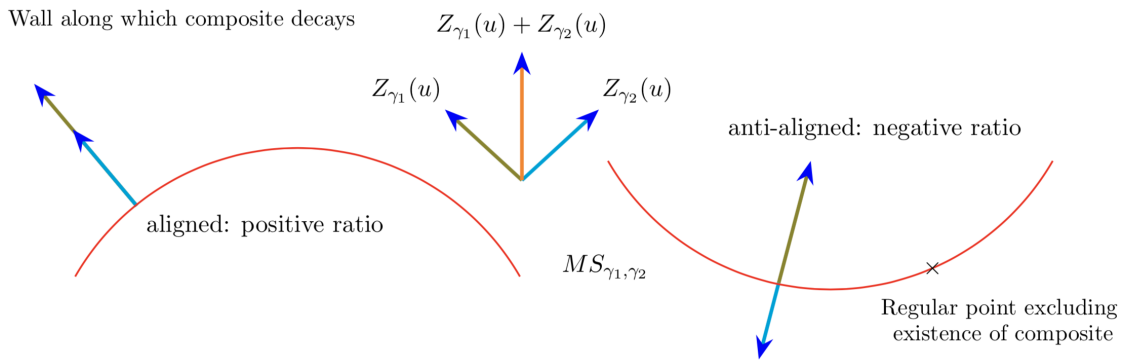


Figure 8.5: Alignment and anti-alignment of central charges on different general segments of a wall of marginal stability.

From this one can see that in the outer region A these higher linear combinations flow to and are excluded by a regular point on the lower segment of the wall, like the sum, but this time shifted according to the ratio $\frac{n}{m}$. This is because of the anti-alignment of the central charges on this segment. We present a table (8.3) here representing the ratios of the central charges along a path (8.2.6) on the wall from

$$1 \longrightarrow -1 \longrightarrow 1, \quad (8.2.6)$$

along the lower segment then the upper segment respectively. Within the inner region B things become more involved and one must consider the logarithmic branch cuts $[\pm 1, \infty)$. In this case, we find that for $n\gamma_1 + m\gamma_2$ within the inner chamber, the flow line for $nZ_{\gamma_1}(u) + mZ_{\gamma_2}(u)$, $\forall n, m \geq 1$ also ends at a regular point on the lower segment of the wall.

However, as with the case for $Z_{\gamma_1}(u) + Z_{\gamma_2}(u)$, it flows through the branch cuts before it can reach the point. Again, we must act with the corresponding monodromies from (7.2.22) around the singular points to transform the central charges and then analytically continue

ratios along path				
paths between singular points	$Z_{\gamma_1}(u)$	$Z_{\gamma_2}(u)$	$Z_{\gamma_1}(u)/Z_{\gamma_2}(u)$	$Z_{\gamma_2}(u)/Z_{\gamma_1}(u)$
1	0	$2.29i$	$+\infty$	0
-1	2.29	0	0	$\pm\infty$
1	0	$2.29i$	$-\infty$	0

Table 8.3: Ratio of central charges at singular points along wall.

through the branch cut.

Excluding higher combinations using range of ratio

Unlike $Z_{\gamma_1}(u) + Z_{\gamma_2}(u)$, the higher combinations $n, m > 1, n \neq m$ do not become the basis states when flowing through the branch cuts, instead they remain states with $m, n > 1, n \neq m$, and the ratio $\frac{n}{m}$ keeps the same sign. This means the states will continue to flow and terminate at another regular point on the lower segment of the wall. Therefore, as with the previous parameterisation, states of the form, $n\gamma_1 + m\gamma_2$ $n, m \geq 1, \frac{n}{m}, \frac{m}{n} > 1$ are excluded in the inner region B as well and hence do not exist/ are unstable anywhere in the moduli space.

Example

Non - existing BPS states				
Flow line	----->		----->	
Charges	$3\gamma_1 + 2\gamma_2$		$\gamma_1 + 2\gamma_2$	
Forked flow lines	----->	----->	----->	----->
Charges	$\gamma_1 + \gamma_2$	$2\gamma_1 + \gamma_2$	γ_2	$\gamma_1 + \gamma_2$

Table 8.4: Forked flow lines of non-existing BPS states on Fig. 8.6.

An example flow -----> in chamber B (the dotted black line) is given by $3Z_{\gamma_1}(u) + 2Z_{\gamma_2}(u)$ and is shown in the diagram Fig. 8.6 above. As it passes through the branch cut between B1 and B2, we act with an M_{+1} (from (7.2.22)) in a counter-clockwise direction and transform

$$3Z_{\gamma_1}(u) + 2Z_{\gamma_2}(u) \mapsto 3Z_{\gamma_1}(u) + 2(Z_{\gamma_2}(u) - Z_{\gamma_1}(u)) \mapsto Z_{\gamma_1}(u) + 2Z_{\gamma_2}(u). \quad (8.2.7)$$

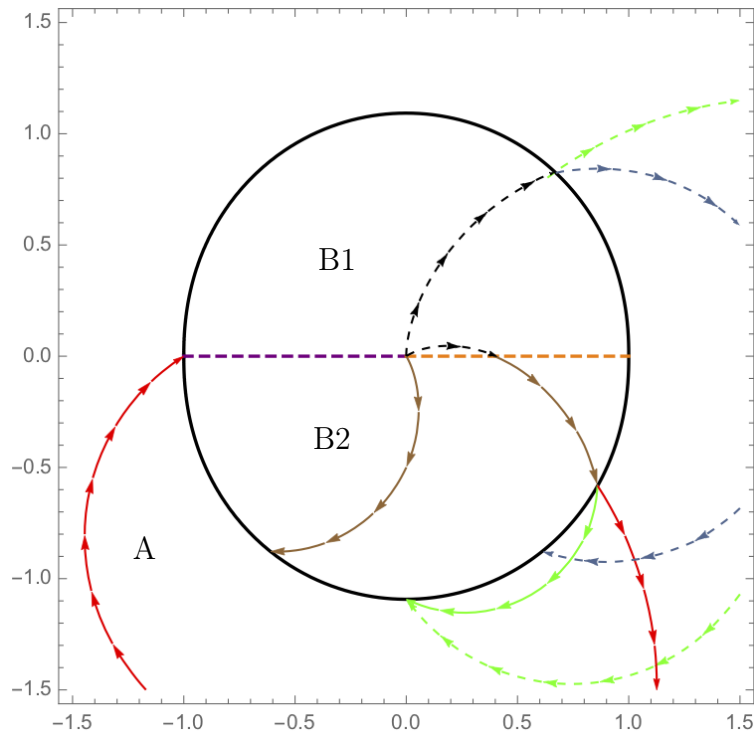


Figure 8.6: The black dotted line in B1 represents the flow of the charge $3Z_{\gamma_1}(u) + 2Z_{\gamma_2}(u)$. Its flow through the branch cut along $(\infty, 1]$ is shown. In this case, it becomes $Z_{\gamma_1}(u) + 2Z_{\gamma_2}(u)$ in B2, represented by the brown line, which can terminate at a regular point on the wall. The black dotted line splits into the green and blue dashed lines, representing the sum $Z_{\gamma_1}(u) + Z_{\gamma_2}(u)$ and $2Z_{\gamma_1}(u) + Z_{\gamma_2}(u)$ respectively. Similarly, the diagram shows the splitting of the brown line into green and red lines, representing $Z_{\gamma_1}(u) + Z_{\gamma_2}(u)$ and $Z_{\gamma_2}(u)$ on the first cover.

This leaves the branch cut in B2 as \longrightarrow (the brown line). This terminates at a regular point in the lower half plane and is therefore excluded. This then excludes the higher linear combinations in the inner chamber B around infinity. ²

Final existing states in each chamber

The complete tabulation (8.5) for the existing states on the 2 covers discussed in section 8.2.2 in this parameterisation is as follows:

²They are excluded outside in A as they simply flow to another regular point on the lower segment of the wall without encountering a branch cut.

Chamber	Existing charges cover 1	Existing charges cover 2	Count
B1: Central region upper half	$\gamma_1, \gamma_2, \gamma_1 + \gamma_2$	$\gamma_1, \gamma_2, \gamma_1 + \gamma_2$	3
B2: Central region lower half	$\gamma_1, \gamma_2, \gamma_1 - \gamma_2$	$\gamma_1, \gamma_2, -\gamma_1 + \gamma_2$	3
A: Outer region	γ_1, γ_2	γ_1, γ_2	2





Table 8.5: Existing BPS states on both covers, in all chambers.

8.2.3 Attractor flow second realisation

Now we repeat the attractor flow analysis for the second realisation which is described by the curve $\Sigma_{A_2}^{II}$. When one again computes the ratio of the central charges one finds a wall of marginal stability with 5 chambers analogous to that in [9] (see Fig. 8.7). This time this includes a center right and center left inner chamber, an outer chamber, as well as 2 chambers below the upper arc and above the lower arc.

- a.) We continue with the curve $\Sigma_{A_2}^{II}$ and consider flow lines of all possible $Z_{\gamma_i}(u)$.
- b.) We normalise the central charges to $Z_{\gamma_i}(u) \rightarrow \frac{1}{u^2-1} Z_{\gamma_i}(u)$ before plotting the attractor flow lines. This is to produce symmetric results such that all attractor points are on equal footing. This means that, for each existing BPS state, each flow line flows from an infinity of the central charge at 2 singular starting points to a 0 at the third singular point.

The existing flow lines in the inner chambers are shown on the Figure 8.7 below:

Existing BPS states				
Flow line				
Charges	γ_1	γ_2	$\gamma_1 + \gamma_2$	$\gamma_1 - \gamma_2$


Non-existing BPS states: 	
Chamber	Charge
outer, lower half plane	$\gamma_1 + \gamma_2$
center left, above cut	γ_2
center left, below cut	$\gamma_2 - 2\gamma_1$
center right, above cut	γ_1
center right, below cut	$\gamma_1 - 2\gamma_2$

Table 8.6: Flow lines on Fig. 8.7.

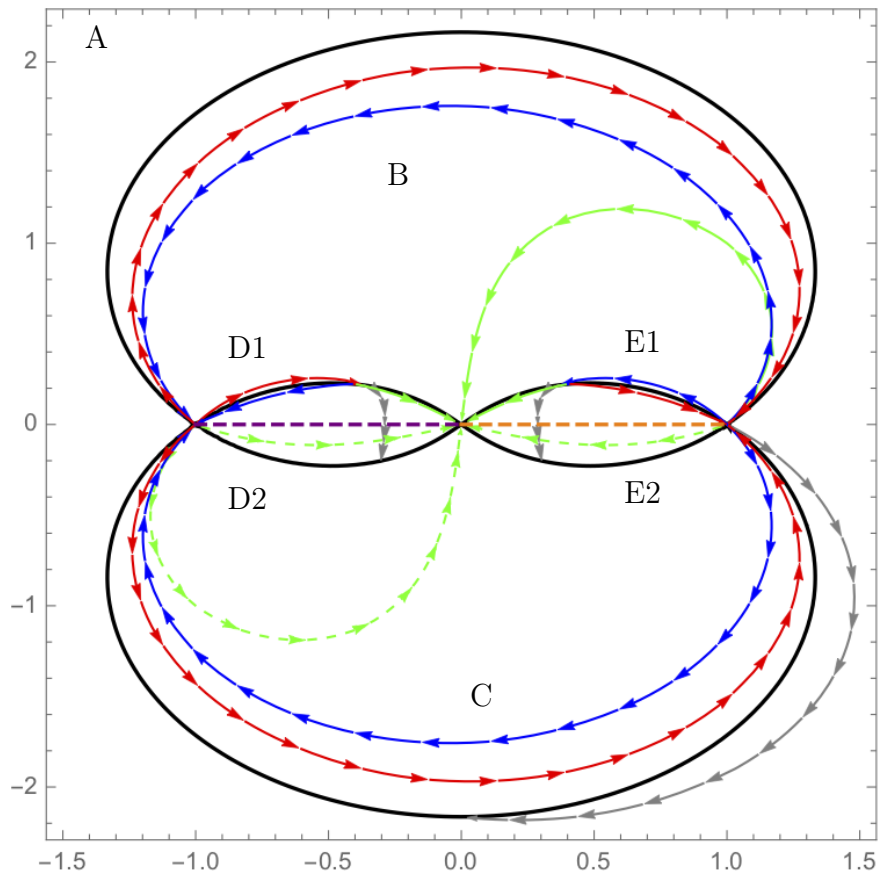


Figure 8.7: Wall of marginal stability in black, the orange and purple lines correspond to branch cuts of $Z_{\gamma_1}(u)$ and $Z_{\gamma_2}(u)$ respectively. The blue and red lines correspond to sample attractor flow lines of $Z_{\gamma_1}(u)$ and $Z_{\gamma_2}(u)$. The green line is a sample flow line for the sum $Z_{\gamma_1}(u) + Z_{\gamma_2}(u)$. It appears as a dashed line on the other side of the branch cuts. The grey lines represent the flow lines continued into unstable regions: $Z_{\gamma_1}(u)$ and $Z_{\gamma_2}(u)$ in the right and left central chambers respectively, and $Z_{\gamma_1}(u) + Z_{\gamma_2}(u)$ in the outer region.

Description of each flow line in outer chambers

The central charges $Z_{\gamma_1}(u), Z_{\gamma_2}(u)$ (7.2.25-7.2.26) are again defined on a particular cover for $u \in \mathbb{P}^1 \setminus [1, \infty)$ and $u \in \mathbb{P}^1 \setminus [-1, \infty)$ respectively. As with the first realisation there are logarithmic branch cuts arising from the $u^a \log u$ terms in the expansion around the singular points. These can again be taken from $[\pm 1, \infty)$ and are represented by the lines $-----$ and $-----$ respectively. The flow lines can be continued through the branch cuts onto a new cover.

- (i) The blue line \longrightarrow corresponds to a sample flow of $Z_{\gamma_1}(u)$: in the 2 chambers B,C within the outer arc, this charge flows from the singular points at $u = +1$ and $u = \infty$ to the termination point at $u = -1$. Therefore, because -1 is a singular point, $Z_{\gamma_1}(u)$

exists within these chambers. The blue line can also be taken in the outer region A, just above the outer arc, and in this case will flow from $+1$ to -1 . So, again, $Z_{\gamma_1}(u)$ exists in this outer region.

- (ii) The red line \longrightarrow corresponds to a sample flow of $Z_{\gamma_2}(u)$: This follows the same flow pattern with the direction of flow reversed: in the regions B,C just below the outer arc, $Z_{\gamma_2}(u)$ flows from $u = -1$ and $u = \infty$ to $u = +1$. Again, $+1$ is a singular point and therefore $Z_{\gamma_2}(u)$ again exists in these chambers as well as the outer region.
- (iii) Finally, the green line \longrightarrow corresponds to a sample attractor flow line of the sum $Z_{\gamma_3}(u) = Z_{\gamma_1}(u) + Z_{\gamma_2}(u)$: shown in the chamber B below the upper outer arc, as well as above the branch cuts in the 2 central chambers, D1 and E1. For this normalisation this state flows from ± 1 to its termination point at $u = \infty$, and therefore exists in these regions, because $u = \infty$ is a singular point.
- (iv) The gray line \longrightarrow represents the sum $Z_{\gamma_1}(u) + Z_{\gamma_2}(u)$ in chamber A outside the wall: here it doesn't exist and terminates at a regular point on the lower arc of the wall. This means that the third state decays across the outer wall in the upper half plane. We have:

$$\begin{aligned} \text{decay pathway outer chamber} \quad Z_{\gamma_3}(u) &\longrightarrow Z_{\gamma_1}(u) + Z_{\gamma_2}(u), & (8.2.8) \\ \text{in terms of charges} \quad \gamma_3 &\longrightarrow \gamma_1 + \gamma_2. \end{aligned}$$

Analytic continuation of $Z_{\gamma_1}(u) + Z_{\gamma_2}(u)$ dyon through the branch cuts

The sum $Z_{\gamma_1}(u) + Z_{\gamma_2}(u)$ also wouldn't exist when evaluated in the chamber C just above the lower arc because it would flow to the same regular termination point. However, we apply the same method as for the previous parameterisation $\Sigma_{A_2}^I$ by taking into account the branch cuts of the basis charges. This sum, represented by the green line \longrightarrow in B, can be analytically continued using the monodromies in (7.2.27), into the lower half plane. Both $Z_{\gamma_1}(u)$ and $Z_{\gamma_2}(u)$ have logarithmic branch cuts in the intervals $(\infty, +1]$ and $[-1, \infty)$ respectively. In these cases, we took the paths around the singular points. The one around -1 is clockwise and we act with

$$(M_{-1})^{-1} : Z_{\gamma_2}(u) \mapsto Z_{\gamma_2}(u) - 2Z_{\gamma_1}(u). \quad (8.2.9)$$

For $+1$ we must consider M_{+1} . However, this time we rotate in a anti-clockwise direction such that

$$M_{+1} : Z_{\gamma_1}(u) \mapsto Z_{\gamma_1}(u) - 2Z_{\gamma_2}(u). \quad (8.2.10)$$

Therefore, the sum becomes

$$Z_{\gamma_1}(u) + Z_{\gamma_2}(u) \mapsto -Z_{\gamma_1}(u) + Z_{\gamma_2}(u) \quad \text{around } -1 \text{ and} \quad (8.2.11)$$

$$Z_{\gamma_1}(u) + Z_{\gamma_2}(u) \mapsto Z_{\gamma_1}(u) - Z_{\gamma_2}(u) \quad \text{around } +1.$$

These combinations are represented on Fig. 8.7 as dotted green lines $\text{-----}\blacktriangleright$. They also flow from ± 1 to ∞ in the chamber C just above the lower arc, and also in the 2 central chambers, D2 and E2, below the branch cut. Therefore, the analytic combination of the sum (8.2.11) can be taken to exist there.

We remember that the sum and its analytic continuation do not exist in the outer region A. Here, on both sides of the branch cuts, the flow lines terminate at a regular point on the wall bounding the outer region. To summarise, this means that, as with the first realisation $\Sigma_{A_2}^I$ in section 8.2.2, there are again 2 covers on which either $\gamma_1 - \gamma_2$ or $-\gamma_1 + \gamma_2$ and their antiparticles can exist in particular regions.

Split flow of $Z_{\gamma_1}(u)$, $Z_{\gamma_2}(u)$ in central two regions

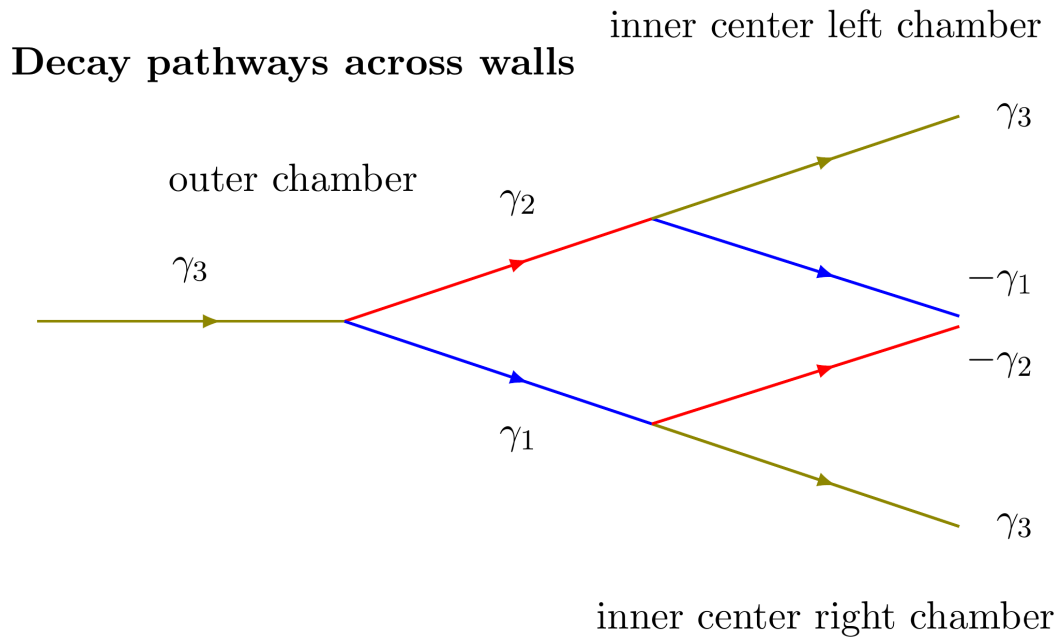
We next consider existence of the basis charges $Z_{\gamma_1}(u)$, $Z_{\gamma_2}(u)$ (7.2.25-7.2.26) in the 2 central regions D and E and their analytic continuation through the branch cuts. Each basis charge has a chamber in the central region near its source point with its logarithmic branch cut passing through it. In these chambers the attractor flow flows into the branch cut. We proceed as before in (8.2.9-8.2.10), by analytically continuing the basis charge through the branch cut by taking a path around the singular point and acting with the corresponding monodromy from (7.2.27). In this case, depending on whether one considers the flow flowing into the branch cut from above or below, the central charges get mapped to

$$Z_{\gamma_{1,2}}(u) \mapsto Z_{\gamma_{1,2}}(u) \pm 2Z_{\gamma_{1,2}}(u). \quad (8.2.12)$$

This always leads to the flow terminating at a regular point on the wall just on the other side of the branch cut, excluding the basis state from existing within the smaller chamber next to its source point. In this case, the central charges $Z_{\gamma_1}(u)$, $Z_{\gamma_2}(u)$ can no longer be considered basis states. Instead, at the wall of marginal stability surrounding the 2 small central chambers D, E, these BPS states decay into the other (now constituent states) that are stable within the chamber:

$$\begin{aligned} \text{decay pathway center right chamber D} \quad Z_{\gamma_1}(u) &\longrightarrow -Z_{\gamma_2}(u) + Z_{\gamma_3}(u), & (8.2.13) \\ \text{in terms of charges} \quad \gamma_1 &\longrightarrow -\gamma_2 + \gamma_3, \end{aligned}$$

and



decay pathway center left chamber E $Z_{\gamma_2}(u) \longrightarrow -Z_{\gamma_1}(u) + Z_{\gamma_3}(u), \quad (8.2.14)$
 $\gamma_2 \longrightarrow -\gamma_1 + \gamma_3,$

These split attractor flow processes (8.2.13-8.2.14) can be seen in the right and left central chambers, D, E, of Fig. 8.7 above respectively. The Fig. 8.8 below shows a zoomed-in version of these chambers:

Existing BPS states		
Flow line	→	
Charges	γ_2	
Split flow lines	→	→
Charges	$-\gamma_1$	$\gamma_1 + \gamma_2$
Non-existing BPS states		
Flow line	→	
Charges	γ_2	above cut
	$\gamma_2 - 2\gamma_1$	below cut

Table 8.7: Split flow lines of γ_2 on Fig. 8.8.

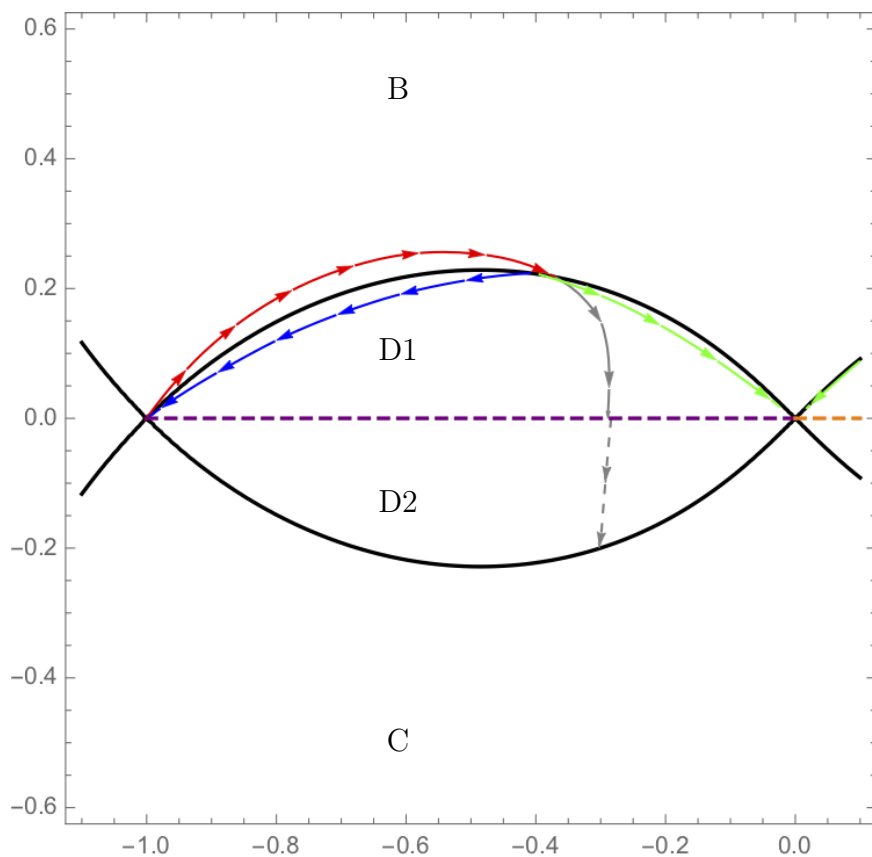


Figure 8.8: Zoomed version of left central chamber D.

- a.) This diagram shows split flow corresponding to $Z_{\gamma_2}(u)$ splitting into $-Z_{\gamma_1}(u) + Z_{\gamma_3}(u)$, where $Z_{\gamma_1}(u)$ in blue exists in the chamber and flows to $u = -1$. Similarly, $Z_{\gamma_3}(u)$ in green exists by flowing to $u \rightarrow \infty$.
- b.) The gray line shows the flow line of $Z_{\gamma_2}(u)$ in D1 continued into its non-existing chamber D2. This gray flow line is analytically continued through the branch cut by mapping $Z_{\gamma_2}(u) \mapsto Z_{\gamma_2}(u) - 2Z_{\gamma_1}(u)$, which is represented by the dashed line.
- c.) This flow then crashes at a regular point on the lower wall, hence excluding the state.

Exclusion of general $n\gamma_1 + m\gamma_2$

Now we consider again, as in 8.2.2, the general states of the form

$$n\gamma_1 + m\gamma_2 \text{ for } n > 1, m \neq 0, 1 \text{ or } m > 1, n \neq 0, 1. \quad (8.2.15)$$

Such states in (8.2.15) are again found not to exist. They flow to a regular point, analogous to a solution of (8.2.5), but for this realisation of the curve. The equation for this point is again

$$nZ_{\gamma_1}(u) + mZ_{\gamma_2}(u) = 0. \quad (8.2.16)$$

To proceed, we again consider the alignment of the central charges along all segments of the wall and determine the sign of the ratio of the central charges, as well as its range of values between the singular points. As with the first parameterisation we tabulate these data in a table (8.8) below. We find that the alignment reverses discontinuously at the point at infinity. In particular, the alignment of $Z_{\gamma_1}(u)$ reverses as the wall passes through this point.

The final table (8.8) shows the ratios and the normalised central charges along the path on the wall: ³

$$1 \longrightarrow -1 \longrightarrow \infty \longrightarrow 1 \longrightarrow -1 \longrightarrow \infty. \quad (8.2.17)$$

ratios along path				
paths between singular points	$Z_{\gamma_1}(u)$	$Z_{\gamma_2}(u)$	$Z_{\gamma_1}(u)/Z_{\gamma_2}(u)$	$Z_{\gamma_2}(u)/Z_{\gamma_1}(u)$
1	∞	0	$+\infty$	0
-1	0	∞	0	$+\infty$
∞	∞	∞	± 1	± 1
1	∞	0	$-\infty$	0
-1	0	∞	0	$-\infty$
∞	∞	∞	∓ 1	∓ 1

Table 8.8: Central charges and their ratio at the singular points.

Exclusion of combinations with $\frac{m}{n} > 1$

³The double tabulated singular points represent the different paths between the singular points along different arcs on the wall to show the range of the ratios along these arcs.

From this table (8.8) above it can be seen that, for $Z_{\gamma_1}(u)/Z_{\gamma_2}(u)$, the arc from $[\infty, 1]$ in the u -plane gives a range of $Z_{\gamma_1}(u)/Z_{\gamma_2}(u)$ from $[-1, -\infty]$. Given that this ratio is a continuous analytic function, it will take any value in this range. Hence, the equation

$$nZ_{\gamma_1}(u) + mZ_{\gamma_2}(u) = 0 \longrightarrow \frac{Z_{\gamma_1}(u)}{Z_{\gamma_2}(u)} = -\frac{m}{n}, \quad (8.2.18)$$

will have a solution along the $[\infty, 1]$ segment corresponding to an attractor point of vanishing central charge at a regular point in the moduli space - meaning such a (n, m) , $\frac{m}{n} > 1$ BPS state doesn't exist.

Exclusion of combinations with $\frac{n}{m} > 1$

Furthermore, we can see that also for $Z_{\gamma_1}(u)/Z_{\gamma_2}(u)$, the arc from $[-1, \infty]$ in the u -plane gives a range of $Z_{\gamma_2}(u)/Z_{\gamma_1}(u)$ from $[-\infty, -1]$. Again, because of the continuity and analyticity of the ratio, the equation (8.2.18) must also have a solution in the range $[-1, \infty]$ by the same argument meaning BPS states of the form (n, m) , $\frac{n}{m} > 1$ also don't exist. Hence, $\forall n, m \neq 0, \frac{n}{m} = 1$.⁴

Flow of higher linear combinations through the branch cuts

Continuation of $Z_{\gamma_2}(u)$ flow						
Flow line						
Charge	γ_2	γ_2	$\gamma_2 - 2\gamma_1$	$-2\gamma_1 + 5\gamma_2$	$-2\gamma_1 - 3\gamma_2$	$\gamma_2 - 4\gamma_1$
Cover number	1	1	2	3	4	5

Table 8.9: Continuation of Z_{γ_2} flow through branch cut.

There are many possible ways that the attractor flow of a general linear combination $n\gamma_1 + m\gamma_2$ can flow through a branch cut.

It can be shown that all these flows are excluded by regular termination points after they are analytically continued through the cut, unless the states take the form $\pm\gamma_1, \pm\gamma_2, \pm\gamma_1 \pm \gamma_2$. The states flow through the logarithmic branch cuts

$$u^a \log u \quad [-1, \infty) : \text{-----} \quad \text{and} \quad (8.2.19)$$

⁴Note that $\frac{Z_{\gamma_1}(u)}{Z_{\gamma_2}(u)} \in [-\infty, 0]$ along the lower $[1, -1]$ segment. However, this doesn't exclude any linear combination of BPS states as they pass through the wall or a branch cut before flowing to a termination point on the lower segment.

cover that terminate at a regular point on the segment of the wall just on the other side of the branch cut - excluding this and the initial state. In the other chamber, the flow lines flow into the branch cut (8.2.19) in one half of the chamber where they are again analytically continued to states on a second cover that terminate at a regular point on the part of the wall bounding the other half of the chamber.⁵

Description of each flow line

In Fig. 8.9 above and Fig. 8.10 we give an example initially of $Z_{\gamma_2}(u)$ represented by a dashed red line $---->$ and the gray line \longrightarrow after it crosses the wall of D1: in this case we analytically continue the flow of $Z_{\gamma_2}(u)$, shown in the previous diagrams, and table (8.9), onto the cover it flows to when passing through the branch cut (8.2.19) between D1 and D2. As mentioned before in (8.2.9), when continuing through the branch cut, we act with the monodromy $(M_{-1})^{-1}$ (from (7.2.27)) in a clockwise direction and obtain

$$(M_{-1})^{-1} : Z_{\gamma_2}(u) \mapsto Z_{\gamma_2}(u) - 2Z_{\gamma_1}(u). \quad (8.2.21)$$

This flow then emerges from the branch cut (8.2.19), in D2, as the brown line \longrightarrow , and flows to a regular point on the segment bounding the lower half of the center left chamber D2 between $[-1, \infty]$. The flow of $Z_{\gamma_2}(u) - 2Z_{\gamma_1}(u)$ is represented by the brown line in the rest of the figure. One can see that in the large lower chamber C the state also flows to this attractor point on the lower wall of the center left chamber and is thus excluded. In the outer region A and large upper chamber B, the state flows to a regular point on the upper segment of chamber B between $[1, -1]$.

We now consider the various ways the state $Z_{\gamma_2}(u) - 2Z_{\gamma_1}(u)$, represented by \longrightarrow , can flow through the logarithmic branch cuts between $[-1, \infty)$ and $(\infty, 1]$:

- (i) We have already described how the flow emerges from the branch cut in the lower half of the central left chamber D2 from the $Z_{\gamma_2}(u)$ state on a second cover. However, on the same cover as the emerging flow in the lower half of the chamber, in the upper half of the chamber D1, $Z_{\gamma_2}(u) - 2Z_{\gamma_1}(u)$ from (8.2.21) flows into the branch cut (8.2.19). Here we again act with $(M_{-1})^{-1}$ in a clockwise direction, such that

$$(M_{-1})^{-1} : Z_{\gamma_2}(u) - 2Z_{\gamma_1}(u) \mapsto (Z_{\gamma_2}(u) - 2Z_{\gamma_1}(u)) - 2Z_{\gamma_1}(u) \mapsto Z_{\gamma_2}(u) - 4Z_{\gamma_1}(u). \quad (8.2.22)$$

This state, represented by the dotted dark gray line $---->$, then emerges from the cut in the lower half of the chamber D2 again, but on a new cover, on which it also

⁵On the original cover in the lower half of this chamber the state has a flow out of the branch cut (from an analytic continuation of a state on a third cover) which then also flows to a different regular point on the wall segment bounding the lower half. This is the same attractor point that the lines in the lower large chamber flow to and are excluded by.

terminates at a regular point (on the left of the previous attractor point) on the lower segment of the wall bounding the half chamber D2, and is hereby excluded.

- (ii) The state $Z_{\gamma_2}(u) - 2Z_{\gamma_1}(u)$ from (8.2.21) also flows into the logarithmic branch cut in the center right chamber E from $(\infty, 1]$, from both above and below on the same cover. When it flows up into the branch cut (8.2.20) from the lower half of the chamber E2 one acts with $(M_{+1})^{-1}$ and

$$(M_{+1})^{-1} : Z_{\gamma_2}(u) - 2Z_{\gamma_1}(u) \mapsto Z_{\gamma_2}(u) - 2(Z_{\gamma_1}(u) + 2Z_{\gamma_2}(u)) \mapsto -2Z_{\gamma_1}(u) - 3Z_{\gamma_2}(u), \quad (8.2.23)$$

which emerges in E1 as the dashed black line $---\rightarrow$ on a new cover, shown in the Figures 8.9, 8.10. This flow then terminates on a regular point on the upper segment bounding the upper half of E1, and is excluded.

- (iii) In the upper half of the center right chamber E1 on the initial cover, $Z_{\gamma_2}(u) - 2Z_{\gamma_1}(u)$ flows downwards into the branch cut (8.2.20). This time we act with M_{+1} in a counterclockwise direction and the state becomes:

$$M_{+1} : Z_{\gamma_2}(u) - 2(Z_{\gamma_1}(u) - 2Z_{\gamma_2}(u)) \mapsto -2Z_{\gamma_1}(u) + 5Z_{\gamma_2}(u). \quad (8.2.24)$$

This flow, represented by a dashed grey line $---\rightarrow$, then emerges from the branch cut on another cover in E2. Again, the line terminates at a regular point - this time on the lower segment of the wall bounding the lower half of E2, and the state is once again excluded.

Summary

Hence, we have determined that the state $Z_{\gamma_2}(u) - 2Z_{\gamma_1}(u)$ is always excluded because all possible flows in all possible regions of the moduli space end at a regular point, including all possible flows through branch cuts. This means this state can never exist as part of the BPS spectrum. As shown in the diagram below (Fig. 8.10) this can be successively continued to other combinations, such as $-2Z_{\gamma_1}(u) - 3Z_{\gamma_2}(u)$ from (8.2.23), that are also excluded as BPS states (Fig. 8.10 below shows that, like $Z_{\gamma_2}(u) - 2Z_{\gamma_1}(u)$, this state has a second regular termination point on the outer arc). If we also consider analytic continuations of the non-existing $Z_{\gamma_1}(u) + Z_{\gamma_2}(u)$ flow, this process of flowing through the cuts can continue until all linear combinations except for the charges $\pm\gamma_1, \pm\gamma_2, \pm\gamma_1 \pm \gamma_2$ are excluded.

Final existing states in each chamber

Therefore, we now know the combination of states that exist in each region of the moduli space. We find 3 BPS states existing in the 2 chambers below the outer arc and 2 BPS

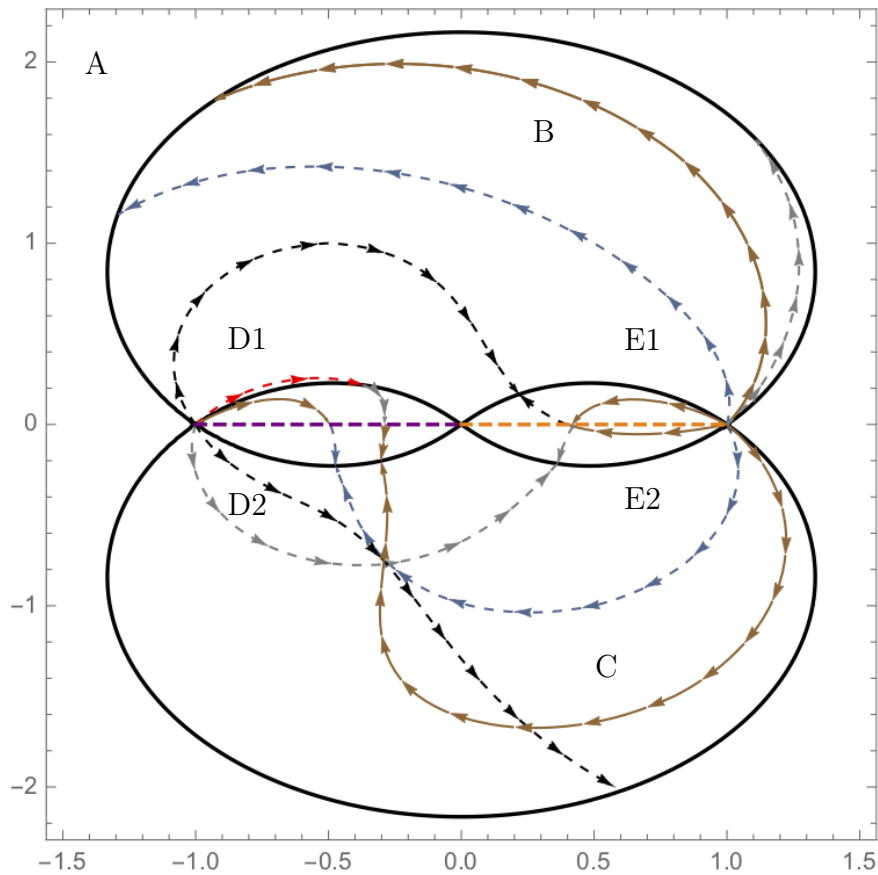


Figure 8.10: This diagram shows the continuation of the higher combinations on the other side of the branch cuts to their second termination points on that cover: $-4Z_{\gamma_1}(u) + Z_{\gamma_2}(u)$ is the light blue line, $-2Z_{\gamma_1}(u) - 3Z_{\gamma_2}(u)$ in black, and $-2Z_{\gamma_1}(u) + 5Z_{\gamma_2}(u)$ in grey. In all cases the flow terminates at a regular point on a segment bounding one of the inner chambers D, E, as well as one on the segment bounding the large outer chamber A opposite to the first regular point - hence such states are excluded.

states existing in the remaining 3 chambers. This is as we expect from the literature e.g. in Shapere and Vafa [9]. Each cycle $\gamma_1, \gamma_2, \gamma_3$ exists in 4 out of 5 regions in the moduli space. The exact description of the BPS existence in the moduli space is given in the table (8.10) below.

Now we take into account the branch cuts on the diagram and remember that in the region on the diagram below the 2 branch cuts (8.2.19, 8.2.20), but still above the outer lower arc ⁶, the central charge of the sum $Z_{\gamma_1}(u) + Z_{\gamma_2}(u)$ becomes either $Z_{\gamma_1}(u) - Z_{\gamma_2}(u)$ or $-Z_{\gamma_1}(u) + Z_{\gamma_2}(u)$ depending on which branch cut the analytic continuation is done through (8.2.11) and hence which of the two possible covers one considers for the central charge. The

⁶This contains the lower part of the central 2 chambers D2, E2 and the full lower chamber C above the lower arc.

Chamber	Existing charges	Count
D: Central left	γ_1, γ_3	2
E: Central right	γ_2, γ_3	2
B: Upper arc	$\gamma_1, \gamma_2, \gamma_3$	3
C: Lower arc	$\gamma_1, \gamma_2, \gamma_3$	3
A: Outside wall	γ_1, γ_2	2

Table 8.10: Existing BPS states in each chamber labelled by γ_1, γ_2 and γ_3 .

complete tabulation is shown in the table (8.11).

Chamber	Existing charges cover 1	Existing charges cover 2	Count
D1: Central left upper half	$\gamma_1, \gamma_1 + \gamma_2$	$\gamma_1, \gamma_1 + \gamma_2$	2
D2: Central left lower half	$\gamma_1, -\gamma_1 + \gamma_2$	$\gamma_1, \gamma_1 - \gamma_2$	2
E1: Central right upper half	$\gamma_2, \gamma_1 + \gamma_2$	$\gamma_2, \gamma_1 + \gamma_2$	2
E2: Central right lower half	$\gamma_2, \gamma_1 - \gamma_2$	$\gamma_2, -\gamma_1 + \gamma_2$	2
B: Upper arc	$\gamma_1, \gamma_2, \gamma_1 + \gamma_2$	$\gamma_1, \gamma_2, \gamma_1 + \gamma_2$	3
C: Lower arc	$\gamma_1, \gamma_2, \gamma_1 - \gamma_2$	$\gamma_1, \gamma_2, -\gamma_1 + \gamma_2$	3
A: Outside wall	γ_1, γ_2	γ_1, γ_2	2

Table 8.11: Existing BPS states, this time distinguishing $\gamma_3 = \gamma_1 + \gamma_2$ from $\gamma_3 = \gamma_1 - \gamma_2$.

8.3 Attractor flow in Seiberg-Witten SU(2)

We also carry out the analysis of deriving the Picard-Fuchs equation, the solutions and the BPS central charges for Seiberg-Witten $SU(2)$ [1]. As for the Argyres–Douglas theory, we determine the attractor flow and use it to reproduce the spectrum of BPS states in each chamber. We hereby reproduce the BPS spectrum of the quiver theory [4] with just 2 basis states γ_1, γ_2 in one chamber, and infinitely many in the other chamber, with charges of the form $n\gamma_1 + (n+1)\gamma_2, (n+1)\gamma_1 + n\gamma_2$. We use a similar set of steps as for the A_2 theory.

The central charges (7.2.30-7.2.31) we derived from the solutions of the Picard-Fuchs equations were found to be

$$\begin{aligned}
Z_{\gamma_1}(u) = & -\frac{2^{\frac{1}{2}}}{\pi^{\frac{1}{2}}}\Gamma\left(\frac{3}{4}\right)^2 F_2^1\left(-\frac{1}{4}, -\frac{1}{4}, \frac{1}{2}, u^2\right) \\
& - u \frac{\Gamma\left(\frac{1}{4}\right)^2}{4\sqrt{2}\pi} F_2^1\left(\frac{1}{4}, \frac{1}{4}, \frac{3}{2}, u^2\right), \quad u \in \mathbb{P}^1 \setminus [1, \infty),
\end{aligned} \tag{8.3.1}$$

$$\begin{aligned}
Z_{\gamma_2}(u) = & -\frac{-i\sqrt{\pi}\Gamma(-\frac{1}{4})}{8\Gamma(\frac{5}{4})}F_2^1(-\frac{1}{4}, -\frac{1}{4}, \frac{1}{2}, u^2) \\
& -\frac{i\sqrt{\pi}\Gamma(\frac{5}{4})}{\Gamma(\frac{3}{4})}uF_2^1(\frac{1}{4}, \frac{1}{4}, \frac{3}{2}, u^2), \quad u \in \mathbb{P}^1 \setminus [-1, \infty),
\end{aligned} \tag{8.3.2}$$

on a particular cover. There are $u^e \log u$ branch cuts at $[-1, \infty)$ and $[1, \infty)$ that are represented by $-----$ and $-----$ on Fig. 8.11.

Spectrum from attractor flow

This behaves very similarly to the A_2 case in the new parameterisation, looking at the plot below (Fig. 8.11), the behavior is almost identical. However, (e.g. from the quiver theory) we expect the spectrum to contain infinitely many BPS states in the chamber B around infinity. To verify this, we first consider the monodromies from (7.2.32) and transformations of the central charges around the singular points, and through the branch cuts ending there.

We recall from (7.2.32) that at -1 the transformations are: ⁷

$$\underline{\text{Monodromy transformations}} \tag{8.3.3}$$

$$(Z_{\gamma_1}(u), Z_{\gamma_2}(u)) \begin{pmatrix} 1 & \pm 2 \\ 0 & 1 \end{pmatrix},$$

such that $Z_{\gamma_1}(u) \mapsto Z_{\gamma_1}(u)$ and $Z_{\gamma_2}(u) \mapsto Z_{\gamma_2}(u) + 2Z_{\gamma_1}(u)$.

At $+1$ we have:

$$(Z_{\gamma_1}(u), Z_{\gamma_2}(u)) \begin{pmatrix} 1 & 0 \\ \mp 2 & 1 \end{pmatrix}, \tag{8.3.4}$$

such that the transformations can be written as:

$$Z_{\gamma_2}(u) \mapsto Z_{\gamma_2}(u), \quad \text{and} \quad Z_{\gamma_1}(u) \mapsto Z_{\gamma_1}(u) - 2Z_{\gamma_2}(u).$$

Now consider the attractor flow: combinations of the form $\pm nZ_{\gamma_1}(u) \pm mZ_{\gamma_2}(u)$ always flow to a point on the wall for $n, m \geq 1$. For $\frac{n}{m} \geq 0$ the flow terminates on the lower arc and for $\frac{n}{m} \leq 0$ on the upper arc. To avoid all states being excluded from existence by flowing to the regular point, we consider the flow entering the branch cuts $[-1, \infty)$ and $(\infty, 1]$ between B1 and B2. At the branch cuts we can combine the flows by acting with the transformations (8.3.3-8.3.4). These must have flows continuous with those on the other side of the branch cut and cannot terminate at a regular point if the original state exists. This can only happen if the ratio changes sign from $\frac{n}{m} \geq 0$ to $\frac{n}{m} \leq 0$ or vice versa.

⁷The sign on the ± 2 is determined by the direction of the loop taken around the singular point.

Infinite tower of existing BPS states

Hence, we can use the monodromies in (8.3.3-8.3.4) to generate the set of all existing states not excluded by the regular points, by acting with the monodromy transformations that reverse this ratio. Initially we act in a similar way to the A_2 case when considering a rotation (starting in the upper half plane) of the form $u = -1 + \epsilon e^{-i\theta}$, $\theta : 0 \rightarrow +2\pi$ around -1 and $u = +1 + \epsilon e^{-i\theta}$, $\theta : -\pi \rightarrow +\pi$ around $+1$, where $\epsilon \in \mathbb{R}^+$.

Therefore, the transformations become $+1$: $Z_{\gamma_1}(u) \mapsto Z_{\gamma_1}(u) - 2Z_{\gamma_2}(u)$ and -1 : $Z_{\gamma_2}(u) \mapsto Z_{\gamma_2}(u) + 2Z_{\gamma_1}(u)$, a change of sign happening because we are considering a rotation from the lower half plane. Knowing that the basis states $Z_{\gamma_1}(u), Z_{\gamma_2}(u)$ exist in the chamber B around infinity, we can consider the transformations that generate the full spectrum by acting with these monodromies:

First examples from first basis state (8.3.5)

$$\begin{aligned}
+1 : Z_{\gamma_1}(u) &\mapsto Z_{\gamma_1}(u) - 2Z_{\gamma_2}(u), \\
-1 : Z_{\gamma_1}(u) - 2Z_{\gamma_2}(u) &\mapsto Z_{\gamma_1}(u) - 2(Z_{\gamma_2}(u) + 2Z_{\gamma_1}(u)) \mapsto -3Z_{\gamma_1}(u) - 2Z_{\gamma_2}(u), \\
+1 : -3Z_{\gamma_1}(u) - 2Z_{\gamma_2}(u) &\mapsto -3(Z_{\gamma_1}(u) - 2Z_{\gamma_2}(u)) - 2Z_{\gamma_2}(u) \mapsto -3Z_{\gamma_1}(u) + 4Z_{\gamma_2}(u), \\
-1 : -3Z_{\gamma_1}(u) + 4Z_{\gamma_2}(u) &\mapsto -3Z_{\gamma_1}(u) + 4(Z_{\gamma_2}(u) + 2Z_{\gamma_1}(u)) \mapsto 5Z_{\gamma_1}(u) + 4Z_{\gamma_2}(u), \\
+1 : 5Z_{\gamma_1}(u) + 4Z_{\gamma_2}(u) &\mapsto 5(Z_{\gamma_1}(u) - 2Z_{\gamma_2}(u)) + 4Z_{\gamma_2}(u) \mapsto 5Z_{\gamma_1}(u) - 6Z_{\gamma_2}(u), \quad \dots
\end{aligned}$$

In general

$$\begin{aligned}
(n+1)Z_{\gamma_1}(u) + nZ_{\gamma_2}(u) &\mapsto (n+1)(Z_{\gamma_1}(u) - 2Z_{\gamma_2}(u)) + nZ_{\gamma_2}(u) \mapsto \\
(n+1)Z_{\gamma_1}(u) - (n+2)Z_{\gamma_2}(u) \quad m = n+1 &\mapsto mZ_{\gamma_1}(u) - (m+1)Z_{\gamma_2}(u), \quad \dots
\end{aligned}$$

First examples from second basis state (8.3.6)

$$\begin{aligned}
-1 : Z_{\gamma_2}(u) &\mapsto Z_{\gamma_2}(u) - 2Z_{\gamma_1}(u), \\
+1 : Z_{\gamma_2}(u) - 2Z_{\gamma_1}(u) &\mapsto Z_{\gamma_2}(u) - 2(Z_{\gamma_1}(u) + 2Z_{\gamma_2}(u)) \mapsto -3Z_{\gamma_2}(u) - 2Z_{\gamma_1}(u), \\
-1 : -3Z_{\gamma_2}(u) - 2Z_{\gamma_1}(u) &\mapsto -3(Z_{\gamma_2}(u) - 2Z_{\gamma_1}(u)) - 2Z_{\gamma_1}(u) \mapsto -3Z_{\gamma_2}(u) + 4Z_{\gamma_1}(u), \\
+1 : -3Z_{\gamma_2}(u) + 4Z_{\gamma_1}(u) &\mapsto -3Z_{\gamma_2}(u) + 4(Z_{\gamma_1}(u) + 2Z_{\gamma_2}(u)) \mapsto 5Z_{\gamma_2}(u) + 4Z_{\gamma_1}(u), \\
-1 : 5Z_{\gamma_2}(u) + 4Z_{\gamma_1}(u) &\mapsto 5(Z_{\gamma_2}(u) - 2Z_{\gamma_1}(u)) + 4Z_{\gamma_1}(u) \mapsto 5Z_{\gamma_2}(u) - 6Z_{\gamma_1}(u), \quad \dots
\end{aligned}$$

In general

$$\begin{aligned}
(n+1)Z_{\gamma_2}(u) + nZ_{\gamma_1}(u) &\mapsto (n+1)(Z_{\gamma_2}(u)) - 2Z_{\gamma_1}(u) + nZ_{\gamma_1}(u) \mapsto \\
(n+1)Z_{\gamma_2}(u) - (n+2)Z_{\gamma_1}(u), \quad m = n+1 &\mapsto mZ_{\gamma_2}(u) - (m+1)Z_{\gamma_1}(u) \quad \dots
\end{aligned}$$

These are the existing states in the model that are not excluded by termination at a regular point. One obtains the same pattern starting with $Z_{\gamma_1}(u) + 2Z_{\gamma_2}(u)$. Hence, all the combinations are of the form: $nZ_{\gamma_2}(u) \pm (n+1)Z_{\gamma_1}(u)$ and $nZ_{\gamma_1}(u) \pm (n+1)Z_{\gamma_2}(u)$, which was previously expected. We also expect another state to exist in chamber B around infinity. This corresponds to a W-boson. In our basis its central charge is the sum of the central charges $Z_{\gamma_1}(u) + Z_{\gamma_2}(u)$. Some examples of sample attractor flow lines, for particular central charges, are shown in the diagrams (Figs. 8.11, 8.12) below:



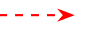
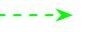
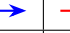

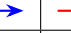







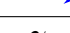
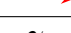


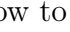
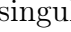
Split flow lines for example existing BPS states									
Flow line									
Charges	$\gamma_1 + \gamma_2$		$\gamma_1 - 2\gamma_2$		$\gamma_2 - 2\gamma_1$		$\gamma_1 - \gamma_2$		
Split flow lines									
Charges	γ_1	γ_2	γ_1	γ_2	γ_1	γ_2	γ_1	γ_2	
Non-existing BPS states									
Flow line									
Charges	$3\gamma_1 + \gamma_2$				$\gamma_1 + \gamma_2$				
Forked flow lines									
Charges	γ_1		γ_2						

Table 8.12: Split flow lines of BPS states on Fig. 8.11.

Analytic continuation for monopole and dyon

The diagram Fig. 8.11 shows the first example of the existing states generated by analytically continuing the central charges of the basis states (the monopole and dyon) through the branch cuts - the diagram shows

$$\begin{aligned}
M_{+1} : \quad Z_{\gamma_1}(u) - 2Z_{\gamma_2}(u) &\mapsto Z_{\gamma_1}(u) \quad \text{and} \\
(M_{-1})^{-1} : \quad -2Z_{\gamma_1}(u) + Z_{\gamma_2}(u) &\mapsto Z_{\gamma_2}(u)
\end{aligned} \tag{8.3.7}$$

as dashed blue  and red  lines in B2 becoming the basis charges in B1, shown by  and , that flow to singular points and exist everywhere. This process can be continued indefinitely, generating the $nZ_{\gamma_2}(u) \pm (n+1)Z_{\gamma_1}(u)$ tower. However, these higher combinations only exist in the central chamber B - all such states split at the wall into their composite basis states and flow to ± 1 . If the linear combination were to be continued in the

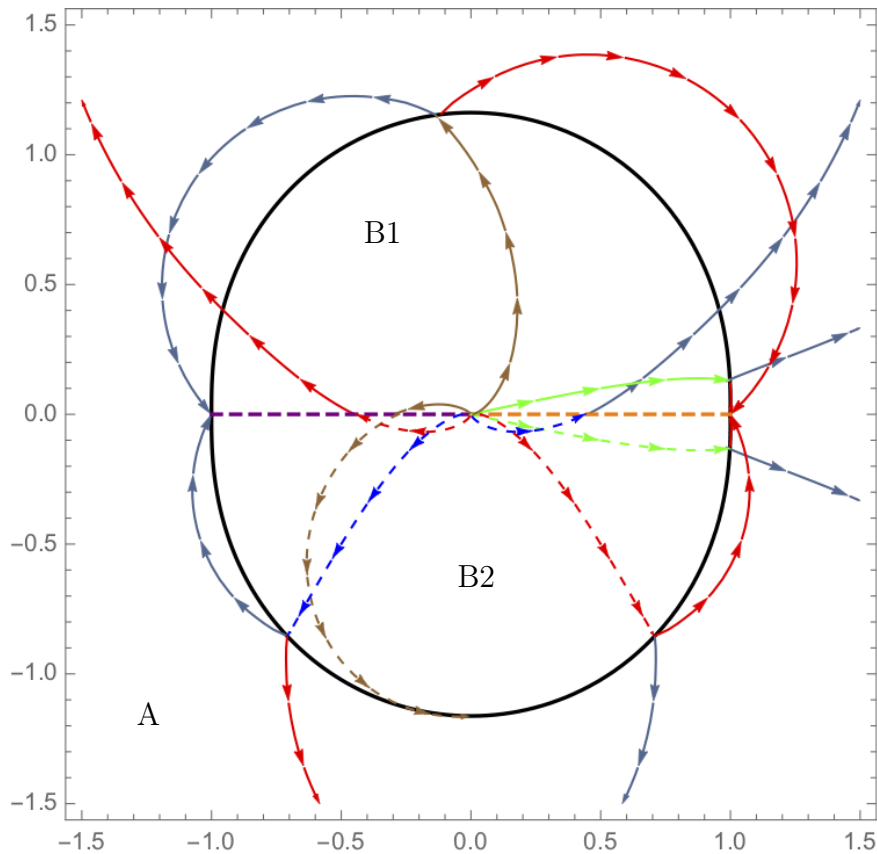


Figure 8.11: Sample attractor flow lines at infinity for Seiberg-Witten $SU(2)$. The wall of marginal stability is in black.

- a.) The solid blue and red lines represent the flows of $Z_{\gamma_1}(u)$ and $Z_{\gamma_2}(u)$ respectively flowing to ± 1 .
- b.) The dashed blue and red lines correspond to $Z_{\gamma_1}(u) - 2Z_{\gamma_2}(u)$ and $-2Z_{\gamma_1}(u) + Z_{\gamma_2}(u)$ - they flow through the branch cut and become the respective basis charges.
- c.) The green line corresponds to $Z_{\gamma_1}(u) + Z_{\gamma_2}(u)$ this flows parallel to the branch cut and its analytic continuation $Z_{\gamma_1}(u) - Z_{\gamma_2}(u)$ is shown by the dashed green line.
- d.) The non-existing brown line corresponds to $3Z_{\gamma_1}(u) + Z_{\gamma_2}(u)$ and flows through the branch cut to become $Z_{\gamma_1}(u) + Z_{\gamma_2}(u)$ on a new cover, where it flows to a regular point on the lower wall.

All higher linear combinations split at the wall into the basis flows.

outer chamber A around $u = 0$ it would flow to a regular point on the wall and be excluded.

Flow for W-boson

The combination $Z_{\gamma_1}(u) + Z_{\gamma_2}(u)$ (the green line \longrightarrow) exists in chamber B1 and is interesting because it flows in parallel to the branch cut rather than flowing through it. When analytically continued through the cut, to $Z_{\gamma_1}(u) - Z_{\gamma_2}(u)$ in B2 (represented by the dashed green line \dashrightarrow), the flow is symmetric with that above the cut. Therefore, this state exists within the central chamber B on 2 covers, but again splits at the wall into the basis states for the same reason as the other higher combinations. It therefore doesn't exist in the outer region A. Physically this should correspond to the W-boson in the spectrum.

Example of flow for non-existing state

Finally the state $3Z_{\gamma_1}(u) + Z_{\gamma_2}(u)$ (represented by the brown line \longrightarrow in B1) flows into the branch cut onto a new cover where it becomes $Z_{\gamma_1}(u) + Z_{\gamma_2}(u) \dashrightarrow$ in B2 and terminates at a regular point on the lower part of the wall. This means it is one of the states excluded by the existence conditions and is not in the spectrum of BPS states. Other non-existing higher combinations follow a similar flow pattern.

Below we show a diagram, Fig. 8.12, showing more closely the central region B with the flow lines passing through the branch cuts. This table describes the flow lines on this diagram:

		Existing BPS states			Non-existing BPS states
Cover 1	Flow line	\dashrightarrow	\dashrightarrow	\dashrightarrow	\dashrightarrow
	Charges	$\gamma_1 - \gamma_2$	$\gamma_1 - 2\gamma_2$	$\gamma_2 - 2\gamma_1$	$\gamma_1 + \gamma_2$
Cover 2	Split flow lines	\longrightarrow	\longrightarrow	\longrightarrow	\longrightarrow
	Charges	$\gamma_1 + \gamma_2$	γ_1	γ_2	$3\gamma_1 + \gamma_2$

Table 8.13: Flow lines through branch cuts on Fig. 8.12.

Final existing states in each chamber

We now have all the required information to write down the spectrum of existing BPS states in each chamber, which we present in table (8.14) below:

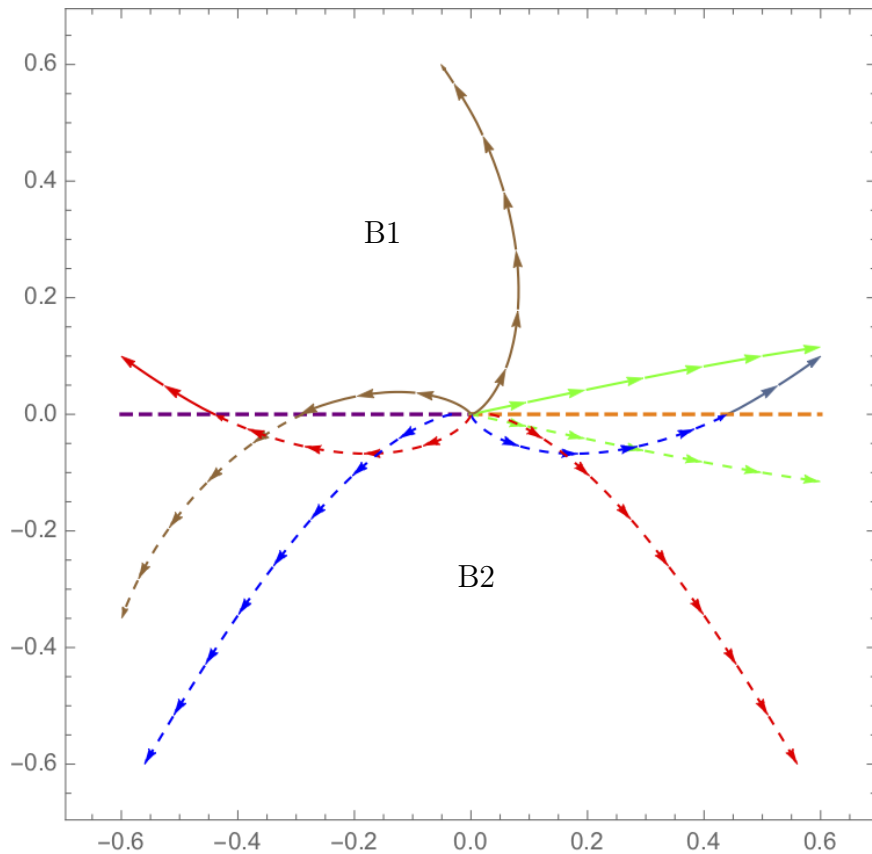


Figure 8.12: Zoom in around infinity of the attractor flow on the previous diagram: this shows the flow of $Z_{\gamma_1}(u) - 2Z_{\gamma_2}(u) \rightarrow Z_{\gamma_1}(u)$, $-2Z_{\gamma_1}(u) + Z_{\gamma_2}(u) \rightarrow Z_{\gamma_2}(u)$, $Z_{\gamma_1}(u) + Z_{\gamma_2}(u) \rightarrow Z_{\gamma_1}(u) - Z_{\gamma_2}(u)$ and $3Z_{\gamma_1}(u) + Z_{\gamma_2}(u) \rightarrow Z_{\gamma_1}(u) + Z_{\gamma_2}(u)$ in blue, red, green and brown respectively.

8.3.1 Concluding remarks

Therefore, we have now reproduced the count of BPS states in every chamber for the Argyres-Douglas theories A_1 , A_2 and Seiberg-Witten theory. Hence, the attractor flow method gives the same results as those from the other methods in the literature, such as the quantum dilogarithms from section 3.1.2 and quiver representations from chapter 4. This then can be considered to be a useful method that could in future be generalised to other BPS structures, such as other models with an ADE type quiver description. Although there has to be a method for initially deriving the central charges for a theory before this can be done. Once these are known it should then become possible to find the walls of marginal stability, existence conditions and attractor flow lines. Which, as in these cases, should allow for the

All existing states in all chambers			
Chamber	Existing charges cover 1	Existing charges cover 2	Count
B1: Central region upper half	$-\gamma_1, -\gamma_2, -\gamma_1-\gamma_2$ $-(n+2)\gamma_1-(n+3)\gamma_2$ $-(n+2)\gamma_2-(n+3)\gamma_1$	$\gamma_1, \gamma_2, \gamma_1 + \gamma_2$ $n\gamma_1 + (n+1)\gamma_2$ $n\gamma_2 + (n+1)\gamma_1$	Infinite
B2: Central region lower half	$-\gamma_1, -\gamma_2, \gamma_1-\gamma_2$ $(n+4)\gamma_1-(n+3)\gamma_2$ $(n+4)\gamma_2-(n+3)\gamma_1$	$\gamma_1, \gamma_2, -\gamma_1 + \gamma_2$ $-(n+2)\gamma_1+(n+1)\gamma_2$ $-(n+2)\gamma_2+(n+1)\gamma_1$	Infinite
A: Outer region	$\pm\gamma_1, \pm\gamma_2$	$\pm\gamma_1, \pm\gamma_2$	2

Table 8.14: Existing states in Seiberg-Witten theory on 2 covers.

determination of the BPS spectrum.

9 | $\mathcal{N} = 4$ black hole partition functions

In the previous two chapters 7 and 8 we used attractor flow to count BPS states in different regions of the moduli space. The next stage of this thesis involves reviewing wall crossing and BPS counting in $\mathcal{N} = 4$ theories, including generating functions for $\frac{1}{4}$ BPS black holes. The idea is then to find mathematical analogs for $\frac{1}{2}$ BPS states in $\mathcal{N} = 2$ theories to the counting functions of $\mathcal{N} = 4$ $\frac{1}{4}$ BPS states that count the BPS states in the same way. Firstly, this derives a new way of BPS state counting which again reproduces the wall crossing, described in section 3.1.2 and chapter 4, and could be generalised to other BPS structures. Furthermore, if a function in $\mathcal{N} = 2$ is found to encode the BPS spectrum and wall crossing phenomena in exactly the same way as in the $\mathcal{N} = 4$ example then it is reasonable to conjecture that the counting function has or is related to the same physical interpretation e.g. in terms of a partition function as in the $\mathcal{N} = 4$ example. After first reviewing the $\mathcal{N} = 4$ example and its derivation in section 9.3, we construct a new analog of the dyon counting function in the second work “Generating functions for $\mathcal{N} = 2$ BPS structures” contained in chapters 10-11 of this thesis. Here in section 9.1 we start by reviewing the history, background and physical significance of black hole partition functions.

9.1 History of black hole partition functions

It is important to first review the history and development of the complete partition functions for black hole microstates in $\mathcal{N} = 4$ string theories. This starts from the development of black hole entropy by Strominger and Vafa, [39] discussed in section 9.1.1, and the definition of the degeneracies (sec. 9.2). The derivation of the 4d generating function, initially carried out by Dijkgraaf, Verlinde and Verlinde [40], is covered in section 9.3. This will then be the generating function, also appearing in the work of Cheng and Verlinde [52, 53], for which limits can be taken and used to construct $\mathcal{N} = 2$ analogs.

9.1.1 Black hole entropy in Strominger-Vafa black holes

The macroscopic black hole entropy formula was derived by Bekenstein and Hawking [164, 165] and is given by

$$S = \frac{k_B c^3 A}{4G\hbar},$$

for area A , with c, k_B, \hbar and G being the speed of light, Boltzmann constant, Planck's constant and the gravitational constant respectively.

However, a formula that derived the black hole entropy from the microstates remained unknown until the work of Strominger and Vafa [39] which derived the entropy for a 5d BPS extremal black hole ¹ for the first time from these microstates in a string theory context. This involved an $\mathcal{N} = 4$ black hole in type IIB string theory, with a target $K3 \times S^1$, with the microstates at weak coupling corresponding to a D1-D5 system in 5 dimensions. When the microstates of this D1-D5 system are counted and the black hole partition function is derived one can calculate the entropy which, at leading order, reproduces the result of Bekenstein-Hawking. These microstates correspond to $\frac{1}{4}$ BPS states in the theory and the partition function counts degeneracies of the black hole charges $d(Q_F, Q_H)$. Here the charges Q_F and Q_H are axion and electric charges respectively. Strominger and Vafa [39] evaluate the entropy by taking large Q_H, Q_F to suppress both string loop and spacetime quantum corrections. This is done by evaluating $S_{stat} = \log d(Q_F, Q_H)$, and the result is obtained as

$$S_{stat} = 2\pi \sqrt{Q_H \left(\frac{1}{2} Q_F^2 + 1 \right)}. \quad (9.1.1)$$

When one takes large Q_F this takes the form of $S_{stat} = 2\pi \sqrt{\frac{1}{2} Q_H Q_F^2}$. This result can also be obtained when one takes the low energy supergravity limit and derives the Bekenstein-Hawking entropy from the action. From this action it is possible to expand the black hole entropy in terms of the charges, such that the Bekenstein-Hawking result is obtained in the limit of large charges when there are fewer quantum corrections from the string theory. The method used for $K3 \times S^1$ can also be applied to $K3 \times T^2$, given that a degeneracy formula for the BPS states has been derived in this case. Here the result for the entropy [166], to leading order, becomes $S = \pi \sqrt{Q^2 P^2 - (P \cdot Q)^2}$ ².

9.2 BPS charges and degeneracies in $\mathcal{N} = 4$ black holes

To proceed from here, we must define the degeneracies of BPS states in a Hilbert space \mathcal{H}_{BPS} of states as described for BPS states in 4d $\mathcal{N} = 2$ theories in chapter 3. We should also note that Harvey and Moore [43, 44] defined the notion of a BPS algebra of this vector space with a tensor product. There are special sectors correspond to a Generalised Kac-Moody algebra with roots encoding BPS charges. In the example we are looking at here,

¹Extremal black holes are those with minimum mass given a fixed charge and angular momentum.

²Here P and Q are electric and magnetic charges of the 4d black hole

we can take the Hilbert space to be the space of quantum states labelled by a particular combination of integers (k, l, m) . Each state also has a particular occupation number N^I . Therefore, these states can be labelled by $N_{k,l,m}^I$ and represented in the Hilbert space by the vector $|N_{k,l,m}^I\rangle$. If one has a charge vector of electric and magnetic charges denoted by (P, Q) the degeneracy of this state $d(P, Q)$ is defined as the number of independent quantum states which have these charges. Specifically, in this case, it represents the difference in the number of bosonic – fermionic BPS multiplets [40, 43, 167]. In this theory these charges are those of the BPS states of a fivebrane soliton with target space $K3 \times S^1 \times \mathbb{R}$. There are several dual string theory perspectives that arise from this fivebrane (see Fig. 9.1), including a type II string theory on $K3 \times T^2$ as well as a heterotic description with a toroidal target space, which is derived from a dimensional reduction. One can also interpret this setup by considering both electric and dual magnetic fivebranes wrapped on the 2 different cycles that are present within the T^2 .

Closed string theories have a relation called the level matching condition relating the number operators of left and right moving string modes and is described in many introductory texts, e.g. [168, 169]. It is generated by the reparameterization invariance of the worldsheet. In this case, we have a generalisation of the heterotic level matching conditions involving the dyon counting formula. These relations constrain the BPS degeneracies by relating the vectors of electric and magnetic charges and the quantum numbers. Here there are 3 level matching conditions [40]:

$$\frac{1}{2}P^2 + \sum_{k,l,m,I} k N_{k,l,m}^I = 1, \quad (9.2.1)$$

$$\frac{1}{2}Q^2 + \sum_{k,l,m,I} l N_{k,l,m}^I = 1, \quad (9.2.2)$$

$$P \cdot Q + \sum_{k,l,m,I} m N_{k,l,m}^I = 1. \quad (9.2.3)$$

An $SL(2, \mathbb{Z})$ duality can exchange the electric and magnetic charges by acting on them in a matrix representation as $\Lambda_{P,Q} \rightarrow \gamma \Lambda_{P,Q} \gamma^t$ (see subsection 9.5.1). All the charges (in the heterotic theory) can be given by 28 electric and magnetic charges respectively [170] that are written as the vectors P, Q . Here we must consider Lorentzian charge lattices which are self-dual and can be written as $\Gamma^{a,b}$ [43]. One can now say that the vectors of electric and magnetic charges are contained in a lattice given by $\Gamma^{22,6}$ [170]. The inner products $P^2 = P \cdot P$, $Q^2 = Q \cdot Q$ and $P \cdot Q$ are defined using the inner product of the charges on this $\Gamma^{22,6}$ lattice, which can now be arranged into a second type of charge vector:

$$\Lambda_{P,Q} = \begin{pmatrix} P \cdot P & P \cdot Q \\ P \cdot Q & Q \cdot Q \end{pmatrix}. \quad (9.2.4)$$

For the dyon counting formula we can give the physical interpretation of the quantum numbers (k, l, m) . In this case, the quantum numbers associated to a string on this space

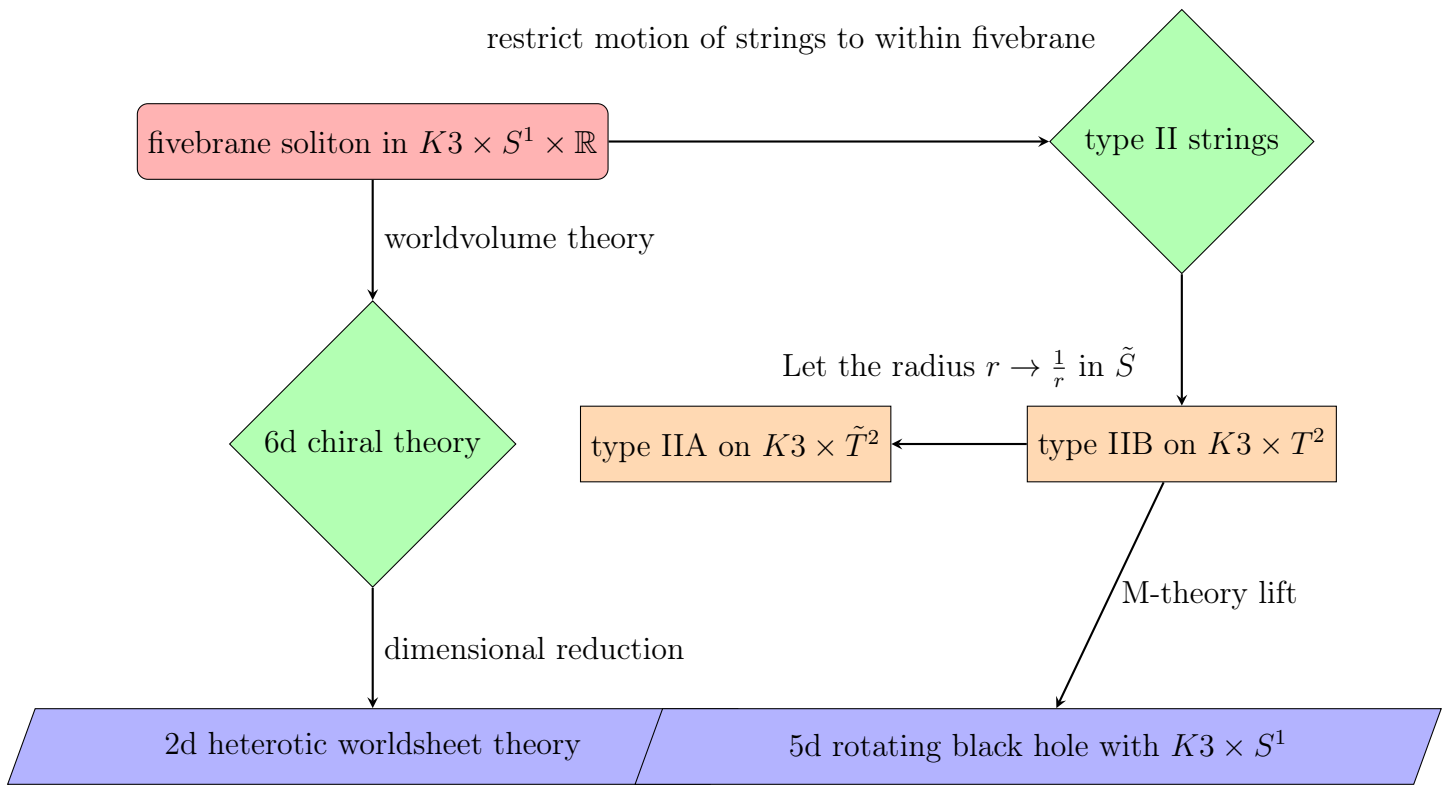


Figure 9.1: Dualities resulting from the fivebrane soliton.

include a momentum number l around the circle, as well as a winding number k , and the helicity of the string m . For this example, these quantum numbers can be arranged into another Lorentzian lattice $\Gamma^{2,1}$, again with an electric - magnetic duality represented by $SL(2, \mathbb{Z})$ [40]. The lattice vectors themselves this time have a square length of $m^2 - 4kl$.

If we assume that we are dealing with a $K3$ in the target space we must look at the expansion coefficients of the elliptic genus formula to define our quantum state vectors. These are denoted by $c(4kl - m^2)$ and the range of the index I for a particular combination of the other quantum numbers is given by the absolute value of the expansion coefficient $|c(4kl - m^2)|$ described further in section 9.3.3 [40]. This means that the index I runs from $I : 1, \dots, |c(4kl - m^2)|$ and hence completes the description of the quantum states $|N_{k,l,m}^I\rangle$.

9.3 Derivation of generating function for black hole

As for the result of Strominger and Vafa, described in subsection 9.1.1 [39], the generating function for the $\frac{1}{4}$ BPS black holes in 4 dimensions has also been derived. This gives a dyon counting formula for $\frac{1}{4}$ BPS states with electric and magnetic charges. In fact, Strominger, Shih and Yin [41] used an M-theory lift to relate the degeneracies of the 4d and 5d model.

As mentioned in section 9.1.1, the 4d model can also be used to reproduce the Bekenstein-Hawking entropy. This has been done for 4d extremal black holes, and can be derived in the standard way by taking the limit of large charges and using the Wald entropy formula [171] for the low energy effective action. The target space of this 4d model in a type II framework is given by $K3 \times T^2$, but there is also a dual heterotic theory [172, 173] on a torus. Here we follow the original derivation by Dijkgraaf, Verlinde, Verlinde [40] of this 4d dyonic generating function, which later appears in the work of Cheng and Verlinde [52, 53], and the literature this is built on.

9.3.1 Heterotic description for purely electric and magnetic states

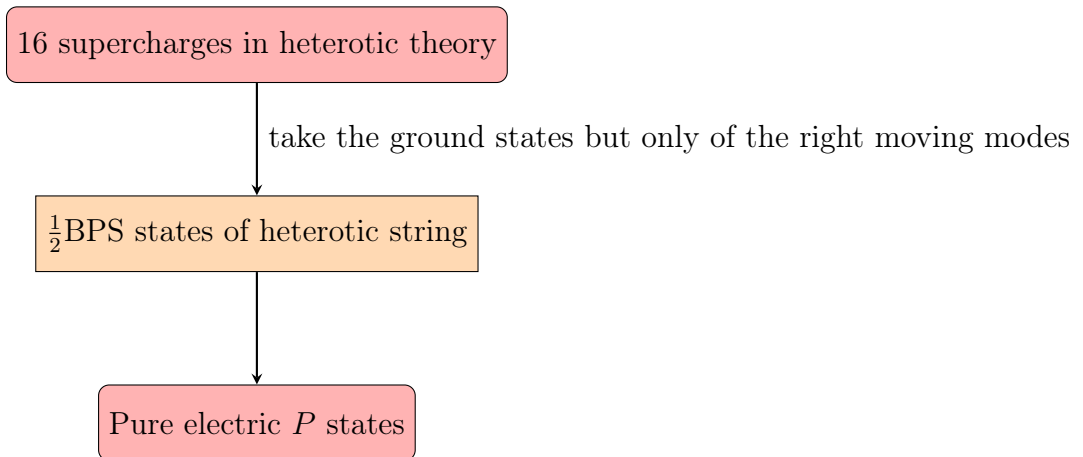
Before we look at the full generating function of the dyons we will start by understanding the derivation in the purely electric/magnetic case in two of the dual string descriptions. Firstly, the heterotic string framework has been used to analyse these $\frac{1}{2}$ BPS states and to derive the counting formula for their degeneracies. We will start with this description here. This degeneracy formula - from the charge lattice, is invariant under the duality group [170, 174, 40], which is given by

$$SL(2, \mathbb{Z}) \times SO(22, 6, \mathbb{Z}),$$

where $SO(22, 6, \mathbb{Z})$ is a T-duality subgroup. To determine the generating function we look for BPS states, which have charges that are contained in a subset of this lattice. These states should, as BPS states, be annihilated by the supercharges, and for the string theory correspond to the ground states associated to the superconformal algebra describing the theory. This particular heterotic string description has 16 supersymmetry charges in total. There are purely electric states and purely magnetic states that annihilate $\frac{1}{2}$ of the supercharges and dyonic states that annihilate $\frac{1}{4}$ of the supercharges. The generating function for the $\frac{1}{2}$ BPS states is fairly easy to determine using half of the possible ground states. This can be computed by just choosing the ground states of the right moving modes [175] of the heterotic string theory that break only half the supersymmetry and hence are $\frac{1}{2}$ BPS. This function is known [40, 175] and is given by

$$d(P) = \oint_{\mathcal{C}} d\sigma \frac{e^{i\pi\sigma P^2}}{\eta(\sigma)^{24}}. \quad (9.3.1)$$

Now a contour \mathcal{C} is taken in the sigma plane such that $\sigma \in [0, 1]$. The function $\eta(\sigma) = \prod_{n=1}^{\infty} (1 - e^{2\pi in\sigma})^{-24}$. The numerator contains the square of the electric charge P^2 . This is invariant under the transformation under $SO(22, 6)$.



Heterotic theory from dimensional reduction of fivebrane

Using the dualities, we can see that the computation of equation (9.3.1) above can either be derived by directly computing the heterotic string partition function for the relevant ground states, as described previously, or by looking at the dual type II theory [172, 173] (see section 9.3.2). The heterotic-type II duality manifests itself in the fivebrane wrapped on the $K3$ manifold in the target space, from which the heterotic string worldsheet is constructed by dimensional reduction [40]. This fivebrane exists as a soliton in the type II descriptions. Its dimensional reduction, to the heterotic theory, is reviewed below.

Worldvolume theory of fivebrane before dimensional reduction

We will now continue here with the explanation of the heterotic fivebrane description. The fivebrane has a 6d chiral theory on its worldvolume. In general, all the existing charged BPS states can be understood as oscillating fields on this worldvolume of the fivebrane. Alternatively, one can consider the fivebrane as oscillating within the full target space of the string theory. The fields, or fluctuations with long wavelength, are known as the 0-modes (of fields with 10 components and no mass). These fields can be arranged into a $\mathcal{N} = (2, 0)$ supermultiplet ³:

<u>Field content of (2,0) multiplet</u>	scalars	fermions	3 index tensor T_3	(9.3.2)
	5	4	1	

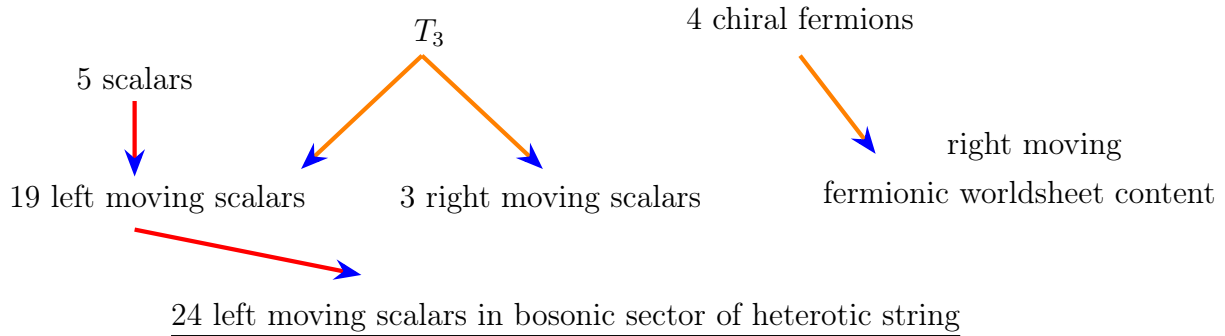
This fivebrane description can be related back to the heterotic string theory using a 6d \rightarrow 2d dimensional reduction [173, 40]. At the moment we recall that we are looking at a 6d

³The last tensor field is also self-dual [176, 40].

chiral theory with an interpretation as the worldvolume theory on the fivebrane.

Heterotic worldsheet theory after dimensional reduction

This is now dimensionally reduced to a 2 dimensional theory embedded within the $K3$ manifold. In this case, the field content in the supermultiplet (9.3.2) reduces.



These correspond to fields that exist on the worldsheet of heterotic string theory with toroidal target space and hence completes the string duality with the type II strings (see section 9.3.2). The momentum lattice for the heterotic strings now becomes that for the cohomology of $K3$ which can be written as $\Gamma^{20,4}$. The subset of electric charges P^A that are contained in this lattice can be found by integrating the tensor field over the 2 cycles Σ^A within the $K3$ as well as along one of the circles S^1 [177, 40]. This flux of the tensor reads as

$$P^A = \int_{S^1 \times \Sigma^A} T_3. \tag{9.3.3}$$

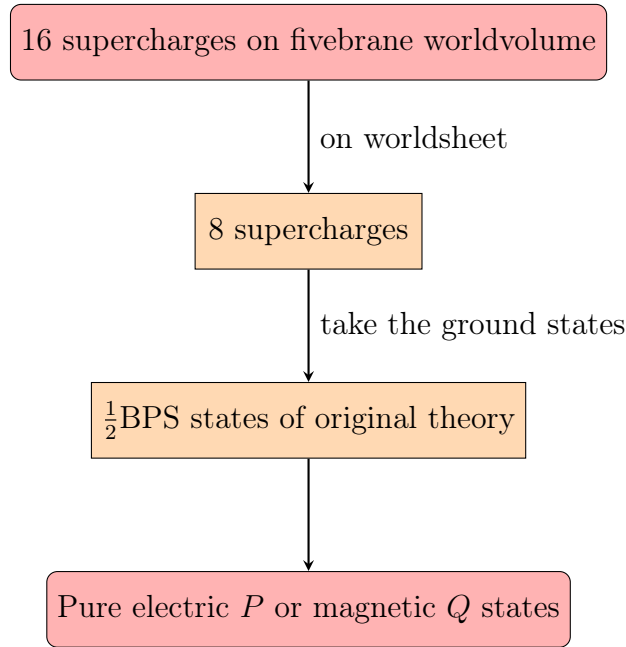
9.3.2 Type II description of electric and magnetic states

So far, the generating function for the purely electric and magnetic BPS states was looked at from the heterotic string perspective. We can now briefly describe the type II interpretation of the fivebrane as a soliton [178], that was further developed in [177] and [176], and use it to recover the purely electric generating function. This is done by considering this worldvolume theory with 5+1 dimensions as a string theory of the type II strings with their motion restricted to within the fivebrane⁴. This theory has (4, 4) supersymmetry in total on the string worldsheet. The target space remains $K3 \times T^2$ and the fivebrane oscillates transversely to the $K3$ manifold⁵. To describe the $\frac{1}{2}$ BPS states one must again look at only the ground states of this string that retain half of the supersymmetry - that existed within the original

⁴This also has a description in terms of D-branes such that the string worldsheet is formed from intersecting D-branes that are contained within the fivebrane worldvolume.

⁵One can define a current algebra from the commutators of current density operators in the theory. This particular superconformal worldsheet theory has a current algebra described by the group $SU(2)_L \times SU(2)_R$

worldvolume theory. The string worldsheet theory already has half the supersymmetry of the fivebrane worldvolume so one can proceed just by looking at all the ground states, without having to choose right or left movers.



Partition function for electric and magnetic states

One must now continue by finding a partition function that counts these $\frac{1}{2}$ BPS states on the fivebrane using the type II perspective. This partition function can be written as the exponential of the free energy $\mathcal{Z} = e^{\mathcal{F}}$. In this theory, because of the $\mathcal{N} = 4$ supersymmetry, the higher loop order terms and terms describing string interactions do not contribute to the free energy. In this case, this calculation proceeds in a similar way to one in a topological string theory for which one can compute the free energy, but only up to a one loop term. The partition function, in [40], now reads as

$$\mathcal{Z} = e^{\mathcal{F}_{0\text{-modes}} + \mathcal{F}_{1\text{-loop}}}, \quad (9.3.4)$$

where the 0-modes of the fivebrane are those discussed in sec. 9.3.1. From the partition function one obtains a dependence on the moduli in the worldvolume theory of the fivebrane. These must be integrated over to get the degeneracies. We are first looking at the purely electric and magnetic BPS states which correspond to the ground states of the string and preserve half of the supersymmetry⁶. The ground states of this string (moving within the fivebrane worldvolume) on the $K3$ manifold are described by harmonic forms. These are

which will become important for dyon counting in sec. 9.3.3.

⁶This partition function should also reproduce the one for the infinite tower of heterotic Dabholkar, Harvey states originally looked at in [179, 180].

the well known [181, 182] differential forms that exist on Riemannian manifolds that are annihilated by the Laplace operator. There are 24 harmonic forms on a $K3$ manifold, which must therefore be factored into the free energy. As the target space is $K3 \times T^2$ we must also include the contributions from the T^2 . This means both the numbers describing momentum and winding around the cycles.

Moduli of torus

These momentum and winding numbers of the string are contained in $\Gamma^{2,2}$, which is also known as the Narain lattice. There are 2 complex moduli that parameterise the torus. Here we have ρ that measures the volume and the field B on T^2 . This is the Kähler modulus of T^2 . We also have a complex structure modulus σ . The 1-loop free energy of this configuration [40], remembering the 24 harmonic forms, can be written as

$$\mathcal{F}_{1-loop} = \frac{1}{2} \int \frac{d^2\tau}{\tau_2} \sum_{(p_L, p_R) \in \Gamma^{2,2}} e^{i\pi(\tau p_L^2 - \bar{\tau} p_R^2)} 24, \quad (9.3.5)$$

where this sum can be split into 2 terms contributing from the momentum modes and winding modes that couple to the parameters ρ and σ respectively. The result of the sum was originally found by [183]⁷, and used again by [40]

$$\mathcal{F}_{1-loop} = 24 \log(\rho_2^{\frac{1}{2}} |\eta(\rho)|^2) + 24 \log(\sigma_2^{\frac{1}{2}} |\eta(\sigma)|^2) + C. \quad (9.3.6)$$

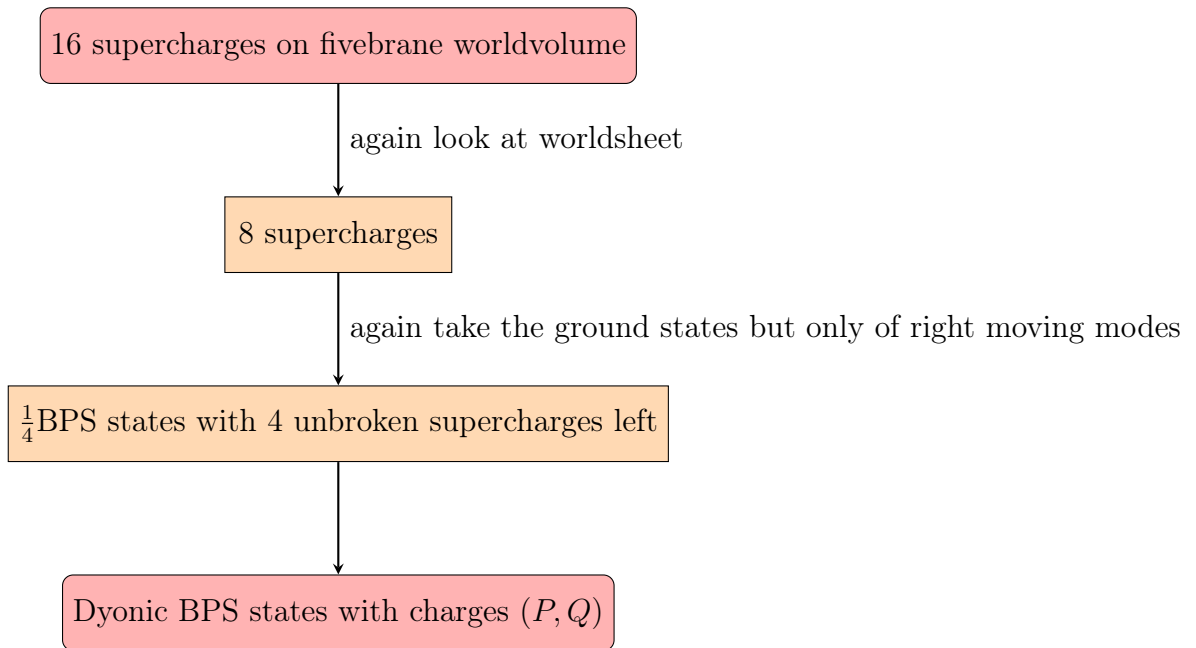
The 2 terms in (9.3.6) represented by parameters ρ and σ can be shown to represent electric and magnetic charges: if we take the first term to represent electric charges, the second then represents magnetic charges. One can look at this duality between the electric charges P and the magnetic charges Q from the type IIA perspective following [184]. Here we can use a T-duality map on the T^2 by inverting the radius of the cycles. This map exchanges the complex structure and volume moduli and shows that this fivebrane encodes both electric and magnetic charges [40] (in fact, it can be interpreted as dual branes wrapping around different cycles in the torus). The heterotic string partition function, discussed before for the ground states of the right moving mode, can be recovered by taking the holomorphic part of the free energy (9.3.6) and including the contributions from the fivebrane 0-modes. Then one reproduces the result shown in equation (9.3.1).

9.3.3 Partition function of dyons from type II description

Now that we have looked at the partition function for purely electric and magnetic $\frac{1}{2}$ BPS states, in subsection 9.3.2, we can generalise to dyonic $\frac{1}{4}$ BPS states which are formed by

⁷This was used to calculate a 1-loop threshold correction.

combining these electric and magnetic BPS states. These will be the states that ultimately appear in the work of Cheng and Verlinde [52, 53] and we later use to construct $\mathcal{N} = 2$ analogs. To understand these states we again consider the type II strings on the fivebrane and the $\mathcal{N} = (4, 4)$ superconformal algebra. As we noted before there are 16 supercharges in total for the spacetime and 8 on the worldsheet. The $\frac{1}{4}$ BPS states are those that break $\frac{3}{4}$ of the original 16 spacetime supersymmetries. Therefore, because the worldsheet supersymmetry is already half of that in spacetime, one must only have half of this worldsheet supersymmetry to obtain the $\frac{1}{4}$ BPS states. This is again achieved by considering the ground states of only the right moving modes of the string and hereby retaining only 4 unbroken supercharges.



Elliptic genus

These states are counted by the trace in the Ramond-Ramond RR-sector of the string theory (from strings satisfying two Ramond boundary conditions). This corresponds to the (2, 2) elliptic genus. As the fivebrane is wrapped on the $K3$, the elliptic genus [40, 42, 51] is taken on this manifold

$$\chi_{(q,y)}(K3) = \text{Tr}_{RR}(-1)^{F_R+F_L} y^{J_{L_0}} q^{(L_0-\frac{c}{24})} \bar{q}^{(\bar{L}_0-\frac{c}{24})}, \quad (9.3.7)$$

$$\chi_{(\tau,z)}(K3) = \text{Tr}(-1)^{F_R+F_L} e^{2\pi i(\tau(L_0-\frac{c}{24})+zF_L)}, \quad (9.3.8)$$

$\tau \in \mathbb{H}^+$, $z \in \mathbb{C}$, $q = e^{2\pi i\tau}$, $y = e^{2\pi iz}$, J_{L_0} is in general a left-moving $U(1)$ charge operator,

L_0, \bar{L}_0 are Virasoro generators for the left and (the restricted) right moving modes respectively,

c is the central charge of the Virasoro superalgebra, $c(K3) = 6$.

This trace is taken over these quantum numbers. To understand (9.3.8), one must now remember the current algebra discussed in section 9.3.2. It has left and right moving 0-modes which are represented by states with fermion numbers on the worldsheet given by $F_L = m \in \mathbb{Z}$, $F_R = 0, \pm 1$, where F_R are those for the right moving ground states. The latter being the only states considered for the right movers.

The quantum number m also becomes the helicity of the states as it represents an $SU(2)_L$ symmetry which is within the Lorentz group in spacetime, (the $SU(2)_L$ also being embedded in the current algebra and containing a $U(1)$ from which the 0-modes are taken) [185, 186, 187, 40]⁸.

3 complex variables ρ, σ, v in partition function

The fermion/helicity numbers m can now be added to the Narain lattice $\Gamma^{2,2}$ introduced in section 9.3.2, which already contains the momentum and winding numbers of the string around the torus T^2 . When these extra numbers are added the lattice becomes $\Gamma^{3,2}$ [40]. In the context of the type IIA string theory with T-duality this means that the lattice has $SO(3, 2, \mathbb{Z})$ invariance. The lattice now requires 3 complex variables to parameterise its underlying geometry. So far, in the previous subsection 9.3.2, we only have 2 variables σ and ρ associated to T^2 so we include a third parameter v ⁹. The parameters themselves transform in the $SL(2, \mathbb{Z})$ subgroup in the form of a vector representation.

The elliptic genus of $K3$, shown above in (9.3.7) [42], can be expanded in terms of Fourier coefficients in the form of $c(4h - m^2)$, where $h = kl$ can be written to compare with the occupation numbers, described in section 9.2, for the quantum states

$$\chi_{(\tau, z)}(K3) = \sum_{h \geq 0, m \in \mathbb{Z}} c(4h - m^2) e^{2\pi i(h\tau + mz)}. \quad (9.3.9)$$

Now, as before, one must look for the free energy \mathcal{F} so that one can find the partition function in the form of $\mathcal{Z} = e^{\mathcal{F}}$. For this free energy, as with the purely electric and magnetic examples in sec. 9.3.2, it is known that the higher loop order terms do not contribute. Therefore, one can again look for the 1-loop integral. In this case, one sums over the momentum modes in the $\Gamma^{3,2}$ lattice and factors in the coefficients from the $K3$ in (9.3.9) [40, 42]. This is to

⁸It can also be seen as a bundle over the torus within the target space

⁹Physically this represents a Wilson loop in the theory that can be taken in the volume occupied by the fivebrane [40].

include all possible combinations of modes wrapped within the $K3$ manifold ¹⁰

$$\mathcal{F}_{1-loop} = \frac{1}{2} \int_{\mathbb{F}} \frac{d^2\tau}{\tau_2} \sum_{\substack{p_R, p_L \in \\ \Gamma^{3,2}}} e^{i\pi(\tau p_L^2 - \bar{\tau} p_R^2)} c(n) e^{i\pi \frac{n}{2}}, \quad (9.3.10)$$

where, for the coefficients, we have $c(n) = c(4h - m^2)$ from the $K3$ elliptic genus in (9.3.9) above. $\epsilon = 0, 1$ for even and odd m respectively. Both the left and right moving momentum modes [188], denoted by p_L and p_R , can be written in terms of the parameters ρ, σ, v

$$\frac{1}{2} p_R^2 = \frac{1}{4Y} |m_1 \rho + m_2 + n_1 \sigma + n_2 (\rho \sigma - v^2) + bv|^2, \quad (9.3.11)$$

$$\frac{1}{2} (p_L^2 - p_R^2) = \frac{1}{4} b^2 - m_1 n_1 + m_2 n_2, \quad (9.3.12)$$

where the numbers m_1, m_2, n_1, n_2, b can be taken as any integer. Here $Y = \rho_2 \sigma_2 - v_2^2$ represents the determinant of the matrix given by the imaginary parts of the complex parameters $\rho = \rho_1 + i\rho_2$, $\sigma = \sigma_1 + i\sigma_2$, $v = v_1 + iv_2$.

9.3.4 Expansion of $K3$ elliptic genus

The $K3$ elliptic genus, described previously in subsection 9.3.3, can be written in terms of theta functions. This is because the affine $SU(2)$ Lie algebra is a subalgebra within the $\mathcal{N} = 4$ algebra that describes the full superconformal sigma model on the $K3$ target space. This decomposition [42, 188] can be written as

$$\chi_{(\tau, z)}(K3) = h_0(\tau) \theta_{01}(\tau, 2z) + h_1(\tau) \theta_{11}(\tau, 2z), \quad (9.3.13)$$

$$\theta_{01}(\tau, 2z) = \sum_{b \in 2\mathbb{Z}} q^{\frac{b^2}{4}} y^b, \quad \theta_{11}(\tau, 2z) = \sum_{b \in 2\mathbb{Z}-1} q^{\frac{b^2}{4}} y^b, \quad (9.3.14)$$

where the theta functions in (9.3.13) are expanded on the second line in terms of odd or even integer powers. The functions $h_0(\tau)$ and $h_1(\tau)$ encode the expansion coefficients of the $K3$ elliptic genus [42]. The first terms in the series are shown here

$$h_0(\tau) = \sum_{N \equiv 0 \pmod{4}} c(N) q^{\frac{N}{4}} = 20 + 216q + 1616q^2 + 8032q^3 + 33048q^4 + 117280q^5 + \dots, \quad (9.3.15)$$

$$h_1(\tau) = \sum_{N \equiv -1 \pmod{4}} c(N) q^{\frac{N}{4}} = q^{-\frac{1}{4}} (2 - 128q - 1026q^2 - 5504q^3 - 23550q^4 - 86400q^5 + \dots).$$

¹⁰The integral is over the worldsheet torus which has a modular group with fundamental domain \mathbb{F} .

We can read off the first few coefficients as

$$c(-1) = 2, \quad c(0) = 20. \quad (9.3.16)$$

This can also be seen by expanding the elliptic genus as

$$\chi_{(\tau,z)}(K3) = 2y + 2y^{-1} + 20 + O(q). \quad (9.3.17)$$

When one takes the limit $y \rightarrow 1$ one obtains the Witten index of $K3$ which is given as: $\chi_{(\tau,z)}(K3) = 24$.

9.3.5 The 1-loop integral

The 1-loop integral (9.3.10) can be written in terms of the functions $h_0(\tau)$, $h_1(\tau)$ and the momentum modes [42]. In this case, the integers m_1, m_2, b are summed over

$$\mathcal{I} = \int_{\mathbb{F}} \frac{d^2\tau}{\tau_2} \sum_{m_1, m_2, n_1, n_2} \left(\sum_{b \in 2n} q^{p_L^2} \bar{q}^{p_R^2} h_0(\tau) + \sum_{b \in 2n+1} q^{p_L^2} \bar{q}^{p_R^2} h_1(\tau) - c(0) \right). \quad (9.3.18)$$

The next step here is to explicitly compute the one loop integral (9.3.10) in terms of the moduli - this integral formulation for BPS algebras has been developed in the literature [43, 183], and explicitly computed for this example in [42, 51], by splitting it into 3 contributions

$$\mathcal{I} = \mathcal{I}_0 + \mathcal{I}_{deg} + \mathcal{I}_{nd}. \quad (9.3.19)$$

These describe the contributions from 0-orbits \mathcal{I}_0 , degenerate orbits \mathcal{I}_{nd} , and non-degenerate orbits \mathcal{I}_{nd} under the action of the $SL(2, \mathbb{Z})$ group describing the modularity of this integral. The results for the 3 integrals can be written as:

$$\mathcal{I}_0 = \frac{Y}{\rho_2} \int_{\mathbb{F}} \frac{d^2\tau}{(\tau_2)^2} \chi_{(\tau,0)}(K3) = \frac{Y}{\rho_2} \frac{\pi}{3} 24, \quad (9.3.20)$$

$$\mathcal{I}_{nd} = -\log \prod_{k>0, l \geq 0, b \in \mathbb{Z}} |1 - e^{k\rho + l\sigma + mv}|^{c(4kl - m^2)}, \quad (9.3.21)$$

$$\begin{aligned} \mathcal{I}_{deg} = & -\frac{\pi}{3} c(0) \sigma_2 - \log(Y)^{c(0)} - \log \prod_{l>0} |1 - e^{l\sigma}|^{4c(0)} + (\gamma_\epsilon - 1 - \log \frac{8\pi}{3\sqrt{3}}) c(0) + \\ & 4\pi \left(\frac{v_2^2}{\sigma_2} + v_2 + \frac{\sigma_2}{6} \right) c(-1) - \log \prod_{l>0, b=\pm 1} |1 - e^{l\sigma + mv}|^{4c(-m^2)} + \log \prod_{l>0, b=\pm 1} |1 - e^{mv}|^{4c(-m^2)}. \end{aligned} \quad (9.3.22)$$

Now the sum of the 3 contributions is computed to obtain $\mathcal{I} = \mathcal{I}_0 + \mathcal{I}_{deg} + \mathcal{I}_{nd}$. This then becomes

$$\mathcal{I} = -2 \log kY^{10} |e^{\rho+\sigma+v} \prod_{k>0, l \geq 0, b \in \mathbb{Z}} (1 - e^{k\rho+l\sigma+mv})^{c(4kl-m^2)}|^2, \quad (9.3.23)$$

where $k = (\frac{8\pi}{3\sqrt{3}}e^{1-\gamma_E})^{10}$. The Euler Mascheroni constant is denoted by γ_E . Here the integral has become a product involving factors over all the possible integer multiples of the moduli. The coefficients of the elliptic genus expansion $c(4kl-m^2)$ are now present as the exponents of the factors. The function [45, 46, 47], which is a Siegel modular form of weight 10, is known as the Igusa cusp form

$$\Phi_{10}(\Omega) = e^{\rho+\sigma+v} \prod_{k>0, l \geq 0, m \in \mathbb{Z}} (1 - e^{k\rho+l\sigma+mv})^{c(4kl-m^2)}, \quad (9.3.24)$$

where

$$\Omega = \begin{pmatrix} \sigma & v \\ v & \rho \end{pmatrix}, \quad (9.3.25)$$

such that we can now write the 1-loop integral in terms of this Igusa cusp form

$$\mathcal{I} = -2 \log(kY^{10} |\Phi_{10}(\Omega)|^2). \quad (9.3.26)$$

As in the case of the half-BPS states, we have the modulus squared of the product and to find the partition function we must only take the holomorphic part. The free energy then can also be written in the form

$$\mathcal{F}_{1-loop} = -\log(kY^{10} |\Phi_{10}(\Omega)|^2) = \log(Y^{10} |\Phi_{10}(\Omega)|^2) + const, \quad (9.3.27)$$

and the partition function can [40], like the half-BPS states, be written as

$$\mathcal{Z} = e^{\mathcal{F}_{1-loop}} = e^{\mathcal{I}} = e^{-\log(kY^{10} |\Phi_{10}(\Omega)|^2)} = e^{-\log(k) + \log(Y^{10} |\Phi_{10}(\Omega)|^2)}. \quad (9.3.28)$$

Finally, to construct the dyon counting formula, we must include the fivebrane 0-mode contribution as both this and the 1-loop order contribute to the free energy. This 0-mode contribution can be taken as the exponential of the electric and magnetic charges (P, Q) [40], using their square, product and the moduli in the form

$$e^{i\pi(P^2\rho+Q^2\sigma+2P\cdot Qv)}.$$

From this it now becomes possible to construct the dyon counting formula [40, 52, 53] in the work of Cheng and Verlinde for BPS states by putting together the contributions from

all the above factors. For the charges (P, Q) this can be put together to find $d(P, Q)$ as ¹¹

$$d(P, Q) = \oint d\sigma d\rho dv \frac{e^{i\pi(P^2\rho + Q^2\sigma + 2P\cdot Qv)}}{\Phi_{10}(\Omega)}. \quad (9.3.29)$$

9.4 Generating function as partition function

The denominator of this dyon degeneracy formula, derived in [40], can be considered a partition function for the charges such that it counts the number of possible configurations of a black hole with charge (P, Q) . This function is also the Igusa cusp form introduced in this section in (9.3.24). It is reviewed in great detail in [54], ¹² and is indeed the 3 parameter partition function of dyonic $\frac{1}{4}$ BPS states discussed in the more recent literature [52, 53, 54] describing the $\mathcal{N} = 4$ wall crossing phenomena. To remind ourselves, the expression for the cusp form is

$$\Phi_{10}(\Omega) = qyp \prod_{k,l,m>0} (1 - q^k y^l p^m)^{2C_0(4kl-m^2)}, \quad (9.4.1)$$

where $C_0(4kl - m^2)$ are the Fourier coefficients of the Jacobi form $\phi_{0,1}(\tau, z)$ used in the multiplicative lift. This is still also a multiplicative lift of the elliptic genus from (9.3.7), which is now written in terms of the Jacobi form $\chi_{(\tau,z)}(K3) = 2\phi_{0,1}(\tau, z)$, meaning that the Fourier coefficients in the exponent are redefined by a factor of 2. We have also redefined the variables from the previous subsection 9.3.5 such that $\rho \rightarrow \sigma, \sigma \rightarrow \tau$. They can now be written as exponentials $p = e^{2\pi i\sigma}, q = e^{2\pi i\tau}, y = e^{2\pi iv}$ and organised into the matrix

$$\Omega = \begin{pmatrix} \tau & v \\ v & \sigma \end{pmatrix}. \quad (9.4.2)$$

This is the period matrix of a genus 2 Riemann surface [40]. The partition function for the dyons is now given by

$$Z(\Omega) = \frac{1}{\Phi_{10}(\Omega)} = \frac{1}{p} \prod_{k>0, l \geq 0, m} \frac{1}{\eta^{18}(\tau) \theta_1^2(\tau, v) (1 - q^k y^l p^m)^{2C_0(4kl-m^2)}} = \sum_{r \geq -1, s \geq -1, t} e^{2\pi i(r\tau + s\rho + tv)} g(r, s, t), \quad (9.4.3)$$

$$\eta(\tau) = e^{\frac{i\pi\tau}{12}} \prod_{n=1}^{\infty} (1 - e^{2n\pi i\tau}) \quad \text{is the dedekind eta function,}$$

$$\theta_1(\tau, v) = -e^{\frac{1}{4}\pi i\tau + \pi i(v + \frac{1}{2})} \theta\left(\tau, v + \frac{1}{2}\tau + \frac{1}{2}\right),$$

¹¹One can let $d(P, Q) = (-1)^{P\cdot Q+1} D(P, Q)$, where the factor was introduced by [41, 189] to relate the 4d and 5d degeneracies.

¹²This function is a is the unique weight 10 cusp form defined in [45, 46].

is an auxiliary theta function that can be mapped to the Jacobi theta function.

This is the full description of the cusp form mentioned in (9.3.24), and is also known as a product representation of a Siegel modular form. These are generalisations of elliptic modular forms in which the arguments are period matrices of higher genus Riemann surfaces with positive definite imaginary part. This function can also be written in terms of the root system of the Borcherds-Kac-Moody algebra of which this is the Weyl denominator. The auxiliary theta function $\theta_1^2(\tau, v)$ contains the Weyl denominator of the \hat{A}_1 subalgebra. This will become important later in sec. 10.3 as we look at the generating functions for subalgebras.

The degeneracy of dyonic BPS states with electric and magnetic charge (P, Q) is now defined as

$$d(P, Q) = g\left(\frac{1}{2}Q^2, \frac{1}{2}P^2, P \cdot Q\right) \quad \text{where} \quad \frac{1}{2}Q^2, \frac{1}{2}P^2, P \cdot Q, \quad (9.4.4)$$

are the 3 T-duality invariants that can be formulated in terms of these charges. We can also transform $v \rightarrow -v$. From the expansion above one can see this is also the Fourier coefficient of the Igusa cusp form ¹³

$$d(P, Q) = \oint d^3\Omega \frac{e^{\pi i \Lambda_{P,Q}(\Omega)}}{\Phi_{10}(\Omega)}, \quad (9.4.5)$$

where the charge vector, and a basis of roots of the lattice of possible charge vectors, can be written as

$$\Lambda_{P,Q} = \begin{pmatrix} P \cdot P & P \cdot Q \\ P \cdot Q & Q \cdot Q \end{pmatrix}, \quad (9.4.6)$$

$$\alpha_1 = \begin{pmatrix} 0 & -1 \\ -1 & 0 \end{pmatrix}, \quad \alpha_2 = \begin{pmatrix} 2 & 1 \\ 1 & 0 \end{pmatrix}, \quad \alpha_3 = \begin{pmatrix} 0 & 1 \\ 1 & 2 \end{pmatrix}.$$

Therefore the charge vector $\Lambda_{P,Q}$ is now a linear combination of a basis of 3 positive roots of the Borcherds-Kac-Moody algebra, $\Lambda_{P,Q} \in (\mathbb{Z}_+\alpha_1 + \mathbb{Z}_+\alpha_2 + \mathbb{Z}_+\alpha_3)$. The roots of a basis are those used by Cheng and Verlinde [53] to look at possible splittings of a dyon into electric and magnetic constituents.

¹³In this way the degeneracy and the Igusa cusp form is written as in Cheng and Verlinde [53].

9.5 Modularity, contour prescription, and wall crossing

Now one can discuss the contour prescription used to extract the Fourier coefficients from the factors in the generating function. Specifically, the example of \hat{A}_1 will be considered using a contour in terms of 2 of the 3 complex variables. To consider a modular formulation of this contour prescription it is important to understand how this works in the original $\mathcal{N} = 4$ dyon counting function from which this limit is taken.

9.5.1 Modularity and limits of Igusa cusp form

As explained in sec. 9.3 the full dyon counting formula was originally derived as the weight 10 Igusa cusp form $\Phi_{10}(\Omega)$. This is a Siegel modular form. Physically, the modularity represents the S-duality transformations acting on the charges and moduli of the theory. We can remember that the matrix Ω from (9.4.2) is a period matrix of a genus 2 Riemann surface in the parameters. For now it can be understood as a general Riemann surface but in section 9.5.3 we will see that the imaginary parts of the periods are proportional to the normalised central charges. Various limits can be taken of this Riemann surface to make it easier to visualise the situation with the charges.

Possible limits that can be taken

For example, one can see that when $v = 0$ the genus 2 surface can be split into 2 tori. In this case, the electric and magnetic charges correspond to cycles around the loops of the 2 tori respectively. However, one can also look at a different limit where $\sigma = 0$. For this second example, one expects the generating function to include the combinations of the periods of a genus 1 Riemann surface matching the action of the $PSL(2, \mathbb{Z})$ modular group from the Jacobi-theta function. Therefore, in the latter case one chooses the subgroup acting just on the upper part of this matrix (τ, v) . In these two cases the period matrix can be taken as

$$\Omega_{v=0} = \begin{pmatrix} \tau & 0 \\ 0 & \sigma \end{pmatrix}, \quad \Omega_{\sigma=0} = \begin{pmatrix} \tau & v \\ v & 0 \end{pmatrix}. \quad (9.5.1)$$

Furthermore, a simpler limit can be taken to give an expression just in (τ, v) , including the Jacobi-theta function. This is the limit $\sigma \rightarrow +i\infty$. This is ideal for studying wall crossing just in these two variables and will be revisited in sec. 10.2.1.

Modularity

The Siegel upper-half plane \mathbb{H}^+ is defined by $\text{Im}[\tau], \text{Im}[\sigma] > 0$ and $\det(\text{Im}[\Omega]) > 0$. The arguments of the Igusa cusp form must take values in this plane in order for this function

to retain the modular property. One can then act on this plane with the group elements $g \in Sp(2, \mathbb{Z})$ [50, 52, 54]. The period matrix then becomes

$$\Omega \rightarrow \frac{A\Omega + B}{C\Omega + D}. \quad (9.5.2)$$

Here the group elements are defined by $gJg^t = J$ where

$$J = \begin{pmatrix} 0 & -I_2 \\ I_2 & 0 \end{pmatrix}. \quad (9.5.3)$$

This means that the block matrices satisfy the relations

$$AB^t = BA^t, \quad CD^t = DC^t, \quad \text{and finally } AD^t - BC^t = I_2. \quad (9.5.4)$$

When one writes the Igusa cusp form as $1/\Phi_{10}(\Omega)$, one can generate the location of the poles of this function by starting with one pole (e.g. at $y = 1$) and acting with elements g of the group to generate the full set. The other poles then arise as images under the action of this group.

For this Igusa cusp form, one can embed the $PSL(2, \mathbb{Z})$ modular group within the $Sp(2, \mathbb{Z})$ group from (9.5.2 - 9.5.3). This can be considered the S-duality transformation acting on the T-duality invariants of the charges from (9.4.6) ¹⁴

$$\Lambda_{P,Q} = \begin{pmatrix} P \cdot P & P \cdot Q \\ Q \cdot P & Q \cdot Q \end{pmatrix}.$$

This matrix transforms under S-duality by action of elements of the $PSL(2, \mathbb{Z})$ subgroup, while, as described above, the full $Sp(2, \mathbb{Z})$ generates all the poles of the Igusa cusp form. This means that the $SL(2, \mathbb{Z})$ subgroup in matrix representation acts on the charges as: $\Lambda_{P,Q} \rightarrow \gamma \Lambda_{P,Q} \gamma^t$, and on the period matrix as $\Omega \rightarrow (\gamma^t)^{-1} \Omega \gamma^{-1}$. This transformation can then be embedded within the $Sp(2, \mathbb{Z})$ group [52, 54]. The embedding works as:

$$\begin{pmatrix} A & B \\ C & D \end{pmatrix} = \begin{pmatrix} (\gamma^t)^{-1} & O \\ O & \gamma \end{pmatrix} = \begin{pmatrix} d & -c & 0 & 0 \\ -b & a & 0 & 0 \\ 0 & 0 & a & b \\ 0 & 0 & c & d \end{pmatrix}. \quad (9.5.5)$$

9.5.2 Contour prescription

One can now consider the integral over the $\mathcal{N} = 4$ dyon counting function for a particular charge and consider what happens to this integral when one acts with the $Sp(2, \mathbb{Z})$ transformation. From this one can look to see if the contour in Ω shifts under this transfor-

¹⁴This is the matrix representing the charges in [52, 53].

mation. The aim of the contour prescription is to keep this contour invariant under S-duality transformations. In practice the degeneracies can be found by deforming S-duality invariant contours for different charges into each other and picking up extra contributions to the degeneracies from the poles.

Prescription for degeneracies

The degeneracies of the charges in (9.4.5), now written together as one vector $\vec{Q} = (P, Q)$, are extracted from the Igusa cusp form before and after the S-duality transformation respectively [50] using the formula

$$d(\vec{Q}) = \oint_{\mathcal{C}} d^3\Omega \frac{e^{-i\pi\vec{Q}^t \cdot \Omega \cdot \vec{Q}}}{\Phi_{10}(\Omega)}, \quad d(\vec{Q}') = \oint_{\mathcal{C}} d^3\Omega' \frac{e^{-i\pi\vec{Q}'^t \cdot \Omega' \cdot \vec{Q}'}}{\Phi_{10}(\Omega')}, \quad (9.5.6)$$

where \mathcal{C} is the contour. To determine the degeneracy for the new charge \vec{Q}' one has to understand the $Sp(2, \mathbb{Z})$ transformation of $\Omega \rightarrow \Omega'$ and act on the contour with this. Under this transformation one knows that the form of the differential remains invariant as well as the form of the inner product of charges in the numerator such that one can write: $d^3\Omega = d^3\Omega'$. Furthermore, the Igusa cusp itself is invariant $\Phi_{10}(\Omega) = \Phi_{10}(\Omega')$, as well as the product in the numerator $\vec{Q} \cdot \Omega \cdot \vec{Q}^t = \vec{Q}' \cdot \Omega' \cdot \vec{Q}'^t$. So, the contour prescription set up for \mathcal{C} must also be one which is also invariant under this transformation. This can be taken as a 3 torus in the Siegel upper half-plane [52, 48, 190, 49, 50] which takes the form in the 3d complex space τ, σ, v :

$$\text{Re}[\tau] \in [0, 1], \quad \text{Re}[\sigma] \in [0, 1], \quad \text{Re}[v] \in [0, 1]. \quad (9.5.7)$$

The imaginary part of this contour is taken to be a large positive constant such that one has:

$$\text{Im}[\tau] \in N_1, \quad \text{Im}[\sigma] \in N_2, \quad \text{Im}[v] \in N_3. \quad (9.5.8)$$

There is another way of writing this contour. One can remember that these variables are defined as complex numbers in the Siegel upper-half plane such that: $\text{Im}[\tau], \text{Im}[\rho] > 0$ and $\text{Im}[\tau]\text{Im}[\rho] > (\text{Im}[v])^2$. The Fourier coefficients are extracted by choosing a particular contour prescription for a charge when specifying N_1, N_2, N_3 (see sec. 9.5.3 below). This contour is typically chosen at fixed imaginary part deeply within the Siegel upper-half plane such that $\text{Im}[\tau]\text{Im}[\sigma] \gg (\text{Im}[v])^2 + 1$. One then integrates over the real part of the contour such that we can finally write the contour \mathcal{C} as

$$0 \leq \text{Re}[\tau], \text{Re}[\sigma], \text{Re}[v] < 1, \quad \text{Im}[\tau]\text{Im}[\sigma] \gg (\text{Im}[v])^2 + 1. \quad (9.5.9)$$

Moving between degeneracies

S-duality for the degeneracies defined as $d(\vec{Q}) = d(\vec{Q}')$, however, works only if there is no possible crossing of walls of marginal stability. If one can cross a wall of marginal stability the degeneracy can jump. To compute the degeneracies in general one must look for a different contour prescription for each charge \vec{Q} and \vec{Q}' separately as \mathcal{C} and \mathcal{C}' . The contour, before any poles are crossed, must be S-duality invariant for each charge satisfying the relations (9.5.8-9.5.9) above.

Therefore, in general one can deduce [50] that the way to extract degeneracies from the pole structure of the theory is to:

- (i) For each charge define a specific contour under which the degeneracies are initially S-duality invariant: that is invariant under $SL(2, \mathbb{Z})$. In general, one can expect to find different contours for different charges.
- (ii) Start with a particular contour \mathcal{C} for which one knows the degeneracies of charges in the part of the charge lattice belonging to the fundamental cell.
- (iii) Deform this contour \mathcal{C} into another \mathcal{C}' .
- (iv) Now during the deformation between 2 contours one can cross poles. So, these poles contribution must then be added to the degeneracy.

9.5.3 Walls and central charges in $\mathcal{N} = 4$

It has been determined that [49, 52, 53, 54] the walls of marginal stability correspond to the boundaries of the regions of the moduli space where the different multi-centered dyonic black hole solutions can exist. These multi-centered solutions are $\frac{1}{4}$ BPS, but they are bound states of single-centered $\frac{1}{2}$ BPS states with parallel electric and magnetic charges that can be transformed under S-duality into either pure electric or magnetic states. The walls of marginal stability are the regions of the moduli space where the mass of the multi-centered state is equal to the sum of the single-centered solutions. That is, there is a $\frac{1}{4}$ BPS dyonic state that splits into two $\frac{1}{2}$ BPS states when

$$M_{(P,Q)} = M_{(P_1,Q_1)} + M_{(P_2,Q_2)}.$$

Walls and central charges

To see where the walls occur one must define a moduli dependence of the contour by writing the period matrix Ω in terms of central charges. In this $\mathcal{N} = 4$ model this can be described by this matrix taking the form of: $\text{Im}[\Omega] = \frac{1}{\epsilon}X$, where X is a unit vector obtained by normalising the central charges. The real part is given by $\text{Re}[\Omega] \in [0, 1]$. Here ϵ is a small

positive real number that takes the contour out to infinity by having $\epsilon \rightarrow 0$ such that the components of Ω take large positive values that only depend on the sign of the components of X but not their magnitude. The $\mathcal{N} = 4$ central charge dependence can be written explicitly in terms of a unit vector, such that $X = \frac{\mathcal{Z}_{P,Q}}{|\mathcal{Z}_{P,Q}|}$, where $\mathcal{Z}_{P,Q}$ is the central charge of the dyon with charges $\vec{Q} = (P, Q)$ ¹⁵. Here P, Q are the charges corresponding to the root from which one wants to extract the degeneracy, and by the prescription given above (9.5.8-9.5.9), also define the contour.

The space of possible unit vectors with $|X| = 1$ is hyperbolic. Therefore, one can now [53] parameterise these vectors as:

$$X = \frac{1}{\tau_2} \begin{pmatrix} |\tau|^2 & \tau_1 \\ \tau_1 & 1 \end{pmatrix}. \quad (9.5.10)$$

Here $\tau = \tau_1 + i\tau_2 \in \mathbb{H}^+$ is the parameter mapping the hyperbola of unit vectors into the upper half-plane. In this case, this can be incorporated into the contour prescription discussed above. For this the large imaginary part in the contour becomes:

$$N_1 = \frac{1}{\epsilon} \frac{|\tau|^2}{\tau_2}, \quad N_2 = \frac{1}{\epsilon} \frac{1}{\tau_2}, \quad N_3 = \frac{1}{\epsilon} \frac{\tau_1}{\tau_2}. \quad (9.5.11)$$

Discrete attractors and Weyl chambers

The equations for the walls are given by the inner product $\alpha_i(X) = (X, \alpha_i) = 0$.¹⁶ The walls are also the boundaries of the Weyl chambers W associated with the Weyl group of the root system (9.4.6). If X varies in such a way that it crosses this locus of vanishing product with a positive root then one crosses a wall, or equivalently a pole, and hence this state ceases to contribute to the degeneracy. Here one can interpret this as a composite dyonic BPS state with a particular charge decaying into 2 product states. This process then repeats itself when the same initial charge can be split into a different combination of 2 product states. The decay pattern then continues iteratively, such that one obtains a cascading discrete attractor flow [53]¹⁷ of composite BPS states, with a particular total charge but different combinations of constituents disappearing across walls bounding infinitely many chambers. This then ultimately reaches the fundamental Weyl chamber W_F . Here one finds only the states that can not further be decomposed - the so called ‘‘immortal dyons’’ in [52, 54].

¹⁵The central charge can be presented in terms of the normalised charge vector and the axion-dilaton moduli [49, 53].

¹⁶Here $\alpha_i \in \Delta^+$ (the set of positive roots). The inner product is defined by $(X, Y) = -\det(Y)\text{Tr}(XY^{-1})$ [53].

¹⁷The attractor equation, this time for the $\mathcal{N} = 4$ theory, is again derived from the central charge and the flow is analogous for the attractor flow in sections 7 and 8 for the $\mathcal{N} = 2$ examples [140, 191] but with the difference that the flow is a discrete pattern of jumping across the walls in the direction of more unstable BPS states.

10 | $\mathcal{N} = 4$ BPS generating function and Lie algebras

In this thesis a generating function is derived which counts the BPS states in the different chambers of the moduli space and from which BPS degeneracies can be extracted. This is also presented in the work “Generating functions for $\mathcal{N} = 2$ BPS structures” and is covered here in this chapter 10 and the following chapter 11.

We restrict the $\mathcal{N} = 4$ generating function to that of subalgebras and use these to reproduce the wall crossing for $\mathcal{N} = 2$ analogs such as Argyres-Douglas and Seiberg-Witten theories [1, 5]. The existence of BPS states in particular regions in the moduli space of these theories was already looked at in the initial part of our research on attractor flow, described in chapters 7 and 8 using the special geometry of the moduli space. In the following sections we derive a generating function for theories with a BPS spectrum described by the roots of the Lie algebras \hat{A}_1 and A_2 . These generating functions have the potential to be generalised to CY 3-folds with ADE-type singularities. They should also encode the wall crossing and the existence conditions for the BPS states. Given that the singularities are ADE-type, and the BPS states are represented by roots of the corresponding Lie algebra, one is looking for associated invariants of the root system within the chambers bounded by walls. To determine what they could be, one can look at what is known in this area so far in the literature [40, 52, 53, 54, 50, 48, 190, 49] on generating functions of $\mathcal{N} = 4$ black holes introduced in section 9.3 and proceed to find an analog that matches the $\mathcal{N} = 2$ wall crossing in these examples.

The generating function derived in section 9.3, for $\mathcal{N} = 4$, $\frac{1}{4}$ BPS states in 4d, culminated in a Lie algebraic prescription for wall crossing for which analogs in $\mathcal{N} = 2$ theories can be found. It has been previously conjectured [42] and worked out explicitly in the work of Cheng and Verlinde [53], that the dyon counting formula in (9.3.29) is related to the Borchers-Kac-Moody algebra. In particular, it corresponds to its Weyl denominator - the Igusa cusp form from (9.3.24). This algebra and its Weyl denominator are described in detail by Gritsenko and Nikulin [45, 46, 47]. In our research we use this result to extract generating functions for subalgebras that match the root systems of $\mathcal{N} = 2$ theories, such as \hat{A}_1 . We then use these as an analogy from which to conjecture a more general approach to generating functions in $\mathcal{N} = 2$ theories with BPS root systems corresponding to other Lie algebras, such as the ADE type Argyres-Douglas theories, previously discussed in sections

3.1.2, 4.3 and chapter 5.1. It should also be noted that BPS algebras of this form have also been discussed for 4d $\mathcal{N} = 2$ heterotic string theory in an old result by Harvey and Moore [172, 43] in which a generating function was also derived. However, the most recent prescriptions for extracting degeneracies and understanding wall crossing are given by Cheng and Verlinde [52, 53].

As the $\mathcal{N} = 4$ walls are Weyl chamber boundaries we can match these with the BPS walls introduced for the framed BPS states from GMN [17] in section 5.3 as well as the Jafferis-Moore [37] D6-D2-D0 boundstates reviewed in section 5.4. This is done by defining the $\mathcal{N} = 2$ moduli used as the argument of the generating function. This means defining the analog of the central charge function $X = \frac{Z_{P,Q}}{|Z_{P,Q}|}$ in terms of central charges for the $\mathcal{N} = 2$ theory such that the BPS walls match correctly. If we use the attractor flow existence conditions from chapter 7 to exclude the BPS walls ending at a regular point in the moduli space then we reproduce the scattering diagrams and wall crossing phenomena for the vanilla BPS states. These are derived by Bridgeland [124] from Konsevich-Soibelman operators [30] (see section 5.3) and reviewed in [58]. It is also interesting to note that the BPS algebra originally defined by Harvey and Moore has been recently matched [192] with the algebra describing the scattering for the framed BPS states.

The dyon counting formula from [53] can be rewritten in terms of the root system in the form of Weyl denominator for the Borcherds-Kac-Moody algebra. In this case, the formula [53] from (9.3.29) becomes

$$(-1)^{P \cdot Q + 1} D(P, Q) = \oint_{\mathcal{C}} d^3\Omega \left(\frac{e^{i\pi(\frac{1}{2}\Lambda_{P,Q} + \rho, \Omega)}}{\prod_{\alpha \in \Delta^+} (1 - e^{-i\pi(\alpha, \Omega)})^{\text{mult}(\alpha)}} \right)^2, \quad (10.0.1)$$

where $\Lambda_{P,Q}$ is the charge vector, $\text{mult}(\alpha)$ is the multiplicity of the root α and $\alpha(\Omega) = (\alpha, \Omega)$ ¹. One can now interpret the degeneracy as enumerating the number of ways one can write the numerator of the dyon counting formula as a sum of 2 sets of roots, the sums being positive. One can now let $\Lambda = \frac{1}{2}\Lambda_{P,Q} + \rho$ be the highest weight of a Verma module² such that the stable composite BPS states can be counted as contributions to this weight. Therefore, wall crossing causes a jump in the highest weight, which is an invariant within the Weyl chambers. This principle is generalisable to Verma modules in $\mathcal{N} = 2$ analogs.

10.1 Wall crossing and BPS generating function for subalgebras

We now start by deriving generating functions for subalgebras from the $\mathcal{N} = 4$ dyon counting function that can give us information about wall crossing in $\mathcal{N} = 2$ theories. These should act on a subset of the root lattice that one can choose. This can be done by looking at

¹This inner product is defined by $(X, Y) = -\det(Y)\text{Tr}(XY^{-1})$.

²See section 11.1.1 for a definition.

the wall crossing for $\frac{1}{4}$ BPS dyons that have charges corresponding to those we know exist in $\mathcal{N} = 2$ theories with affine A_1 (also denoted by \hat{A}_1) root lattice, such as Seiberg-Witten theory or the D6-D2-D0 bound states described by Jafferis-Moore [37]. Then we can use such a generating function as an analog counting function to determine existence of such BPS states in these theories.

However, we first review the $\mathcal{N} = 4$ interpretation. One can start by extracting BPS degeneracies from the generating function (10.0.1) in the full $\mathcal{N} = 4$ case. They are extracted in the Siegel upper half-plane \mathbb{H}^+ . Once this is done one can then look at their wall crossing phenomena. As discussed above in sec. 10, it is understood that this generating function describes the wall crossing phenomenon of the splitting of multi-centered BPS black hole dyons. This has been shown to work from 2 perspectives: the first is directly from the generating function [53] and the second is by a contour prescription [52]. Starting with the generating function (10.0.1), for particular values of the moduli, the function can be expanded as a series expansion of the form ³

$$\frac{1}{\Phi_{10}(\Omega)} = \sum_{p,q,r=-1}^{\infty} F_{KM}(p,q,r) e^{-p\alpha_1(\Omega) - q\alpha_2(\Omega) - r\alpha_3(\Omega)}, \quad (10.1.1)$$

where $\alpha_1, \alpha_2, \alpha_3$ are a basis of positive roots $\Delta_{(A,S)}^+$ of the Borcherds-Kac-Moody superalgebra $\mathfrak{g}(A,S)$ ⁴ and $F_{KM}(p,q,r)$ are the Fourier coefficients of the square Weyl denominator. However, remembering the condition from the work of Cheng and Verlinde [53], the series expansion is only well defined for $\text{Im}[i\alpha_j(\Omega)] > 0$ ⁵ for all roots α_j that occur within the product in the Weyl denominator. Only in this case do we know how to extract the Fourier coefficients. This means that at a point in the moduli space where one has a finite number of roots with negative vanishing imaginary part

$$\text{Im}[i\alpha_j(\Omega)] < 0, \quad \forall j \in \{1, \dots, n\}, \quad \text{Im}[i\alpha_k(\Omega)] > 0, \quad \forall k \neq j. \quad (10.1.2)$$

One must now rewrite the generating function such that it has only factors in the denominator with exponents all in the form $\text{Im}[i\alpha_j(\Omega)] > 0, \quad \forall j \in \{1, \dots, n\}$. It can then be expanded again as a Fourier series where coefficients can be extracted. However, in this case the coefficients will jump. This is because, in rewriting the equation, one moves the exponential factors into the numerator from which one obtains a shift in the degeneracies, meaning that the degeneracies of a particular electric and magnetic charge before wall crossing become those of a different charge on the other side of the wall. In this case, one can use S-duality to change the basis used in the denominator back to one of positive roots, such that the denominator is again written in terms of these roots, as it was before the jump occurred.

³Here we have redefined $\alpha(\Omega)$ by absorbing the factor $i\pi$ into the complex variables in Ω .

⁴We are using the notation of [45] such that A represents the Cartan matrix of the BKM algebra and S is a subset of the indices labelling the generators.

⁵The factor i is inserted here, following the convention of [52, 53], as $\text{Re}[\alpha_j(\Omega)] > 0$ for the sum to converge.

Alternatively, according to the second prescription [52], this can be understood in terms of the contour \mathcal{C} in (10.0.1) and the poles. The walls of marginal stability occurring at the points $\text{Im}[i\alpha_j(\Omega)] = 0$ are passed as the contour crosses the poles at $\alpha_j(\Omega) = 0$. For every wall crossed, the BPS state associated to the root α_i disappears from the spectrum.

10.2 Subalgebras of Borchers-Kac-Moody

Remembering that our aim is to gain information about wall crossing in $\mathcal{N} = 2$ supersymmetric QFTs, we now start looking at multi-centered BPS dyons that decay in this theory that are analogous to the BPS states with corresponding electric and magnetic charges existing in $\mathcal{N} = 2$ theories. These charges should exist as subsets of the root lattice of the Borchers-Kac-Moody superalgebra $\mathfrak{g}(A, S)$ discussed in [53], with an S-duality group that leaves this sublattice invariant. Examples include the algebras $\mathfrak{g}_{A_1} \subset \mathfrak{g}_{\hat{A}_1} \subset \mathfrak{g}(A, S)$ with root systems $\Delta_{A_1} \subset \Delta_{\hat{A}_1} \subset \Delta_{(A, S)}$. In particular, one can look at the simplest case of the A_1 Lie algebra which just describes a single BPS state. For this case a discussion was started in [50]. In this algebra, the only change of basis of the roots that can be done corresponds to permuting the positive and negative root $\pm\alpha \rightarrow \mp\alpha$. Furthermore, there is also the case of the affine Lie algebra denoted by \hat{A}_1 . This has an S-duality and modular group given by $PSL(2, \mathbb{Z})$ [52, 53]. Both the Weyl denominators of A_1 and \hat{A}_1 exist as factors within the Weyl denominator of the Borchers-Kac-Moody algebra. It should therefore be possible to proceed by extracting suitable degeneracies which correspond to the BPS states formed from the expansions of the roots that occur in this subalgebra, and determine the jumps of these degeneracies as the BPS states decay. This then acts as an analog for $\mathcal{N} = 2$ BPS states with a matching set of charges described by the same roots and where particular roots can disappear across a wall.

10.2.1 Weyl denominator for the subalgebras

First, we must find the Weyl denominators for the subalgebras within the Weyl denominator for the Borchers-Kac-Moody algebra. To do this we can write the partition function (10.0.1-10.1.1) more explicitly in the form of

$$\frac{1}{\Phi_{10}(\Omega)} = e^{-2\pi i\tau} \prod_{n=1}^{\infty} (1 - e^{2\pi i n\tau})^{-18} \prod_{l=1}^{\infty} \frac{\mathcal{Z}(\Omega)}{(1 - e^{2\pi i l\tau})^2 (1 - e^{2\pi i l\tau + 2\pi i v})^2 (1 - e^{2\pi i l\tau - 2\pi i v})^2} \frac{e^{-2\pi i v}}{(1 - e^{-2\pi i v})^2}, \quad (10.2.1)$$

where here the partition function from (10.0.1-10.1.1) is split into the various components of the center of mass motion of a 5d rotating black hole, the Kaluza-Klein monopole contribution, and a factor that contains the rest of the partition function from the D1-D5 Strominger-Vafa system, as discussed in [48, 54]. This contains the third complex variable

σ . We call this $\mathcal{Z}(\Omega)$. This can be written as follows ⁶

$$\mathcal{Z}(\Omega) = e^{-2\pi i\sigma} \prod_{l \geq 0, k > 0, m}^{\infty} \frac{1}{(1 - e^{2\pi i l \tau + 2\pi i m v + 2\pi i k \sigma})^{c(4kl - m^2)}}. \quad (10.2.2)$$

Now that we know the partition function, one can extract the Weyl denominators for the subalgebras A_1 and its affinisation \hat{A}_1 . These should be present within the partition function (10.2.1) on the first line. Specifically, these can be read off from the partition function as

$$\frac{1}{\Phi_{10}(\Omega)} = \left(\prod_{l=1}^{\infty} \frac{e^{-2\pi i l \tau}}{(1 - e^{2\pi i l \tau})^2 (1 - e^{2\pi i l \tau + 2\pi i v})^2 (1 - e^{2\pi i l \tau - 2\pi i v})^2} \left(\frac{e^{-2\pi i v}}{(1 - e^{-2\pi i v})^2} \right)_{A_1} \right)_{\hat{A}_1} \prod_{n=1}^{\infty} (1 - e^{2\pi i n \tau})^{-18} \mathcal{Z}(\Omega). \quad (10.2.3)$$

The factors shown here in the brackets labelled by A_1 and \hat{A}_1 are the Weyl denominators of the subalgebras. Hence, as described in chapter 10, these roots exist as here as multi-centered dyons and also undergo wall crossing across the boundary of the corresponding Weyl chamber. Next one can extract particular degeneracies that know about the wall crossing for the subalgebras. For example, if we take the limit of large σ such that we have $\sigma \rightarrow +i\infty$, this ensures that none of the walls in the $\mathcal{Z}(\Omega)$ partition function are crossed, because the imaginary parts of the products with the roots are well above the walls of marginal stability. This also means that the contour \mathcal{C} from [52], used to extract the degeneracies of the roots, is always satisfied. This is because, for: $\text{Im}[\tau]\text{Im}[\sigma] \gg (\text{Im}[v])^2 + 1$, one can let $\text{Im}[\tau]$ and $\text{Im}[v]$ be small and still well within the bound because of the large value for $\text{Im}[\sigma]$.

10.2.2 Degeneracies

Now, considering the fact that the partition function determines black hole degeneracies [40, 53, 54] and their jumps during wall crossing [53], we now look to extract the particular degeneracies that contain the Weyl denominators in (10.2.3). These will thereby exhibit wall crossing of the roots in the subalgebra. We look at particular sets of Fourier coefficients. These Fourier coefficients can be extracted from the dyon degeneracy formula (10.0.1) for the Borcherds-Kac-Moody algebra. This generating function can be written more explicitly in terms of the electric and magnetic charge invariants, and in general takes the form ⁷

$$(-1)^{P \cdot Q + 1} D(P, Q) = \oint_{\mathcal{C}} d\rho d v d \sigma e^{i\pi \Lambda_{P, Q}(\Omega)} \left(\frac{e^{-(\pi i v + \pi i \tau + \pi i \sigma)}}{\prod_{\alpha \in \Delta^+} (1 - e^{-i\pi(\alpha, \Omega)})^{\frac{1}{2}c(|\alpha|^2)}} \right)^2. \quad (10.2.4)$$

⁶ $c(4kl - m^2)$ are Fourier coefficients of the $K3$ elliptic genus.

⁷ $c(|\alpha|^2)$ are again Fourier coefficients of the $K3$ elliptic genus defined by the value $|\alpha|^2$ [53].

The charge vector in $\mathcal{N} = 4$ can in general be written as: $\Lambda_{P,Q}(\Omega) = -P \cdot P \tau - Q \cdot Q \sigma - 2P \cdot Q v$. One can define integers ⁸

$$l = \frac{1}{2}P \cdot P, \quad k = \frac{1}{2}Q \cdot Q, \quad m = P \cdot Q, \quad (10.2.5)$$

and use these to relabel the degeneracies in terms of the Fourier coefficients introduced in (10.1.1) for these integers called

$$(-1)^{P \cdot Q + 1} D(P, Q) = F_{KM}(k, l, m). \quad (10.2.6)$$

One can extract degeneracies in such a way that the coefficients describe the wall crossing associated with a particular Weyl denominator of a chosen subalgebra. This can be done by choosing a suitable sublattice of charges. One does this by fixing some of the above invariants in the lattice, while letting others vary. For example, one could fix $k = 1$. From this, one can define further degeneracies as

$$F_{KM}(1, l, m) = f(l, m) = \oint_{\mathcal{C}} e^{2\pi i m v + 2\pi i l \tau} d\rho d v d\sigma \left(\frac{e^{-(\pi i v + \pi i \tau)}}{\prod_{\alpha \in \Delta^+} (1 - e^{-i\pi(\alpha, \Omega)})^{\frac{1}{2}c(\alpha^2)}} \right)^2. \quad (10.2.7)$$

Now if we start with the 3 dimensional complex integral over ρ, v and σ we can integrate out σ , so that what is left is a complex 2 dimensional integral over ρ and τ . Now the degeneracies we are left with depend just on 2 charges l, m . These degeneracies then produce an integer valued count of the roots in the algebra also defined as in Cheng and Verlinde [53] as a ‘‘second quantised multiplicity’’ of the roots. This is a count of how many combinations of roots can add to produce the root associated to the charge vector in the degeneracy, where one can choose 2 sets of positive roots that one can use to form the combinations.

10.3 \hat{A}_1 as a subalgebra

We can now go back to the original equation (10.2.3) and extract a different set of coefficients. This time we look for the Weyl denominator of \hat{A}_1 , which is a form of the Jacobi-theta function or Jacobi triple product. This affine Lie algebra is another subalgebra of the Borcherds-Kac-Moody algebra which the generating function for the $\frac{1}{4}$ BPS states describes. This can be seen clearly when looking at the (real part of the) Cartan matrix for the Borcherds-Kac-Moody algebra used in [40, 53]. In this case, the inner product between the roots α_i, α_j $i, j = 1, 2, 3$ of the form $C_{i,j} = (\alpha_i, \alpha_j)$. The construction of this algebra was already classified and related to the Igusa cusp form by Gritsenko and Nikulin in [45, 46, 47]. For the affine Lie algebra \hat{A}_1 the basis only has 2 elements such that α_i, α_j $i, j = 1, 2$. Here

⁸The inner product is invariant under $SO(22, 6)$ and is defined on the lattice $\Gamma^{22,6}$ [40, 170, 174].

we again consider $c_{ij} = (\alpha_i, \alpha_j)$ the 2 matrices become

$$C_{i,j} = \begin{pmatrix} 2 & -2 & -2 \\ -2 & 2 & -2 \\ -2 & -2 & 2 \end{pmatrix}, \quad c_{i,j} = \begin{pmatrix} 2 & -2 \\ -2 & 2 \end{pmatrix}, \quad (10.3.1)$$

where we can see that we can embed the matrix $c_{i,j}$ within the larger matrix and hence one can see how the \hat{A}_1 Lie algebra is contained within that for the Borcherds-Kac-Moody algebra. In fact, we can see that there are now 2 different ways that the Cartan matrix \hat{A}_1 , $c_{i,j}$ is contained in the larger Cartan of the Borcherds-Kac-Moody algebra $C_{i,j}$. This information can be used to find the Weyl chambers, degeneracies, and wall crossing phenomena of \hat{A}_1 within the construction for the Kac-Moody algebra.

This Weyl denominator can again be extracted as a generating function of particular degeneracies of the full Borcherds-Kac-Moody algebra. As discussed in sec. 10.2.2 the degeneracies of the sum of roots (10.1.1-10.2.6) in the Kac-Moody algebra, given by $F_{KM}(p, q, r)$ ⁹, are then a product of those of the subalgebras including that of the \hat{A}_1 . This can be seen by decomposing the generating function

$$\begin{aligned} F_{KM}(p, q, r) &= \oint d^3\Omega \frac{e^{p\alpha_1(\Omega)+q\alpha_2(\Omega)+r\alpha_3(\Omega)}}{\Phi_{10}(\alpha_1, \alpha_2, \alpha_3)(\Omega)} = \oint d^3\Omega \frac{e^{p\alpha_1(\Omega)+q\alpha_2(\Omega)+r\alpha_3(\Omega)}}{\theta(\alpha_1, \alpha_2)(\Omega)^2 \tilde{\Phi}_{10}(\alpha_1, \alpha_2, \alpha_3)(\Omega)} \\ &= \oint d^3\Omega e^{p\alpha_1(\Omega)+q\alpha_2(\Omega)+r\alpha_3(\Omega)} \left(\sum_{k', h'} f_{\hat{A}_1}(k', h') e^{-k'\alpha_1(\Omega)-h'\alpha_2(\Omega)} \right) \left(\sum_{c, d, e} d_{\tilde{\Phi}}(c, d, e) e^{-c\alpha_1(\Omega)-d\alpha_2(\Omega)-e\alpha_3(\Omega)} \right), \end{aligned} \quad (10.3.2)$$

where we have decomposed the denominator into the product of the degeneracies of the affine Lie algebra $f_{\hat{A}_1}(k, h)$ and that of the partition function left over $f_{\tilde{\Phi}}(c, d, e)$ after the factor corresponding to the affine Lie algebra is extracted. After this is done, the degeneracies of the Kac-Moody algebra can be written as the product

$$F_{KM}(k' + c, h' + d, e) = \sum_{k', h', c, d} f_{\hat{A}_1}(k', h') d_{\tilde{\Phi}}(c, d, e). \quad (10.3.3)$$

The next step for us is to look at the degeneracies $f_{\hat{A}_1}(k, h)$ of the affine Lie algebra \hat{A}_1 , where we change the labelling $k', h' \rightarrow k, h$ as we restrict to the roots of this subalgebra. The degeneracies $d_{\tilde{\Phi}}(c, d, e)$ then come from the rest of the product including the factor $\eta(\tau)^{-18}$ from (10.2.3).

⁹Here, in general, we can re-write $F_{KM}(k, l, m)$ as $F_{KM}(p, q, r)$ by using a different basis of roots.

10.3.1 Extracting generating function for \hat{A}_1

The factor $f_{\hat{A}_1}(k, h)$ itself in (10.3.3) is not directly a degeneracy (of the form $f(l, m)$ in (10.2.7)) of the Borchers-Kac-Moody Weyl denominator because of the removal of the factor of $\eta(\tau)^{-18}$. However, it contains all the information about the wall crossing. This is because this is factor containing only imaginary roots such that it does not change under the Weyl reflections associated to the permutations of the other roots. Furthermore, the wall $\text{Im}[\tau] = 0$ is not crossed in the $\mathcal{N} = 4$ theory because the moduli stay within the Siegel upper half-plane. If one considers only functions with 2 complex variables, this can be interpreted as preserving the modularity of the eta and theta functions, with τ being defined on the complex upper half plane. If we look back to the product of the different partition functions (10.2.3) and look at what is contained in the bracket, we can extract Fourier coefficients of the function as

$$f_{\hat{A}_1}(\tau, v) = \prod_{l=1}^{\infty} \frac{e^{-2\pi i v - 2\pi i \tau}}{(1 - e^{2\pi i l \tau})^2 (1 - e^{2\pi i l \tau + 2\pi i v})^2 (1 - e^{2\pi i l \tau - 2\pi i v})^2 (1 - e^{-2\pi i v})^2}. \quad (10.3.4)$$

Now one can write this in terms of the roots of the affine Lie algebra:

$$\alpha_0(u) = -2\pi i v, \quad v \in \mathbb{C} \quad \text{and} \quad \delta(u) = -2\pi i \tau, \quad \tau \in \mathbb{H}^+. \quad (10.3.5)$$

Then we can write the function in the form

$$f_{\hat{A}_1}(u) = \prod_{m=1}^{\infty} \frac{e^{\alpha_0(u) + \delta(u)}}{(1 - e^{-m\delta(u)})^2 (1 - e^{-m\delta(u) + \alpha_0(u)})^2 (1 - e^{-m\delta(u) - \alpha_0(u)})^2 (1 - e^{\alpha_0(u)})^2} = \prod_{m=1}^{\infty} \frac{e^{\alpha_0(u) + \delta(u)}}{(1 - e^{-m\delta(u)})^2 (1 - e^{-(m-1)\delta(u) + \alpha_0(u)})^2 (1 - e^{-m\delta(u) - \alpha_0(u)})^2}. \quad (10.3.6)$$

Now the coefficients we want to extract become

$$f_{\hat{A}_1}(k, h) = \oint_{\gamma} d\alpha_0(u) d\delta(u) e^{k\alpha_0(u) + h\delta(u)} \frac{e^{\alpha_0(u) + \delta(u)}}{\prod_{m=1}^{\infty} (1 - e^{-m\delta(u)})^2 (1 - e^{-(m-1)\delta(u) + \alpha_0(u)})^2 (1 - e^{-m\delta(u) - \alpha_0(u)})^2}, \quad (10.3.7)$$

where the contour $\gamma \subset \mathcal{C}$ is again that which was previously defined in the Siegel upper half-plane, but this time restricted to the τ and v planes. We define the charge vector restricted to the \hat{A}_1 subalgebra as

$$\lambda_{k,h} = k\alpha_0 + h\delta. \quad (10.3.8)$$

We assume that the imaginary part of σ is large so that it satisfies the contour \mathcal{C} (see third part of contour):

$$0 \leq \operatorname{Re}[\tau], \operatorname{Re}[v] < 1, \quad \operatorname{Im}[\tau] > 0, \quad \operatorname{Im}[\tau](\operatorname{Im}[\sigma] \rightarrow +\infty) \gg (\operatorname{Im}[v])^2, \quad (10.3.9)$$

so the generating function now becomes

$$f_{\hat{A}_1}(k, h) = \oint_{\gamma} d\alpha_0(u) d\delta(u) e^{\lambda_{k,h}(u)} \frac{e^{\alpha_0(u)+\delta(u)}}{\prod_{m=1}^{\infty} (1 - e^{-m\delta(u)})^2 (1 - e^{-(m-1)\delta(u)+\alpha_0(u)})^2 (1 - e^{-m\delta(u)-\alpha_0(u)})^2}. \quad (10.3.10)$$

Now we see that we have a function that acts in the same way (extracting the multiplicity) of particular roots just for the affine Lie algebra \hat{A}_1 as it does for the Borcherds-Kac-Moody Lie algebra in (10.0.1). However, now we are just looking at the $PSL(2, \mathbb{Z})$ part of the full modular group in the Igusa cusp form.

S-duality

This generating function and coefficients $f_{\hat{A}_1}(k, h)$ from (10.3.3) can be rewritten using an S-duality transformation. These are $PSL(2, \mathbb{Z})$ transformations that act as Weyl reflections, or automorphisms on the fundamental Weyl chamber, of the \hat{A}_1 Lie algebra at each point in the moduli space. However, the S-duality condition of constant $f_{\hat{A}_1}(k, h)$ at u and u' does not hold across the walls where roots can enter or leave the spectrum depending on which direction the wall is crossed. The imaginary roots are not transformed under S-duality.

10.3.2 Contour prescription for \hat{A}_1

To apply the contour prescription \mathcal{C} discussed in [52] for the full Bocherds-Kac-Moody algebra to the \hat{A}_1 part $\gamma \subset \mathcal{C}$ one must again separate the degeneracies associated to \hat{A}_1 Lie algebra (10.3.2-10.3.3) from that associated to the other roots of the Kac-Moody algebra and then restrict the possible contours one can take to those extracting the degeneracies of \hat{A}_1 roots.

For this we look at the contour prescription again but this time only over the 2 variables v and τ . As before we define the contour in a modular invariant way. This time it must remain invariant under $PSL(2, \mathbb{Z})$. Here we are again left with the contour:

$$\operatorname{Re}[\tau] \in [0, 1], \quad \operatorname{Re}[v] \in [0, 1]. \quad (10.3.11)$$

As before the imaginary part of this contour is a large positive constant such that we have:

$$\text{Im}[\tau] \in N_1, \quad \text{Im}[v] \in N_2, \quad (10.3.12)$$

where $N_1, N_2 \rightarrow +\infty$. This contour is taken to enclose part of the fundamental domain of the $PSL(2, \mathbb{Z})$ group. This means that every element in this region is contained here only once for the orbit of this group. In the Figure 10.1 below we show 2 domains and enclose the first one by a contour. For this contour, following [52], we are now looking at the pole at $v = 0$ on the real axis but in general there are for \hat{A}_1 also poles at $v + n\tau, v - n\tau = 0$, $n \in \mathbb{Z}$ that can be mapped to the $v = 0$ pole under the modular transformations. The imaginary part $\text{Im}[v]$ is defined in such a way that the contour crosses the real axis as it jumps from a large positive $+N_2$ to a large negative number $-N_2$ as the modulus changes sign

$$\text{Im}[v] > 0 \longrightarrow \text{Im}[v] < 0. \quad (10.3.13)$$

As the contour must remain invariant as this happens one must deform it back to its original position. In doing so one picks up the contribution of the pole as the contour crosses the real axis. This is the cause of wall crossing of the generating function. The residue from this pole creates the jump in the degeneracies.

This should also give a consistent description for the other poles. These are crossed when the contour for the particular charge one wants to extract the degeneracy of crosses $\text{Im}[v \pm n\tau] = 0$. As long as the contour is taken to be at a sufficiently large imaginary value, then only one pole (and one wall) is crossed at a time. This is because only that particular combination of moduli change sign.

10.4 Wall crossing for \hat{A}_1 in $\mathcal{N} = 4$

Now we understand how the degeneracies of $\frac{1}{4}$ BPS dyons can be extracted from the Igusa cusp form as Fourier coefficients using a contour prescription. These degeneracies including both single and multi-centered black holes. We have also seen how wall crossing represents the split of a multi-centered black hole into 2 electric and magnetic $\frac{1}{2}$ BPS states and its effect on the dyon degeneracies as the multi-centered contribution to the wall is removed. We have seen in (10.1.1) that this wall crossing can be encoded in a jump in the Fourier coefficients representing the degeneracies. We know from [53] that this wall crossing for the full Borcherds-Kac-Moody algebra can be encoded in a change in the highest weight of a Verma module¹⁰ which counts the BPS states. We will now proceed to show that this also holds in the case of the \hat{A}_1 subalgebra. So far, the Weyl denominator of \hat{A}_1 has been found as a factor in the generating function and the contour prescription found in a limit of the 3 complex variables in the full Igusa cusp form. What remains is the Lie algebraic formulation

¹⁰See section 11.1.1 equation (11.1.6) for a definition.

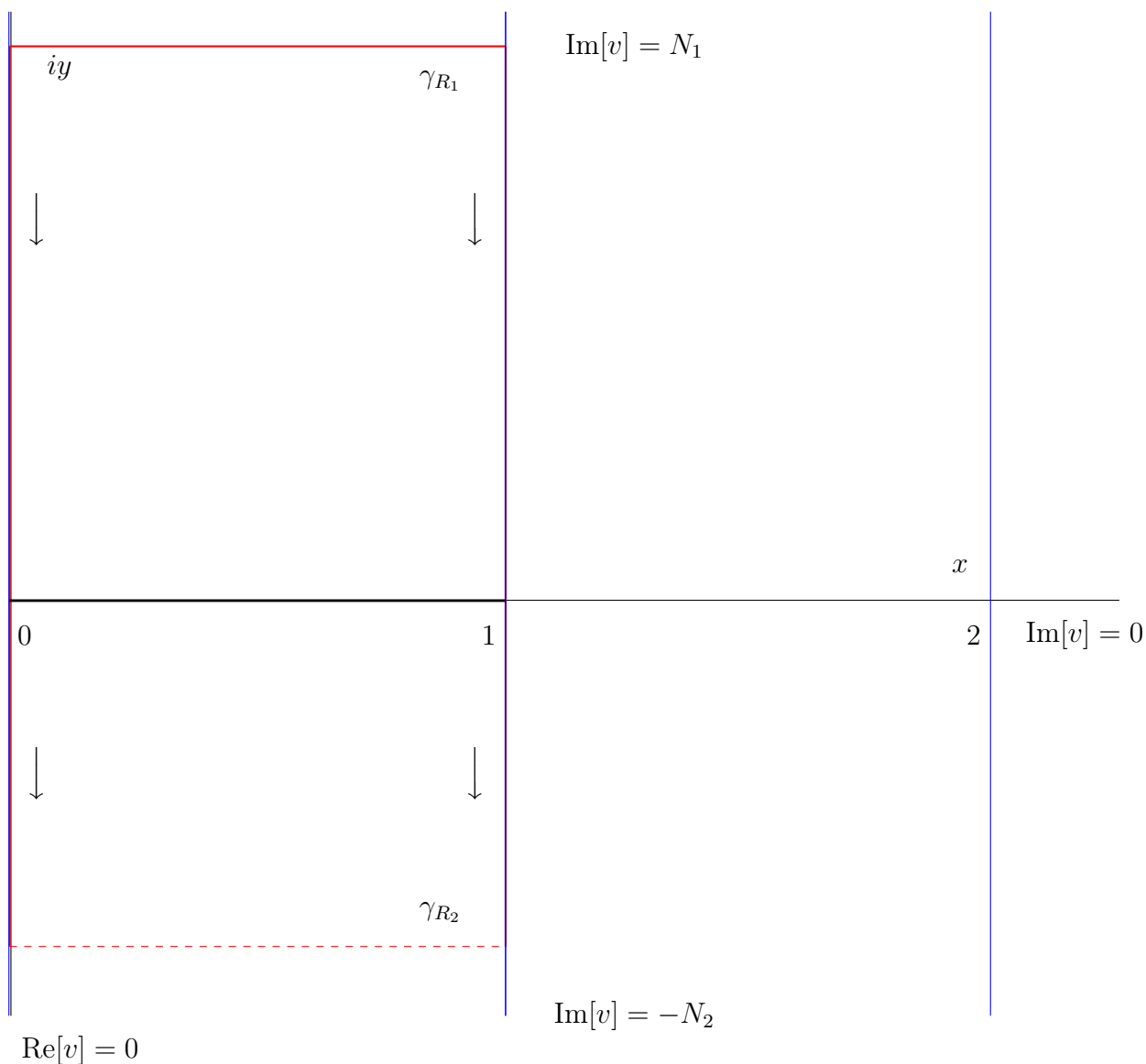


Figure 10.1: This diagram shows the part of the contour γ_{R_1} in the v plane used to extract the Fourier coefficients. This is depicted as the solid red line. The pole at $v = 0$ is crossed as the contour jumps to γ_{R_2} from positive to negative infinity. In this case, a wall is crossed.

of the wall crossing in terms of Verma modules. In the section 10.4.1 below we explicitly calculate the change in the highest weight in the different chambers of \hat{A}_1 .

10.4.1 Wall crossing

The function we have above in (10.3.4) exhibits wall crossing behavior as the roots disappear from the spectrum. This happens when the imaginary part of a particular root shown

in the Weyl denominator vanishes and changes sign. As we remember from (10.1.1) the exponentials must have modulus less than 1 for a well defined series expansion which is convergent and allows one to extract the Fourier coefficients. This means that in our case, for the Weyl denominator written in terms of the roots of the affine Lie algebra, shown in (10.3.10), we must have:

$$|e^{-m\delta(u)}| < 1, \quad |e^{-(m-1)\delta(u)+\alpha_0(u)}| < 1, \quad |e^{-m\delta(u)-\alpha_0(u)}| < 1, \quad m \geq 1. \quad (10.4.1)$$

Or equivalently this means that the imaginary parts $\text{Im}[im\delta(u) + i\alpha_0(u)]$, $\text{Im}[i(m-1)\delta(u) - i\alpha_0(u)] > 0$. If we, as in the $\mathcal{N} = 4$ black hole literature [48, 190, 52, 53, 51, 54], stay in the Siegel upper half plane, or in the case of the Jacobi theta function just the modular upper half plane, we must also constrain $\text{Im}[im\delta(u)] > 0$. So, we can now look at what happens when a particular root crosses a wall:

$$\text{Im}[i(m-1)\delta(u) - i\alpha_0(u)] > 0 \longrightarrow \text{Im}[i(m-1)\delta(u) - i\alpha_0(u)] < 0. \quad (10.4.2)$$

We assume all the other roots retain a positive imaginary part. For this wall, a particular root $-(m-1)\delta + \alpha_0$ disappears or appears (depending on the direction) from the spectrum while all other roots remain in the spectrum. This is therefore an example of wall crossing. In this case, the denominator formula must be rewritten such that all the roots in the denominator again satisfy the conditions on the imaginary part. This can be done by moving a root, for example the $-(m-1)\delta + \alpha_0$ root from (10.4.2), into the numerator.

10.4.2 Jumping between chambers

We can start with a simple example: we start in a chamber in which no root exists - the fundamental Weyl chamber W_F and we move in a direction in the moduli space such that at the first wall of marginal stability a root appears. But only this root and no other roots. For example, if we let a root $-\delta - \alpha_0$ enter the spectrum. The generating function from (10.3.10) is rewritten as:

$$\begin{aligned} f_{\hat{A}_1}(k, h) &= \oint_{\gamma} d\alpha_0(u) d\delta(u) e^{\lambda_{k,h}(u)} \quad (10.4.3) \\ &\frac{e^{\alpha_0(u)+\delta(u)}}{\prod_{l=1}^{\infty} (1 - e^{-l\delta(u)})^2 (1 - e^{-(l-1)\delta(u)+\alpha_0(u)})^2 \prod_{m=1, m \neq 1}^{\infty} (1 - e^{-m\delta(u)-\alpha_0(u)})^2} \\ &\frac{1}{(1 - e^{-\delta(u)-\alpha_0(u)})^2} \\ &\longrightarrow \oint_{\gamma} d\alpha_0(u) d\delta(u) e^{\lambda_{k,h}(u)} \end{aligned}$$

$$\frac{e^{\alpha_0(u)+\delta(u)}}{\prod_{l=1}^{\infty} (1 - e^{-l\delta(u)})^2 (1 - e^{-(l-1)\delta(u)+\alpha_0(u)})^2 \prod_{m=1, m \neq 1}^{\infty} (1 - e^{-m\delta(u)-\alpha_0(u)})^2} \frac{e^{2\delta(u)+2\alpha_0(u)}}{(1 - e^{\delta(u)+\alpha_0(u)})^2}. \quad (10.4.4)$$

Now it can again be expanded in terms of the positive roots within the denominator, but with an additional factor in the numerator. This factor causes a jump in the degeneracies of the various roots. Depending on which region of the moduli space one is in, or in which Weyl chamber W , there can be many of these factors which one must move into the numerator. In general, we can keep moving in that direction such that we cross k walls of marginal stability. If we start within the fundamental Weyl chamber we now have $n \in 1 \dots k$ additional roots in the spectrum. This is a finite set of roots for which one must modify the generating function as:

$$f_{\hat{A}_1}(k, h) = \oint_{\gamma} d\alpha_0(u) d\delta(u) e^{\lambda_{k,h}(u)} \quad (10.4.5)$$

$$\frac{e^{\alpha_0(u)+\delta(u)}}{\prod_{l=1}^{\infty} (1 - e^{-l\delta(u)})^2 (1 - e^{-(l-1)\delta(u)+\alpha_0(u)})^2 \prod_{m=k+1}^{\infty} (1 - e^{-m\delta(u)-\alpha_0(u)})^2} \frac{1}{\prod_{m=1}^k (1 - e^{-m\delta(u)-\alpha_0(u)})^2},$$

$$= \oint_{\gamma} d\alpha_0(u) d\delta(u) e^{\lambda_{k,h}(u)} \frac{e^{\alpha_0(u)+\delta(u)}}{\prod_{l=1}^{\infty} (1 - e^{-l\delta(u)})^2 (1 - e^{-(l-1)\delta(u)+\alpha_0(u)})^2 \prod_{m=k+1}^{\infty} (1 - e^{-m\delta(u)-\alpha_0(u)})^2} \frac{\prod_{m=1}^k e^{2m\delta(u)+2\alpha_0(u)}}{\prod_{m=1}^k (1 - e^{m\delta(u)+\alpha_0(u)})^2}. \quad (10.4.6)$$

Again, this is rewritten in a way such that the denominator is now expandable in terms of Fourier coefficients which can then be extracted by the charge vector $\lambda_{k,h}$ introduced in (10.3.7-10.3.10). There is an alternative way to cross the walls. If one moves in the other direction starting in W_F , where no roots initially exist, a different set of roots start to appear. In this case, the product formula after rewriting in a way that can be expanded as a Fourier series, then becomes:

$$f_{\hat{A}_1}(k, h) = \oint_{\gamma} d\alpha_0(u) d\delta(u) e^{\lambda_{k,h}(u)} \quad (10.4.7)$$

$$\frac{e^{\alpha_0(u)+\delta(u)}}{\prod_{l=1}^{\infty} (1 - e^{-l\delta(u)})^2 (1 - e^{-l\delta(u)-\alpha_0(u)})^2 \prod_{m=k+1}^{\infty} (1 - e^{-(m-1)\delta(u)+\alpha_0(u)})^2} \frac{\prod_{m=1}^k e^{2(m-1)\delta(u)-2\alpha_0(u)}}{\prod_{m=1}^k (1 - e^{(m-1)\delta(u)-\alpha_0(u)})^2}. \quad (10.4.8)$$

This time it is the other set of roots that appear in the spectrum and cause a shift in the degeneracies.

10.4.3 Wall crossing in terms of highest weights

As done in Cheng and Verlinde [53] we can again write this in terms of a Verma module associated to the affine Lie algebra with highest weight

$$\lambda = \frac{1}{2}(\lambda_{k,h} + \alpha_0 + \delta). \quad (10.4.9)$$

In this case, the formula as with the Bocherds-Kac-Moody algebra in Cheng and Verlinde can be written as a square:

$$f_{\hat{A}_1}(k, h) = \oint_{\gamma} d\alpha_0(u) d\delta(u) \left(\frac{e^{\lambda(u)}}{\prod_{m=1}^{\infty} (1 - e^{-m\delta(u)})(1 - e^{-(m-1)\delta(u)+\alpha_0(u)})(1 - e^{-m\delta(u)-\alpha_0(u)})} \right)^2. \quad (10.4.10)$$

This can be used to see that each Weyl chamber W can be associated to a highest weight for a particular representation, W_{λ} as when one moves in the moduli space, for example starting in the fundamental Weyl chamber and moving in a particular direction, this highest weight picks up a certain number of roots with each root corresponding to a particular wall that has been crossed. So, as one starts in the fundamental chamber and moves, the highest weight of the representation is modified in a way such that

$$\lambda + \sum_{m=1}^k ((m-1)\delta - \alpha_0), \quad (10.4.11)$$

in one direction, and

$$\lambda + \sum_{m=1}^k (m\delta + \alpha_0), \quad (10.4.12)$$

in the other direction. One can use the S-duality transformations to map the denominator that is expandable in terms of a new Fourier series into one containing positive roots. Here one can see that in every chamber the highest weight is different - representing a different Fourier series and different black hole degeneracies.

Highest weight in the different chambers

The Weyl chambers of \hat{A}_1 are shown in Fig. 10.2 below. Each region in the moduli space has a unique combination of roots, with the combinations of roots shown in the Figure that

exist within each chamber.

All possible highest weights	
Highest weight in one direction	In other direction
$\lambda + \sum_{n=1}^{\infty} (n\delta + \alpha_0)$	$\lambda + \sum_{m=1}^{\infty} ((m-1)\delta - \alpha_0)$
$\lambda + \sum_{n=1}^k (n\delta + \alpha_0)$	$\lambda + \sum_{m=1}^h ((m-1)\delta - \alpha_0)$
λ	

Table 10.1: Highest weight in modular upper half plane representing existing BPS boundstates. This is also shown in Fig. 10.2.

This shows how one can start in a chamber with none of the roots existing and move to a chamber, where the roots that exist appear when crossing a finite number of walls in either direction. In the $\mathcal{N} = 4$ theory one obtains discrete attractor flow as one moves towards the fundamental Weyl chamber from either side.

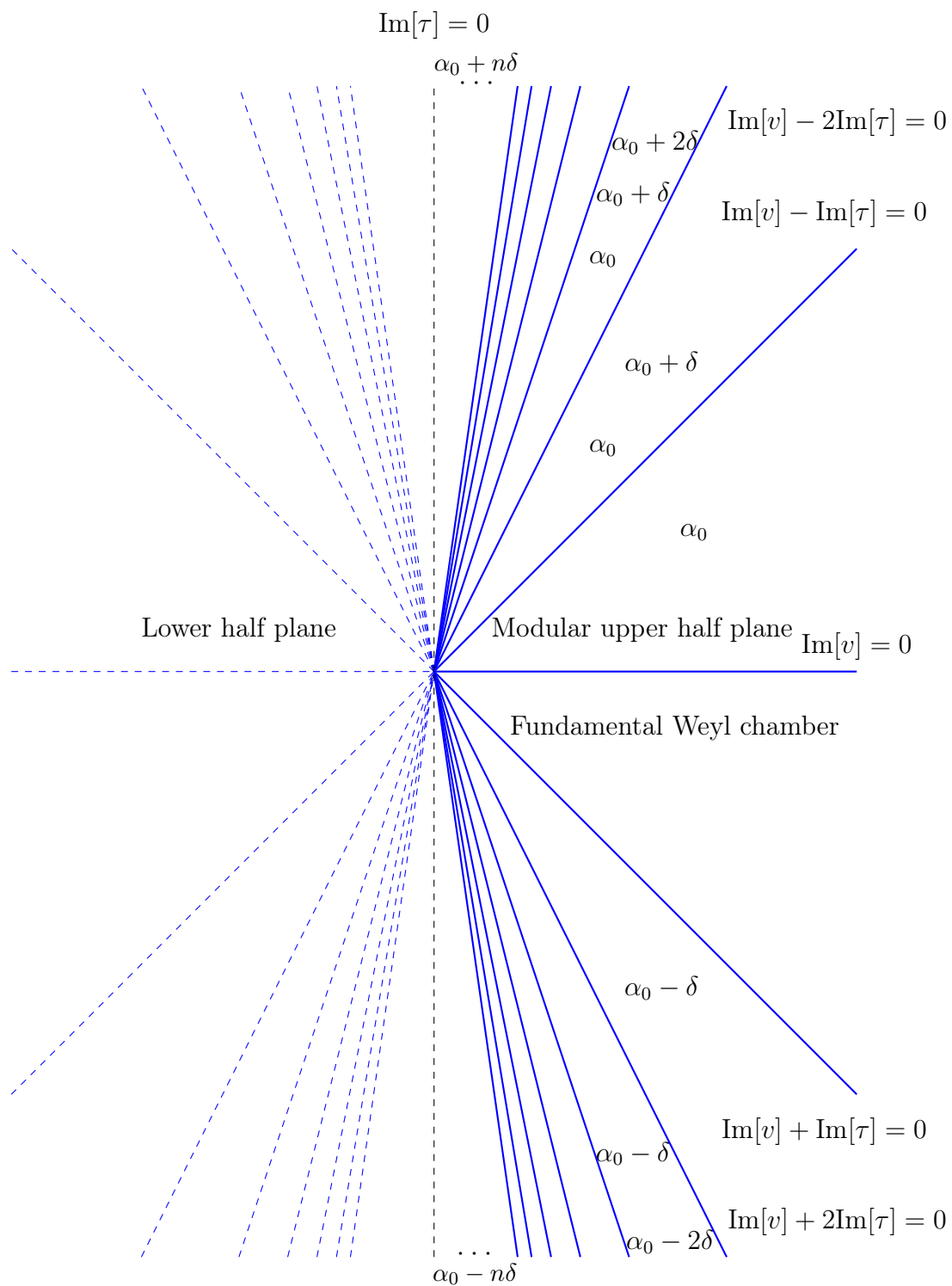


Figure 10.2: This figure shows the walls associated with the \hat{A}_1 roots. These are the blue lines and are found in the modular upper half of the τ -plane. The dashed blue lines shown are the continuation into the lower half plane.

11 | $\mathcal{N} = 2$ analogs of the generating functions

A generating function has been found in section 10.3 for BPS states described by the \hat{A}_1 root system in $\mathcal{N} = 4$. In this case, the BPS degeneracies of states with particular charges can be read off as Fourier coefficients or extracted using a contour integration. These were found to encode wall crossing through either a jump in the Fourier coefficients or in the highest weight of a Verma module (see Eq. 11.1.6). We now look for analog generating functions in $\mathcal{N} = 2$ theories from which one can observe the wall crossing phenomena in the same way, and that can hence also act as counting functions for BPS states. This is done for the \hat{A}_1 Lie algebra as well as the A_2 root system. This is an ideal testing case that can in future be generalised to further theories with BPS states described by ADE type root systems. We conjecture that this generating function is the Weyl denominator associated to the root system of the particular quiver describing the BPS states in the theory. Seiberg-Witten theory and the Argyres-Douglas A_2 theory are good models to start with. We look for a different spectrum of framed BPS states existing in each Weyl chamber and also expect the additional wall of marginal stability to be encoded in the generating function. To do this we first introduce (in the next section 11.1) the definition of a root system in a Lie algebra.

11.1 BPS root systems and Lie algebras

The generating function of the degeneracies of the $\frac{1}{4}$ BPS dyons studied in [52, 53, 54] is a function of the Cartan subalgebra $\mathfrak{h}(A, S)$ of the Borchers-Kac-Moody Lie superalgebra $\mathfrak{g}(A, S)$ associated with the $\mathcal{N} = 4$ supersymmetric string theory on $K3 \times T^2$ that describes the black holes. In this example the positive roots of the Lie algebra represent the possible BPS states that can exist in the theory. The Weyl chambers represent the regions in which these states are stable - the boundaries can be connected back to the moduli space of the theory. This is also the case for the Lie algebras representing analogous BPS states in $\mathcal{N} = 2$ theories. Here one can also consider the Lie algebra for each theory and look at the roots of the Lie algebra to represent all the charge vectors in the theory. A quiver can be constructed from the Cartan matrix, and mutations in the quiver correspond to Weyl transformations, or changes in sign, of the roots, depending on which side of the wall of marginal stability

one does the analysis.

The general construction of a Lie algebra and its root system Δ is well known and reviewed for example in [193, 194, 195, 196, 197, 198, 199]. A good introduction to infinite dimensional examples such as affine and Kac-Moody algebras is given by Kac [200]. A Lie algebra can be decomposed as $\mathfrak{g} = \mathfrak{h} \oplus_{\alpha \in \Delta} \mathfrak{g}_\alpha$ where $\mathfrak{h} \subset \mathfrak{g}$ is the Cartan subalgebra. The root subspaces are defined as $\mathfrak{g}_\alpha = \{x, [h, x] = \alpha(h)x, \forall h \in \mathfrak{h}\}$. A root therefore corresponds to an eigenvalue of the action of the linear adjoint operators on a vector in the eigenspace \mathfrak{g}_α . The explicit action on the coordinates can be written as $Ad_h(x_b) = [h, x_b] = \alpha_b(h)x_b$. These roots live in the dual linear vector space $\Delta \subset \mathfrak{h}^*/\{0\}$. One can also consider a representation V of \mathfrak{g} , for which the weight space which is given by $V_\lambda := \{v \in V : \forall h \in \mathfrak{h}, h \cdot v = \lambda(h)v\}$. One can then generate all the weights in a representation from the root system using: $h \cdot (x \cdot v) = [(\lambda + \alpha)(h)](x \cdot v)$. If a root is simple it cannot be written as a linear combination of other basis roots. If not it can be written in such a linear combination.

Definition 11.1.1. The Killing form is an inner product represented by the trace normalization for adjoint representation generators. Consider $a, b \in \mathfrak{g}_\mathbb{C}$. Their Killing form is represented by

$$(a, b) = \text{Tr}[Ad_a, Ad_b], \quad \mathfrak{g} \times \mathfrak{g} \rightarrow \mathbb{C}. \quad (11.1.1)$$

This can be computed by finding matrices representing adjoint operators for a particular basis and then calculating matrix products.

Alternatively, this can also be calculated by writing the form in terms of brackets as $Ad_{a_i} Ad_{b_j}(x_k) = [x_i, [x_j, x_k]]$. We remember that the root space is in the dual \mathfrak{h}^* of the Cartan subalgebra \mathfrak{h} which can be understood in terms of a Killing form. For every root $\alpha \in \mathfrak{h}^*$, there exists an isomorphism $\mathfrak{h}^* \rightarrow \mathfrak{h}$ such that we have $u, h_\alpha \in \mathfrak{h}$ such that $\alpha(u) = (\alpha, u) = (h_\alpha, u)$. Hence, the contours from sec. 10.3.2 one can take to obtain the BPS degeneracies are parameterised in the Cartan subalgebra $u \in \mathfrak{h}$. From this one can also define another inner product between roots and real linear combinations of them

$$\langle \alpha, \beta \rangle = (h_\alpha, h_\beta), \quad \mathfrak{h}^* \times \mathfrak{h}^* \rightarrow \mathbb{R}. \quad (11.1.2)$$

Now we can construct the Cartan matrix for any Lie algebra from its root system and the inner product shown here. We show the examples for A_1, \hat{A}_1 and A_2 . The matrix contains entries of the form

$$A_{i,j} = 2 \frac{\langle \alpha_i, \alpha_j \rangle}{\langle \alpha_i, \alpha_i \rangle}. \quad (11.1.3)$$

$$A_1 : \quad (2) \quad \bullet$$

$$\hat{A}_1 : \begin{pmatrix} 2 & -2 \\ -2 & 2 \end{pmatrix} \quad \bullet \rightrightarrows \bullet$$

$$A_2 : \begin{pmatrix} 2 & -1 \\ -1 & 2 \end{pmatrix} \quad \bullet \longrightarrow \bullet$$

A quiver can be constructed from this by plotting the roots and the arrows between them. These are shown above to the right of the Cartan matrices. Finally, the Weyl group is a subgroup of the isometry group of the root system which is generated by reflections through the spaces perpendicular to the roots. These represent quiver mutations in the quiver encoding the roots representing the BPS states. The transformations are generated by the map

$$s_\alpha(u) = u - 2 \frac{(\alpha, u)}{(\alpha, \alpha)} \alpha. \quad (11.1.4)$$

11.1.1 Weyl denominator and generating function

From a general root system associated to a Lie algebra one can define the Weyl denominator formula, which was introduced for the Borcherds-Kac-Moody algebra in (10.0.1), and its subalgebras (10.2.1) as the inverse of a product of factors involving all the positive roots of the Lie algebra. We aim to find a generating function for BPS degeneracies corresponding to a particular root for the $\mathcal{N} = 2$ examples following the approach previously carried out for the $\mathcal{N} = 4$ cases. In general, as in the literature [52, 54, 48, 49], we expect this to take the form of a contour integral over the Weyl denominator, although it should be possible to read off the BPS state count from the denominator itself in terms of a highest weight. We conjecture the following general result for this formula, that an integral of the Weyl denominator over the Cartan subalgebra is related to a degeneracy of a particular root or combination of roots representing BPS states in the Lie algebra.

Definition 11.1.2. Now to proceed, one must define the Weyl denominator with an additional charge factor as

$$\frac{e^{\Lambda(u) - \rho(u)}}{\prod_{\alpha \in \Delta^+} (1 - e^{-\alpha(u)})}, \quad (11.1.5)$$

where r is the rank of the Lie algebra and Λ is analogous to the charge vector in [53]. The product is over positive roots $\alpha \in \Delta^+$. The Weyl vector ρ is the half sum of positive roots $\rho = \frac{1}{2} \sum_{\alpha \in \Delta^+} \alpha_i$. All roots α_i and weights λ_i are contained in a charge lattice $\alpha_i, \lambda_i \in \Gamma$.

There is another object one can define in general from a semi-simple Lie algebra \mathfrak{g} and its Borel (maximally solvable) subalgebra \mathfrak{b} . This is the Verma module. A detailed review of

Verma modules is given in [201].

Definition 11.1.3. One first considers the Cartan subalgebra \mathfrak{h} again. Then one can define a Verma module M_λ , with highest weight $\lambda \in \mathfrak{h}^*$, in the adjoint by

$$\mathrm{Hom}_{\mathfrak{g}}(M_\lambda, V) = \mathrm{Hom}_{\mathfrak{b}}(\mathbb{C}_\lambda, V), \quad (11.1.6)$$

where V is a representation of \mathfrak{g} , and \mathbb{C}_λ is the one-dimensional module on which elements of \mathfrak{h} act on with λ .

Verma modules are infinite dimensional, but one can take quotient modules with highest weights that correspond to those of representations of finite semi-simple Lie algebras. The character of a Verma module is (up to a shift by the Weyl vector $\Lambda(u) \rightarrow \lambda(u)$ ¹) the inverse of the Weyl denominator. The exponent in the numerator of (11.1.5) should extract Fourier coefficients from the denominator and can also be assigned a representation of the Lie algebra or module to which it is the highest weight. Hence, we expect the stability of BPS states to coincide with the stability of representations.

Definition 11.1.4. A Lie algebra also has a character function which includes a numerator summing over the possible Weyl transformations of the representation in question. The full Weyl character formula takes the form

$$ch_\lambda = \frac{\sum_{w \in W} (\det w) e^{w(\lambda + \rho)(u)}}{e^{\rho(u)} \prod_{\alpha \in \Delta^+} (1 - e^{-\alpha(u)})}, \quad (11.1.7)$$

where w are elements of the Weyl group and λ is the highest weight of the representation chosen.

Our work in this chapter 11 determines how this generating function counts BPS states in simple Argyres-Douglas examples. In the table below we list what we expect the generating function to become when we substitute the Weyl denominators of the respective Lie algebras into the general formulation. This is expected to be the function which determines what BPS states exist in each chamber of the moduli space and will be verified as such in the following subsections. This should reproduce the counts that have been obtained from other methods such as quiver representations. In the next sections we look explicitly at each example to reproduce the BPS state counts described for these theories in the literature and describe the wall crossing in the new language involving root systems and Weyl chambers.

¹One can redefine $\lambda(u) = \Lambda(u) - \rho(u)$ to absorb this shift if one is working with an inverse product to move between these definitions.

Generating function	$\frac{\sum_{w \in W} (\det w) e^{w(\lambda + \rho)(u)}}{e^{\rho(u)} \prod_{\alpha \in \Delta^+} (1 - e^{-\alpha(u)})}$	The denominators are shown below
A_1	$\frac{e^{\Lambda(u)}}{e^{\rho(u)} (1 - e^{-\alpha(u)})}$	
\hat{A}_1	$\frac{e^{\Lambda(u)}}{e^{\rho(u)} \prod_{m=1}^{\infty} (1 - e^{-m(\alpha_0(u) + \alpha_1(u))}) (1 - e^{-m(\alpha_0(u) + \alpha_1(u)) - \alpha_1(u)}) (1 - e^{-(m-1)(\alpha_0(u) + \alpha_1(u)) + \alpha_1(u)})}$	
A_2	$\frac{e^{\Lambda(u)}}{e^{\rho(u)} (1 - e^{-\alpha_1(u)}) (1 - e^{-\alpha_2(u)}) (1 - e^{-\alpha_3(u)})}$	

11.2 \hat{A}_1 root system in $\mathcal{N} = 2$

One can start by looking at the root system for the affine Lie algebra \hat{A}_1 . This root system is important because it describes several interesting examples of wall crossing in $\mathcal{N} = 2$ QFTs. This includes both the D6-D2-D0 brane system described by Jafferis and Moore [37] as well as Seiberg-Witten theory. The generating function for this affine \hat{A}_1 Lie algebra is already known from the subalgebra of the $\mathcal{N} = 4$ example and is the Weyl denominator formula. This was already established in section 10.3 by extracting particular degeneracies from the Borcherds-Kac-Moody algebra Weyl denominator in Cheng and Verlinde [52, 53]. The wall crossing for this generating function has been found in sections 10.4 and 10.4.1. This is depicted in Fig. 10.2 and is encoded in a change in highest weight of a Verma module.

It is important to note that in the $\mathcal{N} = 4$ example, this only holds in the Siegel upper half plane. This is because the Jacobi-theta function and the full Igusa cusp form are Jacobi and Siegel modular forms respectively. This means that to preserve modularity of the Siegel modular form, or of the Jacobi theta and eta functions, the analysis in section 10.4 as well as that in the literature [40, 52, 53, 54], of which we have taken a limit here, must be confined to the values $\text{Im}[\tau] > 0$. Here the variable τ , from (10.3.5), can be parameterised as the τ parameter of an elliptic curve, which always has a positive imaginary part.

Definition 11.2.1. We can define the imaginary or ‘‘affine’’ wall as the wall $\text{Im}[\tau] = 0$ separating the 2 half-planes corresponding to the 2 domains of definition of the modular form and the Fourier coefficients.

Hence, the imaginary or affine wall is never crossed in the $\mathcal{N} = 4$ theory. This is interpreted in the work of Cheng and Verlinde as imaginary roots never leaving the spectrum which is not the case in $\mathcal{N} = 2$ theories we are looking at. If one is to use this function as an analog counting function for theories in $\mathcal{N} = 2$, to obtain the full spectrum for example of Seiberg-Witten theory, one must analytically continue to a region where the full spectrum of \hat{A}_1 exists. Now values of $\text{Im}[\tau] < 0$ are allowed. This then gives 2 domains of definition of the expansion coefficients.

One can start by considering that the theta function is defined for τ in the upper half plane as $\theta(\tau, v)$. However, in the $\mathcal{N} = 2$ examples the parameter τ has an imaginary part that

changes sign at the affine wall. For this one must define an analytic continuation of the generating function into the lower half plane and hereby define a region in which all the roots can exist including the imaginary root.

Definition 11.2.2. In this case, the actions of the roots on the Cartan subalgebra can be written as 2 complex variables given by

$$\delta(u) = -2\pi i\tau, \tau \in \mathbb{C} \quad \text{and} \quad \alpha_0(u) = -2\pi i v, v \in \mathbb{C}, \quad (11.2.1)$$

following (10.3.5) up to the extension of the range of τ from \mathbb{H}^+ to \mathbb{C} .

Now the highest weight changes in all the possible chambers on both sides of the imaginary wall starting in the fundamental chamber where none of the roots exist. For the other domain of definition one can start in a chamber opposite to the first fundamental chamber. In this chamber all the roots exist. One can then work backwards from this to find the highest weight in other chambers.

11.2.1 Change in highest weight

Here we continue on from sections 10.4 and 10.4.1 by looking at the wall crossing of the generating function (10.4.10), this time focussing on the function inside the square, which we label as $f'_{\hat{A}_1}(u)$. This is done by using the highest weight of the Verma module associated to the Weyl denominator for \hat{A}_1 . However, this is now generalised to wall crossing beyond the affine wall. First, we recall that the generating function (10.4.10) in the fundamental Weyl chamber can be written as

$$f'_{\hat{A}_1}(u) = \frac{e^{\lambda(u)}}{\prod_{m=1}^{\infty} (1 - e^{-m\delta(u)})(1 - e^{-(m-1)\delta(u)+\alpha_0(u)})(1 - e^{-m\delta(u)-\alpha_0(u)})}. \quad (11.2.2)$$

This is written in terms of a highest weight $\lambda = \frac{1}{2}(\lambda_{k,h} + \alpha_0 + \delta)$ of a Verma module as is also done in Cheng and Verlinde [53]. As one crosses into different regions in the moduli space the highest weight jumps, depending on how many Weyl chambers are crossed and what direction one moves in. For example, we can start by moving to ²

$$f'_{\hat{A}_1}(u) = \frac{e^{\lambda'(u)}}{\prod_{l=1}^{\infty} (1 - e^{-l\delta(u)})(1 - e^{-l\delta(u)-\alpha_0(u)}) \prod_{m=k+1}^{\infty} (1 - e^{-(m-1)\delta(u)+\alpha_0(u)}) \prod_{m=1}^k (1 - e^{(m-1)\delta(u)-\alpha_0(u)})}.$$

²If one considers the generating function just in this form one also has a factor of -1 for every jump. For example, we can include $(-1)^k$ in this equation.

This is now a different representation with a different highest weight given by λ' . Following (10.4.11) the relationship between the highest weights is given by

$$\lambda' = \lambda + \sum_{m=1}^k \left((m-1)\delta - \alpha_0 \right).$$

The remaining jumps to all the different chambers are discussed extensively in appendix section B.1.1. We can keep passing through the remaining chambers until the full BPS spectrum exists

$$f'_{\hat{A}_1}(u) = \frac{e^{\lambda(u)} \prod_{l=1}^{\infty} e^{l\delta(u) + \alpha_0(u)}}{\prod_{l=1}^{\infty} (1 - e^{l\delta(u) + \alpha_0(u)})} \frac{\prod_{l=1}^{\infty} e^{l\delta(u)}}{\prod_{l=1}^{\infty} (1 - e^{l\delta(u)})} \frac{\prod_{m=1}^{\infty} e^{(m-1)\delta(u) - \alpha_0(u)}}{\prod_{m=1}^{\infty} (1 - e^{(m-1)\delta(u) - \alpha_0(u)})}, \quad (11.2.3)$$

and the highest weight is

$$\lambda' = \lambda + \sum_{m=1}^{\infty} \left((m-1)\delta - \alpha_0 \right) + \sum_{l=1}^{\infty} l\delta + \sum_{n=1}^{\infty} \left(n\delta + \alpha_0 \right).$$

It is possible to move in the other direction in which the later BPS states enter the spectrum first. An example was also given by (10.4.12). The representations can be ordered in the following way, such that one can write all the possible λ' in the table below. This is also shown in Fig. 11.1 below. Here all the boundaries of the Weyl chambers which are also the walls are shown in blue. These are now written in terms of the inner products with the roots first given in (10.3.5). The roots that exist within each chamber are also shown.

11.2.2 Counting roots and weights in Verma modules

The BPS states with particular charge are represented by the roots of the Lie algebra. To count these roots one uses the weight system of the Verma module as defined in (11.1.6). The roots representing the charges of the BPS states are found by taking the differences between the weights. One can start in the fundamental Weyl chamber where none of the BPS states exists. One chooses an initial weight from (11.2.2) called $\lambda_i \in \Gamma$. One can then move in the 2 possible directions and pick up roots, which are added to the highest weight. For every highest weight λ'_i all the possible weights under it exist. One can use the indices in the table above h, k, l to label the weights. This means we can write $\lambda = \lambda_{0,0,0}$ and $\lambda' = \lambda_{h,k,l}$ and for a particular representation which can run to infinity for $\lambda_{h,k,l}$ where all possible weights exist.

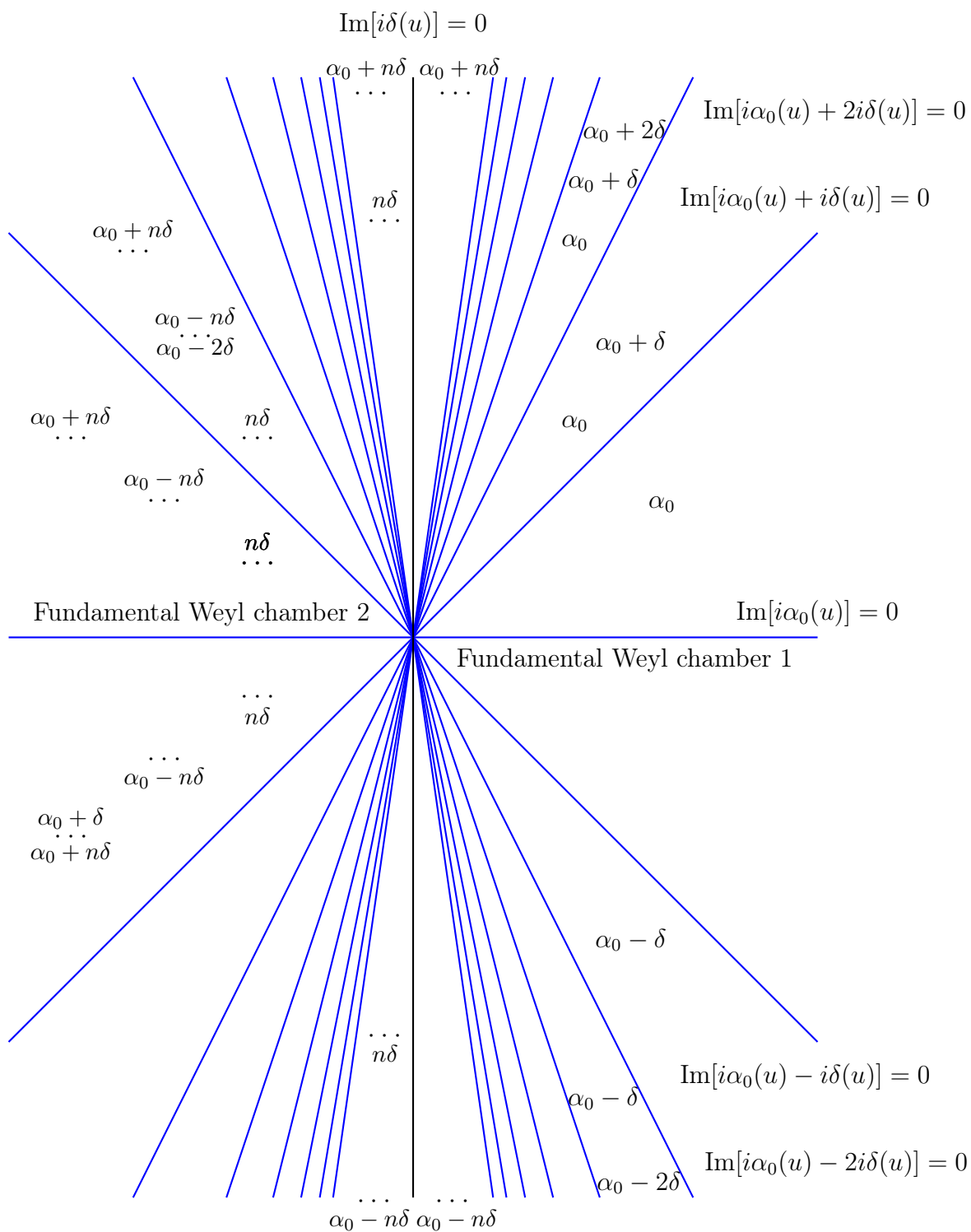


Figure 11.1: This diagram again shows the standard walls of the Weyl chambers of the affine Lie algebra \hat{A}_1 but this time extended into the lower half plane after the continuation described above. The blue lines represent the BPS walls.

All possible highest weights	
$\lambda + \sum_{m=1}^{\infty} \left((m-1)\delta - \alpha_0 \right) + \sum_{l=1}^{\infty} l\delta + \sum_{n=1}^{\infty} \left(n\delta + \alpha_0 \right)$	
$\lambda + \sum_{m=h+1}^{\infty} \left((m-1)\delta - \alpha_0 \right) + \sum_{l=1}^{\infty} l\delta + \sum_{n=1}^{\infty} \left(n\delta + \alpha_0 \right)$	$\lambda + \sum_{m=1}^{\infty} \left((m-1)\delta - \alpha_0 \right) + \sum_{l=1}^{\infty} l\delta + \sum_{n=k+1}^{\infty} \left(n\delta + \alpha_0 \right)$
$\lambda + \sum_{l=1}^{\infty} l\delta + \sum_{n=1}^{\infty} \left(n\delta + \alpha_0 \right)$	$\lambda + \sum_{m=1}^{\infty} \left((m-1)\delta - \alpha_0 \right) + \sum_{l=1}^{\infty} l\delta$
$\lambda + \sum_{n=1}^{\infty} \left(n\delta + \alpha_0 \right)$	$\lambda + \sum_{m=1}^{\infty} \left((m-1)\delta - \alpha_0 \right)$
$\lambda + \sum_{n=1}^k \left(n\delta + \alpha_0 \right)$	$\lambda + \sum_{m=1}^h \left((m-1)\delta - \alpha_0 \right)$
λ	

Table 11.1: All possible highest weights in the $\mathcal{N} = 2$ analog of the \hat{A}_1 Lie algebra. This is also shown on Fig. 11.1.

Inclusion of modules

In each chamber there is then a different highest weight labelling a sub-module of a module in a higher chamber denoted by $M(\lambda_{h,k,l}) \subset M(\lambda_{h',k',l'})$. This is also known as the weak Bruhat ordering of the highest weights $\lambda_{h,k,l} \rightarrow \lambda_{h',k',l'}$. Here this is extended across the affine wall such that it covers two domains of definition of Weyl chambers and Verma modules M and \tilde{M} . One now includes an additional module $G(\lambda_{\infty,\infty,\infty l})$ between the 2 domains. One can start in one fundamental Weyl chamber and move in two possible directions. For the first direction, one can write the sequence of submodules as:

$$M(\lambda_{0,0,0}) \subset M(\lambda_{1,0,0}) \subset M(\lambda_{2,0,0}) \dots M(\lambda_{m-1,0,0}) \subset M(\lambda_{m,0,0}) \dots \quad (11.2.4)$$

$$M(\lambda_{\infty-2,0,0}) \subset M(\lambda_{\infty-1,0,0}) \subset M(\lambda_{\infty,0,0}) \subset G(\lambda_{\infty,\infty,\infty l}) \subset$$

$$\tilde{M}(\lambda_{\infty,\infty-1,\infty l}) \subset \tilde{M}(\lambda_{\infty,\infty-2,\infty l}) \dots \tilde{M}(\lambda_{\infty,k+2,\infty l}) \subset \tilde{M}(\lambda_{\infty,k+1,\infty l}) \subset$$

$$\tilde{M}(\lambda_{\infty,k,\infty l}) \dots \tilde{M}(\lambda_{\infty,2,\infty l}) \subset \tilde{M}(\lambda_{\infty,1,\infty l}).$$

This is the weight system in 1 direction, and these are all the weights that exist for a particular representation in one direction one can take from the fundamental Weyl chamber to the opposite chamber where all states can exist.

Difference in weights

Now one can define a prescription for determining whether a particular root exists. For this we have a rule that the difference in the weights must be a sum of integer combinations of roots, meaning that

$$\lambda_{h,k,l} - \lambda_{h',k',l'} = \sum_i n_i \alpha_i \in \Gamma. \quad (11.2.5)$$

This means that if we know a set of weights that exist one can deduce the roots that exist by taking the difference of each pair of weights and determining what the roots, that are present, must be that span the differences. In the setup of the weight system above a new root enters existence as the highest weight jumps. We have the differences as

$$\lambda_{m,0,0} - \lambda_{m-1,0,0} = (m-1)\delta - \alpha_0, \quad (11.2.6)$$

and

$$\lambda_{\infty,n,\infty l} - \lambda_{\infty,n+1,\infty l} = n\delta + \alpha_0. \quad (11.2.7)$$

When these differences exist in the weight system the roots also enter the spectrum. For the imaginary roots we have

$$\lambda_{\infty,\infty,\infty l} - \lambda_{\infty,0,0} = \sum_{l=1}^{\infty} l\delta \in \Gamma. \quad (11.2.8)$$

So, the imaginary roots enter the spectrum with this highest weight. Now that we have a prescription for counting roots from highest weight Verma modules in (11.2.4) we can apply this to counting BPS states in various $\mathcal{N} = 2$ theories. Now, remembering (11.2.1), we have inner products of the roots and vectors within a complex 2d moduli space of the form $\alpha_0(u) \in \mathbb{C}$ and $\delta(u) \in \mathbb{C}$ for all examples. However, for each specific example one can write these complex numbers in terms of different complex numbers associated to the particular theory, for example the central charges. Therefore, the same root system can give rise to different wall crossing phenomena in different $\mathcal{N} = 2$ theories.

11.3 Example 1: Jafferis-Moore D6-D2-D0 bound state

Jafferis and Moore [37] define a class of generalised Donaldson-Thomas invariants that count D6-D2-D0 boundstates which undergo successive jumps at walls defined by \hat{A}_1 Weyl chamber boundaries. In the region with the maximal number of boundstates, also known as the Szendrői region [59], they are defined in terms of non-commutative Donaldson-Thomas invariants [19]. Here the relevant central charges, expressed in terms of the Kähler parameter $t = z\mathcal{P} + \Lambda e^{i\phi}\mathcal{P}'$, $\mathcal{P}, \mathcal{P}' \in H^2(X, \mathbb{R})$, are $Z_{\gamma_1}(t) = \Lambda^3 e^{3i\phi}$ and $Z_{\gamma_2}(t) = -mz - n$, $n, m \in \mathbb{Z}$ [37]. For this example, the parameters z and ϕ are also those found in the topological string partition function derived by A.S.T.T. [61] which reproduces the wall crossing for these framed BPS states³. When related to a topological string theory, the variables are identified as the argument of the topological string coupling $\arg(\lambda') = 3\phi$ and the complexified Kähler parameter $z = t'$. The central charges are obtained by taking the positive real parameter $\Lambda \rightarrow \infty$. In this case, the stability condition on the central charges takes the form

$$\langle \gamma_1, \gamma_2 \rangle \text{Im}[Z_{\gamma_1}(t)\bar{Z}_{\gamma_2}(t)] = -n\Lambda^3 \text{Im}[e^{3i\phi}(-mz^* - n)] > 0. \quad (11.3.1)$$

The physical walls that correspond to D6-D2-D0 bound states can be further be simplified to: $m = \pm 1, 0$ such that the stability conditions become:

$$-n\text{Im}[-z^*e^{3i\phi} - ne^{3i\phi}] > 0, \quad -n\text{Im}[z^*e^{3i\phi} - ne^{3i\phi}] > 0, \quad -n\text{Im}[-ne^{3i\phi}] > 0. \quad (11.3.2)$$

Example 11.3.1. This can be matched to the parameters we have defined in (10.3.5) for the $\mathcal{N} = 4$ theory and can also be used in the $\mathcal{N} = 2$ analog for the generating function in (11.2.2). In this example, the analog is constructed from the \hat{A}_1 root system by writing the roots in terms of the central charges

$$\pm\alpha_0(u) + n\delta(u) = -iZ_{\gamma_1}(t)\bar{Z}_{\gamma_2}(t), \quad n \in \mathbb{Z}, \quad (11.3.3)$$

so that we now have the walls at $\text{Im}[\pm i\alpha_0(u) + ni\delta(u)] = 0$, and can define the imaginary part of the contour as⁴

$$\underline{\text{Relation of roots to central charges}} \quad (11.3.4)$$

$$\begin{aligned} \text{Im}[\pm i\alpha_0(u) + ni\delta(u)] &= \text{Im}[Z_{\gamma_1}(t)\bar{Z}_{\gamma_2}(t)], \\ \text{Im}[i\alpha_0(u)] &= \frac{\text{Im}[z^*e^{3i\phi}]}{\epsilon}, \end{aligned}$$

³This is done by taking the Borel transformation of the topological free energy along different rays.

⁴We follow a contour prescription analogous to the $\mathcal{N} = 4$ case discussed in section 10.3.2.

$$\mathrm{Im}[i\delta(u)] = -\frac{\mathrm{Im}[e^{3i\phi}]}{\epsilon}, \quad \text{where } \frac{1}{\epsilon} = \Lambda^3.$$

This will generate the wall crossing of the Jafferis-Moore BPS states with splitting given by charges $(\pm 1, n)$ if $\mathrm{Im}[\pm\alpha_0(u) + n\delta(u)]$ changes sign. Each Weyl chamber in the lower half of the $\mathrm{Im}[\delta(u)]$ axis then contains a different combination of BPS states. Examples of the possible combinations of the moduli parameters include:

Combinations of roots acting on moduli (11.3.5)

$$\begin{aligned} \pm\mathrm{Im}[i\alpha_0(u)] &= \pm\frac{\mathrm{Im}[z^*e^{3i\phi}]}{\epsilon}, \\ \pm\mathrm{Im}[i\alpha_0(u)] - \mathrm{Im}[i\delta(u)] &= \pm\frac{\mathrm{Im}[z^*e^{3i\phi}]}{\epsilon} + \frac{\mathrm{Im}[e^{3i\phi}]}{\epsilon}, \\ \pm\mathrm{Im}[i\alpha_0(u)] - 2\mathrm{Im}[i\delta(u)] &= \pm\frac{\mathrm{Im}[z^*e^{3i\phi}]}{\epsilon} + 2\frac{\mathrm{Im}[e^{3i\phi}]}{\epsilon}, \\ \pm\mathrm{Im}[i\alpha_0(u)] - 3\mathrm{Im}[i\delta(u)] &= \pm\frac{\mathrm{Im}[z^*e^{3i\phi}]}{\epsilon} + 3\frac{\mathrm{Im}[e^{3i\phi}]}{\epsilon}, \\ &\dots = \dots \\ -n\mathrm{Im}[i\delta(u)] &= n\left(\frac{\mathrm{Im}[e^{3i\phi}]}{\epsilon}\right). \end{aligned}$$

If these equations are set to 0 these represent the walls, for the bound state in 2 parameters. In this case, the lower half plane for the BPS walls for the \hat{A}_1 root system matches the wall crossing described in [37, 59, 19]. Below this is shown in Figure 11.2.

11.4 Example 2: Seiberg-Witten theory

Seiberg-Witten theory is represented by affine $SU(2)$ Lie algebra or \hat{A}_1 . It was introduced by Seiberg and Witten in [1] and reviewed extensively in e.g. [66]. The theory has also been described by a 2 node quiver with 2 arrows $\bullet \rightrightarrows \bullet$ (see [100, 97, 2, 4]). Another way of looking at this is through the Seiberg-Witten curve, an elliptic curve that defines the central charges and monodromies of the theory and is parameterised by a complex one-dimensional modulus $w \in \mathbb{P}^1 \setminus \{-1, 1, \infty\}$. The number and type of BPS states that exist within the theory depends on the region within this one-dimensional moduli space - there exist two chambers. In one chamber this theory has infinitely many BPS states given by the hypermultiplet dyons $-m(\alpha_0 + \alpha_1) - \alpha_1$, $-(m-1)(\alpha_0 + \alpha_1) + \alpha_1$ and the W-boson with a charge corresponding to the roots $\alpha_0 + \alpha_1$. In the other chamber only the 2 states (a monopole and a dyon) exist as a basis α_1 and α_0 . These results have been previously derived through other methods including quiver mutations and attractor flow but are also derivable via the generating function.

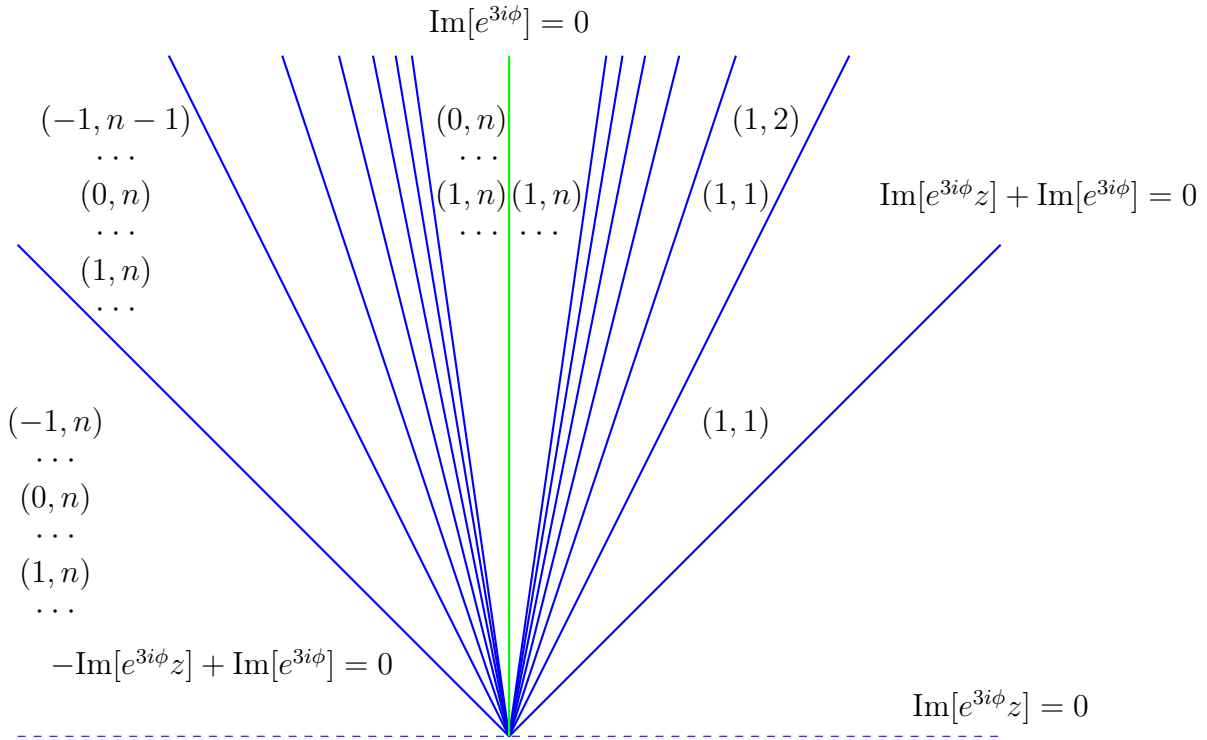


Figure 11.2: Walls for the bound states of D2-D0 branes to a large D6 brane.

As with the previous examples, to derive the BPS state counts through the generating function one must read off the highest weight using the Weyl denominator of the \hat{A}_1 Lie algebra.

Definition 11.4.1. Again, we remember from (10.3.5-11.2.1) that the roots act on the Cartan subalgebra, such that we have 2 complex variables:

$$\alpha_1(u) = \tau \in \mathbb{C}, \quad \alpha_0(u) = z \in \mathbb{C} \quad \text{and} \quad \delta(u) = \alpha_0(u) + \alpha_1(u) = \tau + z. \quad (11.4.1)$$

Here we have redefined our basis of roots given in (10.3.5-11.2.1) by exchanging $\alpha_0(u)$ and $\alpha_1(u)$ to better compare to the charges existing in Seiberg-Witten theory.

One can also integrate to find Fourier coefficients in different chambers as in the $\mathcal{N} = 4$ example in section 10.3.2. The counting function itself can be written as ⁵

$$f'_{\hat{A}_1}(u) = \frac{e^{n\alpha_0(u)+l\alpha_1(u)}}{\prod_{m=1}^{\infty} (1 - e^{-m(\alpha_0(u)+\alpha_1(u))})(1 - e^{-m(\alpha_0(u)+\alpha_1(u)-\alpha_1(u))})(1 - e^{-(m-1)(\alpha_0(u)+\alpha_1(u)+\alpha_1(u)})}, \quad (11.4.2)$$

$$= \frac{e^{n\tau+mz}}{\prod_{m=1}^{\infty} (1 - e^{-m(z+\tau)})(1 - e^{-m(z+\tau)-\tau})(1 - e^{-(m-1)(z+\tau)+\tau})},$$

⁵The highest weight can now be written as $\lambda = n\alpha_0(u) + l\alpha_1(u)$.

where we follow (11.2.2) but with the roots exchanged and the introduction of a new labelling of the highest weight using $n, l \in \mathbb{Z}$.

11.4.1 Seiberg-Witten walls

In Seiberg-Witten theory there is only 1 complex variable w parameterising the moduli space of the Seiberg-Witten curve that enters the stability condition. The equation for the wall of marginal stability can then be written as: $\text{Im}[Z_{\alpha_1}(w)\bar{Z}_{\alpha_2}(w)] = 0$. We know that in Seiberg-Witten theory there is one region of the moduli space with just 2 basis BPS states existing and 1 other region on the other side of the wall with infinitely many BPS states existing - the full spectrum of roots of the \hat{A}_1 Lie algebra. This means, if we are to match this with the chambers of the generating function, we must jump from one chamber to another and thus obtain a change in BPS degeneracies that matches this. For this we must choose a moduli prescription under which this jumping occurs.

For this we must be careful to distinguish the framed BPS states described in the work of GMN [17] from the original vanilla BPS states described in the theory. The framed halo BPS states are bound to a large core charge and the walls for these boundstates to form are the BPS walls. The vanilla BPS states can also bind with each other when the second type of wall, the wall of marginal stability, is crossed. The walls are labelled by:

$$MS_{\alpha_0, \alpha_1} : \text{Wall of marginal stability} \quad (11.4.3)$$

$$W_{\alpha_i} : \text{BPS wall} \quad (11.4.4)$$

If we write the walls in terms of the central charges of the theory, then the walls become not the walls of marginal stability MS_{α_0, α_1} for the BPS invariants of Seiberg-Witten theory itself, but are those for the framed halo BPS states⁶ W_{α_i} discovered in the paper of GMN [17] and re-interpreted in the work of Andriyash, Denef, Jafferis and Moore [18] from a supergravity perspective. These represent boundstates of the α_i to a large core charge. However, the intersection of these BPS walls W_{α_i} occurs on the wall of marginal stability. This is because if the imaginary part of all the central charges is vanishing, or in general $\text{Im}[Z_{\alpha_i}(w)/\mu] = 0, \forall \alpha_i$, where $\mu \in \mathbb{C}$ is a complex parameter then the ratio of all the $Z_{\alpha_i}(w)/\mu$ must be real. Hence, the condition on the wall of marginal stability $\text{Im}[Z_{\alpha_i}(w)\bar{Z}_{\alpha_j}(w)] = 0$ is satisfied.

Therefore, one can consider that the walls for the framed halo BPS states W_{α_i} form a cone for which in the upper region exists the full infinite Seiberg-Witten BPS spectrum and in the lower just the 2 basis states. Which region is which can be determined by the existence conditions on the central charges discussed in our work on attractor flow following the ideas

⁶These are known as BPS walls.

in [55, 57, 56].

Example 11.4.2. The identification between the roots and the central charges is as follows:

$$\alpha_0(u) = \frac{Z_{\alpha_0}(w)}{\mu}, \quad \alpha_1(u) = \frac{Z_{\alpha_1}(w)}{\mu}, \quad \delta(u) = \frac{1}{\mu}(Z_{\alpha_0}(w) + Z_{\alpha_1}(w)). \quad (11.4.5)$$

Here we can take $\mu = \epsilon\zeta$, where $\zeta := e^{i\theta}$, $\theta \in \{0, 2\pi\}$ is a phase, and $\epsilon \in \mathbb{R}$ is a small parameter that can be used to define the contour (see sec. 10.3.2) when extracting Fourier coefficients. This is analogous to the $\mathcal{N} = 4$ examples in [52, 53] where one takes contours at infinity $\epsilon \rightarrow 0$ to generate a consistent jumping of dyon degeneracies. In $\mathcal{N} = 2$ language the phase ζ is a complex parameter representing the phase of an infinitely heavy dyon to which the framed particles are bound.

Now we will briefly review the wall crossing for the framed halo BPS states: On the upper half plane the jumping occurs at the walls $\pm \text{Im}[i\alpha_0(u)] + m \text{Im}[i\alpha_1(u) + i\alpha_0(u)] = 0$, $m \in \mathbb{Z}$. We can choose the moduli that give the matched jumping for the framed halo BPS states. The walls are given by the vanishing locus of the imaginary parts of the central charges:

Imaginary parts of central charges on one side of affine wall $W_{\alpha_0+\alpha_1}$

$$\begin{aligned} \text{Im}[i\alpha_0(u)] &= \text{Im}\left[\frac{Z_{\alpha_0}(w)}{\mu}\right], & (11.4.6) \\ \text{Im}[i\alpha_0(u)] + \text{Im}[i\alpha_1(u) + i\alpha_0(u)] &= \text{Im}\left[\frac{2Z_{\alpha_0}(w) + Z_{\alpha_1}(w)}{\mu}\right], \\ \text{Im}[i\alpha_0(u)] + 2\text{Im}[i\alpha_1(u) + i\alpha_0(u)] &= \text{Im}\left[\frac{3Z_{\alpha_0}(w) + 2Z_{\alpha_1}(w)}{\mu}\right], \\ &\dots = \dots \end{aligned}$$

where the dots represent an infinite continuation of this pattern of BPS walls. Now we can look at the combinations on the other side of the affine wall and determine what happens as these BPS walls are crossed:

On other side, and including $W_{\alpha_0+\alpha_1}$ (11.4.7)

$$\begin{aligned} -\text{Im}[i\alpha_0(u)] &= -\text{Im}\left[\frac{Z_{\alpha_0}(w)}{\mu}\right], \\ -\text{Im}[i\alpha_0(u)] + \text{Im}[i\alpha_1(u) + i\alpha_0(u)] &= \text{Im}\left[\frac{Z_{\alpha_1}(w)}{\mu}\right], \\ -\text{Im}[i\alpha_0(u)] + 2\text{Im}[i\alpha_1(u) + i\alpha_0(u)] &= \text{Im}\left[\frac{Z_{\alpha_0}(w) + 2Z_{\alpha_1}(w)}{\mu}\right], \end{aligned}$$

$$\begin{aligned}
-\mathrm{Im}[i\alpha_0(u)] + 3\mathrm{Im}[i\alpha_1(u) + i\alpha_0(u)] &= \mathrm{Im}\left[\frac{2Z_{\alpha_0}(w) + 3Z_{\alpha_1}(w)}{\mu}\right], \\
&\dots = \dots \\
n\mathrm{Im}[i\alpha_1(u) + i\alpha_0(u)] &= n\mathrm{Im}\left[\frac{Z_{\alpha_0}(w) + Z_{\alpha_1}(w)}{\mu}\right].
\end{aligned}$$

All these walls intersect on the wall of marginal stability MS_{α_0, α_1} for the vanilla states. This produces a cone with the full \hat{A}_1 spectrum on one side and the basis states on the other. The diagram below Fig. 11.3 shows the existence conditions for the framed halo BPS states of Seiberg-Witten theory. The walls of the framed halo BPS states all intersect on the wall of the vanilla BPS degeneracies. The inside of the wall represents the region where only 2 vanilla BPS states exist.

Reminder of Attractor flow existence conditions

Now to give an explanation of the wall crossing at MS_{α_0, α_1} we can look back at the existence conditions for the attractor flow used by [57, 56] and applied again in [58, 62].

- (i) We remember that for a BPS state to exist the endpoint of the flow must terminate at a singular point.
- (ii) If the flow terminates at a regular point in Seiberg-Witten and Argyres-Douglas theories the central charges vanish. This can be interpreted as contradictory, as the central charges vanish at a point where the cycles in the elliptic curve do not pinch. Hence, the BPS state does not exist.

One way of looking at the flow lines is as lines of constant phase, and indeed the BPS walls W_{α_i} satisfy these conditions because $Z_{\alpha_i}(w)/\mu \in \mathbb{R}$ on the W_{α_i} . Therefore, we can use the attractor flow existence conditions on the BPS walls W_{α_i} by excluding walls that pass through regular attractor points at which the central charge vanishes.

Existence conditions from generating function

In terms of the generating function, this condition can be stated such that the generating function must not have any poles at regular points in the moduli space. To do this one can redefine the factor in the denominator that contains the pole, at the wall of marginal stability MS_{α_0, α_1} , where the central charges align. This can be done by writing the central charge that causes the pole at a regular point in terms of a real function multiplying one of the other central charges that vanishes at a regular point. Then one can choose such a function that can be continued across the wall of marginal stability MS_{α_0, α_1} . This is then no longer a root and can no longer be written as the linear combination of the other roots. Hence, this BPS state doesn't exist or contribute to any count of BPS states in a highest

weight of a representation or module. One can then just consider the factor in the generating function for the non-existing BPS state as just a normalisation.

We start by explicitly writing the generating function (11.4.2) in terms of central charges

$$\frac{e^{\lambda(w)}}{\prod_{m=1}^{\infty} \left(1 - e^{-\frac{m}{\mu}(Z_{\alpha_0}(w)+Z_{\alpha_1}(w))}\right) \left(1 - e^{-\frac{m}{\mu}(Z_{\alpha_0}(w)+Z_{\alpha_1}(w)-\frac{Z_{\alpha_1}(w)}{\mu})}\right) \left(1 - e^{-\frac{(m-1)}{\mu}(Z_{\alpha_0}(w)+Z_{\alpha_1}(w)+\frac{Z_{\alpha_1}(w)}{\mu})}\right)}.$$
(11.4.8)

Now we can write the factors representing central charges that vanish at regular points in terms of ratios of the central charges such that:

Central charges in terms of ratio

$$\begin{aligned} -\frac{Z_{\alpha_1}(w)}{\mu} \left(1 + \frac{Z_{\alpha_0}(w)}{Z_{\alpha_1}(w)}\right) m &= \frac{Z_{\alpha_1}(w)}{\mu} r_m(w), \\ \frac{Z_{\alpha_1}(w)}{\mu} \left(1 - (m-1) \left(1 + \frac{Z_{\alpha_0}(w)}{Z_{\alpha_1}(w)}\right)\right) &= \frac{Z_{\alpha_1}(w)}{\mu} r_{m+1,m}(w), \\ \frac{Z_{\alpha_1}(w)}{\mu} \left(-1 - m \left(1 + \frac{Z_{\alpha_0}(w)}{Z_{\alpha_1}(w)}\right)\right) &= \frac{Z_{\alpha_1}(w)}{\mu} r_{m,m+1}(w), \end{aligned}$$
(11.4.9)

$$r_m(w) = -\left(1 + \frac{Z_{\alpha_0}(w)}{Z_{\alpha_1}(w)}\right) m, \quad r_{m+1,m}(w) = 1 - (m-1) \left(1 + \frac{Z_{\alpha_0}(w)}{Z_{\alpha_1}(w)}\right), \quad m > 2, \quad (11.4.10)$$

$$r_{m,m+1}(w) = -1 - m \left(1 + \frac{Z_{\alpha_0}(w)}{Z_{\alpha_1}(w)}\right).$$

On the wall of marginal stability, the ratio of the central charges is real. Therefore, we have on the wall of marginal stability: $r_m(w)$, $r_{m+1,m}(w)$, $r_{m,m+1}(w) \in \mathbb{R}$.

Example of continuation through wall of marginal stability MS_{α_0,α_1}

Now we find a continuation of the generating function through the wall of marginal stability MS_{α_0,α_1} with a function that avoids the poles at a regular point in the moduli space. This is done for the central charges in the exponents that would otherwise vanish at a regular point on the other side of the wall by choosing real continuations of $r_m(w)$, $r_{m+1,m}(w)$, and $r_{m,m+1}(w)$, such that the central charges now behave as those that flow to singular points.

Definition 11.4.3. For example, one can choose ⁷

$$r_m(w) = -\left(1 + \left|\frac{Z_{\alpha_0}(w)}{Z_{\alpha_1}(w)}\right|\right)m, \quad r_{m+1,m}(w) = 1 - (m-1)\left(1 + \left|\frac{Z_{\alpha_0}(w)}{Z_{\alpha_1}(w)}\right|\right), \quad m > 2, \quad (11.4.11)$$

$$r_{m,m+1}(w) = -1 - m\left(1 + \left|\frac{Z_{\alpha_0}(w)}{Z_{\alpha_1}(w)}\right|\right),$$

on the other side of the wall of marginal stability MS_{α_0,α_1} .

Now the generating function avoids all poles at regular points. Essentially the BPS walls W_{α_i} have collapsed into 2 walls representing the basis states. This means there are 2 BPS states that exist in this region as the generating function can maximally count only 2 active BPS states in its highest weight.

Example 11.4.4 (Excluded BPS states).

The exponents of the non-existing BPS states are no longer in the lattice of positive roots $Z_{\alpha_1}(w)/\mu \ r_m(w)$, $Z_{\alpha_1}(w)/\mu \ r_{m,m+1}(w)$, $Z_{\alpha_1}(w)/\mu \ r_{m+1,m}(w)$, $m > 2 \notin \Delta^+$. This is because

$$\frac{Z_{\alpha_1}(w)}{\mu}r_m(w) \neq m'\delta(u), \quad \frac{Z_{\alpha_1}(w)}{\mu}r_{m,m+1}(w) \neq \alpha_0(u) - m'\delta(u) \quad \text{and} \quad (11.4.12)$$

$$\frac{Z_{\alpha_1}(w)}{\mu}r_{m+1,m}(w) \neq -\alpha_0(u) - m'\delta(u).$$

Example 11.4.5 (Existing BPS states).

Now the only BPS states that can still be written as roots include $\alpha_0(u) = Z_{\alpha_0}(w)/\mu$ and $\alpha_0(u) - \delta(u) = -\alpha_1(u) = -Z_{\alpha_1}(w)/\mu$ as these were not modified at the wall. The attractor flow for these states terminates at singular points.

Continuation of generating function through MS_{α_0,α_1}

On this side of the wall of marginal stability MS_{α_0,α_1} the generating function (11.4.8) can be re-written as

$$\frac{e^{\lambda(u)}}{(1 - e^{-\frac{Z_{\alpha_0}(w)}{\mu}})(1 - e^{-\frac{Z_{\alpha_1}(w)}{\mu}}) \prod_{m=1}^{\infty} (1 - e^{-\frac{Z_{\alpha_1}(w)}{\mu}r_m(w)})(1 - e^{-\frac{Z_{\alpha_1}(w)}{\mu}r_{m,m+1}(w)}) \prod_{m=3}^{\infty} (1 - e^{-\frac{Z_{\alpha_1}(w)}{\mu}r_{m+1,m}(w)})},$$

⁷This is only one possible choice of continuation - in general there can be many possible continuations one could choose.

such that it now becomes

$$\frac{e^{\lambda(w)}}{(1 - e^{-\frac{Z_{\alpha_0}(w)}{\mu}})(1 - e^{-\frac{Z_{\alpha_1}(w)}{\mu}})} f\left(\frac{Z_{\alpha_1}(w)}{\mu} r_m(w), \frac{Z_{\alpha_1}(w)}{\mu} r_{m,m+1}(w), \frac{Z_{\alpha_1}(w)}{\mu} r_{m+1,m}(w)\right), \quad (11.4.13)$$

where this is now a generating function of 2 BPS states only. All BPS walls W_{α_i} have collapsed onto two and the function $f\left(\frac{Z_{\alpha_1}(w)}{\mu} r_m(w), \frac{Z_{\alpha_1}(w)}{\mu} r_{m,m+1}(w), \frac{Z_{\alpha_1}(w)}{\mu} r_{m+1,m}(w)\right)$ in (11.4.13) can be treated now just as a normalisation. The framed wall crossing on this side of the wall of marginal stability can now be tabulated.

Highest weight on side with 2 BPS states
$\lambda + (\alpha_0 - \delta) + \alpha_0$
$\lambda + \alpha_0 - \delta$
λ

Table 11.2: Highest weights of the modules when only 2 BPS states exist. Shown on lower half of Fig. 11.3.

A complete tabulation (11.3) of crossing of both the BPS walls W_{α_i} and the wall of marginal stability MS_{α_0, α_1} can now also be written down.

The wall crossing on both sides of MS_{α_0, α_1} is depicted in Fig. 11.3. The crossing of MS_{α_0, α_1} can clearly be seen by looking at just the 2 outer BPS walls. These can be used to construct a cone with upper and lower region. The upper region contains the full spectrum and the lower just the 2 basis states. The parameter ζ can be varied such that the cone can be taken at any point along the wall. On Fig. 11.3 we directly show the intersection of the BPS walls W_{α_i} with the wall of marginal stability MS_{α_0, α_1} . We choose a parameter $\zeta_1 = 1$. One can change the parameter from ζ_1 to ζ_2 . This changes the intersection point of the BPS walls with the wall of marginal stability, and gives a different cone, with the same wall crossing behaviour. Such cones can be used to sweep all regions inside and outside the wall of marginal stability. Indeed, we have actually reproduced the scattering diagram for Seiberg-Witten theory developed by Bridgeland [124, 58].

This therefore reproduces the spectrum of Seiberg-Witten theory (see table (11.4)) with 2

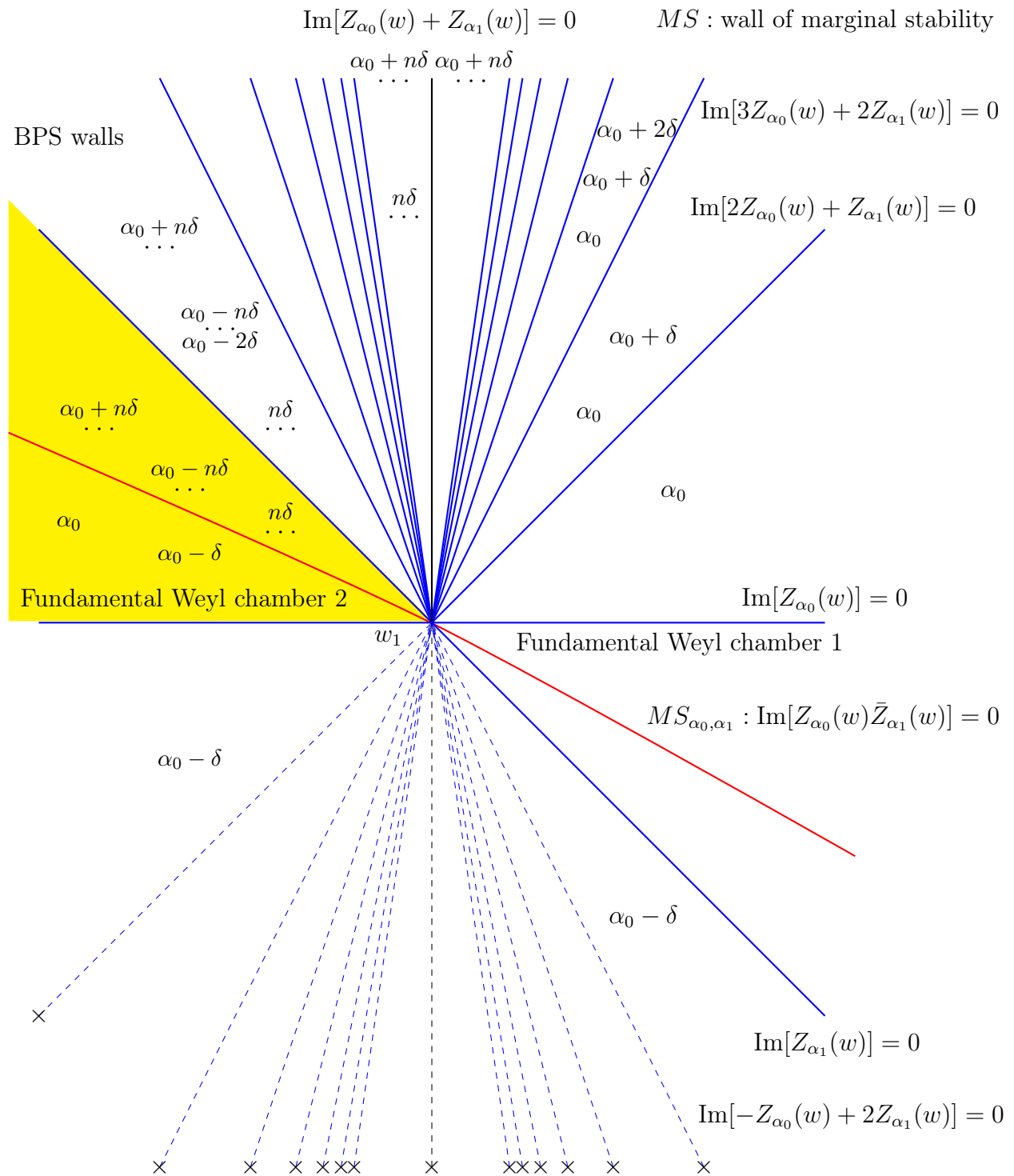


Figure 11.3: This diagram again shows the walls of the Weyl chambers of the affine A_1 Lie algebra, but with the wall of marginal stability for the vanilla BPS states in red. This time we show the intersection of the BPS walls at the point w_1 on the wall of marginal stability. Here the existing BPS walls for Seiberg-Witten theory are shown in dark blue. The dashed blue lines are those excluded by the existence condition of vanishing central charges at regular points represented by the crosses on the ends of the line.

Tabulation on both sides of the wall of marginal stability MS_{α_0, α_1}	
Side with full \hat{A}_1 spectrum	Side with 2 basis states
$\lambda + \sum_{m=2}^{\infty} ((m-1)\delta - \alpha_0) + \sum_{l=1}^{\infty} l\delta + \sum_{n=0}^{\infty} (n\delta + \alpha_0)$	$\lambda + (\delta - \alpha_0) + \alpha_0$
$\lambda + \sum_{m=h+1}^{\infty} ((m-1)\delta - \alpha_0) + \sum_{l=1}^{\infty} l\delta + \sum_{n=0}^{\infty} (n\delta + \alpha_0)$	$\lambda + \delta - \alpha_0$
$\lambda + \sum_{l=1}^{\infty} l\delta + \sum_{n=0}^{\infty} (n\delta + \alpha_0)$	$\lambda + \delta - \alpha_0$
$\lambda + \sum_{n=0}^{\infty} (n\delta + \alpha_0)$	$\lambda + \delta - \alpha_0$
$\lambda + \sum_{n=0}^k (n\delta + \alpha_0)$	$\lambda + \delta - \alpha_0$
λ	

Table 11.3: Complete tabulation of all highest weights for the Seiberg-Witten analog. The first column is on the side of the wall with the full infinite spectrum. Second column is on the side with just the 2 basis states. This is shown on Fig. 11.3.

BPS states in chambers	
Chamber 1	$\pm(\alpha_0 - \delta), \pm\alpha_0$
Chamber 2	$\pm\alpha_0 + n\delta, \pm\delta$

Table 11.4: Final existing BPS states in Seiberg-Witten theory on both sides of the wall of marginal stability represented by the red line in Fig. 11.3.

basis states on one side of the wall and infinitely many on the other.

11.5 Argyres-Douglas A_2

In this example, we look at Argyres-Douglas theory represented by a 2 node quiver with 1 arrow $\bullet \rightarrow \bullet$. This theory has BPS states described by the root system of the $SU(3)$ Lie algebra [5]. As with Seiberg-Witten theory, this theory is parameterised by a complex 1d moduli space of an elliptic curve consisting of a single parameter $w \in \mathbb{P}^1 \setminus \{-1, 1, \infty\}$. As with Seiberg-Witten theory the number of BPS states that exist in the theory depends on the region of the moduli space. It has been found that in one chamber this theory has 2 basis BPS states given by electric and magnetic monopoles α_1 and α_2 . In the other chamber 3 BPS states exist including the 2 monopoles α_1, α_2 and a dyon $\alpha_3 = \alpha_1 + \alpha_2$.

11.5.1 Introduction to counting function for Argyres-Douglas A_2 theory

One can conjecture that a similar generating function exists for other ADE Lie Algebras that are not affine. The second part of the research in this work involves finding a similar generating function and wall crossing behaviour for the Argyres-Douglas A_2 theory [5] following the methods detailed in Cheng and Verlinde [53]. In this case, we again look for a match between the boundaries of the Weyl chambers and the walls. If such a match is found one can use an analogous formulation to that in Cheng and Verlinde to count the existence of certain BPS states by looking at how many additional roots are added to the highest weight in each Weyl chamber. For this example, only the Weyl denominator is needed to determine the change in the highest weight of the Verma module. However, one can also show that the full character also transforms in such a way under wall crossing. This means it remains invariant up to an additional root being added or subtracted to the highest weight every time a boundary of a Weyl chamber is crossed. When in the full character the highest weight is of a representation.

11.5.2 A_2 Weyl character

The Weyl character formula can be generalised from the characters of Borchers-Kac-Moody algebras to those for ADE type Lie algebras. In this way one can compare the prescription for highest weights in Borchers-Kac-Moody algebras to those in models with the A_1, A_2 and \hat{A}_1 root systems. Again, following from sec. 11.1.1 for these roots systems the analog counting function is written as the Weyl denominator that is simple to expand as a geometric series. This being the denominator of the character (recall eq. 11.1.7) [199]

$$ch_\lambda = \frac{\sum_{w \in W} (\det w) e^{w(\lambda + \rho)(u)}}{e^{\rho(u)} \prod_{\alpha \in \Delta^+} (1 - e^{-\alpha(u)})}, \quad (11.5.1)$$

where the vector $\rho = \frac{1}{2} \sum_{\alpha_i \in \Delta^+} \alpha_i$ is again the Weyl vector - written as the half sum of the positive roots. As mentioned before in section 11.1.1 w are the Weyl group elements and one chooses a representation to start with that has a highest weight λ .

The number and charge of the roots representing the BPS states should be distinct for every possible Weyl chamber. As with Seiberg-Witten theory in 11.4.1 such a match again exists for the framed BPS states from [17, 18]. In Cheng and Verlinde [53] the generating function corresponds to the Weyl denominator of the Borcherds-Kac-Moody algebra. In this case, we just look at the simple case of the $SU(3)$ Weyl denominator. One can also look at the full character of this Lie algebra. This is the Weyl character for the $SU(3)$ Lie Algebra. One can choose a complex 2 dimensional moduli parameter for example $u = (u_1, u_2)$ to define in which chamber one is in. This can then be substituted into the character formula.

Definition 11.5.1. The character itself reads:

$$\frac{e^{\lambda(u) - \frac{2}{(\alpha_1, \alpha_1)}((\lambda + \frac{1}{2}(\alpha_1 + \alpha_2 + \alpha_3)), \alpha_1)\alpha_1(u)} + e^{\lambda(u) - \frac{2}{(\alpha_2, \alpha_2)}((\lambda + \frac{1}{2}(\alpha_1 + \alpha_2 + \alpha_3)), \alpha_2)\alpha_2(u)} + e^{\lambda(u) - \frac{2}{(\alpha_3, \alpha_3)}((\lambda + \frac{1}{2}(\alpha_1 + \alpha_2 + \alpha_3)), \alpha_3)\alpha_3(u)}}{(1 - e^{-\alpha_1(u)})(1 - e^{-\alpha_2(u)})(1 - e^{-\alpha_3(u)})} \quad (11.5.2)$$

The highest weight of the representation is denoted as λ and the roots system of the algebra contains $\alpha_1, \alpha_2, \alpha_3 = \alpha_1 + \alpha_2$.

We know, e.g. from the quiver representation theory, that these roots correspond to BPS states and that we should observe at least 2 chambers with 2 and 3 BPS states respectively. The wall of marginal stability does however not match the Weyl chambers directly as these Weyl chamber boundaries (as in the Seiberg-Witten example in sec. 11.4) correspond to the BPS walls W_{α_i} for the framed halo BPS states [17], which are different from the wall of marginal stability MS_{α_1, α_2} . Here we will first look at the wall crossing for the BPS walls W_{α_i} in which there is one chamber with all the halo BPS states existing and another (which we can label the fundamental Weyl chamber) with none of the BPS states existing.

Therefore, as with the $\mathcal{N} = 4$ black hole example in the work of Cheng and Verlinde [53], and the analogs of the \hat{A}_1 Lie algebra, we again find wall crossing behavior with the BPS walls corresponding to the boundaries $\text{Im}[i\alpha_i(u)] = 0$. Furthermore, this again manifests itself either as a shift in the highest weight or in the Fourier expansion coefficients jumping between distinct Weyl chambers. For example, in the transition from the chamber $\text{Im}[i\alpha_i(u)] > 0, \quad \forall i \in 1, 2, 3$ to $\text{Im}[i\alpha_1(u)] < 0, \quad \text{Im}[i\alpha_2(u)] > 0, \quad \text{Im}[i\alpha_3(u)] > 0$, we determined that the highest weight changes such that $ch_{\lambda_2} = ch_{\lambda_1 - \alpha_2'}$ after a suitable basis transformation. In the following section 11.5.3 and in the appendix B.2.1 we calculate this change for all the remaining chambers just from the denominator.

11.5.3 Wall crossing and change of basis for denominator

As with the affine Lie algebra we look at the denominator and try to expand it in the different Weyl chambers. This alone should encode the wall crossing for the BPS walls in

the same way that the Verma modules do in the \hat{A}_1 case. The Weyl denominator of a general Lie algebra, introduced in (11.1.5), is what can be expanded in the different Weyl chambers. As with the case of degeneracies in $\mathcal{N} = 4$ examples we can multiply the denominator by an additional charge factor $e^{\Lambda(u)}$ and write it as a Verma module character

$$\frac{e^{\Lambda(u)}}{e^{\rho(u)} \prod_{\alpha \in \Delta^+} (1 - e^{-\alpha(u)})} = \frac{e^{\lambda(u)}}{\prod_{\alpha \in \Delta^+} (1 - e^{-\alpha(u)})}, \quad (11.5.3)$$

The product is over all positive roots and the exponentials must be negative to allow a convergent geometric series expansion ⁸

$$\frac{1}{\prod_{\alpha \in \Delta^+} (1 - e^{-\alpha(u)})} = \sum_{\beta \in \mathbb{N}\Delta^+} K(\beta) e^{\beta(u)}, \quad (11.5.4)$$

where $K(\beta)$ is the count of all the possible combinations in which β can be expressed in terms of an integral linear combination of positive roots [199]. Now we look at the specific case of (11.5.3) for the A_2 Weyl denominator

$$\frac{e^{\lambda(u)}}{(1 - e^{-\alpha_1(u)})(1 - e^{-\alpha_2(u)})(1 - e^{-\alpha_3(u)})}, \quad (11.5.5)$$

where $\alpha_3(u) = \alpha_1(u) + \alpha_2(u)$.

Weyl denominator expansion in different chambers

Now for each Weyl chamber in which we do the expansion we will change the basis of positive roots in such a way that the exponents in the expansion remain negative for all n, m, l , where n, m and l are the term numbers of this expansion. As discussed in [4] this corresponds to taking successive Weyl reflections and can also be thought of as quiver mutations or changes of basis. Physically, this means choosing a basis of particles. Evaluated at a particular modulus outside the fundamental Weyl chamber (after BPS walls have been crossed) one must therefore take Weyl reflections of the form

$$w_{\alpha_i}(\alpha_j) = \alpha_j - \frac{2}{(\alpha_i, \alpha_i)} (\alpha_j, \alpha_i) \alpha_i. \quad (11.5.6)$$

This is done to distinguish whether the expansions in the different Weyl chambers just correspond to a different basis or quiver mutation (see [4]) by successive Weyl reflection, or if they correspond to walls in the moduli space and actually distinguish whether there are different numbers of BPS states present in the model. ⁹

⁸This formula can be expanded in this form [199] and is known as the Kostant partition function.

⁹In addition to the quiver mutation we are also exchanging α'_1 and α'_2 just to better distinguish the state before and after the transformation.

$$\text{Im}[i\alpha_i(u)] > 0 \quad \forall i \in 1, 2, 3 \quad (11.5.7)$$

$$\sum_{n,m,l=0}^{\infty} e^{-(n\alpha_1(u)+m\alpha_2(u)+l\alpha_3(u))}$$

the exponents are $-n\alpha_1(u) - m\alpha_2(u) - l\alpha_3(u)$,

The expansion in the fundamental Weyl chamber is already in the required form with negative exponents so there is no change of basis required.

$$(11.5.8)$$

$$\text{Im}[i\alpha_1(u)] < 0, \text{Im}[i\alpha_2(u)] > 0, \text{Im}[i\alpha_3(u)] > 0$$

$$- \sum_{n,m,l=0}^{\infty} e^{(n+1)\alpha_1(u)-m\alpha_2(u)-l\alpha_3(u)},$$

$$-(n+1)(-\alpha_1(u)) - m\alpha_2(u) - l(\alpha_1 + \alpha_2(u)),$$

$$\text{change basis } \alpha'_1 = \alpha_1 + \alpha_2 = \alpha_3, \alpha'_2 = -\alpha_1, \alpha'_3 = \alpha_2,$$

$$\text{expression becomes } -((n+1)\alpha'_2(u) + m\alpha'_3(u) + l\alpha'_1(u)).$$

In this Weyl chamber the exponent changes sign. We therefore perform a change of basis to restore the negative exponents. This results in a shift in the highest weight by a single root.

So now the denominator in the new basis reads

$$\frac{e^{(\lambda' - \alpha'_2)(u)}}{(1 - e^{-\alpha'_1(u)})(1 - e^{-\alpha'_2(u)})(1 - e^{-\alpha'_3(u)})}, \quad (11.5.9)$$

such that the module jumps to one with highest weight $\lambda' - \alpha'_2$ relative to that in (11.5.5). We have continued the computation for the expansion of the Weyl denominator in the remaining Weyl chambers. All the changes in the possible expansions are listed in appendix B.2.1. For the remaining expansions it was always possible to write the expansion in terms of a set of negative exponents. When this was done we always obtained a shift in one of the coefficients.

Therefore, it is always possible to change the basis in such a way that all the exponents in the expansion are negative in n, m and l for all n, m, l . These basis changes also correspond to rotations of the positive plane. We have not found any obstructions to this. So, the expansions are distinguished but only by which and how many roots are shifted by one in the exponent and the negative pre-factor in front of the sum. This means that this shift does in fact represent a jump in the number of existing BPS states and is not just a basis change.

Inclusion of modules and structure of chambers

In this way 6 chambers are found with different highest weight modules $M(\lambda_{n,m})$ which can be defined in the same way as for the \hat{A}_1 root system in (11.2.4). One can again write this in terms of inclusions if we write $\lambda_{n,m} = \lambda + n\alpha_1 + m\alpha_2$.¹⁰ In one direction we have

$$M(\lambda_{0,0}) \subset M(\lambda_{1,0}) \subset M(\lambda_{2,1}) \subset M(\lambda_{2,2}), \quad (11.5.10)$$

and in the other

$$M(\lambda_{0,0}) \subset M(\lambda_{0,1}) \subset M(\lambda_{1,2}) \subset M(\lambda_{2,2}). \quad (11.5.11)$$

This means that there is indeed a non-trivial jump in the number of BPS states when the series is expanded in different Weyl chambers. This can be seen by distinct expansion coefficients and can be encoded in the distinct highest weight module.

Therefore, we have found 6 chambers with a different combination of roots (representing the BPS charges) existing in each chamber. This should then correspond to 1 chamber with no roots existing another with just α_1 existing but with no other roots, another with α_2 and no other roots, another with α_2, α_3 , one with α_1, α_3 and finally one with all 3 roots existing as $\alpha_1, \alpha_2, \alpha_3$. This corresponds to the wall crossing for the framed BPS states. This can be shown in a table.

All possible highest weights	
$\lambda + \alpha_1 + \alpha_2 + \alpha_3$	
$\lambda + \alpha_1 + \alpha_3$	$\lambda + \alpha_2 + \alpha_3$
$\lambda + \alpha_1$	$\lambda + \alpha_2$
λ	

Table 11.5: Highest weight states representing framed BPS boundstates in 6 Weyl chambers.

Central charge representation of the roots

If one wants to connect this wall crossing to BPS walls one must again write the complex inner products of the roots in terms of central charges. These walls can then be mapped

¹⁰To continue on from (11.5.9) we must let $\alpha'_i \rightarrow \alpha_i$.

into the moduli space to see the wall crossing at the wall of marginal stability MS_{α_1, α_2} in addition to that at the BPS walls W_{α_i} .

Example 11.5.2. The roots can thus be written as follows:

$$\alpha_1(u) = \frac{Z_{\alpha_1}(w)}{\mu}, \quad \alpha_2(u) = \frac{Z_{\alpha_2}(w)}{\mu}. \quad (11.5.12)$$

Here as with the Seiberg-Witten example we can let $\mu = \epsilon\zeta \in \mathbb{C}$ where $\epsilon \in \mathbb{R}$ is a small parameter defining the contour and $\zeta := e^{i\theta}$, $\theta : 0 \in \{0, 2\pi\}$ is the phase that is chosen.

The BPS walls can be written as the vanishing locus of the imaginary parts of the central charges which read:

$$\text{Im}[i\alpha_1(u)] = \text{Im}\left[\frac{Z_{\alpha_1}(w)}{\mu}\right], \quad \text{Im}[i\alpha_2(u)] = \text{Im}\left[\frac{Z_{\alpha_2}(w)}{\mu}\right], \quad \text{Im}[i\alpha_1(u) + i\alpha_2(u)] = \text{Im}\left[\frac{Z_{\alpha_1}(w) + Z_{\alpha_2}(w)}{\mu}\right].$$

Crossing the wall of marginal stability MS_{α_1, α_2}

At the wall of marginal stability MS_{α_1, α_2} , the central charges align (as is the case for Seiberg-Witten theory in section 11.4) such that their ratio is some real function $r_i(w) \in \mathbb{R}$ along the wall. This means that on the wall of marginal stability MS_{α_1, α_2} one can write the sum of the central charges as

$$\frac{Z_{\alpha_1}(w) + Z_{\alpha_2}(w)}{\mu} = \frac{Z_{\alpha_1}(w)}{\mu} \left(1 + \frac{Z_{\alpha_2}(w)}{Z_{\alpha_1}(w)}\right), \quad (11.5.13)$$

and on the wall of marginal stability we have

$$r_3(w) \frac{Z_{\alpha_1}(w)}{\mu},$$

$$\text{where } r_3(w) = 1 + \frac{Z_{\alpha_2}(w)}{Z_{\alpha_1}(w)} \in \mathbb{R}.$$

Now as in the example of Seiberg-Witten theory we follow the attractor flow existence conditions from [57, 56, 58]. We again choose a continuation of the generating function across the wall of marginal stability that avoids a pole at a regular point. The 2 basis charges only have allowed poles at singular points so we must only change the continuation for the composite state (11.5.13) above. For example, a possible continuation one can choose is:

$$r_3(w) = 1 + \left| \frac{Z_{\alpha_2}(w)}{Z_{\alpha_1}(w)} \right| \in \mathbb{R}. \quad (11.5.14)$$

Example 11.5.3 (Exclusion of composite state). The function $r_3(w)Z_{\alpha_1}(w)/\mu \neq \alpha_1(u) + \alpha_2(u)$. It is no longer a positive root in the A_2 Lie algebra $r_3(w)\frac{Z_{\alpha_1}(w)}{\mu} \notin \Delta^+$. Therefore, it does not exist as a BPS state. To illustrate this further one can explicitly write the generating function (11.5.5) in terms of central charges on both sides of the wall.

$$\text{On one side : } \frac{e^{\lambda(u)}}{(1 - e^{-\frac{Z_{\alpha_1}(w)}{\mu}})(1 - e^{-\frac{Z_{\alpha_2}(w)}{\mu}})(1 - e^{-\frac{Z_{\alpha_1}(w)+Z_{\alpha_2}(w)}{\mu}})}. \quad (11.5.15)$$

$$\begin{aligned} \text{On the other : } & \frac{e^{\lambda(u)}}{(1 - e^{-\frac{Z_{\alpha_1}(w)}{\mu}})(1 - e^{-\frac{Z_{\alpha_2}(w)}{\mu}})(1 - e^{-r_3(w)\frac{Z_{\alpha_1}(w)}{\mu}})} = \\ & \frac{e^{\lambda(u)}}{(1 - e^{-\frac{Z_{\alpha_1}(w)}{\mu}})(1 - e^{-\frac{Z_{\alpha_2}(w)}{\mu}})} f\left(r_3(w)Z_{\alpha_1}(w)\right), \end{aligned}$$

where the function $f(r_3(w)Z_{\alpha_1}(w))$ representing the non-existing BPS state can be treated just as a normalisation factor. What is left for the 2 existing basis BPS states is then also a factor in the integral representation of the double gamma function given for example in Narukawa [202]. In this case, the existing 2 BPS states can also be tabulated in terms of framed wall crossing. We can now tabulate all the wall crossing for both the BPS walls W_{α_i}

Highest weight on one side of MS_{α_1, α_2}
$\lambda + \alpha_1 + \alpha_2$
$\lambda + \alpha_2$
λ

Table 11.6: Highest weights representing framed BPS states in all the chambers: this is on the side of the wall of marginal stability where only the 2 basis BPS states in A_2 exist.

and the walls of marginal stability MS_{α_1, α_2} together. This is plotted on Fig. 11.4 below.

We can now see from Fig. 11.4 that the wall crossing for the regular BPS states for the Argyres-Douglas A_2 BPS structure just has 2 regions - that is one region containing all 3

On side with 2	On side with 3
$\lambda + \alpha_1 + \alpha_2$	$\lambda + \alpha_1 + \alpha_2 + \alpha_3$
$\lambda + \alpha_2$	$\lambda + \alpha_1 + \alpha_3$
$\lambda + \alpha_2$	$\lambda + \alpha_1$
λ	

Table 11.7: This is a complete tabulation for framed BPS states in all chambers present on both sides of the wall of marginal stability for primitive wall crossing. See Fig. 11.4.

BPS states and their antiparticles $\pm\alpha_1, \pm\alpha_2, \pm\alpha_3$ and another region with just the 2 basis states $\pm\alpha_1, \pm\alpha_2$. In this case, the wall of marginal stability for the regular BPS states is again the usual locus in the moduli space at which the ratio of the central charges is real. We have also again recovered the scattering diagram for the A_2 quiver from [124, 58]. For this model, we have the following final count of the roots in the different chambers.

BPS states in chambers	
Chamber 1	$\pm\alpha_1, \pm\alpha_2, \pm(\alpha_1 + \alpha_2)$
Chamber 2	$\pm\alpha_1, \pm\alpha_2$

Table 11.8: Final existing BPS states in A_2 Argyres-Douglas on both sides of wall of marginal stability. That is on both sides of red line in Fig. 11.4.

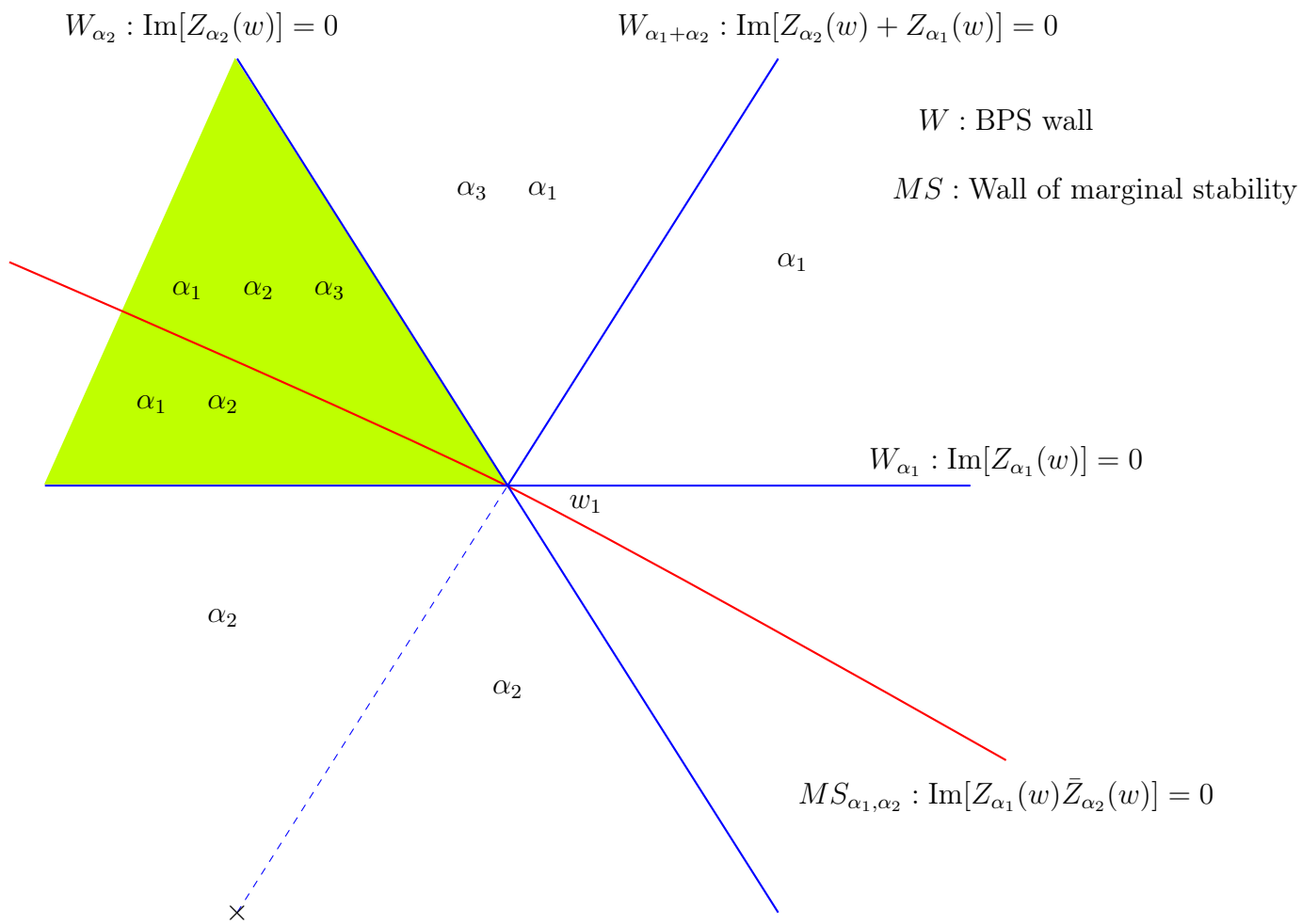


Figure 11.4: The BPS walls are shown by the lines in blue. The wall of marginal stability is shown by the line in red. The dashed blue line is the BPS wall excluded by the existence condition of vanishing central charge at a regular point.

12 | Uncoupled BPS structures and topological strings

A class of BPS structures discussed in this thesis, including those with root systems of A_1 (deformed conifold), and \hat{A}_1 (resolved conifold), are also known as uncoupled BPS structures. This means that BPS states with charges $\gamma_i, \gamma_j \in \Gamma$ and invariants $\Omega(\gamma_i), \Omega(\gamma_j) \neq 0$ have symplectic product $\langle \gamma_i, \gamma_j \rangle = 0$ [20, 203]. They have a description in terms of topological string theory and there should be a relation between the Lie algebraic generating functions discussed in chapter 11 and partition functions of the topological string. These partition functions should also encode the wall crossing phenomena that are seen in the different chambers. Uncoupled BPS structures include those with topological free energies of the form

$$F(\lambda, \{z_\gamma\}) = \frac{1}{24} \sum_{\gamma \in \Gamma} \Omega(\gamma) \log \left(\frac{2\pi i \lambda}{z_\gamma} \right) + \sum_{g \geq 2} \sum_{\gamma \in \Gamma} \frac{\Omega(\gamma) B_{2g}}{4g(2g-2)} \left(\frac{2\pi i \lambda}{z_\gamma} \right)^{2g-2}, \quad (12.0.1)$$

where in this case $\Omega(\gamma)$ are the BPS invariants, $z_\gamma = Z_\gamma$ are the central charges, and λ is the topological string coupling.

12.1 Deformed and resolved conifold

The simplest example of an uncoupled BPS structure is that associated to the A_1 root system. This just contains 1 BPS state with its antiparticle and there are no walls of marginal stability. As mentioned above, this BPS structure arises from the deformed conifold [204, 60]. This is also the simplest example that we looked at for the attractor flow in chapters 7-8. There we showed a single BPS state and its antiparticle existing by showing the flow lines flowing to the attractor point at the origin of the moduli space.

Specifically, in this case of the deformed conifold, the free energy for the B-model topological string [204] takes the form of

$$F(\lambda, a) = \lambda^{-2} \left(\frac{a^2}{2} \log a - \frac{3}{4} a^2 \right) - \frac{1}{12} \log a + \sum_{g=2}^{\infty} \frac{B_{2g}}{2g(2g-2)a^{2g-2}} \lambda^{2g-2}, \quad (12.1.1)$$

where $a = Z_\gamma \in \mathbb{C}$, and we can call the last term $\Phi(\lambda, a)$. We can proceed to take the Borel transform, defined in chapter 6, of this function. However, we first discuss a generating function and relate this to the Bernoulli numbers.

12.1.1 Deformed conifold generating function

One can expect the generating function for the A_1 BPS structure to take the form of, or at least contain the factor, (as the Weyl denominator for the A_1 Lie algebra)

$$\frac{e^x}{(1 - e^x)^2}. \quad (12.1.2)$$

Indeed, we will see in sec. 12.1.1 and sec. 12.2.3, that this term is present in the Borel transform and non-perturbative free energy, for the deformed conifold, respectively. This can also be used (12.1.11) to write the Borel transform of the resolved conifold. For this one must expand this function in terms of Bernoulli numbers. We can start by using the generating function of Bernoulli numbers and substituting it into the required expression.

Bernoulli numbers

The Bernoulli numbers are defined by the expansion of the function

$$\frac{x}{1 - e^x} = \sum_{n=0}^{\infty} B_n \frac{x^n}{n!}. \quad (12.1.3)$$

Connection with Bernoulli numbers

The generating function can be constructed from these Bernoulli numbers

$$\begin{aligned} \sum_{g=2}^{\infty} \frac{B_{2g}}{2g(2g-2)!} x^{2g-2} &= \sum_{g=2}^{\infty} \frac{(2g-1)B_{2g}}{(2g)!} x^{2g-2} = \frac{\partial}{\partial x} \left(\frac{1}{x} \sum_{g=2}^{\infty} \frac{B_{2g}}{(2g)!} x^{2g} \right) = \\ &= \frac{\partial}{\partial x} \left(\frac{1}{x} \left(\sum_{g=0}^{\infty} \frac{B_g}{g!} x^g - \left(1 - \frac{x}{2} + \frac{x^2}{12} \right) \right) \right), \end{aligned} \quad (12.1.4)$$

such that we can now use $\frac{x}{1-e^x} = \sum_{g=0}^{\infty} \frac{B_g}{g!} x^g$. Here we have $B_0 = 1$, $B_1 = -\frac{1}{2}$, $B_2 = \frac{1}{6}$. These terms are substituted in and subtracted from the original series

$$\begin{aligned} \frac{\partial}{\partial x} \left(\frac{1}{1 - e^x} - \frac{1}{x} + \frac{1}{2} - \frac{x}{12} \right) &= \\ &= -\frac{e^x}{(1 - e^x)^2} + \frac{1}{x^2} - \frac{1}{12}, \end{aligned} \quad (12.1.5)$$

rearranging this we obtain the relation

$$\frac{e^x}{(1 - e^x)^2} = \frac{1}{x^2} - \frac{1}{12} - \sum_{g=2}^{\infty} \frac{B_{2g}}{2g(2g-2)!} x^{2g-2}, \quad (12.1.6)$$

such that we have now expanded in terms of Bernoulli numbers. This relation is known e.g. in [20] and is useful both for writing down non-perturbative free energies and in determining Gopakumar-Vafa invariants.

Borel transform

The relation that was derived for the Bernoulli numbers can be used in the Borel transform. We remember defining this in section 6.2.1 in equations (6.2.1-6.2.4). Initially the Borel transform of $\Phi(\lambda, a)$, which reads as $G(\xi, a)$ in the new variable ξ , can be written as

$$G(\xi, a) = \sum_{g=2}^{\infty} \frac{B_{2g}}{2g(2g-2)!} \xi^{2g-3} \frac{1}{a^{2g-2}} = \frac{1}{\xi} \left(\frac{a^2}{\xi^2} - \frac{e^{\xi/a}}{(e^{\xi/a} - 1)^2} - \frac{1}{12} \right), \quad (12.1.7)$$

where the right hand side of the equation is derived by substituting in the relation from (12.1.6). This is indeed the Weyl denominator for the A_1 Lie algebra, which, as we know from chapter 10, can act as a counting function for BPS states.

12.1.2 Resolved conifold

The resolved conifold is another interesting example for the study of the non-perturbative topological string partition function, as was done extensively in [61]. In this case, the free energy expansion is known and one can act on it with a Borel transform along a chosen ray that does not pass through any singularities. One can choose to take the integral between 2 particular singular rays known as stokes rays. If one crosses a singular ray to move between 2 regions one obtains a contribution to the free energy from the singularity known as a stokes jump (remember section 6.2.2). For the resolved conifold it is possible to compute the stokes jumps. This is interesting as the normalised partition function generated by the stokes jumps reproduces the wall crossing for the D6-D2-D0 brane system in section 5.4 derived in Jafferis and Moore [37]. These stokes jumps also encode the jumps of the Weyl denominator for \hat{A}_1 .

Topological free energy for resolved conifold

The topological string free energy of the resolved conifold was derived in [24, 25] and is given by the genus expansion [61]¹

$$F(\lambda, t) = \sum_{g=0}^{\infty} \lambda^{2g-2} \tilde{F}(t) = \frac{1}{\lambda^2} \text{Li}_3(q) + \frac{B_2}{2} \text{Li}_1(q) + \Phi(\hat{\lambda}, t), \quad (12.1.8)$$

where $q = e^{2\pi it}$, $\hat{\lambda} = \lambda/2\pi$, $t, \hat{\lambda} \in \mathbb{C}^*$ and the last term can be written as

$$\Phi(\hat{\lambda}, t) = \sum_{g=2}^{\infty} \hat{\lambda}^{2g-2} \frac{B_{2g}}{2g(2g-2)} \sum_{k \in \mathbb{Z}} (k-t)^{2-2g}, \quad k \in \mathbb{Z}, \quad (12.1.9)$$

From this we can look at the Borel transform $G(\zeta, t) := \mathcal{B}(\Phi(-, t))(\zeta)$ [61] of this term where ζ is the new variable after the transformation

$$G(\zeta, t) = \sum_{g=2}^{\infty} \frac{1}{\zeta} \frac{B_{2g}}{2g(2g-2)!} \sum_{k \in \mathbb{Z}} \frac{(k-t)^{2-2g}}{\zeta^{2-2g}}. \quad (12.1.10)$$

Now we can consider the variables in the form $x_k = \frac{\zeta}{(k-t)}$ so that we can now substitute the relation derived above in (12.1.6) for each k . Then the expression finally becomes

$$G(\zeta, t) = \sum_{k \in \mathbb{Z}} \frac{1}{\zeta} \left(\left(\frac{k-t}{\zeta} \right)^2 - \frac{1}{12} + \frac{e^{\frac{\zeta}{k-t}}}{(1 - e^{\frac{\zeta}{k-t}})^2} \right). \quad (12.1.11)$$

One can see that this function (12.1.11) has poles at $\zeta = 2\pi im(t+k)$, $m \in \mathbb{Z}/\{0\}$ and use this to derive the Stokes jumps across these singular rays. The BPS partition function, as in the case for the $\mathcal{N} = 4$ generating function, can be found by taking the exponent of the free energy $Z_{BPS} = e^{\mathcal{F}}$. When the Stokes jumps are computed one obtains logarithmic factors that when put into this exponent reproduce the D6-D2-D0 partition function (5.4.13) in section 5.4. This means there is a correspondence between the boundaries of Weyl chambers of \hat{A}_1 and the Stokes rays. There is also a map between Donaldson-Thomas and Gromov-Witten invariants [28, 29] one can derive in this case with an appropriate change of variables in the partition function.

12.1.3 Gamma and G -functions

We can remember from chapter 7 that the deformed conifold is realised by the curve $y^2 = x^2 - 4a \in \mathbb{C}^2$, and corresponds to the Argyres-Douglas A_1 BPS structure. The generating

¹The polylogarithms are defined as $\text{Li}_s(q) = \sum_{n=1}^{\infty} \frac{q^n}{n^s}$, $s \in \mathbb{C}$.

function (from the non-perturbative topological free energy), which we just determined is the Weyl denominator of the A_1 Lie algebra, can also be written as a double gamma function.

Difference equation

Another way to determine the non-perturbative free energy is to find a solution to the difference equation [60, 205]. This equation can be written as

$$F(\lambda, a + \lambda) - 2F(\lambda, a) + F(\lambda, a - \lambda) = \frac{\partial^2}{\partial a^2} F^0(a), \quad (12.1.12)$$

where the 0-order term $F^0(a)$ is defined by

$$F^0(a) = \frac{1}{2}a^2 \log a - \frac{3}{4}a^2. \quad (12.1.13)$$

It has been checked [60] that the non-perturbative free energy below uniquely solves the difference equation

$$F_{\text{np}}(\lambda, a) := \log G\left(1 + \frac{a}{\lambda}\right) + \frac{a^2}{2\lambda^2} \log \lambda + \frac{a}{\lambda} \zeta'(0) + \frac{1}{12} \log(\lambda) + \zeta'(-1). \quad (12.1.14)$$

Hence, we see the appearance of the Barnes G -function $G\left(1 + \frac{a}{\lambda}\right)$ and ζ represents the ζ -function. Now we use a relation between the double gamma function and the G -function solution to the difference equation (12.1.12) to derive integral representation of this solution along the real axis, as well as a Wornowitz type integral form.

12.2 Multiple gamma functions

It is interesting to study multiple gamma functions because one can also write the Weyl denominators of A_2 and other Lie algebras, associated to BPS structures covered in this thesis, within this form. This allows one to conjecture a general relation between partition functions for BPS structures, Lie algebras and gamma functions. The general form of the multiple gamma function [202] is given by an integral representation

$$\Gamma_r(z, \omega) = \exp\left(\frac{1}{2\pi i} \int_{\tilde{L}} \frac{e^{-zt}(\log(-t) + \gamma)}{t \prod_{j=1}^r (1 - e^{-\omega_j t})} dt\right), \quad (12.2.1)$$

where we have $\omega = (\omega_1, \dots, \omega_i, \dots, \omega_r)$, $\omega_i, z \in \mathbb{C}$, and γ is defined as Euler's constant. The contour \tilde{L} is shown on Fig. 12.1 below.

However, in this section we will focus on the solution for the deformed conifold (the double gamma function). The function $r = 2$ can be chosen as this is expected to correspond to

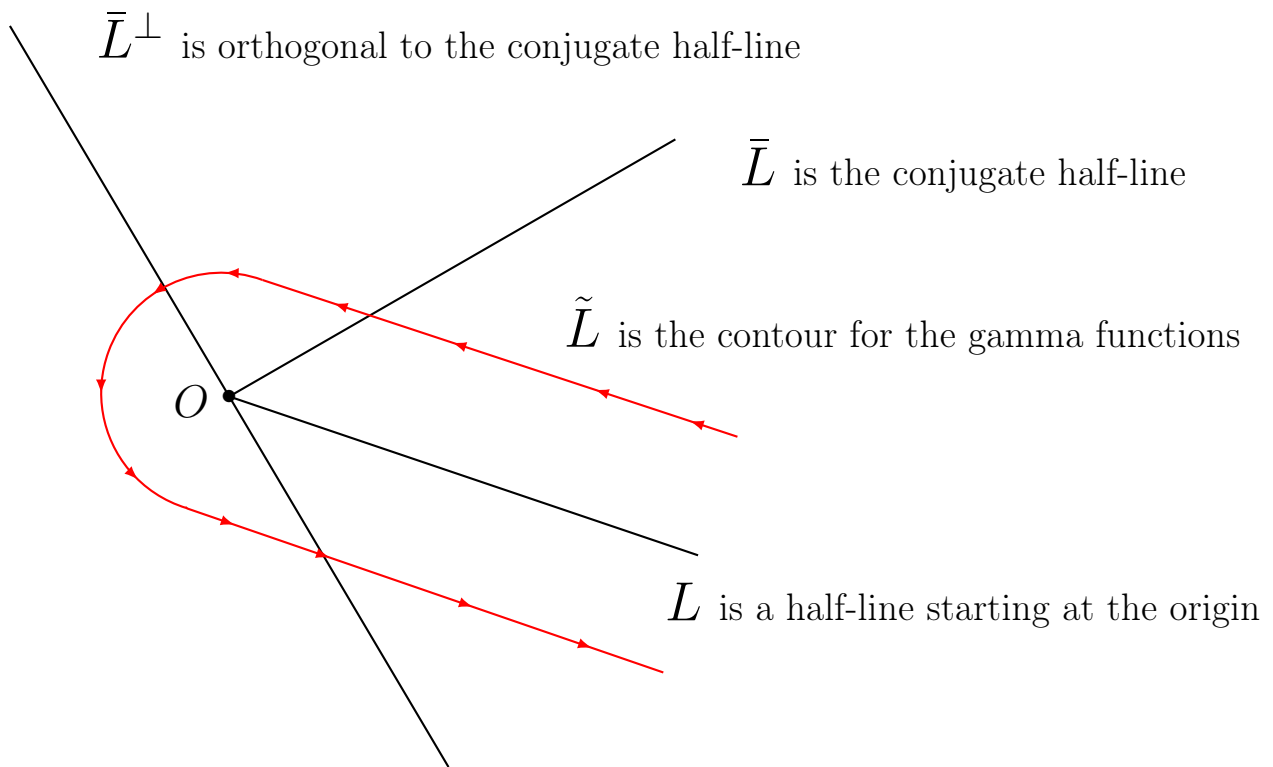


Figure 12.1: Contour prescription for multiple gamma function.

our deformed conifold for a particular choice of ω

$$\Gamma_2(z, \omega_1, \omega_2) = \exp\left(\frac{1}{2\pi i} \int_{\tilde{L}} \frac{e^{-zt}(\log(-t) + \gamma)}{t(1 - e^{-\omega_1 t})(1 - e^{-\omega_2 t})} dt\right). \quad (12.2.2)$$

We can now define the Barnes G -function [206] such that

$$G(z + 1) = (2\pi)^{\frac{z}{2}} e^{-\frac{z+z^2(1+\gamma)}{2}} \prod_{k=1}^{\infty} \left(1 + \frac{z}{k}\right)^k e^{\frac{z^2}{2k} - z}. \quad (12.2.3)$$

The double gamma function for $\omega_1 = \omega_2 = 1$ can be related to the Barnes G function as ²

$$G(z) = \frac{1}{\Gamma_2(z)}. \quad (12.2.4)$$

To connect the general form of the double gamma function (12.2.2) to the double gamma function in the generating function for the A_1 BPS structure one must define the function

²These are the original Barnes gamma functions that have a different normalisation than the Gamma functions in [202]. This is given by the Barnes modular constant k_2 .

as $\Gamma_2(z) = k_2\Gamma_2(z, 1, 1)$. This can be written in terms of the integral representation

$$\Gamma_2(z, 1, 1) = \exp\left(\frac{1}{2\pi i} \int_{\tilde{L}} \frac{e^{-zt}(\log(-t) + \gamma)}{t(1 - e^{-t})^2} dt\right). \quad (12.2.5)$$

12.2.1 Relation between integral representations

In the case of the resolved conifold it is possible to write the non-perturbative free energy in terms of an integral representation on the positive real axis \mathbb{R}_+ called the Woronowicz form. We derive a similar integral representation for the deformed conifold (12.1.14) using the fact that the solution for the free energy can be written as a double gamma (or G) function. Then we relate the double gamma function to an equivalent integral representation on the positive real axis.

Second integral representation

First, we remind ourselves that the G -function can be written in terms of gamma functions such that $G(z) = 1/\Gamma_2(z)$. Also, we know the relation $G(z + 1) = \Gamma_1(z)G(z)$ ³. Our aim here is to relate 2 different integral representations, the first one being the gamma function $\Gamma_2(z, \omega)$, and the second one corresponding to the integral

$$\int_0^\infty \frac{x \log(x^2 + z^2)}{e^{2\pi x} - 1}. \quad (12.2.6)$$

To derive this relation we follow the derivation given in [206] on the theory of the Barnes Function. Firstly, we must take logs of the expression relating the G -function to the gamma functions:

$$\begin{aligned} \log G(z + 1) &= \log(\Gamma_1(z)G(z)) = \log \Gamma_1(z) + \log G(z) = \\ &= \log \Gamma_1(z) - \log \Gamma_2(z), \\ \log \Gamma_2(z) &= \log \Gamma_1(z) - \log G(z + 1), \\ \frac{1}{2\pi i} \int_{\tilde{L}} \frac{e^{-zt}(\log(-t) + \gamma)}{t(1 - e^{-t})^2} dt &= \log \Gamma_1(z) - \log G(z + 1) + \text{const.} \end{aligned} \quad (12.2.7)$$

12.2.2 Relation between G and zeta function

A derivation for $\log G(z + 1)$ is described in [206]. This function can be expressed in terms of the other integral representation. For this we use a relationship with derivatives of the Hurwitz zeta function $\zeta(t, z)$. The derivative is given by $\zeta'(t, z) = \frac{d}{dt}\zeta(t, z)$ and a relation

³ $\Gamma_1(z) = \Gamma(z)$ is the well known Euler Gamma function.

between the G -function and these derivatives exists and is shown in [206]:

$$\log G(z+1) = z \log \Gamma_1(z) + \zeta'(-1, 0) - \zeta'(-1, z). \quad (12.2.8)$$

This can also be written as an integral representation along the positive real axis and is hereby a second integral representation of the double gamma function. This then becomes the Woronowicz form from (12.2.6). This is given in equation (20) of Adamchick [206].

G-function and Woronowicz form

In terms of the G function this is given by

$$\log G(z+1) = \frac{z^2}{2} \log(z) - \frac{3}{4} z^2 + z \frac{\log(2\pi)}{2} + \zeta'(-1, 0) + \int_0^\infty \frac{x \log(x^2 + z^2)}{e^{2\pi x} - 1} dx, \quad (12.2.9)$$

and in terms of the gamma function

$$\begin{aligned} \frac{1}{2\pi i} \int_{\tilde{L}} \frac{e^{-zt}(\log(-t) + \gamma)}{t(1 - e^{-t})^2} dt = \log \Gamma_1(z) - \frac{z^2}{2} \log(z) + \frac{3}{4} z^2 - z \frac{\log(2\pi)}{2} \\ - \zeta'(-1, 0) - \int_0^\infty \frac{x \log(x^2 + z^2)}{e^{2\pi x} - 1} dx + const, \end{aligned} \quad (12.2.10)$$

where the integral along the real axis is the integral representation we are looking for. This therefore becomes a candidate for the Woronowicz form of the non-perturbative free energy (12.1.14) of the deformed conifold. A derivation of this is presented in the appendix part C.

12.2.3 Removal of logarithm in gamma function

The integral form of the multiple gamma functions (12.2.1) contains a logarithm in the numerator when using the contour prescription from Fig. 12.1, taken around a half line. This half line starting at the origin as described in [202]. It would be interesting to see if a contour prescription exists such that the integral representation takes only the form of the Weyl denominator of the Lie algebra (A_1 for the deformed conifold) without any logarithmic terms. Furthermore, we should aim to find an integral form of the double gamma function along the full real axis (see Fig. 12.2) analogous to that for the non-perturbative free energy for the resolved conifold in [61]. So far, we have found the double gamma function as a solution to the deformed conifold difference equation (12.1.12) with a further Woronowicz integral representation (12.2.10) along the positive real axis \mathbb{R}_+ . However, we also look for an exact expression for the double gamma function as an integral along the full real axis \mathbb{R} of the A_1 Weyl denominator.

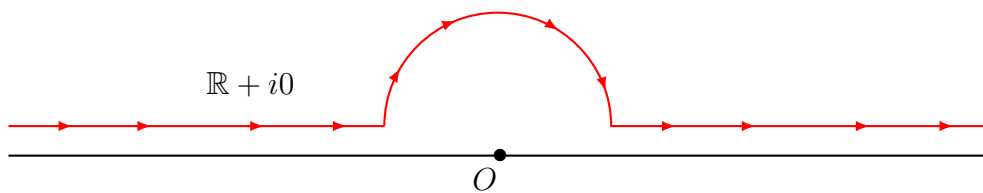


Figure 12.2: New contour for integral representation along real axis.

A difference equation for the multiple gamma functions

Here we will describe the derivation of an equation relating integral representations of gamma functions along the full real axis. There exists a generalisation of the sine function [207, 208] called the multiple sine function. For $\omega = (\omega_1, \dots, \omega_i, \dots, \omega_r)$ [202] this is defined as

$$S_r(z, \omega) = \exp\left((-1)^r \frac{\pi i}{r!} B_{rr}(z, \omega) + \int_{\mathbb{R}+i0} \frac{e^{zt}}{t \prod_{i=1}^r (1 - e^{\omega_i t})} dt\right), \quad (12.2.11)$$

where the $B_{rr}(z, \omega)$ are defined from the Bernoulli polynomials which can be written as an expansion

$$\frac{t^r e^{zt}}{\prod_{i=1}^r (1 - e^{\omega_i t})} = \sum_{n=0}^{\infty} B_{rn}(z, \omega) \frac{t^n}{n!}. \quad (12.2.12)$$

If one looks for the double sine function one must choose $r = 2$ to substitute into the expression. The multiple sine function for $r = 2$ can be written in terms of the double gamma function by substituting into the general relation between gamma and sine functions described in [202, 208, 20]:

$$S_2(z, \omega) = \Gamma_2(z, \omega)^{-1} \Gamma_2(\omega_1 + \omega_2 - z, \omega), \quad (12.2.13)$$

$$\log S_2(z, \omega) = -\log \Gamma_2(z, \omega) + \log \Gamma_2(\omega_1 + \omega_2 - z, \omega). \quad (12.2.14)$$

This can be rearranged to obtain

$$\log \Gamma_2(z, \omega) = -\left(\frac{\pi i}{2!} B_{22}(z, \omega) + \int_{\mathbb{R}+i0} \frac{e^{zt}}{t(1 - e^{\omega_1 t})(1 - e^{\omega_2 t})} dt\right) + \log \Gamma_2(\omega_1 + \omega_2 - z, \omega), \quad (12.2.15)$$

where we have finally replaced the logarithm in the double gamma function (12.2.5) with an integral along the real axis avoiding the origin. Its contour is shown on Fig. 12.2.

Example for deformed conifold

Now we look back to the expression (12.2.15) relating $\log \Gamma_2(z, \omega)$ and $\log \Gamma_2(\omega_1 + \omega_2 - z, \omega)$. We can relate these expressions explicitly by substituting the parameters used in the non-perturbative deformed conifold from (12.1.14), and remembering the inverse relation (12.2.4). For this we let $z = 1 + \frac{a}{\lambda}$ and $\omega_1 = \omega_2 = 1$. Also, we can use the expressions, from [202, 20], for $B_{rr}(z, \omega)$. We look for

$$B_{22}(z, \omega_1, \omega_2) = \frac{z^2}{\omega_1 \omega_2} - \frac{\omega_1 + \omega_2}{\omega_1 \omega_2} z + \frac{\omega_1^2 + \omega_2^2 + 3\omega_1 \omega_2}{6\omega_1 \omega_2}. \quad (12.2.16)$$

Now we can substitute everything into the expression:

$$\begin{aligned} \log \Gamma_2\left(1 + \frac{a}{\lambda}, 1, 1\right) &= -\frac{\pi i}{2} B_{22}\left(1 + \frac{a}{\lambda}, 1, 1\right) - \int_{\mathbb{R}+i0} \frac{e^{(1+\frac{a}{\lambda})t}}{t(1-e^t)^2} dt + \log \Gamma_2\left(1 - \frac{a}{\lambda}, 1, 1\right), \\ &\quad (12.2.17) \\ &\quad - \frac{\pi i}{2} \left(\left(1 + \frac{a}{\lambda}\right)^2 - 2\left(1 + \frac{a}{\lambda}\right) + \frac{5}{6} \right) - \int_{\mathbb{R}+i0} \frac{e^{(1+\frac{a}{\lambda})t}}{t(1-e^t)^2} dt + \log \Gamma_2\left(1 - \frac{a}{\lambda}, 1, 1\right), \end{aligned}$$

$$\log \Gamma_2\left(1 + \frac{a}{\lambda}, 1, 1\right) = - \int_{\mathbb{R}+i0} \frac{e^{(1+\frac{a}{\lambda})t}}{t(1-e^t)^2} dt - \frac{\pi i}{2} \left(\left(1 + \frac{a}{\lambda}\right)^2 - 2\left(1 + \frac{a}{\lambda}\right) + \frac{5}{6} \right) + \log \Gamma_2\left(1 - \frac{a}{\lambda}, 1, 1\right). \quad (12.2.18)$$

Here another difference equation for the double gamma function has been derived, in terms of an integral along the real axis. This can also be rewritten by expanding one of the $\log \Gamma_2\left(1 \pm \frac{a}{\lambda}, 1, 1\right)$, as done in appendix part C, in equation (C.1.2). Therefore, the other gamma function can now be expressed in terms of the integral which can then be interpreted as an integral representation contained within the non-perturbative free energy of the deformed conifold.

12.2.4 Concluding remarks

Here we have seen that the non-perturbative free energy for the deformed conifold contains the Weyl denominator of the A_1 root system so we can conjecture a relation between the wall crossing from Weyl denominators for A_n type root systems and the jumping depending on the ray one chooses for the integral in the Borel transform of the topological free energy. As for the resolved conifold in [61], the spectrum and partition function of framed BPS states originally described by Jafferis and Moore [37] is obtained in this way, hence giving a different partition function in the different chambers. This jumping matches that obtained from the \hat{A}_1 part of the dyon counting in sec. 10.1, on one side of the affine wall.

There should therefore be a general relation for the wall crossing of BPS structures between the generating functions of Cheng and Verlinde [52, 53], describing the splitting of

multi-centered black holes, the Stokes jumps in this section, and wall crossing for the related Harvey-Moore [43, 44] BPS algebras. In the deformed and resolved conifolds one can also notice a pattern of the Borel transformed free energy containing a sum over A_1 Weyl denominator identities for the BPS states in the spectrum which is suggestive for further generalisation. Another direction this research could take is to further match the wall crossing for the framed BPS states of GMN [17, 18] at BPS walls to the Stokes jumps associated to other ADE type BPS structures.

13 | Summary

We can now summarise all the results developed in this thesis. BPS states and their construction in string theory have been introduced. In sections 3.1.2, 4.3, and 5.4 the BPS structures associated with the \hat{A}_1 Lie algebra, including Seiberg-Witten theory and the D6-D2-D0 bound states of type IIA string theory on the resolved conifold, were reviewed, as well as those associated with Argyres-Douglas theories. The current known formulations of the wall crossing phenomena that have been used to determine the number of BPS states in every region of the moduli space and the location of the wall(s) of marginal stability, in these theories, have been reviewed in this thesis.

This includes quantum dilogarithm identities in section 3.1.2 describing matching products of operators on either side of the wall of marginal stability as well as quiver methods in chapter 4 that allow the determination of the BPS spectra on either side of the wall, including the decay of quiver representations 4.2 into subrepresentations as well as the mutation method in 4.2.2. The wall crossing formulae that encode the changes in the BPS indices are reviewed in chapter 5. They are used to explain the wall crossing for framed BPS states [17, 18] of GMN which represent bound states to a large core and have wall crossing across Weyl chamber boundaries known as BPS walls. The discussions have focused on the examples of ADE type Argyres-Douglas theories introduced in section 2.1.2 with particular focus on the examples of A_1 and A_2 . This is because these are the simplest cases and can be used as testing cases to study BPS structures.

In our project “Special geometry, quasi-modularity and attractor flow for BPS structures” [62] described in chapters 7 and 8 we used the attractor flow methods developed in the literature for example in [55, 36, 56] to determine the existence of BPS states based on the conditions of the endpoints of the flow. We applied these methods to Argyres-Douglas theories of type A_1 , A_2 and Seiberg-Witten theory and we found that this indeed reproduces the spectrum of BPS states in these theories if one uses the split attractor flow on the wall and the branch cuts to determine where which BPS states exist. We find the jump from 2 to 3 BPS states in the A_2 model and from 2 basis states to the full infinite \hat{A}_1 spectrum in Seiberg-Witten theory.

In sections 9.2 and 9.3 the black hole literature [40] for the derivation of the generating function of $\frac{1}{4}$ BPS dyons is reviewed and related to the Weyl denominator of the Borcherds-Kac-Moody algebra. The wall crossing for the dyons is reviewed in chapter 10: the connections

of this wall crossing to the Weyl denominator is explained in the work of Cheng and Verlinde [53], via both the highest weights of the Verma modules and the jumps in the coefficients of the Fourier series, which in the $\mathcal{N} = 4$ examples represent degeneracies of black holes with a particular electric and magnetic charge invariants.

In chapters 10-11, in the project “Generating functions for $\mathcal{N} = 2$ BPS structures”, we used this prescription for wall crossing in $\mathcal{N} = 4$ to construct an analog counting, or generating function, that describes $\mathcal{N} = 2$ wall crossing, for example for the BPS structures that arise from Seiberg-Witten and Argyres-Douglas theories.

At first, in chapter 10, we extracted the Weyl denominators for the A_1 and \hat{A}_1 Lie algebras from that of the Borcherds-Kac-Moody Lie algebra, and in chapter 11 (using the existence conditions from 7.1.1), we found that the wall crossing encoded in these subalgebras matches that in $\mathcal{N} = 2$ systems. For example, in section 11.3, we used the fact that the D6-D2-D0 brane system discussed by Jafferis and Moore [37] also has a chamber structure for the framed BPS states corresponding to the root system of \hat{A}_1 . This means that the Weyl denominator for \hat{A}_1 describes this wall crossing. We then proceeded to look for an analog counting function for other $\mathcal{N} = 2$ BPS structures in Argyres-Douglas 11.5 and Seiberg-Witten theory 11.4. Following the same principle as we did for the first \hat{A}_1 example we investigated the Weyl denominator, and the full Weyl character, and found that again the highest weight (and also any Fourier series expansion) jumps depending on which chamber one is in. The proposed Weyl denominator formula is more general and we therefore expect it to encode the wall crossing for further ADE type Argyres-Douglas theories. If one considers the framed halo BPS states in Gaiotto Moore Neitzke [17] one can match the wall crossing with the chambers for these states if one writes the moduli in terms of the central charges and a suitable phase. The walls of the framed halo BPS states then intersect on the wall of marginal stability of the “vanilla” BPS states (of the original unframed theory), for which the counts can then be reproduced. For example, the jump between the 2 basis states and the full \hat{A}_1 root system for Seiberg-Witten theory. We hereby also recovered the scattering diagram for these examples, introduced by Bridgeland in [124].

Finally, in chapter 12, relations to topological string partition functions were reviewed. A result by [61] was studied. This reproduced the framed BPS indices and the wall crossing for the D6-D2-D0 system, using jumps at Stokes rays, in a Borel transform of the free energy. We also determined that the Borel transformed free energy for the deformed conifold contains the A_1 Weyl denominator. From this one can conjecture that the wall crossing of more general framed BPS states, in BPS structures of A_n type, can also be derived from jumping at Stokes rays in topological string free energies.

Conclusions

The conclusion of this thesis is that the construction of the generating function, that counts BPS bound states within a highest weight, generalises from $\mathcal{N} = 4$ dyons to analogs in 4d

$\mathcal{N} = 2$ QFTs. This result is important as it suggests a general formulation for the wall crossing in BPS structures with multiple bound states that have their existence conditions given by Weyl chamber boundaries associated to a particular root system. It suggests that for such a BPS structure there exists both a BPS algebra of the Harvey-Moore type [43, 44], a generalised generating function of the form used in [40, 52, 53, 54], and a BPS count given by highest weight modules in a particular chamber. The pattern of Weyl chambers matches the Bridgeland scattering diagram [124] when one considers the additional wall of marginal stability.

In some examples, the Stokes jumps of the Borel transformed free energy also match this wall crossing, giving a partition function. All of this together indicates that for such a generalised BPS structure there exist 2 generating functions encoding the same wall crossing with a relation to be determined. Dyon counting functions representing microstates have been derived for $\mathcal{N} = 4$ black holes, for example [39] and [40, 49, 48, 190, 52, 53, 54], but are not known in general for $\mathcal{N} = 2$ black holes. The analog generating functions constructed in this thesis, as well as the work on attractor flow existence conditions, helps further our understanding of $\mathcal{N} = 2$ examples in the special cases of A_1, \hat{A}_1 and A_2 Lie algebras. However, with more research it is hoped that these results can in future be generalised to more involved examples. Suitable cases could include further ADE type BPS structures or D4-D2-D0 bound states. Another possible direction is to relate these wall crossing phenomena to walls existing in topological string partition functions via the OSV conjecture developed for $\mathcal{N} = 2$ in [146, 36]. The $\mathcal{N} = 4$ dyon counting function used in this thesis from [40] has been related to a topological partition function in this way in [189]. Further work on this would involve factorising generating functions for new black holes to the absolute value squared of a topological string partition function on the particular target space used for the construction.

Therefore, by constructing a new generating function, this thesis has deepened our understanding of wall crossing in a class of BPS structures and developed a new way of encoding the stability conditions of the BPS bound states in various examples of supersymmetric QFTs, string theory and supergravity. This generating function has also provided a new way of counting the BPS states in the different chambers existing within the moduli spaces of the theories.

A | BPS states and central charges

Here the series expansions are given for the central charges used in the attractor flow in chapters 7 and 8. The expansions are carried out around the singular points.

A.1 Expansion of central charges around singular points

The monodromies M_{u_s} can be read off from these expansions at $+1$ and -1 by collecting the logarithmic terms. For each singular point $u_s \in \mathcal{B}$ we let $u \rightarrow +1 + v$ or $u \rightarrow -1 + v$ respectively before expanding in MATHEMATICA. We separate out the terms that are a prefactor of $\log(v)$.

A.1.1 Argyres-Douglas A_2 realised on $\Sigma_{A_2}^I$

(i) Expansions around $+1$:

$$Z_{\gamma_1}(u) = -v + \frac{5v^2}{144} - \frac{385v^3}{62208} + \frac{85085v^4}{53747712} - \frac{7436429v^5}{15479341056} + \frac{1078282205v^6}{6687075336192} - \frac{167133741775v^7}{2888816545234944} + O(v^8) \quad (\text{A.1.1})$$

$$Z_{\gamma_2}(u) = \frac{167133741775v^7}{5777633090469888} - \frac{1926300758747iv^7}{11555266180939776\pi} + \frac{835668708875iv^7 \log(2)}{5777633090469888\pi} \quad (\text{A.1.2})$$

$$+ \frac{167133741775iv^7 \log(3)}{1925877696823296\pi} - \frac{1078282205v^6}{13374150672384} + \frac{92311189073iv^6}{200612260085760\pi} - \frac{1078282205iv^6 \log(3)}{4458050224128\pi} - \frac{5391411025iv^6 \log(2)}{13374150672384\pi} + \frac{7436429v^5}{30958682112} - \frac{251071813iv^5}{185752092672\pi}$$

$$\begin{aligned}
& + \frac{37182145iv^5 \log(2)}{30958682112\pi} + \frac{7436429iv^5 \log(3)}{10319560704\pi} - \frac{85085v^4}{107495424} + \frac{5616029iv^4}{1289945088\pi} \\
& - \frac{85085iv^4 \log(3)}{35831808\pi} - \frac{425425iv^4 \log(2)}{107495424\pi} + \frac{385v^3}{124416} - \frac{3043iv^3}{186624\pi} + \frac{1925iv^3 \log(2)}{124416\pi} \\
& + \frac{385iv^3 \log(3)}{41472\pi} - \frac{5v^2}{288} + \frac{47iv^2}{576\pi} - \frac{5iv^2 \log(3)}{96\pi} - \frac{25iv^2 \log(2)}{288\pi} + \frac{v \left(i \log \left(\frac{864}{v} \right) + i + \pi \right)}{2\pi} \\
& + \frac{36i}{5\pi} + O(v^8) \\
& \left(- \frac{167133741775iv^7}{5777633090469888\pi} + \frac{1078282205iv^6}{13374150672384\pi} - \frac{7436429iv^5}{30958682112\pi} \right. \\
& \left. + \frac{85085iv^4}{107495424\pi} - \frac{385iv^3}{124416\pi} + \frac{5iv^2}{288\pi} \right) \log(v)
\end{aligned}$$

(ii) Expansions around -1 :

$$\begin{aligned}
Z_{\gamma_1}(u) &= \frac{1926300758747v^7}{11555266180939776\pi} - \frac{167133741775v^7 \log(3)}{1925877696823296\pi} - \frac{835668708875v^7 \log(2)}{5777633090469888\pi} \\
& \tag{A.1.3} \\
& + \frac{92311189073v^6}{200612260085760\pi} - \frac{1078282205v^6 \log(3)}{4458050224128\pi} - \frac{5391411025v^6 \log(2)}{13374150672384\pi} + \frac{251071813v^5}{185752092672\pi} \\
& - \frac{7436429v^5 \log(3)}{10319560704\pi} - \frac{37182145v^5 \log(2)}{30958682112\pi} + \frac{5616029v^4}{1289945088\pi} - \frac{85085v^4 \log(3)}{35831808\pi} \\
& - \frac{425425v^4 \log(2)}{107495424\pi} + \frac{3043v^3}{186624\pi} - \frac{385v^3 \log(3)}{41472\pi} - \frac{1925v^3 \log(2)}{124416\pi} + \frac{47v^2}{576\pi} - \frac{5v^2 \log(3)}{96\pi} \\
& - \frac{25v^2 \log(2)}{288\pi} + O(v^8) + \left(\frac{167133741775v^7}{5777633090469888\pi} + \frac{1078282205v^6}{13374150672384\pi} + \frac{7436429v^5}{30958682112\pi} + \right. \\
& \left. \frac{85085v^4}{107495424\pi} + \frac{385v^3}{124416\pi} + \frac{5v^2}{288\pi} \right) \log(v) + \frac{v \left(\log \left(\frac{v}{864} \right) - 1 \right)}{2\pi} + \frac{36}{5\pi}
\end{aligned}$$

$$Z_{\gamma_2}(u) = iv + \frac{5iv^2}{144} + \frac{385iv^3}{62208} + \frac{85085iv^4}{53747712} + \frac{7436429iv^5}{15479341056} + \frac{1078282205iv^6}{6687075336192} \quad (\text{A.1.4})$$

$$+ \frac{167133741775iv^7}{2888816545234944} + O(v^8)$$

A.1.2 Argyres-Douglas A_2 realised on $\Sigma_{A_2}^{II}$

(i) Expansions around +1:

$$Z_{\gamma_1}(u) = \frac{7i\pi v^5}{16384\sqrt{2}} + \frac{799v^5}{983040\sqrt{2}} - \frac{35v^5 \log(2)}{16384\sqrt{2}} - \frac{5i\pi v^4}{2048\sqrt{2}} - \frac{89v^4}{24576\sqrt{2}} + \frac{25v^4 \log(2)}{2048\sqrt{2}} + \quad (\text{A.1.5})$$

$$\frac{i\pi v^3}{32\sqrt{2}} - \frac{v^3}{192\sqrt{2}} - \frac{5v^3 \log(2)}{32\sqrt{2}} + \frac{i\pi v^2}{4\sqrt{2}} + \frac{5v^2}{8\sqrt{2}} - \frac{5v^2 \log(2)}{4\sqrt{2}} +$$

$$\left(\frac{7v^5}{16384\sqrt{2}} - \frac{5v^4}{2048\sqrt{2}} + \frac{v^3}{32\sqrt{2}} + \frac{v^2}{4\sqrt{2}} \right) \log(v) + \frac{2\sqrt{2}v}{3} + \frac{16\sqrt{2}}{15} + O(v^6)$$

$$Z_{\gamma_2}(u) = -\frac{i\pi v^2}{4\sqrt{2}} - \frac{i\pi v^3}{32\sqrt{2}} + \frac{5i\pi v^4}{2048\sqrt{2}} - \frac{7i\pi v^5}{16384\sqrt{2}} + O(v^6) \quad (\text{A.1.6})$$

(ii) Expansions around -1:

$$Z_{\gamma_1}(u) = \frac{\pi v^2}{4\sqrt{2}} - \frac{\pi v^3}{32\sqrt{2}} - \frac{5\pi v^4}{2048\sqrt{2}} - \frac{7\pi v^5}{16384\sqrt{2}} - \frac{105\pi v^6}{1048576\sqrt{2}} - \frac{231\pi v^7}{8388608\sqrt{2}} + O(v^8) \quad (\text{A.1.7})$$

$$Z_{\gamma_2}(u) = \frac{799iv^5}{983040\sqrt{2}} - \frac{21iv^5 \log(2)}{16384\sqrt{2}} - \frac{7iv^5 \log\left(\frac{4}{v}\right)}{16384\sqrt{2}} + \frac{89iv^4}{24576\sqrt{2}} - \frac{25iv^4 \log(2)}{2048\sqrt{2}} - \frac{iv^3}{192\sqrt{2}} \quad (\text{A.1.8})$$

$$- \frac{5iv^3 \log(2)}{32\sqrt{2}} - \frac{5iv^2}{8\sqrt{2}} + \frac{iv^2 \log(1024)}{8\sqrt{2}} + \left(\frac{5iv^4}{2048\sqrt{2}} + \frac{iv^3}{32\sqrt{2}} - \frac{iv^2}{4\sqrt{2}} \right) \log(v) + \frac{2}{3}i\sqrt{2}v$$

$$- \frac{16i\sqrt{2}}{15} + O(v^6)$$

A.1.3 Seiberg-Witten SU(2) theory

(i) Expansions around +1:

$$\begin{aligned}
Z_{\gamma_1}(u) = & \frac{7623i\pi v^7}{134217728\sqrt{2}} + \frac{188287v^7}{1342177280\sqrt{2}} - \frac{38115v^7 \log(2)}{134217728\sqrt{2}} - \frac{1323i\pi v^6}{8388608\sqrt{2}} \quad (\text{A.1.9}) \\
& - \frac{15981v^6}{41943040\sqrt{2}} + \frac{6615v^6 \log(2)}{8388608\sqrt{2}} + \frac{245i\pi v^5}{524288\sqrt{2}} + \frac{3437v^5}{3145728\sqrt{2}} - \frac{1225v^5 \log(2)}{524288\sqrt{2}} \\
& - \frac{25i\pi v^4}{16384\sqrt{2}} - \frac{665v^4}{196608\sqrt{2}} + \frac{125v^4 \log(2)}{16384\sqrt{2}} + \frac{3v^3}{256\sqrt{2}} + \frac{3i\pi v^3}{512\sqrt{2}} \\
& + \frac{3v^3 \log\left(\frac{v}{32}\right)}{512\sqrt{2}} - \frac{i\pi v^2}{32\sqrt{2}} - \frac{3v^2}{64\sqrt{2}} + \frac{v^2 \log(1024)}{64\sqrt{2}} \\
& + \left(\frac{7623v^7}{134217728\sqrt{2}} - \frac{1323v^6}{8388608\sqrt{2}} + \frac{245v^5}{524288\sqrt{2}} - \frac{25v^4}{16384\sqrt{2}} - \frac{v^2}{32\sqrt{2}} \right) \log(v) \\
& + \frac{i\pi v}{2\sqrt{2}} - \frac{v}{2\sqrt{2}} + \frac{v \log\left(\frac{v}{32}\right)}{2\sqrt{2}} - 2\sqrt{2} + O(v^8)
\end{aligned}$$

$$\begin{aligned}
Z_{\gamma_2}(u) = & -\frac{i\pi v}{2\sqrt{2}} + \frac{i\pi v^2}{32\sqrt{2}} - \frac{3i\pi v^3}{512\sqrt{2}} + \frac{25i\pi v^4}{16384\sqrt{2}} - \frac{245i\pi v^5}{524288\sqrt{2}} + \frac{1323i\pi v^6}{8388608\sqrt{2}} + O(v^7) \quad (\text{A.1.10})
\end{aligned}$$

(ii) Expansions around -1:

$$\begin{aligned}
Z_{\gamma_1}(u) = & -\frac{\pi v}{2\sqrt{2}} - \frac{\pi v^2}{32\sqrt{2}} - \frac{3\pi v^3}{512\sqrt{2}} - \frac{25\pi v^4}{16384\sqrt{2}} - \frac{245\pi v^5}{524288\sqrt{2}} \quad (\text{A.1.11}) \\
& - \frac{1323\pi v^6}{8388608\sqrt{2}} - \frac{7623\pi v^7}{134217728\sqrt{2}} + O(v^8)
\end{aligned}$$

$$\begin{aligned}
Z_{\gamma_2}(u) = & \frac{15981iv^6}{41943040\sqrt{2}} - \frac{1323iv^6 \log(8)}{4194304\sqrt{2}} + \frac{1323iv^6 \log(2v)}{8388608\sqrt{2}} + \frac{3437iv^5}{3145728\sqrt{2}} - \frac{245iv^5 \log(8)}{262144\sqrt{2}} \quad (\text{A.1.12})
\end{aligned}$$

$$\begin{aligned} & + \frac{245iv^5 \log(2v)}{524288\sqrt{2}} + \frac{665iv^4}{196608\sqrt{2}} - \frac{25iv^4 \log(8)}{8192\sqrt{2}} + \frac{25iv^4 \log(2v)}{16384\sqrt{2}} + \frac{3iv^3}{256\sqrt{2}} + \frac{3iv^3 \log\left(\frac{v}{32}\right)}{512\sqrt{2}} \\ & + \frac{3iv^2}{64\sqrt{2}} - \frac{iv^2 \log(8)}{16\sqrt{2}} + \frac{iv^2 \log(v)}{32\sqrt{2}} + \frac{iv^2 \log(4)}{64\sqrt{2}} - \frac{iv}{2\sqrt{2}} + \frac{iv \log\left(\frac{v}{32}\right)}{2\sqrt{2}} + 2i\sqrt{2} + O(v^7) \end{aligned}$$

B | \hat{A}_1 changes in representation

The generating function extracted for the \hat{A}_1 root system in chapter 10 and generalised to $\mathcal{N} = 2$ analogs in chapter 11 encodes highest weight Verma modules.

B.1 Original generating function

Here we look at the changes in the modules in all the chambers of the \hat{A}_1 Lie algebra. First, we look at the change in the generating function itself including the square factor on the whole function and the prefactors from the Weyl vector of the original Borcherds-Kac-Moody algebra. We start just in front of the affine wall as the generating functions before have already been discussed in sec. 10.4 for the $\mathcal{N} = 4$ case.

At first, in the chamber just in front of the affine root the generating function takes the form

$$f(k, l) = \oint_{\gamma} d\alpha_0(u) d\delta(u) e^{\lambda_{k,i}(u)} \frac{e^{\alpha_0(u)+\delta(u)}}{\prod_{l=1}^{\infty} (1 - e^{-l\delta(u)})^2 (1 - e^{-l\delta(u)-\alpha_0(u)})^2} \frac{\prod_{m=1}^{\infty} e^{2(m-1)\delta(u)-2\alpha_0(u)}}{\prod_{m=1}^{\infty} (1 - e^{(m-1)\delta(u)-\alpha_0(u)})^2}. \quad (\text{B.1.1})$$

Now if we are allowed to cross the affine root, the generating function in the chamber just on the other side of the affine root becomes

$$f(k, l) = \oint_{\gamma} d\alpha_0(u) d\delta(u) e^{\lambda_{k,i}(u)} \frac{e^{\alpha_0(u)+\delta(u)}}{\prod_{l=1}^{\infty} (1 - e^{-l\delta(u)-\alpha_0(u)})^2} \frac{\prod_{l=1}^{\infty} e^{2l\delta(u)}}{\prod_{l=1}^{\infty} (1 - e^{l\delta(u)})^2} \frac{\prod_{m=1}^{\infty} e^{2(m-1)\delta(u)-2\alpha_0(u)}}{\prod_{m=1}^{\infty} (1 - e^{(m-1)\delta(u)-\alpha_0(u)})^2}. \quad (\text{B.1.2})$$

Now we can continue to cross the walls

$$f(k, l) = \oint_{\gamma} d\alpha_0(u) d\delta(u) e^{\lambda_{k,i}(u)} \frac{e^{\alpha_0(u)+\delta(u)} \prod_{l=1}^k e^{2l\delta(u)+2\alpha_0(u)}}{\prod_{l=k+1}^{\infty} (1 - e^{-l\delta(u)-\alpha_0(u)})^2 \prod_{l=1}^k (1 - e^{l\delta(u)+\alpha_0(u)})^2} \quad (\text{B.1.3})$$

$$\frac{\prod_{l=1}^{\infty} e^{2l\delta(u)}}{\prod_{l=1}^{\infty} (1 - e^{l\delta(u)})^2} \frac{\prod_{m=1}^{\infty} e^{2(m-1)\delta(u)-2\alpha_0(u)}}{\prod_{m=1}^{\infty} (1 - e^{(m-1)\delta(u)-\alpha_0(u)})^2},$$

until we are in the chamber where all the states exist

$$f(k, l) = \oint_{\gamma} d\alpha_0(u) d\delta(u) e^{\lambda_{k,l}(u)} \tag{B.1.4}$$

$$\frac{e^{\alpha_0(u)+\delta(u)} \prod_{l=1}^{\infty} e^{2l\delta(u)+2\alpha_0(u)}}{\prod_{l=1}^{\infty} (1 - e^{l\delta(u)+\alpha_0(u)})^2} \frac{\prod_{l=1}^{\infty} e^{2l\delta(u)}}{\prod_{l=1}^{\infty} (1 - e^{l\delta(u)})^2} \frac{\prod_{m=1}^{\infty} e^{2(m-1)\delta(u)-2\alpha_0(u)}}{\prod_{m=1}^{\infty} (1 - e^{(m-1)\delta(u)-\alpha_0(u)})^2}.$$

Finally one can reabsorb the factors in the numerator into a new representation such that one can take $\tilde{\lambda}_{k,l} = \lambda_{k,l} + \sum_{k,l,m=1}^{\infty} [(2l\delta + 2\alpha_0) + (2l\delta) + (2(m-1)\delta - 2\alpha_0)]$ so that one can define a new function at infinity where all roots exist as

$$f(k, l) = \oint_{\gamma} d\alpha_0(u) d\delta(u) e^{\tilde{\lambda}_{k,l}(u)} \frac{1}{\prod_{l=1}^{\infty} (1 - e^{l\delta(u)+\alpha_0(u)})^2} \frac{1}{\prod_{l=1}^{\infty} (1 - e^{l\delta(u)})^2} \frac{1}{\prod_{m=1}^{\infty} (1 - e^{(m-1)\delta(u)-\alpha_0(u)})^2}. \tag{B.1.5}$$

Now from this one can extend the diagram with Weyl chambers into the other half plane. This is what is shown in Fig. 11.1. for the $\mathcal{N} = 2$ analogs.

B.1.1 Changes in highest weight

Now we write the generating function back in terms of a highest weight. This highest weight then shifts in all the different chambers in the moduli space. The original generating function is

$$f(k, l) = \oint_{\gamma} d\alpha_0(u) d\delta(u) e^{\lambda_{k,l}(u)} \frac{e^{\alpha_0(u)+\delta(u)}}{\prod_{m=1}^{\infty} (1 - e^{-m\delta(u)})^2 (1 - e^{-(m-1)\delta(u)+\alpha_0(u)})^2 (1 - e^{-m\delta(u)-\alpha_0(u)})^2}, \tag{B.1.6}$$

which we write as

$$f(k, l) = \oint_{\gamma} d\alpha_0(u) d\delta(u) \left(\frac{e^{\lambda(u)}}{\prod_{m=1}^{\infty} (1 - e^{-m\delta(u)}) (1 - e^{-(m-1)\delta(u)+\alpha_0(u)}) (1 - e^{-m\delta(u)-\alpha_0(u)})} \right)^2. \tag{B.1.7}$$

In terms of the highest weight λ . Now we see how the generating function changes as we

cross k walls in one direction

$$f(k, l) = \oint_{\gamma} d\alpha_0(u) d\delta(u) \left(\frac{e^{\lambda(u)}}{\prod_{l=1}^{\infty} (1 - e^{-l\delta(u)}) (1 - e^{-l\delta(u) - \alpha_0(u)}) \prod_{m=k+1}^{\infty} (1 - e^{-(m-1)\delta(u) + \alpha_0(u)})} \right. \\ \left. \frac{\prod_{m=1}^k e^{(m-1)\delta(u) - \alpha_0(u)}}{\prod_{m=1}^k (1 - e^{(m-1)\delta(u) - \alpha_0(u)})} \right)^2. \quad (\text{B.1.8})$$

We can keep moving in this direction such that we let $k \rightarrow \infty$. In this case, the generating function becomes

$$f(k, l) = \oint_{\gamma} d\alpha_0(u) d\delta(u) \left(\frac{e^{\lambda(u)}}{\prod_{l=1}^{\infty} (1 - e^{-l\delta(u)}) (1 - e^{-l\delta(u) - \alpha_0(u)})} \frac{\prod_{m=1}^{\infty} e^{(m-1)\delta(u) - \alpha_0(u)}}{\prod_{m=1}^{\infty} (1 - e^{(m-1)\delta(u) - \alpha_0(u)})} \right)^2. \quad (\text{B.1.9})$$

The new highest weight becomes: $\lambda' = \lambda + \sum_{m=1}^{\infty} ((m-1)\delta - \alpha_0)$ If one proceeds to cross the affine wall then you get an infinite number of affine roots added to the highest weight

$$f(k, l) = \oint_{\gamma} d\alpha_0(u) d\delta(u) \left(\frac{e^{\lambda(u)}}{\prod_{l=1}^{\infty} (1 - e^{-l\delta(u) - \alpha_0(u)})} \frac{\prod_{l=1}^{\infty} e^{l\delta(u)}}{\prod_{l=1}^{\infty} (1 - e^{l\delta(u)})} \frac{\prod_{m=1}^{\infty} e^{(m-1)\delta(u) - \alpha_0(u)}}{\prod_{m=1}^{\infty} (1 - e^{(m-1)\delta(u) - \alpha_0(u)})} \right)^2. \quad (\text{B.1.10})$$

$$\lambda' = \lambda + \sum_{m=1}^{\infty} ((m-1)\delta - \alpha_0) + \sum_{l=1}^{\infty} l\delta$$

One can continue to cross walls in this direction with the integer p decreasing

$$f(k, l) = \oint_{\gamma} d\alpha_0(u) d\delta(u) \left(\frac{e^{\lambda(u)} \prod_{n=k+1}^{\infty} e^{n\delta(u) + \alpha_0(u)}}{\prod_{n=p+1}^{\infty} (1 - e^{l\delta(u) + \alpha_0(u)}) \prod_{n=1}^k (1 - e^{-n\delta(u) - \alpha_0(u)})} \frac{\prod_{l=1}^{\infty} e^{l\delta(u)}}{\prod_{l=1}^{\infty} (1 - e^{l\delta(u)})} \frac{\prod_{m=1}^{\infty} e^{(m-1)\delta(u) - \alpha_0(u)}}{\prod_{m=1}^{\infty} (1 - e^{(m-1)\delta(u) - \alpha_0(u)})} \right)^2. \quad (\text{B.1.11})$$

Now the final highest weight becomes

$$\lambda' = \lambda + \sum_{m=1}^{\infty} ((m-1)\delta - \alpha_0) + \sum_{l=1}^{\infty} l\delta + \sum_{n=p+1}^{\infty} (n\delta + \alpha_0), \quad (\text{B.1.12})$$

in the chamber where all the BPS states exist.

B.2 A_2 Weyl character changes in representation

The full list of basis changes and computations for the change in the highest weight (described in sec. 11.5) of the Weyl character/denominator of $SU(3)$ is shown here. This is distinct in the different Weyl chambers and subsequently reveals which framed halo BPS states exist within each chamber. We then have the 6 chambers with the different possible combinations of BPS states existing.

B.2.1 Weyl denominator expansions

We look at the possible expansions of the Weyl denominator and find that we can write it in terms of negative exponents after a suitable change of basis of positive roots. However, we obtain a shift in the exponents in one of the roots which generates different coefficients. This indicates a wall has been crossed. For clarity, we here write the inner product as $\alpha(u) = (\alpha, u)$:

$$\begin{aligned} \text{Im}[i(\alpha_1, u)] > 0, \text{Im}[i(\alpha_2, u)] < 0, \text{Im}[i(\alpha_3, u)] > 0, & \quad (\text{B.2.1}) \\ - \sum_{n,m,l=0}^{\infty} e^{-n(\alpha_1, u) + (m+1)(\alpha_2, u) - l(\alpha_3, u)} \\ - (n(\alpha_1, u) + (m+1)(-\alpha_2, u) + l(\alpha_1 + \alpha_2, u)), \\ \text{change basis } \alpha'_1 = -\alpha_2, \alpha'_2 = \alpha_1 + \alpha_2 = \alpha_3, \alpha'_3 = \alpha_1, \\ \text{expression becomes } - (n(\alpha'_3, u) + (m+1)(\alpha'_1, u) + l(\alpha'_2, u)), \end{aligned}$$

$$\begin{aligned} \text{Im}[i(\alpha_1, u)] > 0, \text{Im}[i(\alpha_2, u)] < 0, \text{Im}[i(\alpha_3, u)] < 0, & \quad (\text{B.2.2}) \\ \sum_{n,m,l=0}^{\infty} e^{-n(\alpha_1, u) + (m+1)(\alpha_2, u) + (l+1)(\alpha_3, u)} \\ - (n(\alpha_1, u) + (m+1)(-\alpha_2, u) + (l+1)(-\alpha_1 - \alpha_2, u)), \\ \text{change basis } \alpha'_1 = -\alpha_1 - \alpha_2 = -\alpha_3, \alpha'_2 = \alpha_1, \alpha'_3 = -\alpha_2, \\ \text{expression becomes } - (n(\alpha'_2, u) + (m+1)(\alpha'_3, u) + (l+1)(\alpha'_1, u)), \end{aligned}$$

$$\begin{aligned} \text{Im}[i(\alpha_1, u)] < 0, \text{Im}[i(\alpha_2, u)] > 0, \text{Im}[i(\alpha_3, u)] < 0, & \quad (\text{B.2.3}) \\ \sum_{n,m,l=0}^{\infty} e^{(n+1)(\alpha_1, u) - m(\alpha_2, u) + (l+1)(\alpha_3, u)} \\ - ((n+1)(-\alpha_1, u) + m(\alpha_2, u) + (l+1)(-\alpha_1 - \alpha_2, u)), \\ \text{change basis } \alpha'_1 = \alpha_2, \alpha'_2 = -\alpha_1 - \alpha_2 = -\alpha_3, \alpha'_3 = -\alpha_1, \end{aligned}$$

expression becomes $-((n+1)(\alpha'_3, u) + m(\alpha'_1, u) + (l+1)(\alpha'_2, u))$,

$$\begin{aligned} & \operatorname{Im}[i(\alpha_i, u)] < 0, \quad \forall i \in 1, 2, 3, \tag{B.2.4} \\ & \sum_{n,m,l=0}^{\infty} e^{(n+1)(\alpha_1, u) + (m+1)(\alpha_2, u) + (l+1)(\alpha_3, u)} \\ & -((n+1)(-\alpha_1, u) + (m+1)(-\alpha_2, u) + (l+1)(-\alpha_1 - \alpha_2, u)), \\ & \text{change basis } \alpha'_1 = -\alpha_1, \alpha'_2 = -\alpha_2, \alpha'_3 = -\alpha_3 = -\alpha_1 - \alpha_2, \\ & -((n+1)(\alpha'_1, u) + (m+1)(\alpha'_2, u) + (l+1)(\alpha'_3, u)). \end{aligned}$$

C | Integral representations of double gamma function

C.1 Derivation of relation

Following from sec. 12.2.2 we will show a derivation of the alternative integral representation of the double gamma function here - this relation can be derived by taking the log of the gamma function written as

$$\frac{1}{\Gamma_1(z)} = ze^{\gamma z} \prod_{m=1}^{\infty} \left(1 + \frac{z}{m}\right) e^{-\frac{z}{m}}. \quad (\text{C.1.1})$$

Now proceeding with the derivation, we write out in full: $z \log \Gamma_1(z) - \log G(z+1) = -z \log\left(\frac{1}{\Gamma_1(z)}\right) - \log G(z+1)$. This becomes

$$\begin{aligned} & -z \left(\log z + \gamma z + \sum_{m=1}^{\infty} \left(\log\left(1 + \frac{z}{m}\right) - \frac{z}{m} \right) \right) - \\ & \left(\frac{z}{2} \log(2\pi) - \frac{z}{2} - \frac{z^2}{2} - \frac{z^2\gamma}{2} + \sum_{k=1}^{\infty} \left(k \log\left(1 + \frac{z}{k}\right) + \frac{z^2}{2k} - z \right) \right). \end{aligned} \quad (\text{C.1.2})$$

This equation can be rearranged so that

$$\begin{aligned} & \sum_{k=1}^{\infty} \left((z+k) \log\left(1 + \frac{z}{k}\right) - \frac{z^2}{2k} - z \right) = \\ & -z \log z - \frac{z}{2} \log(2\pi) + \frac{z}{2} + \frac{z^2}{2} - \frac{\gamma z^2}{2} - z \log \Gamma_1(z) + \log G(z+1). \end{aligned} \quad (\text{C.1.3})$$

The other stage of this proof (using the method in the book “Special Functions q-series and Related Topics” [209]) involves integrating the log of the gamma function on an interval. Here the interval $[0, z]$ is used. This can then be related back to the equation (C.1.3) above

$$\int_0^z \log \Gamma(x) dx = - \int_0^z \log \left(\frac{1}{\Gamma(x)} \right) dx = \quad (\text{C.1.4})$$

$$-(z \log z - z) - \frac{z^2 \gamma}{2} - \sum_{k=1}^{\infty} \left((z+k) \log \left(1 + \frac{z}{k} \right) - \frac{z^2}{2k} - z \right).$$

This can be further rearranged such that the difference equation can be written in terms of the integral. This becomes

$$\begin{aligned} \int_0^z \log \Gamma(x) dx &= \frac{z(1-z)}{2} + \frac{z}{2} \log(2\pi) + z \log \Gamma(z) - \log G(1+z) \longrightarrow \quad (C.1.5) \\ -\log G(1+z) + z \log \Gamma(z) &= \int_0^z \log \Gamma(x) dx - \frac{z(1-z)}{2} - \frac{z}{2} \log(2\pi). \end{aligned}$$

Finally, we use the known result for this integral in terms of the zeta function, given in [209]

$$\int_0^z \log \Gamma(x) dx = z \frac{1-z + \log(2\pi)}{2} + \zeta'(-1, z) - \zeta'(-1). \quad (C.1.6)$$

So therefore, one can substitute this into the previous equation to obtain the result

$$\log G(z+1) = z \log \Gamma_1(z) + \zeta'(-1, 0) - \zeta'(-1, z). \quad (C.1.7)$$

C.2 Writing relation as an integral representation

Now we can proceed with the rest of the proof starting with the values of the derivatives of the zeta functions. The zeta functions derivatives are given by Adamchik [206] in equation (3) as:

$$\zeta'(-1, z) = \frac{z^2}{2} \log(z) - \frac{z^2}{4} - \frac{z}{2} \log(z) + 2z \int_0^{\infty} \frac{\arctan(\frac{x}{z})}{e^{2\pi x} - 1} dx + \int_0^{\infty} \frac{x \log(x^2 + z^2)}{e^{2\pi x} - 1} dx \quad (C.2.1)$$

$$\zeta'(-1, 0) = 2 \int_0^{\infty} \frac{x \log(x)}{e^{2\pi x} - 1} dx.$$

The value of $\log \Gamma_1(z)$ is also known in terms of z this reads as

$$\log \Gamma_1(z) = \left(z - \frac{1}{2} \right) \log(z) - z + \frac{\log(2\pi)}{2} + 2 \int_0^{\infty} \frac{\arctan(\frac{x}{z})}{e^{2\pi x} - 1} dx. \quad (C.2.2)$$

This is also known as Binet's second formula. Substituting this into the expression below

$$\log G(z+1) = z \left(\left(z - \frac{1}{2} \right) \log(z) - z + \frac{\log(2\pi)}{2} + 2 \int_0^{\infty} \frac{\arctan(\frac{x}{z})}{e^{2\pi x} - 1} dx \right) + \zeta'(-1, 0) - \quad (C.2.3)$$

$$\left(\frac{z^2}{2} \log(z) - \frac{z^2}{4} - \frac{z}{2} \log(z) + 2z \int_0^\infty \frac{\arctan(\frac{x}{z})}{e^{2\pi x} - 1} dx + \int_0^\infty \frac{x \log(x^2 + z^2)}{e^{2\pi x} - 1} dx.\right),$$

and then collecting the terms the expression for the G function:

$$\log G(z + 1) = \frac{z^2}{2} \log(z) - \frac{3}{4} z^2 + z \frac{\log(2\pi)}{2} + \zeta'(-1, 0) + \int_0^\infty \frac{x \log(x^2 + z^2)}{e^{2\pi x} - 1} dx. \quad (\text{C.2.4})$$

This corresponds to the equation (20) in Adamchik [206]. This now relates the 2 possible integral representations of the second gamma function. This expression relating the 2 integrals is written below

$$\begin{aligned} \frac{1}{2\pi i} \int_{\tilde{L}} \frac{e^{-zt}(\log(-t) + \gamma)}{t(1 - e^{-t})^2} dt &= \log(\Gamma_1(z)) - \frac{z^2}{2} \log(z) + \frac{3}{4} z^2 - z \frac{\log(2\pi)}{2} \\ &- \zeta'(-1, 0) - \int_0^\infty \frac{x \log(x^2 + z^2)}{e^{2\pi x} - 1} dx + \text{const}. \end{aligned} \quad (\text{C.2.5})$$

Hence, the double gamma function is now written in terms of an integral along the real axis.

Bibliography

- [1] N. Seiberg and E. Witten, “Electric-magnetic duality, monopole condensation, and confinement in $N=2$ supersymmetric Yang-Mills theory,” *Nuclear Physics B* **426** no. 1, (Sep, 1994) 19–52. [http://dx.doi.org/10.1016/0550-3213\(94\)90124-4](http://dx.doi.org/10.1016/0550-3213(94)90124-4).
- [2] S. Cecotti and C. Vafa, “Classification of complete $N=2$ supersymmetric theories in 4 dimensions,” *Surveys in Differential Geometry* **18** (03, 2011) .
<https://arxiv.org/abs/1103.5832>.
- [3] S. Cecotti, A. Neitzke, and C. Vafa, “R-Twisting and 4d/2d Correspondences,” (2010) , [arXiv:1006.3435](https://arxiv.org/abs/1006.3435) [hep-th].
- [4] M. Alim, S. Cecotti, C. Cordova, S. Espahbodi, A. Rastogi, and C. Vafa, “ $\mathcal{N} = 2$ quantum field theories and their BPS quivers,” *Adv. Theor. Math. Phys.* **18** no. 1, (2014) 27–127, [arXiv:1112.3984](https://arxiv.org/abs/1112.3984) [hep-th].
- [5] P. C. Argyres and M. R. Douglas, “New phenomena in $SU(3)$ Supersymmetric Gauge Theory,” *Nuclear Physics B* **448** no. 1-2, (Aug, 1995) 93–126.
[http://dx.doi.org/10.1016/0550-3213\(95\)00281-V](http://dx.doi.org/10.1016/0550-3213(95)00281-V).
- [6] P. C. Argyres, M. R. Plesser, N. Seiberg, and E. Witten, “New $N = 2$ superconformal field theories in four dimensions,” *Nuclear Physics B* **461** no. 1-2, (Feb, 1996) 71–84. <https://doi.org/10.1016%2F0550-3213%2895%2900671-0>.
- [7] T. Eguchi, K. Hori, K. Ito, and S.-K. Yang, “Study of $N = 2$ superconformal field theories in 4 dimensions,” *Nuclear Physics B* **471** no. 3, (Jul, 1996) 430–442.
<https://doi.org/10.1016%2F0550-3213%2896%2900188-5>.
- [8] A. Gustavsson and M. Henningson, “The light spectrum near the Argyres–Douglas point,” *Physics Letters B* **463** no. 2-4, (Sep, 1999) 201–205.
<https://doi.org/10.1016%2Fs0370-2693%2899%2900935-1>.
- [9] A. D. Shapere and C. Vafa, “BPS structure of Argyres-Douglas superconformal theories,” (1999) , [arXiv:hep-th/9910182](https://arxiv.org/abs/hep-th/9910182).
- [10] S. Cecotti and C. Vafa, “On classification of $N=2$ supersymmetric theories,” *Communications in Mathematical Physics* **158** no. 3, (Dec, 1993) 569–644.
<https://doi.org/10.1007%2Fb02096804>.

- [11] S. Cecotti and C. Vafa, “2d Wall-Crossing, R-Twisting, and a Supersymmetric Index,” (2010) , [arXiv:1002.3638](https://arxiv.org/abs/1002.3638) [hep-th].
- [12] W. Lerche, C. Vafa, and N. P. Warner, “Chiral Rings in $N=2$ Superconformal Theories,” *Nucl. Phys. B* **324** (1989) 427–474.
- [13] S. Cecotti, L. Girardello, and A. Pasquinucci, “Singularity Theory and $N = 2$ Supersymmetry,” *Int. J. Mod. Phys. A* **6** (1991) 2427–2496.
- [14] A. B. Zamolodchikov, “Higher Order Integrals of Motion in Two-Dimensional Models of the Field Theory with a Broken Conformal Symmetry,” *JETP Lett.* **46** (1987) 160–164.
- [15] A. B. Zamolodchikov, “Thermodynamic Bethe Ansatz in Relativistic Models. Scaling Three State Potts and Lee-yang Models,” *Nucl. Phys. B* **342** (1990) 695–720.
- [16] D. Gaiotto, G. W. Moore, and A. Neitzke, “Four-Dimensional Wall-Crossing via Three-Dimensional Field Theory,” *Communications in Mathematical Physics* **299** no. 1, (Jul, 2010) 163–224. <https://doi.org/10.1007/s00220-010-1071-2>.
- [17] D. Gaiotto, G. W. Moore, and A. Neitzke, “Framed BPS States,” *Adv. Theor. Math. Phys.* **17** no. 2, (2013) 241–397, [arXiv:1006.0146](https://arxiv.org/abs/1006.0146) [hep-th].
- [18] E. Andriyash, F. Denef, D. L. Jafferis, and G. W. Moore, “Wall-crossing from supersymmetric galaxies,” *JHEP* **01** (2012) 115, [arXiv:1008.0030](https://arxiv.org/abs/1008.0030) [hep-th].
- [19] D. Joyce and Y. Song, “A theory of generalized Donaldson-Thomas invariants,” *Mem. Amer. Math. Soc.* **217** no. 1020, (2012) iv+199. <https://doi.org/10.1090/S0065-9266-2011-00630-1>.
- [20] T. Bridgeland, “Riemann–Hilbert problems for the resolved conifold and non-perturbative partition functions,” *Journal of Differential Geometry* **115** no. 3, (2020) 395 – 435. <https://doi.org/10.4310/jdg/1594260015>.
- [21] T. Bridgeland, “Riemann–Hilbert problems from Donaldson–Thomas theory,” *Inventiones mathematicae* **216** no. 1, (Dec, 2018) 69–124. <http://dx.doi.org/10.1007/s00222-018-0843-8>.
- [22] S. K. Donaldson and R. P. Thomas, “Gauge theory in higher dimensions,” in *Conference on Geometric Issues in Foundations of Science in honor of Sir Roger Penrose’s 65th Birthday*, pp. 31–47. 6, 1996.
- [23] R. P. Thomas, “A holomorphic Casson invariant for Calabi-Yau 3-folds, and bundles on $K3$ fibrations,” *J. Differential Geom.* **54** no. 2, (2000) 367–438. <http://projecteuclid.org/euclid.jdg/1214341649>.
- [24] R. Gopakumar and C. Vafa, “M-Theory and Topological Strings -I,” 1998. <https://arxiv.org/abs/hep-th/9809187>.

- [25] R. Gopakumar and C. Vafa, “M theory and topological strings-II,” (1998) , [arXiv:hep-th/9812127](https://arxiv.org/abs/hep-th/9812127).
- [26] S. Hosono, M.-H. Saito, and A. Takahashi, “Relative Lefschetz action and BPS state counting,” *Int. Math. Res. Not.* **15** (2001) 783–816, [arXiv:math/0105148](https://arxiv.org/abs/math/0105148).
- [27] S. H. Katz, “Gromov-Witten, Gopakumar-Vafa, and Donaldson-Thomas invariants of Calabi-Yau threefolds,” in *AMS - IMS - SIAM Summer Research Conference on String Geometry*, pp. 43–52. 8, 2004. [arXiv:math/0408266](https://arxiv.org/abs/math/0408266).
- [28] D. Maulik, N. Nekrasov, A. Okounkov, and R. Pandharipande, “Gromov-Witten theory and Donaldson-Thomas theory, i,” *Compositio Mathematica* **142** no. 5, (2006) 1263–1285.
- [29] D. Maulik, N. Nekrasov, A. Okounkov, and R. Pandharipande, “Gromov-Witten theory and Donaldson-Thomas theory, ii,” *Compositio Mathematica* **142** no. 5, (2006) 1286–1304.
- [30] M. Kontsevich and Y. Soibelman, “Stability structures, motivic Donaldson-Thomas invariants and cluster transformations,” (2008) , [arXiv:0811.2435](https://arxiv.org/abs/0811.2435) [[math.AG](https://arxiv.org/abs/math)].
- [31] D. Gaiotto, G. W. Moore, and A. Neitzke, “Wall-crossing, Hitchin systems, and the WKB approximation,” *Adv. Math.* **234** (2013) 239–403, [arXiv:0907.3987](https://arxiv.org/abs/0907.3987) [[hep-th](https://arxiv.org/abs/hep-th)].
- [32] S. Cecotti and C. Vafa, “BPS Wall Crossing and Topological Strings,” 2009. <https://arxiv.org/abs/0910.2615>.
- [33] T. Dimofte, S. Gukov, and Y. Soibelman, “Quantum Wall Crossing in N=2 Gauge Theories,” *Letters in Mathematical Physics* **95** no. 1, (Oct, 2010) 1–25. <http://dx.doi.org/10.1007/s11005-010-0437-x>.
- [34] T. Dimofte and S. Gukov, “Refined, Motivic, and Quantum,” *Letters in Mathematical Physics* **91** no. 1, (Nov, 2009) 1–27. <https://doi.org/10.1007%2Fs11005-009-0357-9>.
- [35] E. Diaconescu and G. W. Moore, “Crossing the wall: Branes versus bundles,” *Adv. Theor. Math. Phys.* **14** no. 6, (2010) 1621–1650, [arXiv:0706.3193](https://arxiv.org/abs/0706.3193) [[hep-th](https://arxiv.org/abs/hep-th)].
- [36] F. Denef and G. W. Moore, “Split states, entropy enigmas, holes and halos,” *JHEP* **11** (2011) 129, [arXiv:hep-th/0702146](https://arxiv.org/abs/hep-th/0702146).
- [37] D. L. Jafferis and G. W. Moore, “Wall crossing in local Calabi Yau manifolds,” (2008) , [arXiv:0810.4909](https://arxiv.org/abs/0810.4909) [[hep-th](https://arxiv.org/abs/hep-th)].
- [38] E. Andriyash, F. Denef, D. L. Jafferis, and G. W. Moore, “Bound state transformation walls,” *JHEP* **03** (2012) 007, [arXiv:1008.3555](https://arxiv.org/abs/1008.3555) [[hep-th](https://arxiv.org/abs/hep-th)].

- [39] A. Strominger and C. Vafa, “Microscopic origin of the Bekenstein-Hawking entropy,” *Physics Letters B* **379** no. 1–4, (Jun, 1996) 99–104.
[http://dx.doi.org/10.1016/0370-2693\(96\)00345-0](http://dx.doi.org/10.1016/0370-2693(96)00345-0).
- [40] R. Dijkgraaf, E. Verlinde, and H. Verlinde, “Counting Dyons in $N = 4$ String Theory,” *Nuclear Physics B* **484** no. 3, (Jan, 1997) 543–561.
[http://dx.doi.org/10.1016/S0550-3213\(96\)00640-2](http://dx.doi.org/10.1016/S0550-3213(96)00640-2).
- [41] A. Strominger, D. Shih, and X. Yin, “Recounting dyons in $N = 4$ string theory,” *Journal of High Energy Physics* **2006** no. 10, (Oct, 2006) 087.
<https://doi.org/10.1088%2F1126-6708%2F2006%2F10%2F087>.
- [42] T. Kawai, “ $N = 2$ heterotic string threshold correction, K3 surface and generalized Kac-Moody superalgebra,” *Physics Letters B* **372** no. 1-2, (Apr, 1996) 59–64.
<https://doi.org/10.1016%2F0370-2693%2896%2900052-4>.
- [43] J. A. Harvey and G. Moore, “Algebras, BPS states, and strings,” *Nuclear Physics B* **463** no. 2-3, (Mar, 1996) 315–368.
<https://doi.org/10.1016%2F0550-3213%2895%2900605-2>.
- [44] J. A. Harvey and G. Moore, “On the Algebras of BPS states,” *Communications in Mathematical Physics* **197** no. 3, (Oct, 1998) 489–519.
<https://doi.org/10.1007%2Fs002200050461>.
- [45] V. A. Gritsenko and V. V. Nikulin, “Siegel automorphic form corrections of some Lorentzian Kac-Moody Lie algebras,” *Amer. J. Math.* **119** no. 1, (1997) 181–224.
http://muse.jhu.edu/journals/american_journal_of_mathematics/v119/119.1gritsenko.pdf.
- [46] V. A. Gritsenko and V. V. Nikulin, “Igusa modular forms and “the simplest” Lorentzian Kac-Moody algebras,” *Sbornik: Mathematics* **187** no. 11, (Dec, 1996) 1601–1641. <https://doi.org/10.1070%2Fsm1996v187n11abeh000171>.
- [47] V. A. Gritsenko and V. V. Nikulin, “On classification of Lorentzian Kac-Moody algebras,” *Russian Mathematical Surveys* **57** no. 5, (Oct, 2002) 921–979.
<https://doi.org/10.1070%2Frm2002v057n05abeh000553>.
- [48] J. R. David, D. P. Jatkar, and A. Sen, “Dyon spectrum in $N = 4$ supersymmetric type II string theories,” *Journal of High Energy Physics* **2006** no. 11, (Nov, 2006) 073. <https://doi.org/10.1088%2F1126-6708%2F2006%2F11%2F073>.
- [49] A. Sen, “Walls of marginal stability and dyon spectrum in $N = 4$ supersymmetric string theories,” *Journal of High Energy Physics* **2007** no. 05, (May, 2007) 039.
<https://doi.org/10.1088%2F1126-6708%2F2007%2F05%2F039>.

- [50] A. Dabholkar, S. Nampuri, and D. Gaiotto, “Comments on the spectrum of CHL dyons,” *Journal of High Energy Physics* **2008** no. 01, (Jan, 2008) 023. <https://doi.org/10.1088%2F1126-6708%2F2008%2F01%2F023>.
- [51] J. R. David, D. P. Jatkar, and A. Sen, “Product representation of dyon partition function in CHL models,” *Journal of High Energy Physics* **2006** no. 06, (Jun, 2006) 064. <https://doi.org/10.1088%2F1126-6708%2F2006%2F06%2F064>.
- [52] M. C. Cheng and E. P. Verlinde, “Dying Dyons Don’t Count,” *Journal of High Energy Physics* **2007** no. 09, (Sep, 2007) 070. <http://dx.doi.org/10.1088/1126-6708/2007/09/070>.
- [53] M. C. N. Cheng and E. P. Verlinde, “Wall Crossing, Discrete Attractor Flow, and Borchers Algebra,” *SIGMA* **4** (2008) 068, [arXiv:0806.2337](https://arxiv.org/abs/0806.2337) [hep-th].
- [54] A. Dabholkar, S. Murthy, and D. Zagier, “Quantum Black Holes, Wall Crossing, and Mock Modular Forms,” (2012) , [arXiv:1208.4074](https://arxiv.org/abs/1208.4074) [hep-th].
- [55] G. Moore, “Arithmetic and Attractors,” 1998. <https://arxiv.org/abs/hep-th/9807087>.
- [56] F. Denef, B. Greene, and M. Raugas, “Split attractor flows and the spectrum of BPS D-branes on the quintic,” *Journal of High Energy Physics* **2001** no. 05, (May, 2001) 012. <https://doi.org/10.1088%2F1126-6708%2F2001%2F05%2F012>.
- [57] F. Denef, “Supergravity flows and D-brane stability,” *Journal of High Energy Physics* **2000** no. 08, (Aug, 2000) 050. <https://doi.org/10.1088%2F1126-6708%2F2000%2F08%2F050>.
- [58] P. Bousseau, P. Descombes, B. Le Floch, and B. Pioline, “BPS Dendroscopy on Local P^2 ,” (2022) , [arXiv:2210.10712](https://arxiv.org/abs/2210.10712) [hep-th].
- [59] B. Szendroi, “Non-commutative Donaldson–Thomas invariants and the conifold,” *Geom. Topol.* **12** no. 2, (2008) 1171–1202, [arXiv:0705.3419](https://arxiv.org/abs/0705.3419) [math.AG].
- [60] M. Alim, “Intrinsic non-perturbative topological strings,” (2021) , [arXiv:2102.07776](https://arxiv.org/abs/2102.07776) [hep-th].
- [61] M. Alim, A. Saha, J. Teschner, and I. Tulli, “Mathematical Structures of Non-perturbative Topological String Theory: From GW to DT Invariants,” *Commun. Math. Phys.* **399** no. 2, (2023) 1039–1101, [arXiv:2109.06878](https://arxiv.org/abs/2109.06878) [hep-th].
- [62] M. Alim, F. Beck, A. Biggs, and D. Bryan, “Special geometry, quasi-modularity and attractor flow for BPS structures,” (2023) , [arXiv:2308.16854](https://arxiv.org/abs/2308.16854) [hep-th].
- [63] K. Nagao and H. Nakajima, “Counting invariant of perverse coherent sheaves and its wall-crossing,” *International Mathematics Research Notices* **2011** no. 17, (2011) 3885–3938. <https://arxiv.org/abs/0809.2992>.

- [64] E. B. Bogomolny, “Stability of Classical Solutions,” *Sov. J. Nucl. Phys.* **24** (1976) 449.
- [65] M. K. Prasad and C. M. Sommerfield, “Exact Classical Solution for the ’t Hooft Monopole and the Julia-Zee Dyon,” *Phys. Rev. Lett.* **35** (Sep, 1975) 760–762.
<https://link.aps.org/doi/10.1103/PhysRevLett.35.760>.
- [66] W. Lerche, “Introduction to Seiberg-Witten theory and its stringy origin,” *Nuclear Physics B - Proceedings Supplements* **55** no. 2, (May, 1997) 83–117.
[http://dx.doi.org/10.1016/S0920-5632\(97\)00073-X](http://dx.doi.org/10.1016/S0920-5632(97)00073-X).
- [67] C. Cordova and S.-H. Shao, “An Index Formula for Supersymmetric Quantum Mechanics,” *J. Singul.* **15** (2016) 14–35, [arXiv:1406.7853](https://arxiv.org/abs/1406.7853) [hep-th].
- [68] M. R. Douglas and G. W. Moore, “D-branes, quivers, and ALE instantons,” (1996) ,
[arXiv:hep-th/9603167](https://arxiv.org/abs/hep-th/9603167).
- [69] M. R. Douglas, B. Fiol, and C. Römelsberger, “The spectrum of BPS branes on a noncompact Calabi-Yau,” *Journal of High Energy Physics* **2005** no. 09, (Sep, 2005) 057. <https://doi.org/10.1088%2F1126-6708%2F2005%2F09%2F057>.
- [70] M. R. Douglas, B. Fiol, and C. Römelsberger, “Stability and BPS branes,” *Journal of High Energy Physics* **2005** no. 09, (Sep, 2005) 006.
<https://doi.org/10.1088%2F1126-6708%2F2005%2F09%2F006>.
- [71] S. Cecotti, “Trieste lectures on wall-crossing invariants,” *available from the authors homepage*, <http://people.sissa.it/cecotti/ictptext.pdf> (2010) .
- [72] C. Hull and P. Townsend, “Unity of superstring dualities,” *Nuclear Physics B* **438** no. 1-2, (Mar, 1995) 109–137.
<https://doi.org/10.1016%2F0550-3213%2894%2900559-w>.
- [73] E. Witten, “String theory dynamics in various dimensions,” *Nuclear Physics B* **443** no. 1-2, (Jun, 1995) 85–126.
<https://doi.org/10.1016%2F0550-3213%2895%2900158-o>.
- [74] P. S. Aspinwall, “Enhanced gauge symmetries and K3 surfaces,” *Physics Letters B* **357** no. 3, (Sep, 1995) 329–334.
<https://doi.org/10.1016%2F0370-2693%2895%2900957-m>.
- [75] M. Bershadsky, C. Vafa, and V. Sadov, “D-strings on D-manifolds,” *Nuclear Physics B* **463** no. 2-3, (Mar, 1996) 398–414.
<https://doi.org/10.1016%2F0550-3213%2896%2900024-7>.
- [76] A. Strominger, “Massless black holes and conifolds in string theory,” *Nuclear Physics B* **451** no. 1-2, (Sep, 1995) 96–108.
<https://doi.org/10.1016%2F0550-3213%2895%2900287-3>.

- [77] A. Strominger, “Black hole condensation and duality in string theory,” *Nuclear Physics B - Proceedings Supplements* **46** no. 1-3, (Mar, 1996) 204–209.
<https://doi.org/10.1016%2F0920-5632%2896%2900023-0>.
- [78] J. Polchinski, “Dirichlet Branes and Ramond-Ramond Charges,” *Physical Review Letters* **75** no. 26, (Dec, 1995) 4724–4727.
<https://doi.org/10.1103%2Fphysrevlett.75.4724>.
- [79] D. Mumford, “Projective invariants of projective structures and applications,” in *Proc. Internat. Congr. Mathematicians (Stockholm, 1962)*, pp. 526–530. 1962.
- [80] C. N. Yang and R. L. Mills, “Conservation of Isotopic Spin and Isotopic Gauge Invariance,” *Phys. Rev.* **96** (Oct, 1954) 191–195.
<https://link.aps.org/doi/10.1103/PhysRev.96.191>.
- [81] H. Georgi and S. L. Glashow, “Unity of All Elementary-Particle Forces,” *Phys. Rev. Lett.* **32** (Feb, 1974) 438–441.
<https://link.aps.org/doi/10.1103/PhysRevLett.32.438>.
- [82] N. Seiberg, “Supersymmetry and Nonperturbative beta Functions,” *Phys. Lett. B* **206** (1988) 75–80.
- [83] A. Klemm, W. Lerche, and S. Theisen, “Nonperturbative Effective Actions of N=2 Supersymmetric Gauge Theories,” *International Journal of Modern Physics A* **11** no. 11, (Apr, 1996) 1929–1973. <https://doi.org/10.1142%2Fs0217751x96001000>.
- [84] P. C. Argyres and A. E. Faraggi, “Vacuum Structure and Spectrum of N=2 supersymmetric SU(N) gauge theory,” *Physical Review Letters* **74** no. 20, (May, 1995) 3931–3934. <https://doi.org/10.1103%2Fphysrevlett.74.3931>.
- [85] N. Seiberg and E. Witten, “Monopoles, duality and chiral symmetry breaking in N = 2 supersymmetric QCD,” *Nuclear Physics B* **431** no. 3, (Dec, 1994) 484–550.
<https://doi.org/10.1016%2F0550-3213%2894%2990214-3>.
- [86] A. Klemm, W. Lerche, S. Yankielowicz, and S. Theisen, “Simple singularities and N = 2 supersymmetric Yang-Mills theory,” *Physics Letters B* **344** no. 1-4, (Jan, 1995) 169–175. <https://doi.org/10.1016%2F0370-2693%2894%2901516-f>.
- [87] T. Eguchi and A. J. Hanson, “Asymptotically flat self-dual solutions to euclidean gravity,” *Physics Letters B* **74** no. 3, (1978) 249–251.
<https://www.sciencedirect.com/science/article/pii/037026937890566X>.
- [88] B. Fiol and M. Mariño, “BPS states and algebras from quivers,” *Journal of High Energy Physics* **2000** no. 07, (Jul, 2000) 031.
<https://doi.org/10.1088%2F1126-6708%2F2000%2F07%2F031>.

- [89] A. Barbieri and J. Stoppa, “Frobenius type and CV-structures for Donaldson-Thomas theory and a convergence property,” *Communications in Analysis and Geometry* **27** no. 2, (2019) 287–327, [arXiv:1512.01176 \[math.AG\]](#).
- [90] S. A. Filippini, M. Garcia-Fernandez, and J. Stoppa, “Stability data, irregular connections and tropical curves,” *Selecta Mathematica* **23** (2017) 1355–1418, [arXiv:1403.7404 \[math.AG\]](#).
- [91] A. Dabholkar, F. Denef, G. W. Moore, and B. Pioline, “Exact and asymptotic degeneracies of small black holes,” *Journal of High Energy Physics* **2005** no. 08, (Aug, 2005) 021. <https://doi.org/10.1088%2F1126-6708%2F2005%2F08%2F021>.
- [92] B. Young, “Computing a pyramid partition generating function with dimer shuffling,” *Journal of Combinatorial Theory, Series A* **116** no. 2, (2009) 334–350.
- [93] L. Faddeev and R. Kashaev, “Quantum Dilogarithm,” *Modern Physics Letters A* **09** no. 05, (Feb, 1994) 427–434. <https://doi.org/10.1142%2Fs0217732394000447>.
- [94] T. Dimofte, S. Gukov, J. Lenells, and D. Zagier, “Exact Results for Perturbative Chern-Simons Theory with Complex Gauge Group,” *Commun. Num. Theor. Phys.* **3** (2009) 363–443, [arXiv:0903.2472 \[hep-th\]](#).
- [95] D.-E. Diaconescu, J. Gomis, and M. R. Douglas, “Fractional branes and wrapped branes,” *Journal of High Energy Physics* **1998** no. 02, (Feb, 1998) 013. <https://doi.org/10.1088%2F1126-6708%2F1998%2F02%2F013>.
- [96] D.-E. Diaconescu and J. Gomis, “Fractional branes and boundary states in orbifold theories,” *Journal of High Energy Physics* **2000** no. 10, (Oct, 2000) 001. <https://doi.org/10.1088%2F1126-6708%2F2000%2F10%2F001>.
- [97] B. Fiol, “The BPS spectrum of N=2 SU(N) SYM and parton branes,” *JHEP* **02** (2006) 065, [arXiv:hep-th/0012079](#).
- [98] D. Gaiotto, “N=2 dualities,” *JHEP* **08** (2012) 034, [arXiv:0904.2715 \[hep-th\]](#).
- [99] M. Alim, S. Cecotti, C. Cordova, S. Espahbodi, A. Rastogi, and C. Vafa, “BPS Quivers and Spectra of Complete N=2 Quantum Field Theories,” *Commun. Math. Phys.* **323** (2013) 1185–1227, [arXiv:1109.4941 \[hep-th\]](#).
- [100] F. Denef, “Quantum Quivers and Hall/Hole halos,” *Journal of High Energy Physics* **2002** no. 10, (Oct, 2002) 023. <https://doi.org/10.1088%2F1126-6708%2F2002%2F10%2F023>.
- [101] C. Voisin, *Hodge Theory and Complex Algebraic Geometry I*, vol. 1 of *Cambridge Studies in Advanced Mathematics*. Cambridge University Press, 2002.
- [102] H. Derksen and J. Weyman, “Quiver representations,” *Notices of the AMS* **52** no. 2, (2005) 200–206.

- [103] R. Schiffler, *Quiver representations*, vol. 1. Springer, 2014.
- [104] A. Kirillov Jr, *Quiver representations and quiver varieties*, vol. 174. American Mathematical Soc., 2016.
- [105] P. S. Aspinwall, T. Bridgeland, A. Craw, M. R. Douglas, A. Kapustin, G. W. Moore, M. Gross, G. Segal, B. Szendrői, and P. M. H. Wilson, *Dirichlet branes and mirror symmetry*, vol. 4 of *Clay Mathematics Monographs*. AMS, Providence, RI, 2009.
- [106] B. Feng, A. Hanany, Y.-H. He, and A. M. Uranga, “Toric duality as Seiberg duality and brane diamonds,” *Journal of High Energy Physics* **2001** no. 12, (Dec, 2001) 035. <https://doi.org/10.1088%2F1126-6708%2F2001%2F12%2F035>.
- [107] D. Berenstein and M. R. Douglas, “Seiberg Duality for Quiver Gauge Theories,” 2002. <https://arxiv.org/abs/hep-th/0207027>.
- [108] C. E. Beasley and M. R. Plesser, “Toric duality is Seiberg duality,” *Journal of High Energy Physics* **2001** no. 12, (Dec, 2001) 001. <https://doi.org/10.1088%2F1126-6708%2F2001%2F12%2F001>.
- [109] F. Cachazo, B. Fiol, K. Intriligator, S. Katz, and C. Vafa, “A geometric unification of dualities,” *Nuclear Physics B* **628** no. 1-2, (Apr, 2002) 3–78. <https://doi.org/10.1016%2Fs0550-3213%2802%2900078-0>.
- [110] V. Ginzburg, “Calabi-Yau algebras,” 2006. <https://arxiv.org/abs/math/0612139>.
- [111] M. Van den Bergh, “Non-commutative crepant resolutions,” in *The Legacy of Niels Henrik Abel: The Abel Bicentennial, Oslo, 2002*, pp. 749–770. Springer, 2004.
- [112] M. Reineke, “Framed quiver moduli, cohomology, and quantum groups,” *Journal of Algebra* **320** no. 1, (2008) 94–115. <https://arxiv.org/abs/math/0411101>.
- [113] H. Nakajima, “Varieties associated with quivers,” *Representation theory of algebras and related topics (Mexico City, 1994)* **19** (1996) 139–157.
- [114] J. Manschot, “Stability and duality in $\mathcal{N} = 2$ supergravity,” *Communications in Mathematical Physics* **299** no. 3, (Aug, 2010) 651–676. <https://doi.org/10.1007%2Fs00220-010-1104-x>.
- [115] J. Manschot, B. Pioline, and A. Sen, “Wall Crossing from Boltzmann Black Hole Halos,” *JHEP* **07** (2011) 059, [arXiv:1011.1258](https://arxiv.org/abs/1011.1258) [hep-th].
- [116] S. Alexandrov and B. Pioline, “Attractor flow trees, BPS indices and quivers,” *Adv. Theor. Math. Phys.* **23** no. 3, (2019) 627–699, [arXiv:1804.06928](https://arxiv.org/abs/1804.06928) [hep-th].
- [117] G. Moore, “PiTP lectures on BPS states and wall-crossing in d=4, N=2 theories,” 2010, accessed 14.10.2022. https://static.ias.edu/pitp/archive/2010files/Moore_LectureNotes.rev3.pdf.

- [118] A. Kapustin, “Wilson-’t Hooft operators in four-dimensional gauge theories and S-duality,” *Phys. Rev. D* **74** (2006) 025005, [arXiv:hep-th/0501015](https://arxiv.org/abs/hep-th/0501015).
- [119] A. Kapustin and E. Witten, “Electric-Magnetic Duality And The Geometric Langlands Program,” *Commun. Num. Theor. Phys.* **1** (2007) 1–236, [arXiv:hep-th/0604151](https://arxiv.org/abs/hep-th/0604151).
- [120] F. Denef, “On the correspondence between D-branes and stationary supergravity solutions of type II Calabi-Yau compactifications,” in *Workshop on Strings, Duality and Geometry*. 3, 2000. [arXiv:hep-th/0010222](https://arxiv.org/abs/hep-th/0010222).
- [121] D. R. Brill, “Splitting of an extremal Reissner-Nordström throat via quantum tunneling,” *Physical Review D* **46** no. 4, (Aug, 1992) 1560–1565. <https://doi.org/10.1103/PhysRevD.46.1560>.
- [122] J. Maldacena, J. Michelson, and A. Strominger, “Anti-de Sitter fragmentation,” *Journal of High Energy Physics* **1999** no. 02, (Feb, 1999) 011. <https://doi.org/10.1088/1126-6708/1999/02/02/011>.
- [123] M. Gross and B. Siebert, “From real affine geometry to complex geometry,” *Annals of mathematics* (2011) 1301–1428. <https://arxiv.org/abs/math/0703822>.
- [124] T. Bridgeland, “Scattering diagrams, Hall algebras and stability conditions,” *Algebraic Geometry* **4** (11, 2017) 523–561. <https://arxiv.org/abs/1603.00416>.
- [125] R. P. Stanley and S. Fomin, *Enumerative Combinatorics*, vol. 2 of *Cambridge Studies in Advanced Mathematics*. Cambridge University Press, 1999.
- [126] B. Young, “Computing a pyramid partition generating function with dimer shuffling,” *Journal of Combinatorial Theory, Series A* **116** no. 2, (2009) 334–350.
- [127] A. Voros, “The return of the quartic oscillator. The complex WKB method,” *Annales de l’I.H.P. Physique théorique* **39** no. 3, (1983) 211–338. http://www.numdam.org/item/AIHPA_1983__39_3_211_0/.
- [128] E. Delabaere and F. Pham, “Resurgent methods in semi-classical asymptotics,” *Annales de l’I.H.P. Physique théorique* **71** no. 1, (1999) 1–94. http://www.numdam.org/item/AIHPA_1999__71_1_1_0/.
- [129] H. Dillinger, E. Delabaere, and F. Pham, “Résurgence de Voros et périodes des courbes hyperelliptiques,” *Annales de l’Institut Fourier* **43** no. 1, (1993) 163–199. <http://www.numdam.org/articles/10.5802/aif.1326/>.
- [130] E. Delabaere, H. Dillinger, and F. Pham, “Exact semiclassical expansions for one-dimensional quantum oscillators,” *Journal of Mathematical Physics* **38** (12, 1997) 6126–6184.

- [131] K. Iwaki and T. Nakanishi, “Exact WKB analysis and cluster algebras,” *J. Phys. A* **47** no. 47, (2014) 474009, 98.
<https://doi.org/10.1088/1751-8113/47/47/474009>.
- [132] S. Codesido and M. Mariño, “Holomorphic anomaly and quantum mechanics,” *Journal of Physics A: Mathematical and Theoretical* **51** no. 5, (Dec, 2017) 055402.
<https://doi.org/10.1088/1751-8121/51/5/055402>.
- [133] K. Ito, M. Mariño, and H. Shu, “TBA equations and resurgent Quantum Mechanics,” *JHEP* **01** (2019) 228, [arXiv:1811.04812](https://arxiv.org/abs/1811.04812) [hep-th].
- [134] A. Grassi, J. Gu, and M. Mariño, “Non-perturbative approaches to the quantum Seiberg-Witten curve,” *JHEP* **07** (2020) 106, [arXiv:1908.07065](https://arxiv.org/abs/1908.07065) [hep-th].
- [135] D. Sauzin, “Introduction to 1-summability and resurgence,” 2014.
<https://arxiv.org/abs/1405.0356>.
- [136] B. Y. Sternin and V. E. Shatalov, *Borel-Laplace transform and asymptotic theory: introduction to resurgent analysis*. CrC Press, 1995.
- [137] A. Voros, “The return of the quartic oscillator. The complex WKB method,” *Annales de l’I.H.P. Physique théorique* **39** no. 3, (1983) 211–338.
http://www.numdam.org/item/AIHPA_1983__39_3_211_0/.
- [138] K. Ito and H. Shu, “ODE/IM correspondence and the Argyres-Douglas theory,” *JHEP* **08** (2017) 071, [arXiv:1707.03596](https://arxiv.org/abs/1707.03596) [hep-th].
- [139] F. Denef, “Attractors at weak gravity,” *Nuclear Physics B* **547** no. 1-2, (May, 1999) 201–220. [https://doi.org/10.1016/S0550-3213\(99\)00096-6](https://doi.org/10.1016/S0550-3213(99)00096-6).
- [140] S. Ferrara, R. Kallosh, and A. Strominger, “ $\mathcal{N} = 2$ Extremal Black Holes,” *Physical Review D* **52** no. 10, (Nov, 1995) R5412–R5416.
<https://doi.org/10.1103/PhysRevD.52.R5412>.
- [141] A. Strominger, “Macroscopic entropy of $N = 2$ extremal black holes,” *Physics Letters B* **383** no. 1, (Aug, 1996) 39–43.
[https://doi.org/10.1016/S0370-2693\(96\)00711-3](https://doi.org/10.1016/S0370-2693(96)00711-3).
- [142] S. Ferrara and R. Kallosh, “Supersymmetry and attractors,” *Physical Review D* **54** no. 2, (Jul, 1996) 1514–1524. <https://doi.org/10.1103/PhysRevD.54.1514>.
- [143] S. Ferrara, G. W. Gibbons, and R. Kallosh, “Black holes and critical points in moduli space,” *Nuclear Physics B* **500** no. 1-3, (Sep, 1997) 75–93.
[https://doi.org/10.1016/S0550-3213\(97\)00324-6](https://doi.org/10.1016/S0550-3213(97)00324-6).
- [144] S. Ferrara, K. Hayakawa, and A. Marrani, “Lectures on attractors and black holes,” *Fortschritte der Physik* **56** no. 10, (Oct, 2008) 993–1046.
<https://doi.org/10.1002/prop.200810569>.

- [145] B. Pioline, “Lectures on black holes, topological strings and quantum attractors,” *Classical and Quantum Gravity* **23** no. 21, (Oct, 2006) S981–S1045.
<https://doi.org/10.1088%2F0264-9381%2F23%2F21%2Fs05>.
- [146] H. Ooguri, A. Strominger, and C. Vafa, “Black hole attractors and the topological string,” *Phys. Rev. D* **70** (2004) 106007, [arXiv:hep-th/0405146](https://arxiv.org/abs/hep-th/0405146).
- [147] S. Alexandrov and B. Pioline, “Attractor flow trees, BPS indices and quivers,” *Adv. Theor. Math. Phys.* **23** no. 3, (2019) 627–699, [arXiv:1804.06928](https://arxiv.org/abs/1804.06928) [hep-th].
- [148] D. Lüst, “Dual string vacua with N=2 supersymmetry in four dimensions,” *Nuclear Physics B - Proceedings Supplements* **62** no. 1-3, (Mar, 1998) 375–403.
<https://doi.org/10.1016%2Fs0920-5632%2897%2900679-8>.
- [149] K. Behmdt, G. L. Cardoso, B. de Wit, R. Kallosh, D. Lust, and T. Mohaupt, “Classical and quantum N = 2 supersymmetric black holes,” *Nuclear Physics B* **488** no. 1-2, (Mar, 1997) 236–260.
<https://doi.org/10.1016%2Fs0550-3213%2897%2900028-x>.
- [150] B. Craps, F. Roose, W. Troost, and A. V. Proeyen, “What is special Kähler geometry?,” *Nuclear Physics B* **503** no. 3, (Oct, 1997) 565–613.
<https://doi.org/10.1016%2Fs0550-3213%2897%2900408-2>.
- [151] P. A. Griffiths, “On the Periods of Certain Rational Integrals: I,” *Annals of Mathematics* **90** no. 3, (1969) 460–495. <http://www.jstor.org/stable/1970746>.
- [152] P. A. Griffiths, “On the Periods of Certain Rational Integrals: II,” *Annals of Mathematics* **90** no. 3, (1969) 496–541. <http://www.jstor.org/stable/1970747>.
- [153] M. Mariño, “Topological strings, matrix models and nonperturbative effects.” http://home.mathematik.uni-freiburg.de/mathphys/konf/Warwick_TQFT/marino.pdf. Lecture notes for Spring School on ‘The geometry and integrability of topological QFT and string theory’ (Warwick 2008) [Accessed 13-09-22].
- [154] M. Abramowitz and I. A. Stegun, *Handbook of Mathematical Functions with Formulas, Graphs, and Mathematical Tables*. Dover, New York, ninth dover printing, tenth gpo printing ed., 1964.
- [155] G. Arfken, *Mathematical Methods for Physicists*. Academic Press, Inc., San Diego, third ed., 1985.
- [156] H. Bateman and A. Erdélyi, *Higher transcendental functions*. California Institute of technology. Bateman Manuscript project. McGraw-Hill, New York, NY, 1955.
<https://cds.cern.ch/record/100233>.
- [157] I. Thompson, *NIST Handbook of Mathematical Functions, edited by Frank WJ Olver, Daniel W. Lozier, Ronald F. Boisvert, Charles W. Clark*. Taylor & Francis, 2011.

- [158] A. Klemm, W. Lerche, P. Mayr, C. Vafa, and N. Warner, “Self-dual strings and $N = 2$ supersymmetric field theory,” *Nuclear Physics B* **477** no. 3, (Oct, 1996) 746–764. <https://doi.org/10.1016%2F0550-3213%2896%2900353-7>.
- [159] S. Katz, A. Klemm, and C. Vafa, “Geometric engineering of quantum field theories,” *Nuclear Physics B* **497** no. 1-2, (Jul, 1997) 173–195. <https://doi.org/10.1016%2Fs0550-3213%2897%2900282-4>.
- [160] A. Klemm, “On the geometry behind $N=2$ supersymmetric effective actions in four-dimensions,” in *33rd Karpacz Winter School of Theoretical Physics: Duality - Strings and Fields*. 5, 1997. [arXiv:hep-th/9705131](https://arxiv.org/abs/hep-th/9705131).
- [161] M. Billó , F. Denef, P. Frè, I. Pesando, W. Troost, A. V. Proeyen, and D. Zanon, “Special geometry of Calabi-Yau compactifications near a rigid limit,” *Fortschritte der Physik* **47** no. 1-3, (Jan, 1999) 133–139. <https://doi.org/10.1002%2F%28sici%291521-3978%28199901%2947%3A1%2F3%3C133%3A%3Aaid-prop133%3E3.0.co%3B2-3>.
- [162] M. Billó , F. Denef, P. Frè, I. Pesando, W. Troost, A. V. Proeyen, and D. Zanon, “The rigid limit in special Kähler geometry: From K3-fibrations to special Riemann surfaces: A detailed case study,” *Classical and Quantum Gravity* **15** no. 8, (Aug, 1998) 2083–2152. <https://doi.org/10.1088%2F0264-9381%2F15%2F8%2F003>.
- [163] E. D’Hoker, T. T. Dumitrescu, and E. Nardoni, “Exploring the strong-coupling region of $SU(N)$ Seiberg-Witten theory,” *JHEP* **11** (2022) 102, [arXiv:2208.11502](https://arxiv.org/abs/2208.11502) [[hep-th](https://arxiv.org/abs/hep-th)].
- [164] J. D. Bekenstein, “Black Holes and Entropy,” *Phys. Rev. D* **7** (Apr, 1973) 2333–2346. <https://link.aps.org/doi/10.1103/PhysRevD.7.2333>.
- [165] S. W. Hawking, “Black holes in general relativity,” *Commun. Math. Phys.* **25** (1972) 152–166.
- [166] A. Sen, “Black hole entropy function, attractors and precision counting of microstates,” *General Relativity and Gravitation* **40** no. 11, (Apr, 2008) 2249–2431. <https://doi.org/10.1007%2Fs10714-008-0626-4>.
- [167] S. Kachru and A. Tripathy, “The hidden symmetry of the heterotic string,” *Adv. Theor. Math. Phys.* **21** (2017) 1729–1745, [arXiv:1702.02572](https://arxiv.org/abs/1702.02572) [[hep-th](https://arxiv.org/abs/hep-th)].
- [168] H. Ooguri and Z. Yin, “TASI Lectures on Perturbative String Theories,” 1996. <https://arxiv.org/abs/hep-th/9612254>.
- [169] D. Tong, “Lectures on String Theory,” 2009. <https://arxiv.org/abs/0908.0333>.

- [170] A. Sen, “Strong–Weak Coupling Duality in Four-Dimensional String Theory,” *International Journal of Modern Physics A* **09** no. 21, (Aug, 1994) 3707–3750. <https://doi.org/10.1142/2Fs0217751x94001497>.
- [171] R. M. Wald, “Black hole entropy is the noether charge,” *Physical Review D* **48** no. 8, (Oct, 1993) R3427–R3431. <http://dx.doi.org/10.1103/PhysRevD.48.R3427>.
- [172] J. A. Harvey and A. Strominger, “The heterotic string is a soliton,” *Nuclear Physics B* **449** no. 3, (Sep, 1995) 535–552. <https://doi.org/10.1016/2F0550-3213%2895%2900310-o>.
- [173] M. Duff, “String solitons,” *Physics Reports* **259** no. 4-5, (Aug, 1995) 213–326. <https://doi.org/10.1016/2F0370-1573%2895%2900002-x>.
- [174] J. P. Gauntlett and J. A. Harvey, “S-Duality and the Spectrum of Magnetic Monopoles in Heterotic String Theory,” 1994. <https://arxiv.org/abs/hep-th/9407111>.
- [175] A. Dabholkar, “Exact counting of black hole microstates,” *Phys. Rev. Lett.* **94** (2005) 241301, [arXiv:hep-th/0409148](https://arxiv.org/abs/hep-th/0409148).
- [176] R. Dijkgraaf, E. Verlinde, and H. Verlinde, “BPS spectrum of the five-brane and black hole entropy,” *Nuclear Physics B* **486** no. 1-2, (Feb, 1997) 77–88. <https://doi.org/10.1016/2Fs0550-3213%2896%2900638-4>.
- [177] R. Dijkgraaf, E. Verlinde, and H. Verlinde, “BPS quantization of the five-brane,” *Nuclear Physics B* **486** no. 1-2, (Feb, 1997) 89–113. <https://doi.org/10.1016/2Fs0550-3213%2896%2900639-6>.
- [178] J. A. Harvey and A. Strominger, “The heterotic string is a soliton,” *Nuclear Physics B* **449** no. 3, (Sep, 1995) 535–552. <https://doi.org/10.1016/2F0550-3213%2895%2900310-o>.
- [179] A. Dabholkar and J. A. Harvey, “Nonrenormalization of the Superstring Tension,” *Phys. Rev. Lett.* **63** (1989) 478.
- [180] A. Dabholkar, G. W. Gibbons, J. A. Harvey, and F. Ruiz Ruiz, “Superstrings and Solitons,” *Nucl. Phys. B* **340** (1990) 33–55.
- [181] G. De Rham, *Differentiable manifolds: forms, currents, harmonic forms*, vol. 266. Springer Science & Business Media, 2012.
- [182] S. Morita, *Geometry of differential forms*. No. 201. American Mathematical Soc., 2001.
- [183] L. J. Dixon, V. Kaplunovsky, and J. Louis, “Moduli dependence of string loop corrections to gauge coupling constants,” *Nucl. Phys. B* **355** (1991) 649–688.

- [184] E. Verlinde, “Global aspects of electric-magnetic duality,” *Nuclear Physics B* **455** no. 1-2, (Nov, 1995) 211–225.
<https://doi.org/10.1016%2F0550-3213%2895%2900431-q>.
- [185] C. Vafa and E. Witten, “A strong coupling test of S-duality,” *Nuclear Physics B* **431** no. 1-2, (Dec, 1994) 3–77.
<https://doi.org/10.1016%2F0550-3213%2894%2990097-3>.
- [186] J. Breckenridge, D. Lowe, R. Myers, A. Peet, A. Strominger, and C. Vafa, “Macroscopic and microscopic entropy of near-extremal spinning black holes,” *Physics Letters B* **381** no. 4, (Jul, 1996) 423–426.
<https://doi.org/10.1016%2F0370-2693%2896%2900553-9>.
- [187] J. Breckenridge, R. Myers, A. Peet, and C. Vafa, “D-branes and spinning black holes,” *Physics Letters B* **391** no. 1-2, (Jan, 1997) 93–98.
<https://doi.org/10.1016%2Fs0370-2693%2896%2901460-8>.
- [188] T. Kawai, Y. Yamada, and S.-K. Yang, “Elliptic genera and $N = 2$ superconformal field theory,” *Nuclear Physics B* **414** no. 1-2, (Feb, 1994) 191–212.
<https://doi.org/10.1016%2F0550-3213%2894%2990428-6>.
- [189] D. Shih and X. Yin, “Exact black hole degeneracies and the topological string,” *JHEP* **04** (2006) 034, [arXiv:hep-th/0508174](https://arxiv.org/abs/hep-th/0508174).
- [190] J. R. David and A. Sen, “CHL dyons and statistical entropy function from D1-D5 system,” *Journal of High Energy Physics* **2006** no. 11, (Nov, 2006) 072.
<https://doi.org/10.1088%2F1126-6708%2F2006%2F11%2F072>.
- [191] T. Mohaupt, “Black hole entropy, special geometry and strings,” *Fortsch. Phys.* **49** (2001) 3–161, [arXiv:hep-th/0007195](https://arxiv.org/abs/hep-th/0007195).
- [192] D. Galakhov, “BPS Hall algebra of scattering Hall states,” *Nuclear Physics B* **946** (Sep, 2019) 114693. <https://doi.org/10.1016%2Fj.nuclphysb.2019.114693>.
- [193] J. E. Humphreys, *Introduction to Lie algebras and representation theory* / J. E. Humphreys. Springer-Verlag New York, 1972.
<http://www.loc.gov/catdir/enhancements/fy0817/72085951-t.html>.
- [194] W. Fulton and J. Harris, “Representation theory,” *volume 129, Graduate Texts in Mathematics* (1991) .
- [195] J. E. Humphreys, *Reflection groups and Coxeter groups*. No. 29. Cambridge university press, 1992.
- [196] B. C. Hall, “An Elementary Introduction to Groups and Representations,” May, 2000. <http://arxiv.org/abs/math-ph/0005032>.

- [197] J.-P. Serre, *Cartan Subalgebras*. Springer Berlin Heidelberg, Berlin, Heidelberg, 2001. https://doi.org/10.1007/978-3-642-56884-8_3.
- [198] Dennis Gaitsgory, Course Notes, “Geometric Representation theory, Math 267y, Fall 2005.”.
- [199] M. A. Walton, “Polytope expansion of Lie characters and applications,” *Journal of Mathematical Physics* **54** no. 12, (Dec, 2013) 121701. <https://doi.org/10.1063%2F1.4834615>.
- [200] V. G. Kac, *Infinite-dimensional Lie algebras*. Cambridge University Press, Cambridge, third ed., 1990.
- [201] J. E. Humphreys, *Representations of semisimple Lie algebras in the BGG category O* / James E. Humphreys. Graduate studies in mathematics ; v. 94. American Mathematical Society, Providence, R.I, 2008.
- [202] A. Narukawa, “The modular properties and the integral representations of the multiple elliptic gamma functions,” *Advances in Mathematics* **189** no. 2, (2004) 247–267.
- [203] K. Iwaki and O. Kidwai, “Topological recursion and uncoupled BPS structures I: BPS spectrum and free energies,” *Adv. Math.* **398** (2022) 108191, [arXiv:2010.05596](https://arxiv.org/abs/2010.05596) [[math-ph](#)].
- [204] D. Ghoshal and C. Vafa, “ $C = 1$ string as the topological theory of the conifold,” *Nucl. Phys. B* **453** (1995) 121–128, [arXiv:hep-th/9506122](https://arxiv.org/abs/hep-th/9506122).
- [205] K. Iwaki, T. Koike, and Y. Takei, “Voros coefficients for the hypergeometric differential Equations and Eynard–Orantin’s topological recursion: Part i—for the Weber equation,” in *Annales Henri Poincaré*, vol. 24, pp. 1305–1353, Springer. 2023.
- [206] V. S. Adamchik, “Contributions to the Theory of the Barnes Function,” 2003. <https://arxiv.org/abs/math/0308086>.
- [207] N. Kurokawa and S.-y. Koyama, “Multiple sine functions,” *Forum Math.* **15** no. 6, (2003) 839–876. <https://doi.org/10.1515/form.2003.042>.
- [208] M. Jimbo and T. Miwa, “Quantum KZ equation with $|q| = 1$ and correlation functions of the XXZ model in the gapless regime,” *Journal of Physics A: Mathematical and General* **29** no. 12, (Jun, 1996) 2923–2958. <https://doi.org/10.1088%2F0305-4470%2F29%2F12%2F005>.
- [209] M. R. Mourad Ismail, David R. Masson, *Special Functions q -series and Related Topics*. American Mathematical Soc., Printed in the United States of America., 1997.